Influence of oxygen on vascular tone during acute hypoxia

A thesis submitted to Cardiff University in accordance with the requirements for the degree of PHILOSOPHIAE DOCTOR (PhD)

Jessica Emma Dada (BSc Hons)

Wales Heart Research Institute

Cardiff University

October 2013

Supervisors: Dr Philip E James & Dr Derek Lang

Declaration

This work has not previously been accepted in substance for any degree and is not concurrently submitted in candidature for any degree.

Signed …… (candidate) Date……

STATEMENT 1
This thesis is being submitted in partial fulfilment of the requirements for the degree of PhD.

Signed …… (candidate) Date ……..

STATEMENT 2
This thesis is the result of my own independent work/investigation, except where otherwise stated. Other sources are acknowledged by explicit references.

Signed …… (candidate) Date ……..

STATEMENT 3
I hereby give consent for my thesis, if accepted, to be available for photocopying and for interlibrary loan, and for the title and summary to be made available to outside organisations.

Signed …… (candidate) Date ……..

To Keith,

Thank you for supporting me every step of the way

&

To my parents,

For always believing in me

Acknowledgements

First and foremost, I would like to thank both of my supervisors, Dr Philip James and Dr Derek Lang, for all their support throughout my PhD. I have learnt so much from both of you and I am very grateful for all your advice.

I would also like to thank Dr Alison May and Mr Lawrence King for their support obtaining samples for the clinical aspects of this work. A special thank you to my former undergraduate project student, Miss Natalie Price, for your efforts in obtaining preliminary data for a chapter within this thesis.

I will very much miss the interesting conversation in office 3/08 with students and staff both past and present, not to mention stimulating lunchtime gossip with Miss Libby Ellins and Dr Kirsten Smith! A special thank you to my closest colleagues and friends: Dr Ewelina Sagan, Dr Shantu Bundhoo, Dr Phillip Freeman, Mr Gareth Willis, Miss Katie Connolly, Dr Laurence Thornhill, Dr Liz Palmer & Miss Sioned Owen for all of your help and encouragement.

I have met some amazing people during my PhD in Cardiff. It's been a truly unforgettable experience.

‘Believe you can and you’re halfway there’

Theodore Roosevelt

Contents

Abstract

It is well acknowledged that molecular oxygen (O_2) constricts vascular tissue under physiological conditions. In hypoxia, the decrease in partial pressure of O_2 (pO_2) within the tissue may be due to either a reduction in O_2 supply or an increased O_2 demand. The pulmonary circulation responds to a decrease in O_2 by inducing vasoconstriction, whereas the systemic circulation induces vasorelaxation. Systemic vasorelaxation in hypoxia occurs by one of two presumed mechanisms, direct, in which smooth muscle cells can no longer sustain adequate contraction, or indirect, in which vasodilatory molecules are produced. Since the early 1990's, several laboratories worldwide hypothesised that the vasodilatory molecules released under hypoxic conditions originated from the red blood cell (RBC). Several mechanisms have been proposed to date, including nitrite (NO_2^-) reduction by haemoglobin (Hb) to nitric oxide (NO), S-nitrosation of Hb to S-nitrosohaemoglobin (HbSNO) and adenosine triphosphate (ATP) binding to P_2Y receptors on the vascular endothelium. Although there has been extensive research within this field, a clear mechanism by which vasorelaxation occurs is yet to be fully elucidated. Therefore, the aims of this thesis were to determine the vasodilatory specie(s) released from RBCs and the mechanism by which vasorelaxation occurs.

Myography experiments were conducted using dissected rabbit thoracic aortae. Rings were equilibrated at various O_2 concentrations, directly influencing tissue pO_2. Bolus administration of oxygenated RBCs, isolated Hb or Krebs-Henseleit (KH) buffer to pre-constricted hypoxic rings induced a transient relaxation which was immediately followed by a post-constriction of equivalent magnitude. Interestingly, oxygenated KH buffer alone could induce relaxation of aortic rings in a similar manner to RBCs and Hb, demonstrating that O_2 itself relaxes hypoxic vascular tissue. In addition, the extent of vasorelaxation was inversely related to the tissue pO_2.

Oxygenated KH buffer alone induced vasorelaxation in hypoxic pre-constricted rings pre-incubated with NOS inhibitor, L-NMMA, indicating an endothelium-independent mechanism. Subsequent experiments investigated the role of soluble guanylate cyclase (sGC) in the context of these findings. A number of studies have shown that sGC does not bind O_2. However, the results present herein demonstrate that O_2 can stimulate an enhanced activity of soluble guanylate cyclase (sGC), increasing the production of cyclic guanosine monophosphate (cGMP). Importantly, this could occur in the absence of NO but was found to be dependent upon the presence of haem.

In order to compare O_2-induced vasorelaxation in a vessel with an alternative function, the left anterior descending (LAD) artery was dissected from porcine hearts. Hypoxic pre-constricted LAD rings relaxed 20% more to a bolus of oxygenated RBCs or KH buffer compared to rabbit aortic rings and this was not due to an increased expression of sGC within the smooth muscle. Further experiments aimed to show whether vessel size had an effect upon the magnitude of O_2-induced vasorelaxation in hypoxia. O_2 induced a greater vasorelaxation in rings of smaller inner diameter. In conclusion, the results within this thesis show a direct relaxant effect of O_2 that is mediated via the sGC-cGMP pathway and suggest a role for O_2 in response of vascular smooth muscle in acute hypoxia.

Abbreviations

AA	Arachidonic acid
AC	Adenylate cyclase
ACh	Acetylcholine
ADP	Adenosine diphosphate
AE-1	Anion exchanger 1
APS	Ammonium persulphate
ATP	Adenosine triphosphate
β^o	Mutation of β-thalassemia which prevents formation of β-chains
β^+	Mutation of β-thalassemia which allows formation of β-chains
BH_4	Tetrahydrobiopterin
BK	Bradykinin
BSA	Bovine serum albumin
Ca^{2+}	Calcium
$[Ca^{2+}]i$	Intracellular calcium concentration
$CaCl_2$	Calcium chloride
CaM	Calmodulin
cAMP	Cyclic adenosine monophosphate
CAT	Catalase
CGD	Chronic granulomatous disease
cGMP	Cyclic guanosine monophosphate
CO	Carbon Monoxide
COX	Cyclooxygenase
d.H_2O	Double distilled water
Da	Dalton
deoxyHb	Deoxyhaemoglobin
d.H_2O	Double distilled water
dL	Decilitre
DNA	Deoxyribonucleic acid
2,3-DPG	2,3-diphosphoglycerate
DPI	Diphenyleneiodonium
EC_{50}	Concentration of a drug which provokes half-maximal response
EDHF	Endothelium-derived hyperpolarising factor
ELISA	Enzyme-linked immunosorbent assay
EPO	Erythropoietin
EPR	Electron paramagnetic resonance spectroscopy
Fe^{2+}	Reduced iron (ferrous)
Fe^{3+}	Oxidised iron (ferric)
g	Gravity
GC	Guanylate cyclase

GTP	Guanosine Triphosphate
GSNO	S-Nitrosoglutathione
GTN	Glyceryl trinitrate
H^+	Hydrogen ion
H_2O	Water
H_2O_2	Hydrogen peroxide
H_2S	Hydrogen sulphide
Hb	Haemoglobin
HbNO	Nitrosyl haemoglobin
HbSNO	S-nitrosohaemoglobin
HCl	Hydrochloric acid
HIF-1	Hypoxia inducible factor – 1
HO	Haem oxygenase
HPLC	High Performance Liquid Chromatography
HRP	Horseradish Peroxidase
H_2O_2	Hydrogen Peroxide
IP_3	Inositol 1, 4, 5-triphosphate
K^+	Potassium
K_{ATP}	ATP-sensitive potassium channel
K_{Ca}	Calcium-dependent potassium channel
KH	Krebs Henseleit
KCl	Potassium chloride
KH_2PO_4	Potassium dihydrogen orthophosphate
K_m	Michaelis Menten constant
LAD	Left anterior descending
L-NAME	N^G-nitro-L-arginine methyl ester
L-NMMA	N^G-monomethyl-L-arginine
M	Molar
Mb	Myoglobin
mg	Milligrams
mRNA	Messenger ribonucleic acid
$MgSO_4$	Magnesium sulphate
min(s)	Minute(s)
ml	Millilitre
mM	Millimolar
N_2	Nitrogen
Na^+	Sodium ion
NAC	N-acetyl cysteine
NaCl	Sodium chloride
NADH	Nicotinamide adenine dinucleotide
NADPH	Nicotinamide adenine dinucleotide phosphate

$NaHCO_3$	Sodium hydrogen carbonate
$NaNO_2$	Sodium nitrite
NaOH	Sodium hydroxide
nm	Nanometre
nmol	Nanomol
NNO	N-nitrosamines
NO	Nitric oxide
NO_2^-	Nitrite
NO_3^-	Nitrate
NOA	Nitric oxide analysis
NOC 9	MAHMA NONOate
NOS	Nitric oxide synthase
NO_x	NO species
NSB	Non-specific binding
OBC	Ozone-based chemiluminescence
OD	Optical density
ODQ	[1*H*-[1,2,4]oxadiazolo-[4,3-*a*]quinoxalin-1-one]
$ONOO^-$	Peroxynitrite
osc	Oscillations
O_2	Oxygen
O_2^-	Superoxide
oxyHb	Oxyhaemoglobin
P_i	Inorganic phosphate
PAGE	Polyacrylamide gel electrophoresis
pCO_2	Partial pressure of carbon dioxide
PDE	Phosphodiesterase
PDT	2,2,6,6-tetra-methyl-4-piperidone
PE	Phenylephrine
pEC_{50}	Negative log of the EC_{50}
PEG	Polyethylene glycol
pGC	Particulate guanylate cyclase
PGI_2	Prostacyclin
PKG	Protein kinase G
pmol	picomol
pO_2	Partial pressure of oxygen
PPE	Personal protective equipment
PVDF	Poly vinylidene fluoride
RBC	Red Blood Cell
RNS	Reactive nitrogen species
ROS	Reactive oxygen species
rpm	Revolutions per minute

s	Seconds
SDS	Sodium dodecyl sulphate
sGC	Soluble guanylate cyclase
(R)SNO	S-Nitrosothiol
SNP	Sodium nitroprusside
SOD	Superoxide dismutase
SR	Sarcoplasmic reticulum
TEMED	Tetramethylethylenediamine
TBS	Tris buffered saline
TBST	Tris buffered saline + Tween-20
tHb	Total haemoglobin
µl	Microlitre
µm	Micrometre
µM	Micromolar
V	Volts
VEGF	Vascular endothelial growth factor
VDCC	Voltage-dependent calcium channels
w/v	Weight in volume

Units conversion

1 Torr = 1 mmHg
1 % O_2 = 10 µM O_2
760 mmHg = 21 % O_2

1 Introduction

It is now well recognised that molecular oxygen (O_2) constricts vascular smooth muscle under physiological conditions. When the partial pressure of O_2 (pO_2) within tissues decreases, pulmonary smooth muscle constricts, decreasing the surface area available for gaseous exchange. Conversley, the systemic circulation responds to a fall in pO_2 by dilating the vasculature, encouraging the diffusion of O_2 into the surrounding hypoxic tissue. The release of a red blood cell (RBC)-derived vasodilatory molecule which transiently dilates vascular tissue in order to match O_2 demand is thought to underlie this response. Indeed, over the past twenty years or so, several groups have suggested molecules which could be involved in promoting vasorelaxation. The results chapters within this thesis focus on the influence of O_2 on vascular tone in this setting.

1.1 Control of O_2 in the vasculature

1.1.1 O_2 sensing

The body utilises several sensing mechanisms to assess the concentration of O_2 within the blood and tissues in order to match supply with demand. These mechanisms will be discussed in more depth in the sections below.

1.1.1.1 The carotid body

Respiration is controlled by specialised chemoreceptors which have the capability to sense variation in pO_2, partial pressure of carbon dioxide (pCO_2) and hydrogen ions (H^+) (1). For instance, two types of cells reside within the carotid body (located near the bifurcation of the carotid artery (2)), type I (glomus) and type II (sustentacular) (3). Such peripheral arterial chemoreceptors and other central chemoreceptors are the key sensory centres

which can facilitate homeostatic control of changes in O_2 as well as drive hyperventilation responses during hypoxia (4) and metabolic acidosis (5).

Glomus cells located in the carotid body are involved in cellular responses in hypoxia. The cells sense a change in arterial O_2 tension and subsequently elicit a response via afferent neurons to the central nervous system (CNS). Responsiveness of the carotid body to acute hypoxia relies on the inhibition of O_2-sensitive potassium (K^+) channels in the type I cells. This ultimately leads to cell depolarisation, calcium (Ca^{2+}) entry and release of transmitters that activate afferent nerve fibres. (6). The mechanism of how a change in O_2 tension leads to a decrease in K^+ conductance remains unknown however there has been some speculation as to how it occurs (7). For instance, one could speculate that several O_2-sensors coexist in the same cell or perhaps are distributed among the different O_2-sensitive cell types.

1.1.1.2 Haem oxygenase-2 (HO-2)

HO-2, a constitutive form of HO, has been implicated as an O_2 sensor in carotid body activation by hypoxia (8). This is an interesting concept considering the enzyme requires both nicotinamide adenine dinucleotide phosphate (NADPH) and O_2 for the generation of carbon monoxide (CO), biliverdin and reduced iron (Fe^{2+}) by the catabolism of haem. Williams *et al* (2004) proposed that under normoxia, HO-2 had the ability to control proteins which would normally be modulated by hypoxia, through the production of CO since O_2 availability was limited (9). Nevertheless, there has been data published in HO-2 knockout mouse models that have variable outcomes. Adachi and colleagues (2004) suggest that the response to hypoxia is blunted in knockout mice (10) however, data reported by Ortega-

Saenz *et al* (2006, 2007) conclude that the response is unaffected (11, 12). Therefore the involvement of HO-2 in the hypoxic response during O_2-sensing remains uncertain.

1.1.1.3 Mitochondria

The production of adenosine triphosphate (ATP) via the electron transport chain requires O_2 to act as an electron acceptor. When hypoxia prevails, cells compromise by acquiring energy by glycolysis, leading to cessation of the electron transport chain. This demonstrates that the mitochondria have a profound ability to sense limited O_2 within a cell. However, it is more difficult to answer whether mitochondria have the ability to detect changes in O_2 within the physiological range (20-40 mmHg (13)). One suggestion states that alteration in redox state of the electron transport chain could contribute to the sensing of O_2 by mitochondria (14). The Michaelis-Menten constant (K_m) for O_2 of cytochrome *c* oxidase has been reported to be < 1 μM, allowing pO_2-independent mitochondrial respiration in state 3 of < 2 Torr (14). If electron transport is not limited by O_2 supply under hypoxic conditions (pO_2 5-50 Torr), it is difficult to see how mitochondrial redox could be affected by O_2 concentration. However, it is possible that pO_2 within cells could be lower than extracellular pO_2 due to gradients between the cell membrane and mitochondrial membrane. It is also noteworthy that the K_m calculation above is usually undertaken with isolated/purified enzyme and may not reflect the whole cell scenario.

1.1.1.3.1 Mitochondrial-derived reactive O_2 species (ROS)

O_2 is reduced to water (H_2O) by cytochrome *c* oxidase during mitochondrial respiration, the resulting energy conserved during ATP synthesis. Early research in the 1950's estimated that ~3 % of the O_2 consumed is not reduced effectively during mitochondrial respiration (15). Superoxide (O_2^-) is generated from the electron transfer to

O_2 and its generation is dependent on factors such as O_2 availability, reduction state of the O_2 carriers, as well as the membrane potential of the mitochondria (16, 17). It has been postulated that the decrease in maximum initial rate of cytochrome *c* oxidase catalysed reactions (V_{max} of cytochrome *c* oxidase) (14) during hypoxia is attributable to the increased mitochondrial redox state which in turn leads to the enhancement of ROS production during anoxic conditions.

1.1.1.4 O_2 sensitive-K^+ channels

Lopez and Barneo (1988) discovered that in type I cells from the adult rabbit carotid body, hypoxia could inhibit a K^+ current (18). Since then, a whole host of O_2-sensitive K^+ channels have been identified (19, 20). However, the mechanisms by which K^+ channels can actually sense O_2 are less certain. For instance, are the channels themselves responsive to changes in O_2 or do they reflect a secondary response initiated by a primary O_2 sensor? The idea of a secondary response has been supported by the fact that O_2-sensitive channels are responsive to oxidising and reducing agents. For example, in 1999, Fearon and colleagues expressed a specific L-type Ca^{2+} channel subunit in human embryonic kidney-293 cells (HEK-293) and established that recordings of Ca^{2+} currents by whole cell patch clamping were dampened by hypoxia (21). Oxidising agent *p*-chloromercuribenzenesulphonic acid abolished the response to hypoxia, suggesting that hypoxia may affect Ca^{2+} channel activity via redox alteration of thiol residues. This is still yet to be confirmed, however, assessment of responsiveness to hypoxia in the absence of other O_2-sensing mechanisms could be demonstrated using a cloned O_2-sensitive channel implanted into a secondary cellular membrane (21).

1.1.1.5 NADPH oxidase

NADPH oxidase is an enzyme which catalyses the production of O_2^- from O_2 and NADPH. The enzyme is made up of several components, two membrane and three cytosolic, in which activation involves the phosphorylation of one of the cytosolic components (22). In terms of O_2 sensing, since the rate of ROS production appears to be dependent on the concentration of O_2, this system could therefore act as a sensor. In a system which involves a membrane oxidase, O_2^- could function as a second messenger, linking the oxidase sensor to the target, namely K^+ channels (section 1.1.1.4). (23).

Components of the NADPH oxidase system have been expressed in several cell types that are known to be O_2-responsive such as type I cells of the carotid body (see section 1.1.1.1) and pulmonary vascular myocytes (24). However, there is some disagreement as to whether NADPH oxidase possesses an O_2 sensing capability. For example, patients with chronic granulomatous disease (CGD) suffer from a defect in one or more NADPH oxidase subunits (25). Based on the theory above, loss of part of this oxidase system would lead to loss of function of the enzyme. Nevertheless, patients with CGD are able to maintain normal erythropoietin (EPO) levels. Under normal physiological circumstances, EPO plays a key role in O_2 homeostasis where production of EPO is stimulated in the kidneys in response to hypoxia (7). This suggests that NADPH oxidase function is not required for O_2-sensing in conjunction with production of EPO. It could be argued that perhaps O_2 sensing in that setting could involve an isoform of NADPH oxidase which is not affected by the CGD. However, the non-selective electron transport inhibitor, diphenyleneiodonium (DPI) should mimic the effect of hypoxia by diminishing ROS production in normoxic conditions through the inhibition of NADPH oxidase (22).

NADPH has also been reported to play a role in O_2 sensing that is fundamental to the mechanism of hypoxic pulmonary vasoconstriction (24) (discussed in more detail in section 1.2.3). Similar to the mechanism mentioned earlier in this section, alveolar hypoxia would lead to a decrease in ROS production and subsequently shift the redox status of pulmonary artery smooth muscle cells (PASMC) to a more reduced state. In addition, this would also cause inactivation of redox-dependent K^+ channels present on the plasma membrane leading to depolarisation, Ca^{2+} influx and smooth muscle cell contraction. In this setting, NADPH oxidase would act as the primary sensor of O_2 and the K^+ channels would function as the effectors, initiating the resultant vasconstrictive response.

A study by Archer *et al* in 1999 disproved the notion that NADPH oxidase could sense O_2 underlying hypoxic pulmonary vasoconstriction (26). Transgenic mice lacking the gp91phox subunit of NADPH oxidase displayed a decrease in the generation of ROS. However, the K^+ current response to hypoxic conditions and lung vasoconstriction response were not inhibited. DPI in this system did not inhibit the constriction response in normoxia as opposed to hypoxia, perhaps ruling out the involvement of NADPH oxidase in O_2 sensing of hypoxic pulmonary vasoconstriction.

An interesting observation of the kinetics of NADPH oxidase is the K_m for O_2 (30-40 μM), as calculated from cell models. This far outweighs the K_m for nitric oxide synthase (NOS) which has been calculated at approximately (6-9 μM) (27). This would infer that at O_2 concentrations between 10 and 30 μM, cells of the endothelium for instance, would maximally produce NO however the concentration of O_2^- would be limited.

1.1.1.6 Hypoxia-inducible factor 1 (HIF-1)

HIF-1 is present in most species which consume O_2. It consists of both α and β subunits, the α playing a role in O_2 sensing and the β subunit possessing the ability to form complexes with other proteins of similar basic helix-loop-helix structure (28). Interestingly, the messenger ribonucleic acid (mRNA) for both subunits are detected under normoxic conditions. While the α subunit protein can be rapidly degraded by the ubiquitin/proteasome breakdown pathway, it is stabilised by hypoxia. Such an action leads to dimer formation, nuclear translocation and deoxyribose nucleic acid (DNA) binding. Activation of HIF-1 in hypoxia increases the levels of certain other proteins inside the cell such as inducible NOS (iNOS) and vascular endothelial growth factor (VEGF) among others, to promote cell survival in low O_2 conditions.HIF acts by binding to HIF response elements (HRE) in the promoters of these genes. Increases in the levels of VEGF promote collateral expansion of endothelial cells to form new blood vessels under low O_2 conditions (29). It is important to mention that the activation of HIF-1 and the processes aforementioned are part of the mechanisms which occur in response to adaptation to chronic hypoxia, such as tumour progression (30).

1.1.2 Blood

Blood is one of the most dynamic fluids within the body. Adult blood contains 4.5-5.8 x 10^{11} cells/dL, males generally having a higher number of cells per volume than females (31) and this comprises ~45 % of total blood volume (haematocrit). The next sections will introduce the different components of the blood and their functional roles within the body.

1.1.2.1 Red Blood Cells (RBCs)

1.1.2.1.1 Production, development & senescence

Erythropoiesis, the process by which RBCs are produced, is primarily stimulated by EPO, a hormone which is synthesised by the kidneys. In neonatal development, the main site of RBC production is the liver however adult RBCs are formed within the bone marrow from precursor stem cells. Prior and immediately after their exit, RBCs are known as reticulocytes, and comprise a small proportion of circulating RBCs. Reticulocytes have the ability to form the polypeptide chains, α and β-globin, as well as protoporphyrin. The combination of these three elements with Fe^{2+} creates a functional adult haemoglobin (HbA) molecule. (32).

The typical lifespan of RBCs is between 100 and 120 days (33). As the RBC ages, there are changes to the plasma membrane which render the cell more susceptible to recognition by scavenging macrophages. The scavenging activity by macrophages occurs at the same rate as RBC production thus the population of RBCs remains relatively constant (34).

1.1.2.1.2 Structure

RBCs are in abundance within blood, approximately 5×10^{11} cells/dL (35). Due to their biconcave shape, RBCs have dimensions of 8 µm in diameter, 2 µm depth on the outer edge and 1 µm inner depth. Their unique structure enables efficient transport of O_2 in the blood by an enhanced surface area. In addition, the membranes of these cells are extremely flexible. Although 8 µm in diameter, RBCs are able to travel through capillaries of only a third of this size. (Figure 1.1). (31).

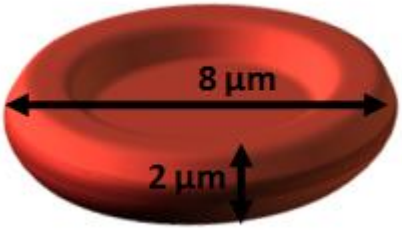

Figure 1.1: Red blood cell structure. *Reproduced with permission by Miss N Price*.

1.1.2.1.3 Haemoglobin (Hb) – O_2 carrier

Hb consists of haem and globin domains. The globin portion is made up of four polypeptide chains, two α subunits and two β subunits (~64,500 Da) (31). The haem portion of Hb is made up of four iron containing haem moieties, each of which can reversibly bind an O_2 molecule. (Figure 1.2).

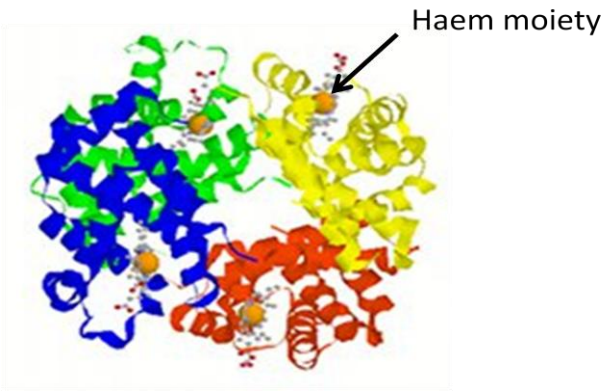

Figure 1.2: Structure of Hb. The haem moieties present in each subunit bind O_2. *Adapted (36).*

The discovery that Hb was made up of 4 subunits which could change conformation in order to accommodate O_2 binding (37, 38), lead to further investigation as to how Hb can alter its affinity for O_2. Cooperative binding of each subunit ensures that the affinity to O_2 increases with subsequent oxygenation (39). This binding capacity with O_2 originates from the two conformational states that Hb can adopt, T (tense) and R (relaxed) (40) (Figure 1.3). When O_2 binds, Hb changes from T state to R state via a number of different stages. The

hydrogen bonding in both $\alpha_1\beta_1$ and $\alpha_2\beta_2$ variants of HbA is extensive and these quaternary structures allow little movement. However, $\alpha_2\beta_1$ and $\alpha_1\beta_2$ confers allosteric movement during the transition from T to R state, resulting in different properties compared to the ligand-bound state (41).

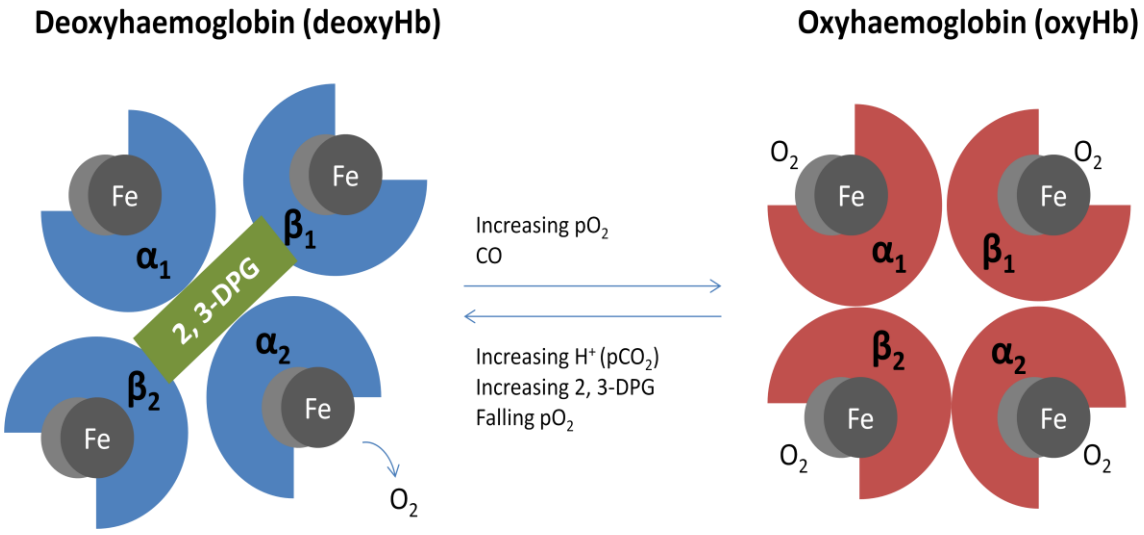

Figure 1.3: O_2 binding and transition from T to R state Hb. 4 O_2 molecules are bound to R state oxyHb. An increase in levels of 2,3-diphosphoglycerate (2,3-DPG) or a fall in either pH or pO_2 favours transition back to T state Hb. An increase in pO_2 or CO favours transition back to R state Hb and subsequent O_2 binding. *Adapted (42).*

Brunori and colleagues discovered that the O_2 affinity in T state was around 70 times lower than that of R state Hb (43). Later, in 1972, Perutz suggested that the low affinity of Hb in T state was possibly due to an increased tension at the haem site which draws the central iron further away from the plane of the porphyrin ring. This could ultimately resist movement into the ring upon O_2 binding (40).

1.1.3 O_2 delivery

The arrival of oxygenated blood to a respiring tissue bed initiates the exchange of O_2 and CO_2 across the vessel/tissue interface. A lower level of O_2 in the tissues, coupled with a high level of CO_2 permits the dissociation of O_2 from Hb and subsequent diffusion to the tissue

bed. The process of O_2 dissociation from Hb is different in comparison to the association of O_2 with Hb in the lungs, mainly due to the differences in tissue thickness (lung alveolar epithelium vs. tissues of the body). (44).

Danish physiologist, August Krogh examined the relationship between the concentration of O_2 in blood and the subsequent gradients of O_2 which develop along the length of a capillary. Krogh's model of O_2 transport through tissues was based on the finding that in many tissues, capillaries are evenly spaced. Thus it was considered that capillaries supply O_2 to specific cylindrical regions which surround each capillary (Figure 1.4) (44, 45).

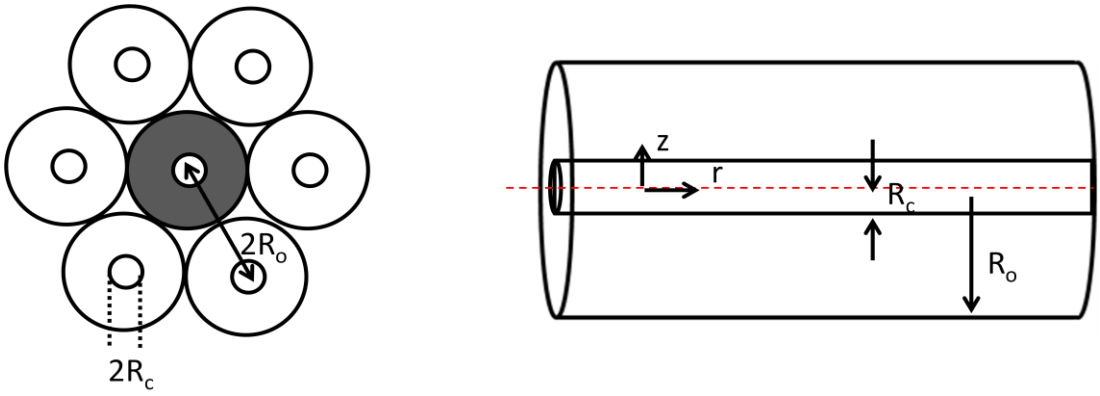

Figure 1.4: Krogh cylinder model. The left hand diagram depicts the cross sectional area of the capillary and surrounding tissue, the right, a capillary through a cylindrical tissue bed. *Half the distance between the centre of the two capillaries (R_o), capillary radius (R_c), distance along capillary (r), centre of capillary (z). Adapted (45).*

1.1.3.1 Normal distribution of O_2 across a vascular bed

Oxygenated blood is transported to tissues and organs to supply respiring cells with O_2 and nutrients to meet the metabolic demand. In skeletal muscle, an increase in metabolic rate decreases the tissue O_2 saturation in the blood compartment. It is possible that this decrease in saturation signals vascular smooth muscle to relax by limiting the production of ATP required for contraction (46). Certainly, in health, decreases in blood O_2 saturation can

in large be countered by increasing flow and tissue perfusion (i.e. the number of open arterioles/capillaries).

As illustrated in Figure 1.5, pO_2 generally decreases during an arterial to venous transit. The Krogh model (section 1.1.3) considers that most O_2 that flows through a capillary network diffuses out in a cylindrical fashion to the adjacent tissue. For the most part, it is assumed that the majority of O_2 is exchanged at this level, implying that large gradients exist between the pO_2 of the blood and tissues. However, the capillary-tissue gradients in pO_2 are much larger in the lung compared to the tissues (50 mmHg/µm vs. 0.5 mmHg/µm) (47). The oxygenation of blood within the capillaries is similar to that of the surrounding tissue, suggesting that the capillaries may not be the primary vessel for tissue oxygenation.

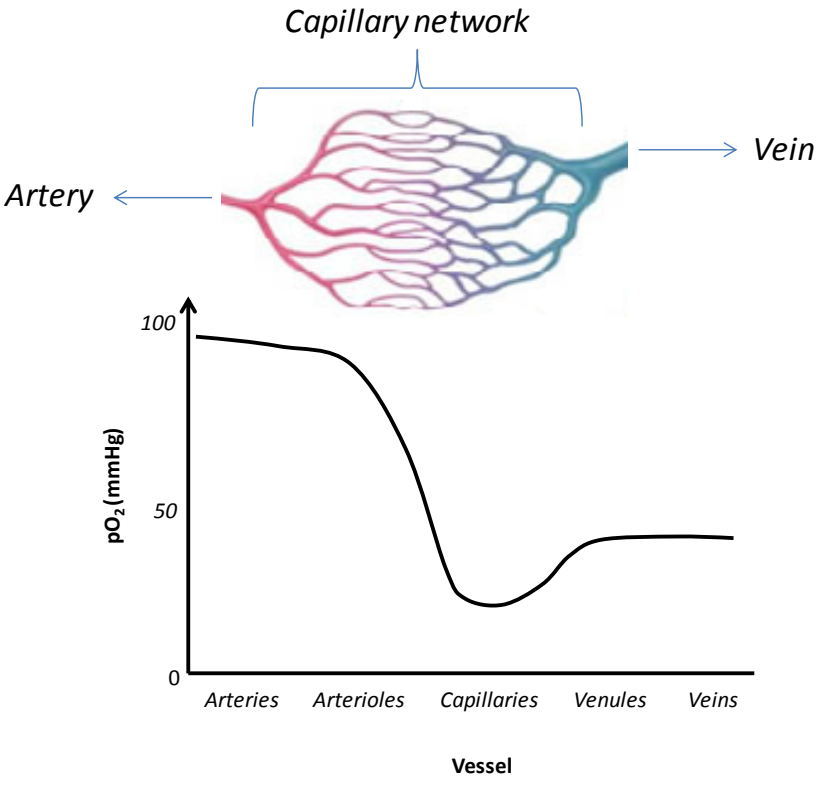

Figure 1.5: Change in pO_2 across a vascular bed. *Adapted (48).*

1.1.3.2 The Bohr Effect

This phenomenon was postulated by the physician, Christian Bohr, in 1904 (49). He stated that Hb affinity for O_2 is inversely related to pH and CO_2 concentrations within the blood. An increase in pCO_2 (or decrease in blood pH) leads to a rightward shift of the O_2 dissociation curve and subsequent offloading of O_2. Thus, a decrease in pCO_2/increase in blood pH leads to the binding of O_2 to Hb. (Figure 1.6).

The mechanism by which the Bohr effect arises ultimately centres on ion transfer between the Hb subunits. In deoxyHb, the N-terminal amino groups of the α subunits and the C-terminal histidines of the β-subunit contribute to ion pairing. This leads to the binding of only one proton to every two O_2 molecules that are released, causing a decrease in acidity. On the other hand, oxyHb lacks ion pairing interaction and thus the acidity increases (50).

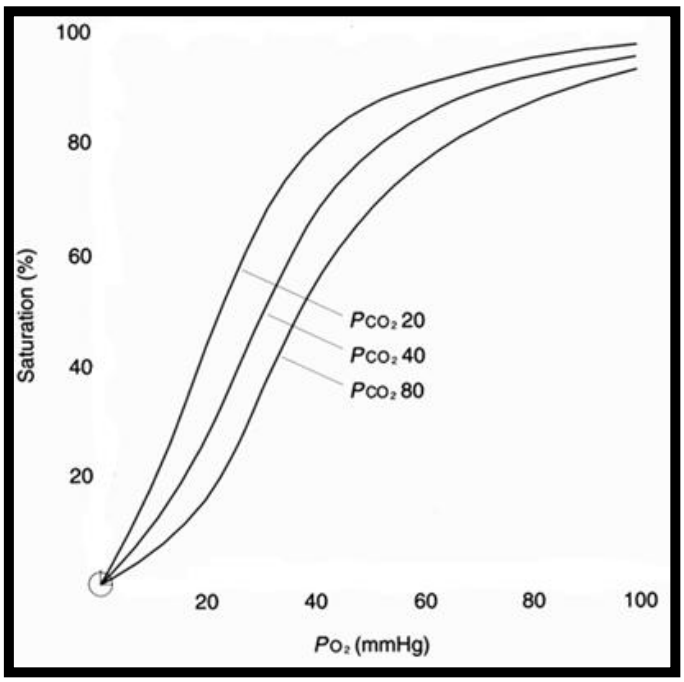

Figure 1.6: Effect of increasing CO_2 (mmHg) on O_2 saturation of Hb. *Adapted (51).*

Haldane first discovered that deoxygenation of blood increases its ability to carry CO_2 and this was later named the Haldane effect (52). The opposite is also true, oxygenated blood displays a lower affinity for CO_2. Both of the effects mentioned in this section are relevant to the changes which occur with an increased metabolic activity where tissues of the body require more O_2, yet the subsequent increase in CO_2 needs to be removed efficiently.

1.1.3.2.1 Metabolism

The correct functioning of Hb and the integrity of the RBC membrane are key to the efficiency of RBC performance. Unique metabolic processes occur within the RBC in order to maintain these functions. This is regulated through the molecules ATP, 2,3-diphosphoglycerate (2,3-DPG) and nicotinamide adenine dinucleotide (NADH) in particular (31).

Glycolysis is the main metabolic pathway in RBCs. Glucose is converted into pyruvate and lactate which can then leave the cell and be further metabolised in the liver during gluconeogensis (53). The RBCs have a particularly high consumption of glucose (the main substrate of glycolysis), utilising 30-40 g per day (31). ATP is also highly consumed mostly by active ion channels in the cell membrane. When ATP is lacking, the ionic balance is disrupted, leading to cell swelling and accumulation of Ca^{2+} (54).

NADH produced by the glycolytic pathway is an electron source for metHb reductase (31). The latter is an enzyme involved in the conversion of metHb back to Hb, using NADH as an electron donor to reduce the haem moieties from Fe^{3+} to Fe^{2+}.

2,3-DPG is a metabolite only found within RBCs. At a concentration of between 4 and 5 mM, it is in equimolar proportion to Hb. However, the quantity of free metabolite is dependent upon Hb saturation, deoxyHb contains as little as 0.5 mM (55). 2,3-DPG binds in a 1:1 ratio to deoxyHb (Lysine 82, Histidine 143 and N-terminal groups on β subunits) and decreases the affinity of Hb for O_2. This occurs through binding of 2,3-DPG to T state Hb which ultimately leads to a preference in O_2 offloading (31).

1.1.3.3 Plasma

The plasma component of blood comprises about 55 % of the total volume and accounts for the fluidity of whole blood. Plasma itself is made up of several constituents (Table 1.1).

Table 1.1: Examples of plasma components. *Adapted (56).*

Constituents	
Water	~ 90 % of total plasma volume
Salts, Ions, Electrolytes	NaCl, HCO_3^-, Ca^{2+}, Mg^{2+}, Cl^-, Cu^{2+}, Fe^{2+} NO_2^-, NO_3^-
Low MW compounds	Glucose, ATP, cAMP, vitamins, urea
High MW compounds	Peptides, GP, clotting factors, polysaccharides, DNA
Gases	O_2, CO_2, NO

1.1.3.3.1 Distribution of ions

Similar to other cells of the body, RBCs contain high intracellular K^+ and low sodium (Na^+) and chloride (Cl^-) concentrations. Anions such as bicarbonate (HCO_3^-) and Cl^- are transported across the membrane by facilitated diffusion via the anion exchange protein, rendering the RBC much more permeable to anions than cations. Both Na^+ and K^+ are regulated by the Na^+/K^+-ATPase which transports 3 Na^+ ions out and 2 K^+ ions into the cell, utilising ATP as its energy source. Ca^{2+} which entered the plasma membrane of RBCs via store operated channels is transported out of the cell via Ca^{2+}-ATPase. In RBC senescence, the activity of Ca^{2+}-ATPase diminishes leading to an increase in intracellular Ca^{2+} that eventually initiates cell degradation in the spleen. Hb itself possesses a negative charge, therefore governing the movement of other anions (HCO_3^- and Cl^-) across the cell membrane. (31).

1.1.4 CO_2 in the blood

CO_2 from metabolising cells and tissues of the body diffuses into the blood and into the RBCs. A small proportion of CO_2 can combine with Hb to form carbaminohaemoglobin, however the rest is converted to carbonic acid (H_2CO_3) by the enzyme carbonic anhydrase. This can further dissociate into H^+ and HCO_3^-. (57).

1.1.5 pH

The pH of the blood in a healthy individual is between 7.35 and 7.45. It is critical to keep the pH within this range and so the buffering capacity of the blood is very important. It is mainly the regulation of H^+ which most affects the pH of blood therefore balancing reactions that consume or release this ion are the primary goals. (31). The equation below summarises the series of events which occur in the blood in order to buffer an increase in

H^+. The intermediate H_2CO_3 is involved in a reversible reaction which leads to the formation of H_2O and CO_2.

$$H^+(aq) + HCO_3^-(aq) \rightleftharpoons H_2CO_3(aq) \rightleftharpoons H_2O(l) + CO_2(g)$$

Several factors, for instance exercise, can have a marked influence on blood pH. During aerobic exercise, muscle cells release CO_2 and H^+ (produced during glucose metabolism) into the blood and this can lead to a lowering of the pH. If O_2 supply does not match demand, anaerobic metabolism prevails and produces pyruvate and H^+ during glycolysis. Subsequently lactate dehydrogenase can then convert pyruvate to lactic acid, again lowering blood pH. Importantly, the human body can efficiently deal with a reduction in pH via its innate buffering systems. Hb plays an essential role in "scavenging" the extra CO_2 and H^+ and the lungs and kidneys respond to pH changes by removing CO_2, HCO_3^-, and H^+ (58).

1.2 Hypoxia

1.2.1 Supply vs. demand

In the body, intracellular O_2 ranges from 110 mmHg (16%) in the pulmonary alveoli to less than 20 mmHg (3%) in some areas of the heart, kidney and brain (28). The physiological concentration inside the cells is very much based on homeostasis, the balance between O_2 delivery and O_2 consumption. The response to hypoxia is dependent on whether the insult is temporary (acute) or a chronic adaptation.

1.2.2 Consequences of hypoxia

There are several ways in which the body adapts to hypoxia. At the organismal level, an increase in alveolar ventilation occurs as a response to environmental hypoxia, which

involves the interaction of chemoreceptors, respiratory control centres in the medulla and respiratory muscles in the chest wall. At the tissue level, hypoxic pulmonary vasoconstriction manifests, as discussed in section 1.2.3. At the cellular level (section 1.1.1), neurotransmitters released by glomus cells of the carotid body signal driving hormonal responses which alter the rate of respiration. Production of EPO occurs by the liver and kidneys to encourage RBC production for enhanced O_2 delivery to hypoxic cells. Vascular growth factors are also released as mentioned in section 1.1.1.6, promoting angiogenesis and increasing blood supply to tissues.

1.2.3 Hypoxic pulmonary vasoconstriction

Alveolar hypoxia is the primary determinant of pulmonary vasoconstriction. The process was first identified in 1894 as a rise in pulmonary arterial pressure upon asphyxia (59). Since then, it was confirmed that hypoxia in the absence of hypercapnia induced constriction within the pulmonary circulation (60). This mechanism is the opposite of the systemic response, where the manifestation of tissue hypoxemia leads to vasodilation in order to match perfusion to metabolic demand. A recent study conducted by a former colleague tested the effects of nitrite (NO_2^-) on pulmonary vascular resistance (61). Healthy volunteers were infused with a low dose of sodium NO_2^- (1 µmol/min $NaNO_2$) during exposure to either normoxic (21 % O_2) or hypoxic (12 % O_2) conditions. Analysis of forearm blood flow revealed that infusion of $NaNO_2$ under hypoxic condition caused both pulmonary and systemic vasodilatation.

The threshold for hypoxic pulmonary vasoconstriction is approximately 60 mmHg and while it increases in proportion to the degree of hypoxia, it fails under anoxic conditions (~5 mmHg) (62). The process is mediated by both smooth muscle and endothelial cells (Figure

1.7). In the former, Ca^{2+} is released from the sarcoplasmic reticulum (SR) via ryanodine receptors. Such smooth muscle constriction is augmented through myofilament Ca^{2+} sensitisation (see Figure 1.7) following the release of an unidentified vasoconstrictor from the overlying endothelium. (63).

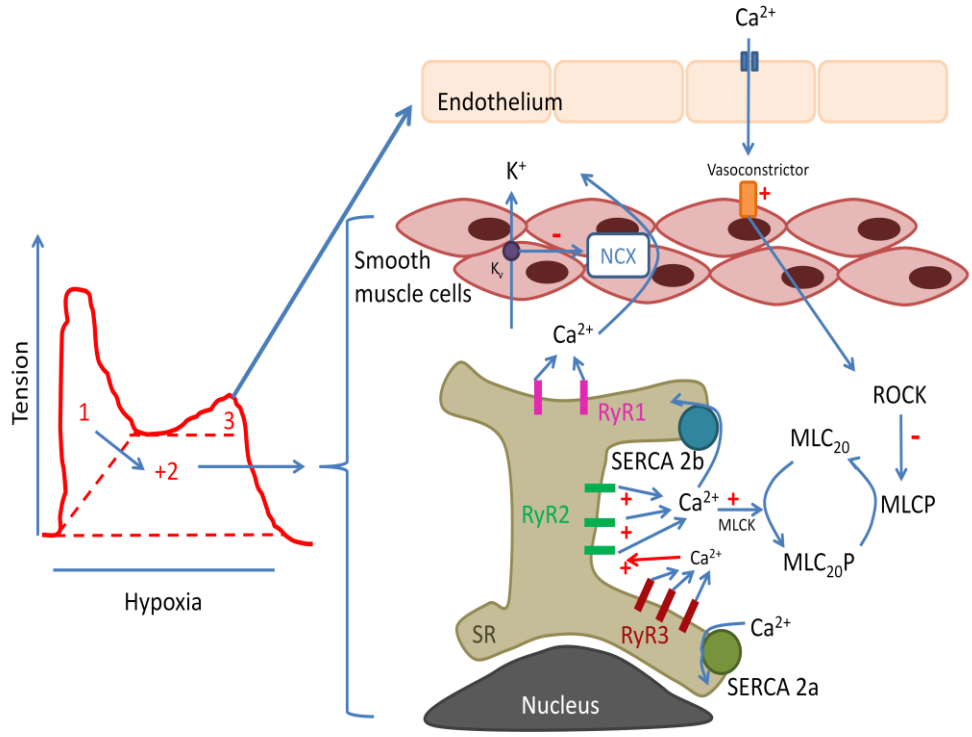

Figure 1.7: Mechanism of hypoxic pulmonary vasoconstriction. The trace on the left depicts the phases observed during hypoxic pulmonary constriction of an isolated pulmonary arterial ring. Phases 1 and 2 enhance Ca^{2+} release from the smooth muscle sarcoplasmic reticulum (SR) via ryanodine receptors (RyR). Sarco/endoplasmic reticulum Ca^{2+}-ATPase (SERCA) subtypes pump Ca^{2+} back into the SR. This imposes a positive inducement (via Ca^{2+}/calmodulin) of myosin light chain kinase (MLCK) leading to phosphorylation of myosin light chain 20 (MLC_{20}). Phase 3 involves vasoconstrictor release from the endothelium which affects Rho associated kinase (ROCK) leading to inhibition of myosin light chain phosphatase (MLCP) and Ca^{2+} sensitisation. *Adapted* (64).

1.3 The vascular endothelium

1.3.1 Structure & function

The endothelium is a monolayer of cells that forms the inner lining of blood vessels. Structural and functional integrity of endothelial cells is imperative for maintenance of

vascular homeostasis and inflammatory status (65). Although endothelial cells line all blood vessels across the entire body, there is geographical variation with regard to their innate responses to the same stimulus (66). This emphasises the multi-faceted functions of these cells and their varied roles in endocrine, paracrine and autocrine processes (65). Several functions of the endothelium are summarised in Figures 1.8 and 1.9.

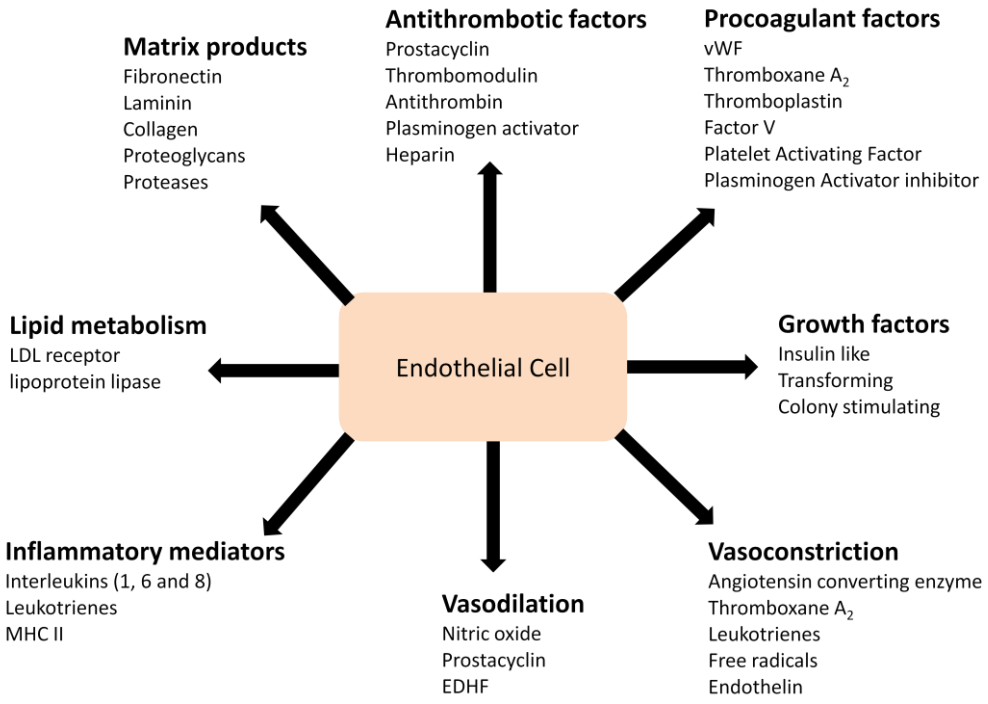

Figure 1.8: Secreted mediators released by endothelial cells that have a profound influence over cellular processes within the body. *Adapted (65).*

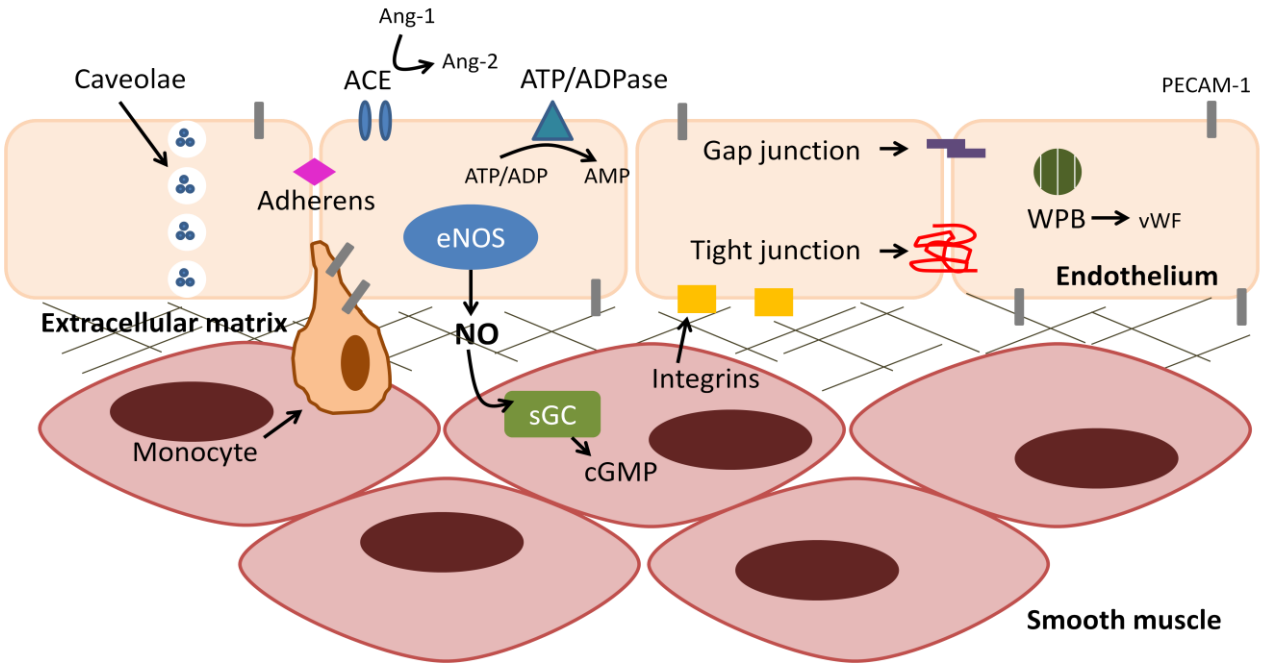

Figure 1.9: Structure and signalling processes of the vascular endothelium. The cells are associated with the extracellular matrix by integrins and proteins including vitronectin and fibronectin. Individual endothelial cells are connected by tight junctions, gap junctions and adherens. Gap junctions permit the rapid transport of Ca^{2+} and inositol triphosphate (IP_3) between endothelial cells. Large molecules such as albumin are transported through the endothelium by caveolae however smaller molecules can migrate between the gaps between adjacent cells. Angiotensin converting enzyme (ACE) catalyses the conversion of Angiotensin 1 (Ang-I) to Angiotensin 2 (Ang-II) causing vasoconstriction. Stimulation of eNOS, which itself is regulated by calmodulin, NADPH and 5, 6, 7, 8-tetrahydrobiopterin (BH_4), catalyses the conversion of L-arginine to L-citrulline, liberating the vasoactive gas, nitric oxide (NO). vWF contained within WPB plays a critical role in platelet adhesion and haemostasis. *Adapted* (67).

Endothelial cells form a semi selective barrier that governs movement of certain molecules between the blood and interstitium (68, 69). In order for this to occur efficiently, the endothelial cells maintain a non-thrombogenic surface (65). Antithrombotic factors (see Figure 1.8) inhibit various coagulation cascades which would normally lead to platelet aggregation (70, 71).

1.3.2 Inflammation

Inflammation is a response within the body to local injury, infection or antigen stimulation (72). Under physiological conditions, inflammation is a key part of our innate immune response to invading pathogens. Endothelial cells are actively involved in inflammation and the subsequent immune response in several ways. Firstly, endothelial cells play a role in antigen presentation and recruitment of inflammatory cells (73). Secondly, they express a variety of adhesion molecules and release chemotactic factors which facilitate the adherence and migration of cells within the blood.

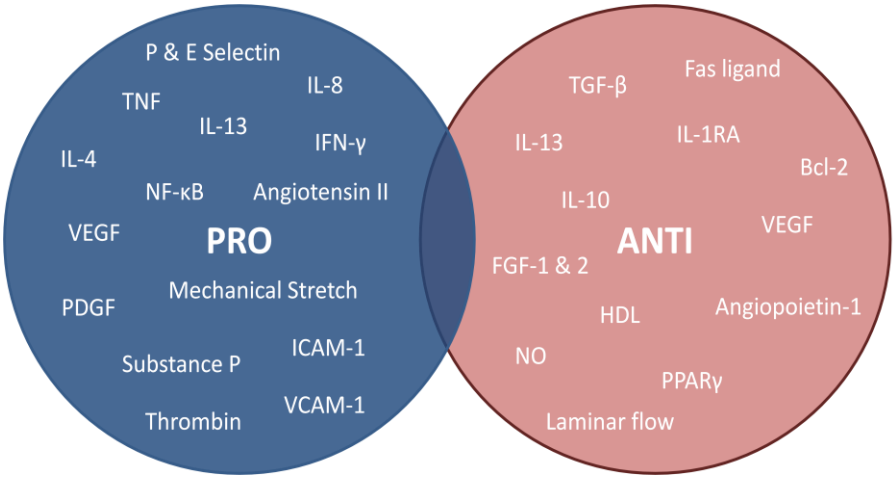

Figure 1.10: Examples of pro and anti inflammatory mediators which affect the vascular system. Abbreviations not defined in text: interleukin (IL), interferon gamma (IFN-γ), nuclear factor kappa B (NF-κB), interleukin adhesion molecule-1 (ICAM-1), vascular cell adhesion molecule-1, tumour growth factor beta (TGF-β), fibroblast growth factor 1 & 2 (FGF-1 & 2), high density lipoprotein (HDL), peroxisome proliferator-activated receptor gamma (PPAR-γ), b cell lymphoma 2 (Bcl-2). *Adapted* (72, 74-76).

1.3.3 ROS & oxidative stress

The definition of a free radical is *'any species capable of independent existence that contains one or more unpaired electrons'* (77). ROS are very important in the maintenance of homeostasis in certain cell types. For example, within the mitochondria, ROS production at complex I (NADH dehydrogenase) and complex III (ubiquinone cytochrome bc1) initiates the signals that control the response to changes in O_2 tension (78).

The activity of NOX oxidases, NOS, xanthine oxidase (XO), cytochrome P450, cyclooxygenase (COX) and mitochondria contribute to the generation of oxy radical species within the vasculature (79) (Figure 1.11). These oxidases are of low activity under physiological conditions in order to maintain vascular homeostasis.

Overproduction of such species, including ROS and reactive N_2 species (RNS), or the failure of antioxidant mechanisms within the body can eventually lead to cellular and tissue

damage (80). For instance, in the endothelium, both responses to shear stress and receptor-mediated activation have been linked to COX, cytochrome P450 and mitochondrial generation of vasoactive levels of hydrogen peroxide (H_2O_2) (81). It has also been documented that the uncoupling of eNOS results in free radical generation (82). In addition, the most detrimental action of free radical species and particularly ROS, is the reaction with NO. These reactions ultimately lead to a decreased bioavailability of NO and endothelial dysfunction.

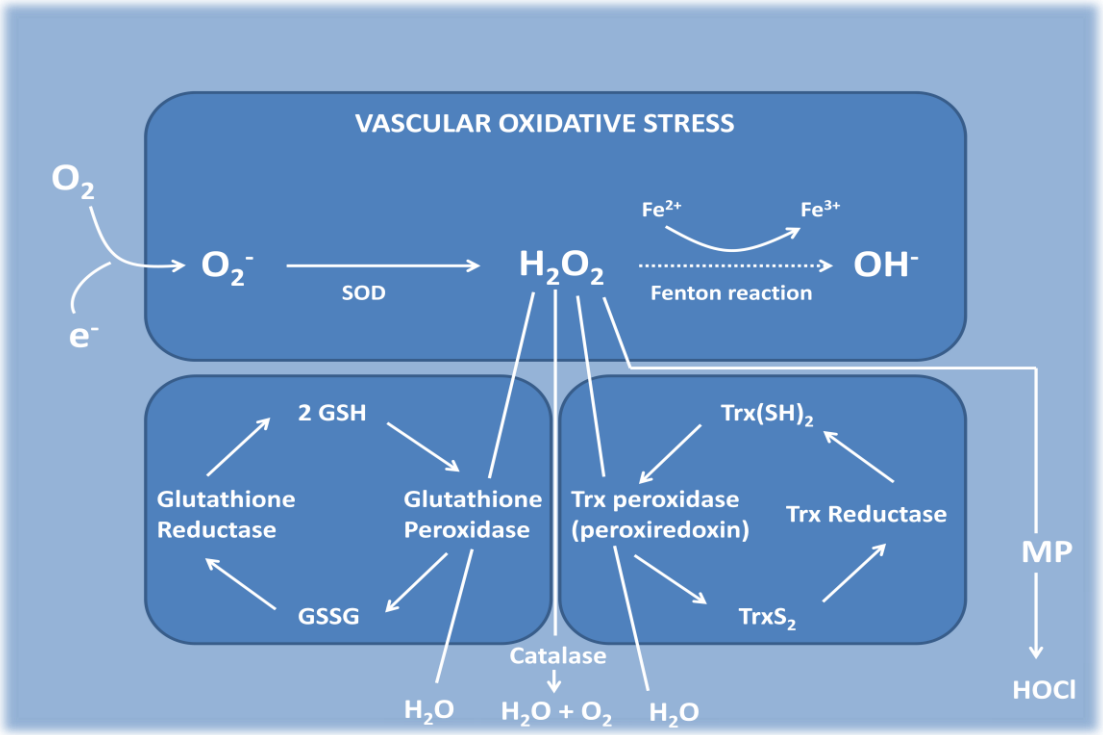

Figure 1.11: Generation and inactivation of ROS. An overproduction of ROS results in vascular oxidative stress. NADPH oxidases, XO, uncoupled eNOS and activated O_2 from mitochondria during oxidative respiration have been implicated as sources of O_2^- in the vascular system. O_2^- is converted to H_2O_2 by superoxide dismutase (SOD). Fenton chemistry propagates the conversion of H_2O_2 to hydroxyl radicals (OH^-) which are very damaging to cells. H_2O_2 can be detoxified by glutathione peroxidase, catalase or peroxiredoxin to H_2O and O_2. Myeloperoxidase (MP) utilises H_2O_2 to oxidise Cl^- to the oxidising agent hypochlorous acid (HOCl) which chlorinates and subsequently deactivates molecules such as L-arginine. MP also has the ability to oxidise NO to nitrite (NO_2^-) in the vascular system. *Adapted* (83).

1.4 NO in the vascular system

1.4.1 Endothelial bioavailability of NO

Extensive production of free radical species results in cell damage, particularly of the vascular endothelium (80). The presence of free radicals can also lead to changes in the vasodilatory capacity of blood vessels since certain radicals (O_2^- in particular) interact rapidly with NO, thus inactivating it.

In the vascular system, NO is one of the most important free radicals, while ROS and other related derivatives of O_2 such as H_2O_2 (which does not possess an unpaired electron) play key roles in oxidant stress. NO and O_2^- radicals have the capacity to instigate oxidant stress and cell damage (84). Importantly, the vascular endothelium produces intracellular O_2^- and H_2O_2 from enzymes such as XO and NADH/NADPH oxidases and has the ability to release these species into the lumen. However, it is not yet apparent whether the endothelial cells produce these radicals constitutively or post-insult, for instance, exposure to cytokines or ischaemia reperfusion. Nevertheless, the equilibrium between the concentrations of NO and O_2^- is pathologically vital (see equation below).

$$\mathbf{O_2^- + NO \rightarrow ONOO^-}$$

An excess of O_2^- leads to vasoconstriction due to the increased formation of the cytotoxic species, peroxynitrite ($ONOO^-$). The latter can oxidise methionine residues and thiol (-SH) groups on cellular proteins and as such, is very damaging to cells (82).

In terms of antioxidant mechanisms in place to deal with O_2^- in particular, SOD enzymes present in the extracellular and intracellular compartments govern the extent of NO/O_2^-

interaction. SOD enzymes all have the capacity to generate H_2O_2 as an end product which can then be further broken down by catalase:

$$O_2^- + O_2^- + 2H^+ \rightarrow H_2O_2 + O_2$$

$$2H_2O_2 \rightarrow 2H_2O + O_2$$

Of course in high concentrations, H_2O_2 is cytotoxic to all cell types and can also react with iron in endothelial cells to produce hydroxyl (OH^-) radicals, causing further cellular damage.

1.4.2 NOS

NOS enzymes were first identified in 1989 and during the early 1990's, three major isoforms of the enzyme were cloned, purified and characterised (85-88). The enzymes are dimers, however once activated, require calmodulin (CaM) binding and therefore adopt a more tetrameric structure (89). NOS enzymes require several essential cofactors for the catalysis of L-arginine to L-citrulline and subsequent liberation of NO (90). These processes are highlighted below (Figure 1.12).

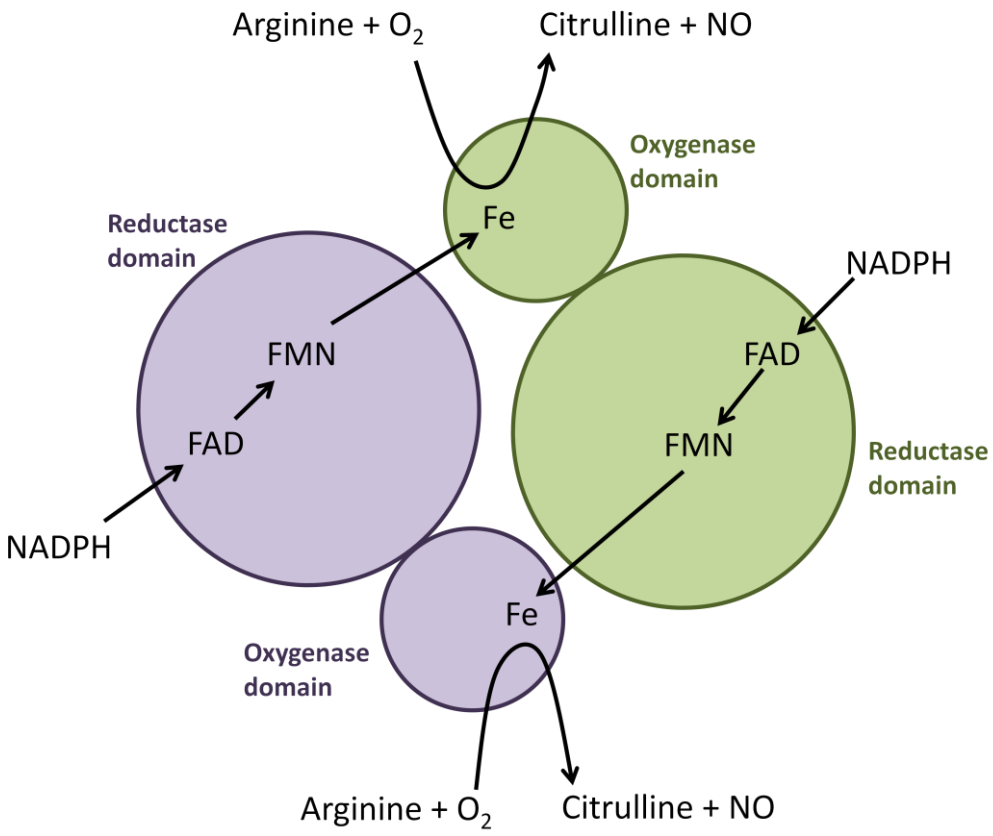

Figure 1.12: Schematic structure of the NOS dimer and overview of cofactor interactions. Electrons (e^-) donated by NADPH to the reductase domain of the enzyme are transported to the oxygenase domain of the enzyme via flavin adenine dinucleotide (FAD) and flavin mononucleotide (FMN). This flow of electrons can only occur in the presence of Ca^{2+}-bound CaM. Once in the oxygenase domain, the electrons interact with the haem iron and tetrahydrobiopterin (BH_4) at the active site of the enzyme to catalyse the reaction of O_2 with L-arginine to release NO. *Adapted (89).*

The three NOS isoforms discovered are: nNOS (neuronal, Type I, NOS-1), iNOS (inducible, Type II, NOS-2) and eNOS (endothelial, Type III, NOS-3) (91). nNOS and eNOS are constitutive and dependent upon the on/off binding nature of Ca^{2+} whereas iNOS is inducible, binding CaM very tightly, rendering the enzyme to long term activation (89). The next section considers the inhibition of these enzymes.

1.4.2.1 Inhibition of NOS

Pharmacological agents can inhibit NO actions by several routes. Arginine-derived analogues such as N^G-monomethyl-L-arginine (L-NMMA) and N^G-nitro-L-arginine methyl

ester (L-NAME) compete with arginine for NOS; such compounds have been useful clinical and *in vitro* tools. The effect of L-NMMA infusion into the body is largely dependent on the route of administration. Infusion into the brachial artery induces vasoconstriction due to the local inhibition of basal NO without influencing systemic blood pressure. However, L-NMMA given intravenously elevates blood pressure and causes vasoconstriction in renal, cerebral, mesenteric and striated muscle resistance vessels (92).

The chemical structures of the main inhibitors of NOS are summarised in Figure 1.13. These compounds show varying degrees of selectivity for the three NOS isoforms and so their use in experimental science needs to be considered.

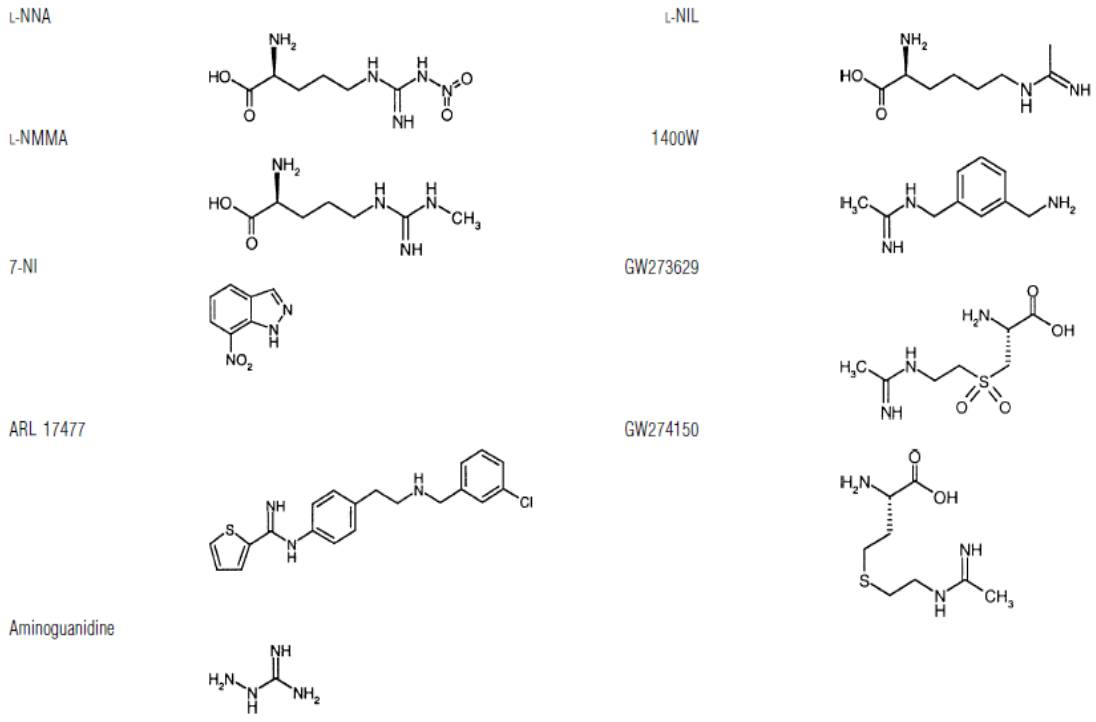

Figure 1.13: Chemical structures of a variety of NOS inhibitors. *Adapted (89).*

1.4.3 NO metabolites

NO is highly reactive and its metabolism can lead to the formation of several by-products within the body. The most frequent reactions of NO are the gain or loss of an

electron, forming NO^- or NO^+, respectively. More specifically, nitrite (NO_2^-), nitrate (NO_3^-) and S-nitrosothiols (RSNO) are metabolites that have been the subjects of particular interest in NO research. These are described in more detail below.

1.4.3.1 NO_2^-

NO_2^- is an inorganic compound found in various foods within our diet including cured and processed meats (93). In terms of the human body, NO_2^- has been implicated in several physiological processes. In 1953, Furchgott demonstrated that sodium nitrite ($NaNO_2$) induced relaxation of rabbit aortic strips (94). However, the concentrations of NO_2^- within these studies (100 µM-1 mM) were not representative of those within the human body (healthy range 100-500 nM). Subsequently, a number of groups have shown that a large dose of inorganic NO_2^- (~3-15 mg/kg body weight) given to spontaneously hypertensive rats lead to a decrease in systemic blood pressure, implying a reduction of NO_2^- to NO (95-97). Interestingly, Tsuchiya and colleagues demonstrated that intake of NO_2^- within the diet lead to rapid increases in nitrosyl haemoglobin (HbNO) levels, again suggestive of systemic conversion of NO_2^- to NO (98).

The oxidoreductase enzyme, XO has been shown to reduce NO_2^- under anaerobic conditions when in the presence of NADH or xanthine as a substrate (99). This was demonstrated by detection of stoichiometric levels of NO versus substrate depletion through ozone based chemiluminescence (OBC).

eNOS is fully functional at a K_m of 6-9 µM O_2. Therefore, when O_2 availability decreases below these levels, usually due to disease such as ischaemic heart disease, eNOS cannot convert L-arginine to L-citrulline and NO. Gautier and colleagues have demonstrated that under anoxic conditions but physiological pH, eNOS can function to reduce NO_2^- to NO

(100). Moreover, this reduction was shown to occur at the oxygenase domain of the enzyme and proceeds independently of BH_4, suggesting a new mechanism for the rapid delivery of NO in hypoxia.

Under such conditions, it is also thought that Hb within RBCs has the capacity to function as a NO_2^- reductase, releasing NO which transiently dilates local vessels, reoxygenating the surrounding tissue (101). Indeed, this process has been implicated as the primary mechanism underlying vascular smooth muscle relaxation in hypoxia (see section 1.9.1.2. for more detail).

1.4.3.2 NO_3^-

NO_3^- is a constituent of leafy green vegetables such as spinach, as well as the root vegetable beetroot (93). Like NO_2^-, NO_3^- has also attracted recent attention in the field of vascular biology. In 2006, Larsen and colleagues conducted a randomised clinical study in which 17 healthy volunteers were administered a 3-day dietary supplementation of sodium nitrate ($NaNO_3$) (0.1 mmol/kg body weight) or NaCl placebo to examine the effects on blood pressure (102). Importantly, decreased diastolic blood pressure was observed in the NO_3^- group suggesting a role for short term NO_3^- supplementation in hypertensive patients. Further investigation by Alhuwalia's group in London in 2008, also demonstrated that a dietary NO_3^- load attenuated endothelial dysfunction caused by an acute ischaemic insult in the human forearm, as well as reduced *ex vivo* platelet aggregation in response to agonists, collagen and adenosine diphosphate (ADP) (103). While mammals themselves do not have the capacity to convert NO_3^- back to NO_2^- and NO, unlike NO_2^-, it has recently been reported that bacteria in the oral microflora possess NO_3^- reductase enzymes which can reduce

saliva-derived NO_3^- to NO_2^- (104). This provides an important additional mechanism of NO production in man.

1.4.3.3 RSNO

RSNOs are formed through the generation of NO^+ or other N-oxides such as dinitrogen trioxide (N_2O_3) (105). RSNOs exert their biological effects by either transnitrosation of NO^+ to various other proteins and also through S-nitrosation of cysteine residues on proteins and can often be dependent on the presence of transition metals and pH (106). S-nitrosation of thiols can have a substantial influence on protein function and subsequent signal transduction (107). To date, an abundance of proteins that can be S-nitrosated have been discovered including heat shock protein 90 (Hsp90) and eNOS (108).

RSNOs have longer half lives than NO and are therefore more stable. It has been proposed that the S-nitrosylation of cysteine thiols signifies a route through which NO can exert its biological effects. Several studies in the late 1990's/early 2000's provided evidence for the existence of protein-linked SNOs in tissue under basal conditions (105, 106, 109-111). More specifically, Mathews and Kerr identified roles for several RSNO compounds in vascular and gastrointestinal smooth muscle relaxation as well as activation of platelet sGC and inhibition of collagen-induced aggregation (112). The study confirmed that the functional group ('R') of each compound affected the potency of relaxation (EC_{50}) in vascular tissue experiments (ranging from 4 nM for S-nitroso-galactopyranose to 220 nM for S-nitroso-N-acetylpenicillamine (SNAP)). Moreover, the biological activity of each compound varied between bioassays, with the order of potency for the compounds being different for each experiment. Collectively, these observations suggest that the functional group can affect both the potency and tissue selectivity of RSNO's.

1.4.4 NO in blood

Once NO leaves endothelial cells, it can either diffuse basally into adjacent smooth muscle cells to bind sGC or apically into the blood vessel lumen. The latter results in NO binding to Hb within RBCs or other interactions with various plasma components as described below.

1.4.4.1 NO in Plasma

Almost all NO in plasma is oxidised to NO_2^-, a compound that is biologically stable for a relatively long period (113, 114):

$$\mathbf{2NO + O_2 \rightarrow 2NO_2^-}$$

$$\mathbf{NO_2^- + NO \rightarrow N_2O_3}$$

The products formed in the equations above are largely hydrolysed into NO_2^- and NO_3^-, respectively.

Much interest has been focussed on the interaction of NO and its metabolites in plasma, with respect to proteins such as albumin (106, 115), which like other proteins possesses a free thiol group that can bind NO to form RSNO (106). Using methods established and characterised in our laboratory, typical values for plasma NO metabolites are displayed in Table 1.2.

Table 1.2: Concentration of NO metabolites in plasma.

Metabolite	Concentration in plasma	Reference
NO_3^-	20-30 μM	(116)
NO_2^-	150-300 nM	(116, 117)
RSNO	10-100 nM	(116, 118)

1.4.4.2 NO in RBCs

Extensive research has now been conducted with regard to the interaction of NO and Hb. The first examination of the conformation, co-operativity and ligand binding of NO with Hb (Fe^{2+}) was by Cassoly in 1975 (119). NO reacts with oxyHb to form metHb and NO_3^- shown by the equation below:

$$\mathbf{HbFe^{2+}O_2 + NO \rightarrow HbFe^{3+}\,(metHb) + NO_3^-}$$

NO also has the capacity to bind to free haem (deoxyHb, T state) to form nitrosylated Hb (HbNO):

$$\mathbf{Fe^{2+} + NO \rightarrow Fe^{2+}NO}$$

The reaction of NO with oxyHb leading to NO_3^- formation ultimately renders NO inactive and is not conducive to preservation of NO bioavailability. However, the interaction of NO with free Hb forms a nitrosylated form of Hb (HbNO) so NO activity can be somewhat preserved (120). HbNO as a source of NO is very controversial due to its long half life in blood (~40 minutes) (121). This prolonged release of NO renders the molecule more susceptible to scavenging by other Hb within the blood.

Both of the reactions described above have been reported to occur at a rate of around 10^7 M^{-1} s^{-1}, which is indeed very rapid (122). However, the dissociation of NO from HbNO is substantially slower, at a rate of around 10^{-5} $M^{-1}s^{-1}$ (123).

In the late 90's, Gow and Stamler published a letter in *Nature* emphasising the importance of Hb allostery in initiating the conversion of T state Hb into the oxygenated R state. This research was driven by the fact that *in vivo*, Hb is only partially nitrosylated (124), whereas earlier studies had only considered the metabolism of fully nitrosylated Hb. It was suggested that partially nitrosylated Hb could release NO upon transition to the R state, which subsequently bind to cysteine residues at position 93 on the β-chain of Hb forming S-nitrosylated Hb (HbSNO) (125). They confirm an 80% formation of HbSNO upon oxygenation under physiological conditions.

It has also been demonstrated that NO_2^- can bind to oxyHb, but this is a slower process than the binding of NO (126). Kosaka *et al* confirmed the equation for the reaction of NO_2^- with oxyHb (127):

$$\mathbf{4HbO_2 + 4NO_2^- + 4H^+ \rightarrow 4Hb^+ + 4NO_3^- + O_2 + 2H_2O}$$

Zavodnik (1999) used metHb formation as a measure of NO_2^- uptake by RBCs and demonstrated that the rates were comparable between RBCs and RBC haemolysates (128). While this suggests that the membrane does not hinder NO_2^- entry into the RBC cytoplasm, the mechanism by which NO_2^- enters the RBC is yet to be fully elucidated. To this end, a stopped-flow spectrofluorometric study conducted by Shingles *et al* demonstrated that NO_2^- efflux in RBC ghosts (intact membrane post-haemolysis) was inhibited by 4,4'-diisothiocyano-2,2'-stilbenedisulphonic acid (DIDS), which is a specific inhibitor of anion

exchanger 1 (AE-1) found in the RBC membrane (129). This suggests that there may be a need for a specific transporter for NO_2^- to cross the cell membrane.

Doyle and colleagues illustrate that the reaction of NO_2^- with deoxyHb is multifaceted (130). A series of equations were formulated to describe how this interaction is dependent upon pH and nitrous acid formation (HONO):

$$H^+ + NO_2^- \rightleftharpoons HONO$$

$$Hb + HONO \longrightarrow metHb + NO + OH^-$$

$$Hb + NO \longrightarrow HbNO$$

$$Hb + NO_2^- \longrightarrow metHb + NO_2^{2-}$$

The product of NO_2^- reduction shown in red is predicted to produce NO and H_2O in a subsequent reaction (130) and could therefore have a significant role in the control of vascular tone.

Using methods established and characterised in our laboratory, typical total NO metabolites within RBC is ~ 100-250nM, with around 30-60nM being NO_2^-.

1.5 Control of vascular tone

1.5.1 Regulation of tone

1.5.1.1 Myogenic response

In 1902, Sir William Bayliss discovered the myogenic response ('Bayliss effect') in the vasculature (131). This effect is simply the response of the vascular smooth muscle cells to a stretch stimulus that is independent of neuronal influences. *In vivo*, this would involve

vasoconstriction in response to an increase in blood pressure and equally, a vasodilatory response to a reduction in pressure (132). In arteries and veins, the force generated by myogenic tone is not substantial enough to significantly affect the diameter of the vessel however, arteriolar diameter is considerably reduced (132).

1.5.1.2 Contractile response

Vascular smooth muscle is one of 6 types of smooth muscle found in the body (vascular, respiratory, urinary, reproductive, gastrointestinal and ocular) (133). Unlike skeletal and cardiac muscle, smooth muscle is not striated in appearance and can be innervated by the autonomic nervous system. Contraction of smooth muscle is controlled by local paracrine/autocrine messengers as well as secreted hormones (92). In addition to this, smooth muscle can also develop contractions in response to changes in load or length. Regardless of the stimulus for contraction, contractile force by smooth muscle cells is generated through formation of actin-myosin cross bridges, utilising Ca^{2+} ions as the initiating driver. Changes in membrane potential in response to action potentials or activation of stretch-sensitive ion channels can also bring about smooth muscle contraction.

All muscle contraction relies on an increase in extracellular Ca^{2+}. In smooth muscle however, the process is not solely dependent on changes in membrane potential. Agonists such as phenylephrine activate the phosphatidylinositol cascade to cause an increase of Ca^{2+} release from the SR. This rise in intracellular Ca^{2+} enhances the binding to CaM and subsequent activation of MLCK to phosphorylate the MLC of myosin II (134). The degree at which MLC is phosphorylated determines the extent of smooth muscle contraction; dephosphorylation therefore leads to relaxation of smooth muscle.

1.5.1.3 Ca^{2+}

As mentioned above, a rise in intracellular Ca^{2+} triggers the mechanisms which generate smooth muscle cell contraction. Activation of the Ca^{2+}/calmodulin complex leads to the activation of myosin light chain kinase (MLCK). Phosphorylation of myosin light chain (MLC) renders the chains more sensitive to Ca^{2+}, allowing for the initiation of contraction even if Ca^{2+} is lacking. Cross bridge formation in smooth muscle involves the association and disassociation of ATP to myosin heads, leading to the sliding movement of actin filaments (135) (Figure 1.14).

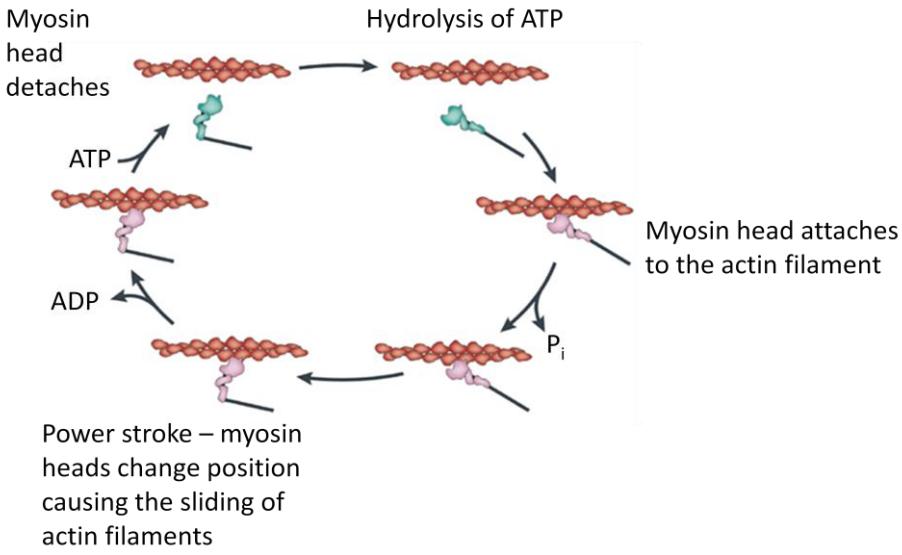

Figure 1.14: Actin-myosin cross bridge formation involved in mechanical contraction of smooth muscle. ADP and inorganic phosphate (P_i) are liberated following each working stroke. *Adapted (136).*

Levels of intracellular Ca^{2+} are tightly controlled despite extremely high extracellular concentrations of Ca^{2+}. Vascular smooth muscle contracts due to a net influx of Ca^{2+} as a result of inositol 1,4,5-trisphosphate (IP_3) induced release from the SR (137, 138).

Several mechanisms are involved in Ca^{2+} influx such as voltage-dependent L-type Ca^{2+} channels, the reverse mode of the Na^{+}/Ca^{2+} exchanger and non-selective cation channels. On the other hand, Ca^{2+} efflux from intracellular stores occurs via IP_3-regulated channels or by Ca^{2+}-induced Ca^{2+} release, regulated by ryanodine receptor-regulated channels (139).

1.5.1.4 Rho Signalling

The GTPase, Rho, has also been implicated in the mechanism of smooth muscle contraction. Importantly, the interaction of Rho with Rho kinase has been shown to be Ca^{2+}-independent, modulating the degree of phosphorylation of MLC of myosin II by inhibiting myosin phosphatase. This has been shown to contribute to agonist-induced Ca^{2+}-sensitisation in smooth muscle contraction (140).

Two signalling pathways have been implicated in the inhibition of myosin phosphatase. The first of which involves the phosphorylation of regulatory subunit, MYPT1 at Thr696 and Thr853 via $G_{12/13}$/Rho-Rho kinase pathway. Phosphorylation at both of these residues has been shown to suppress phosphatase activity. The second mechanism involves the phosphorylation of smooth muscle-specific myosin phosphatase inhibitor protein, CPI-17. Specifically, the phosphorylation at Thr38 enhances the inhibitory effect of CPI-17 on myosin phosphatase by 1000-fold. (141).

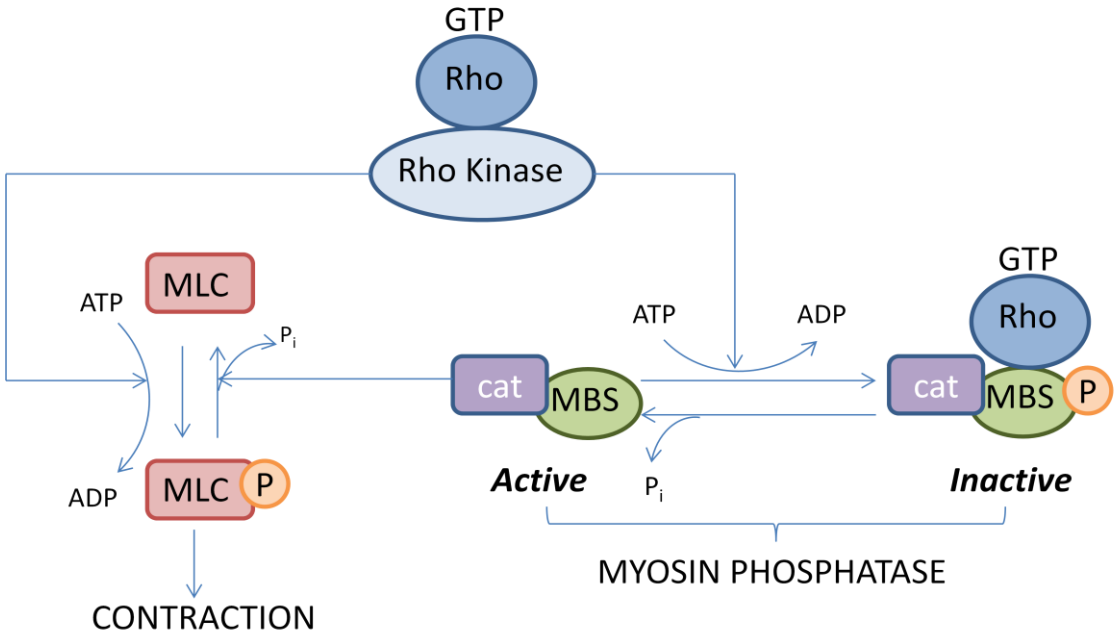

Figure 1.15: Summary of Rho-mediated smooth muscle contraction. Agonists that also stimulate G_q-linked increases in Ca^{2+} can stimulate Rho activity. Rho, which is activated by the binding of guanosine triphosphate (GTP), activates Rho kinase which in turn, phosphorylates the myosin binding subunit (MBS) of myosin phosphatase, inhibiting its activity. Rho kinase also has the ability to phosphorylate the myosin light chain (MLC) directly, mediating further contraction. *Adapted (140).*

1.6 Endothelium-dependent smooth muscle relaxation

1.6.1.1 NO-mediated smooth muscle relaxation

NO is a relatively inert diatomic gas and has the ability to diffuse through the phospholipid bilayer of cell membranes where it then forms a nitrosyl complex with the haem of sGC in the cytosol. Very small amounts of NO (nM) are required to fully activate sGC in this environment, which in turn promotes the conversion of guanosine triphosphate (GTP) to cyclic guanosine monophosphate (cGMP) (142). Interestingly, a study by Mergia and colleagues (2006) demonstrated that the α_2 isoform of guanylate cyclase (GC), which represents only 6 % of total GC within mouse aortic tissue, could elicit a full biological response albeit at higher concentrations of NO (143). This study suggested that in fact most

guanylate cyclase NO 'receptors' function as spare receptors which increase sensitivity to NO *in vivo*. In addition, the large pool of unbound GC (not bound to primary ligand, NO) could advocate a secondary mechanism of GC stimulation/activation.

The mechanism by which endogenous NO induces endothelium-derived smooth muscle relaxation is illustrated in Figure 1.16.

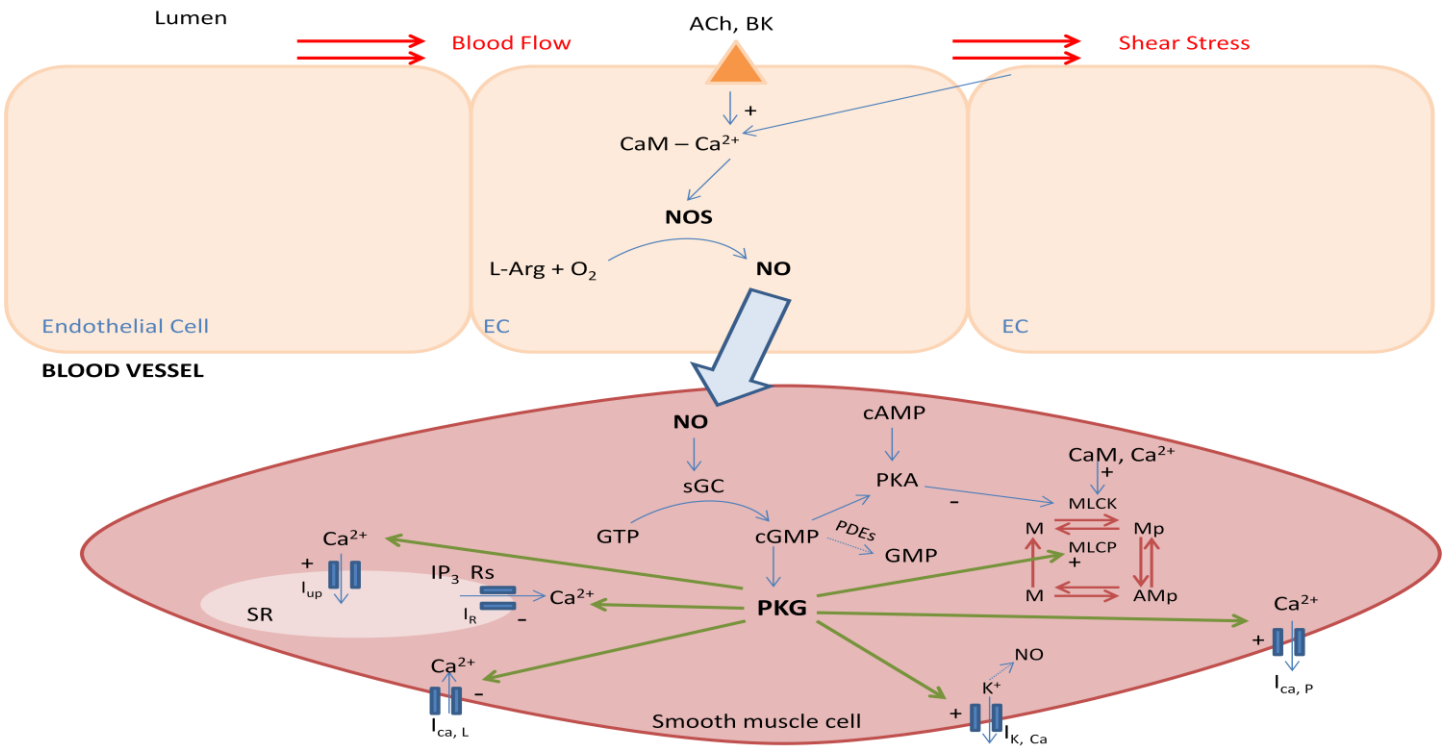

Figure 1.16: Endothelium-mediated smooth muscle relaxation via the NO-cGMP signalling pathway. NO is synthesised in endothelial cells by the conversion of L-arginine to L-citrulline in response to shear stress or receptor-mediated activation. NO diffuses across the endothelial cell membrane into adjacent smooth muscle cells where it binds and activates sGC, increasing intracellular levels of cGMP from GTP. cGMP activates cGMP-dependent protein kinase G (PKG), which in turn regulates a number of important proteins such as Ca^{2+} activated K^{+} channels, L-type Ca^{2+} channels, Ca^{2+}-ATPase pump and MLCP, leading to a fall in the intracellular Ca^{2+} concentration and smooth muscle relaxation. cGMP is degraded by phosphodiesterases (PDEs) into guanosine monophosphate (GMP). Endothelial cells are connected to smooth muscle cells by myoendothelial gap junctions. *Adapted (144).*

1.6.1.2 Prostacyclin (PGI_2)

Eicosanoid, PGI_2, is one of the main products of arachidonic acid (AA) metabolism. Various enzymes are involved in the production of PGI_2 as illustrated in Figure 1.17. Metabolite 6-keto $PGF_{1\alpha}$ is a product of PGI_2 hydrolysis and has subsequently been used in several studies as an index of PGI_2 production (145-147).

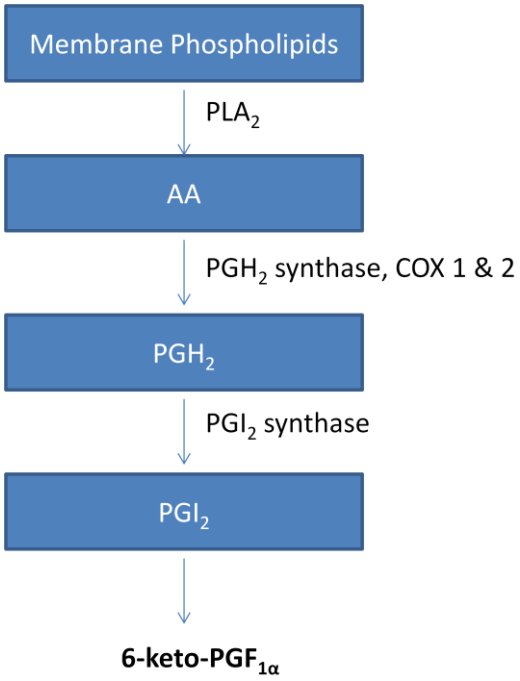

Figure 1.17: PGI_2 production. Phospholipase A_2 (PLA_2) releases AA directly from membrane phospholipids. Prostaglandin H_2 (PGH_2) synthase and cyclooxygenase (COX) 1 and 2 catalyse the conversion of AA to PGH_2 and subsequently PGI_2. Unstable PGI_2 has the capacity to spontaneously hydrolyse into the stable product, 6-keto $PGF_{1\alpha}$. *Adapted (148).*

PGI_2 functions in a similar manner to NO, preventing platelet plug formation and inducing vascular smooth muscle relaxation. However, PGI_2 induces these effects by stimulating the enzyme adenylate cyclase (AC) which in turn, stimulates a rise in the second messenger, cyclic adenosine monophosphate (cAMP) (148).

1.6.1.1 Endothelium-derived hyperpolarising factor (EDHF)

Vascular smooth muscle relaxation may also be elicited following the release of endothelium-derived hyperpolarising factor (EDHF) (Figure 1.18). While this mediator is not fully characterised, there are many suggestions as to its identity including CO and hydrogen sulphide (H_2S), as well as H_2O_2, cytochrome P450 products such as the epoxyeicosatrienoic acids (EETs), the vasodilator peptide, C-type natriuretic peptide and small increases in extracellular K^+ resulting from the opening of endothelial cell intermediate conductance calcium activated potassium channel (IKCa) and small conductance (SKCa) channels (149). In addition to the uncertainty of the mediator(s) involved in this phenomenon, the mechanism of action by which EDHF exerts its effects has also been extensively researched. Griffith and colleagues made a significant contribution to the field of EDHF and myoendothelial gap junction communication (150-154). The observations that endothelial hyperpolarisation depends on the opening of K_{Ca} channels and its subsequent travel through myoendothelial gap junctions contrasts with the idea above that EDHF-type relaxations are mediated by a freely transferable entity that activates smooth muscle K_{Ca} channels such as EETs (152). Further investigation into the morphology of myoendothelial gap junctions have shown their differences from homocellular gap junction and hypotheses suggested that two junctions border each smooth muscle cell in small arteries and thus contribute to the increased sensitivity of these cells to hyperpolarising stimuli (155).

Hyperpolarisation of the plasma membrane is resistant to inhibitors of COX and NOS and thus does not lead to an increase in cyclic second messengers such as cAMP or cGMP (156). EDHF-mediated vasorelaxation is likely to occur in small, resistance vessels (157)

however, in coronary and renal vascular beds, EDHF can also exert its effects in conduit vessels (158).

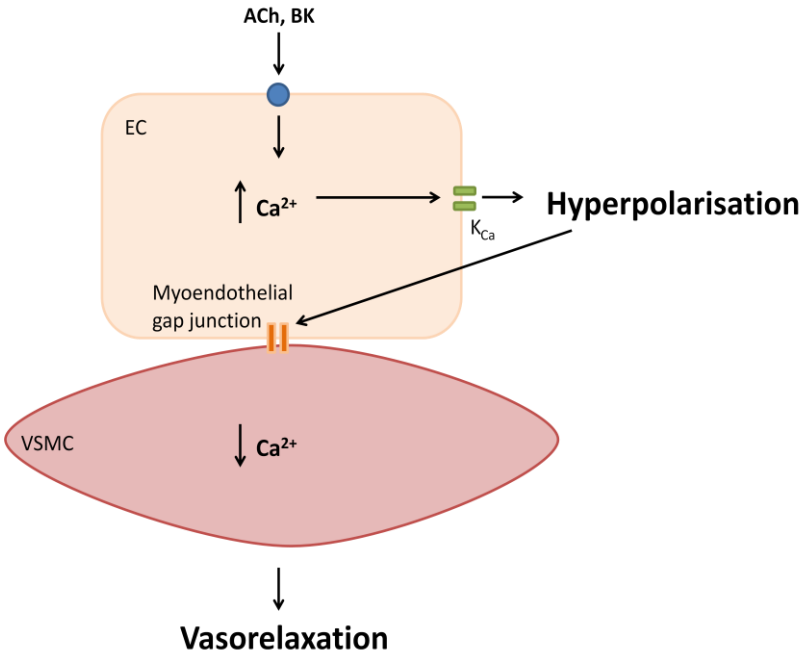

Figure 1.18: The EDHF response. Binding of agonists such as acetylcholine (ACh) and bradykinin (BK) to the endothelium stimulates a rise in intracellular Ca^{2+}, leading to membrane hyperpolarisation. This hyperpolarisation in turn, spreads through to the vascular smooth muscle and leads to a decrease in intracellular Ca^{2+} and vasorelaxation. Vascular smooth muscle cell (*VSMC); endothelial cell (EC). Adapted (159).*

1.7 Endothelium-independent smooth muscle relaxation

As previously mentioned in section 1.6.1.1, endothelium-derived NO can diffuse across the endothelial cell membrane into neighbouring smooth muscle cells to stimulate sGC. However, sGC can also be stimulated directly within the smooth muscle by exogenous NO derived from a range of NO donating compounds.

1.7.1 NO donors & mimetics

In pathophysiology, NO bioavailability is often reduced. The processes outlined in section 1.4.1 describe how oxidative stress can affect NO bioavailability, leading to impaired

vasorelaxation. Endothelial dysfunction is a main factor in cardiovascular diseases such as atherosclerosis, hypertension and coronary artery disease (160). Compounds such as organic nitrates have been used as therapies to treat these diseases however issues such as tolerance and adverse effects due to their metabolism, initiated the search for improved alternatives (160). There is also a question as to whether compounds such as glyceryl trinitrate (GTN) or isosorbide dinitrate (ISDN) actually release NO or a related species to induce relaxation. Alternative NO donors have been developed (NONOates, SNO) which improve the therapeutic half-life and reduce tolerance in patients (161). These drugs can spontaneously release NO (direct NO donors) forming species such as NO^+, NO^- or $NO^\bullet$.

Direct NO donors tend to contain either a nitroso or nitrosyl functional group within their chemical structure. Three of the most common types are NO gas, sodium trioxodinitrate (Angeli's salt) and sodium nitroprusside (SNP). NO gas is freely soluble but has a very short half life *in vivo* (3-5 s (162)) and is highly reactive with molecular O_2. In therapeutic terms, NO gas has been used in clinical practise to treat pulmonary vascular disease, especially persistent pulmonary hypertension of the newborn (PPHN) (163). However, in most cases such therapy has been rendered unsuitable due to the nature of NO and its biochemical properties (164).

The group of compounds known as the diazeniumdiolate ions (Figure 1.19) or NONOates spontaneously donate NO under physiological pH conditions, with half lives ranging from 2 seconds to 20 hours depending on their chemical structure (165). This makes them ideal for controlled release of NO under tight experimental conditions.

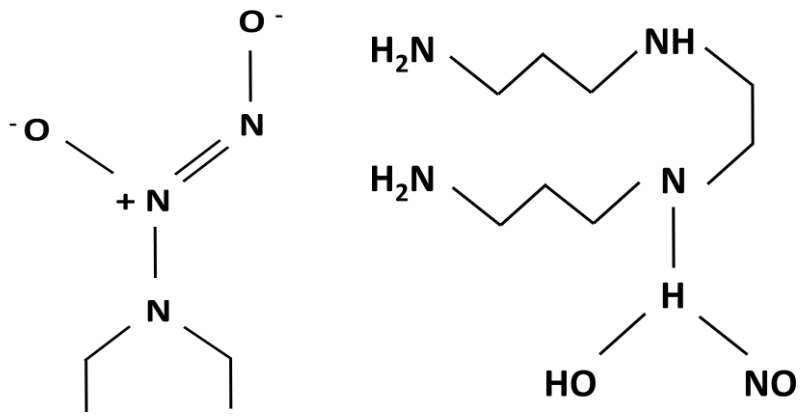

Figure 1.19: Examples of direct NO donor compounds. Left – diethylamino (DEA [N(O)NO]) NONOate, right – Spermine NONOate. *Adapted (160).*

NO donor drugs such as SNO (Figure 1.20 and section 1.4.3.3) have advantages over other similar drugs due to the limited development of tolerance *in vivo*. These compounds are also naturally occurring and in reality release NO^+. Evidence suggests that they are transported into the intracellular compartment through plasma membrane-bound disulphide isomerise and related transnitrosation reactions (166).

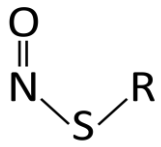

Figure 1.20: SNO structure. Members of the SNO class of compounds include SNO-glutathione, SNO-albumin and SNAP. *Adapted (160).*

1.8 Soluble Guanylate Cyclase (sGC)

1.8.1 Structure

In mammals, sGC is expressed in the cytoplasm of most cell types and was first purified in the early 1980's from bovine lung (167, 168). It is an αβ heterodimer, the molecular weight reported as ~72-80 kDa for the α subunits and ~70 kDa for the β subunits (169). A total of four polypeptides have been characterised to date: α_1, α_2, β_1 and β_2 (170). sGC also

possesses a haem moiety which is bound to the N-terminal region of the β chain. Catalytic regions of the enzyme consist of components originating from both the α and β subunits and reside within the C-terminus. These can also be found in the membrane bound particulate guanylate cyclase (pGC), as well as AC (171). The α and β subunits of sGC also possess a predicted Per/Arnt/Sim (PAS)-like domain, as well as a putative amphipathic helix (172).

Although the enzyme has been purified from tissues of various species for many years, the crystal structure of the whole enzyme is yet to be completed. To this end, much focus has been centred on the development of bacterial expression systems for haem and catalytic domains of sGC (173-176). Moreover, rat β_1 and β_2 homodimers have also been expressed and completely characterised in *Escherichia coli* (177). While the catalytic domain of the αβ heterodimer has also been expressed, the haem domain has been of considerable interest due to its NO binding capacity. Figure 1.21 illustrates the main crystal structure of the haem binding domain of sGC.

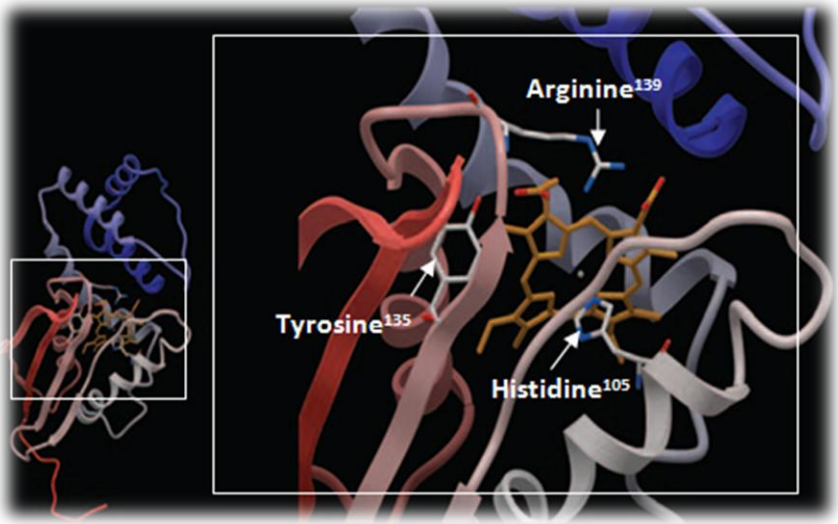

Figure 1.21: Crystal structure of the haem binding domain of human sGC. The enlarged image highlights the three main residues within the haem-binding motif. *Adapted (178).*

1.8.1.1 NO binding

The primary role of sGC is to act as an NO sensor (179). Investigation by Buechler *et al* confirmed that both α_1 and β_1 subunits are required for basal enzyme activity as well as activation by NO (180). This was determined through the deletion of the N-terminal sequence of either the α_1 or β_1 subunits. Deletions of the β subunit lead to a loss of sensitivity to NO whereas deletion of the α subunit did not alter the response to NO. However, the binding of the haem moiety to the enzyme requires the presence of both subunits, illustrating the importance of the α_1 subunit in haem-related processes such as activation (181). Specific investigation into the location of the haem binding region of the enzyme established that the N-terminus of the β_1 subunit (approximately 190 amino acids) was imperative for NO binding. Moreover, residue Histidine105 was revealed to be the proximal haem ligand for the enzyme, allowing for full enzymatic activation by NO (182).

Evidence from Electron Paramagnetic Resonance (EPR) spectroscopy determined that NO binds to the haem moiety of sGC forming a 6-coordinate nitrosyl complex which then breaks to form a 5-coordinate complex through two different means (183, 184). Figure 1.22 shows the model proposed by Stone and Marletta for NO-sGC binding. The model suggests that ~28 % of the haem is converted rapidly to the 5-coordinate complex whereas the remaining haem is converted slowly to the 5-coordinate species and is dependent upon the interaction of NO with a non-haem site.

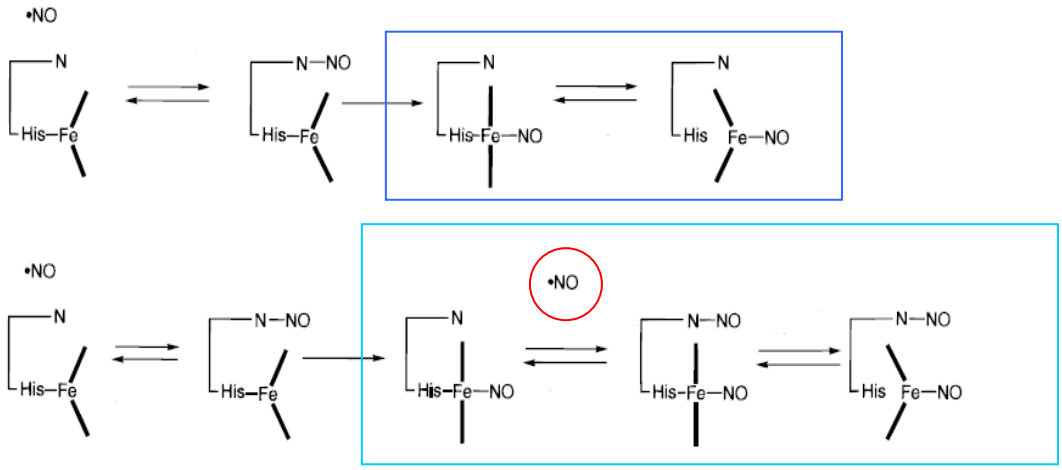

Figure 1.22: Mechanism for NO binding to sGC. This model suggests that NO binding to the enzyme has both a haem-dependent binding site as well as a haem-independent site. Both the top and bottom diagrams show that the initial relocation of NO to the haem is an irreversible reaction. The top mechanism illustrates the binding nature of 28% of haem, whereby there is a quick transition from the 6-coordinate nitrosyl complex to the 5-coordinate complex. The remaining 72% is a much slower process, requiring yet more NO to interact with a non-haem site. *Adapted (184).*

Recent research by Tsai and colleagues has investigated the subsequent binding of further NO molecules, in particular, the second NO to associate with the enzyme. They conducted an EPR study using two isotopes of NO, ^{14}NO and ^{15}NO, to establish whether the haem iron is the site at which the second NO binds. Bioinformatics was used to confirm that the second NO binds at a different site to the first and that this binding occurs simultaneously with the dissociation of the proximal His-105 ligand (185). This work provided evidence for the formation of the 5-coordinate species *after* the binding of the second NO to the enzyme.

1.8.2 NO-independent stimulation of sGC

1.8.2.1 Carbon monoxide (CO) binding

CO is mainly produced by the initial cleavage of haem into CO and biliverdin by HO (186). Two forms of HO exist, the oxidative stress-inducible protein (HO-1) and the constitutive isoform, HO-2 (187).

CO has a high affinity for sGC and binds in the same way as NO, to the prosthetic haem moiety (188). CO binding however, only catalyses a 4 to 6-fold activation of purified sGC and therefore deemed as a relatively poor activator of the enzyme (181, 188). The binding of CO is thought to form only a 6-coordinate species and thus no disruption to the histidine-iron (His-Fe) bond. Since the breakage of this bond is thought to be crucial in how sGC is activated, Kharitonov *et al* and Deinum *et al* suggested that a 5-coordinate intermediate may be formed when CO dissociates from the enzyme which closely resembles the nitrosyl-haem complex (189, 190) allowing the observed 4-fold activation of the enzyme.

1.8.2.2 Synthetic activators/stimulators

As mentioned in section 1.7.1, patients receiving various compounds which donate NO and other organic nitrates have been found to develop tolerance to these drugs following chronic use. This required the development of new pharmacological compounds which reduce these effects. In particular, the German pharma company, Bayer, have developed several compounds which activate/stimulate sGC and are either dependent or independent of NO, some of which are commercially available. YC-1, BAY 41-2272 and BAY 60-2770 discussed in more detail in section 4.1.2.

In addition, compound A-350619 (Figure 1.23, top left) was also found to activate sGC. Studies conducted on this activator in combination with YC-1, revealed that A-350619 would likely share the same binding site (191). Interestingly, the activation of sGC by A-350619 was only partially inhibited by [1*H*-[1,2,4]oxadiazolo-[4,3-*a*]quinoxalin-1-one] (ODQ), suggesting that this compound has the ability to activate sGC via an allosteric site. Protoporphyrin IX (Figure 1.23, top right) has also been reported to activate the sGC (176, 192, 193) in a haem-independent manner (194, 195). Both haem and protoporphyrin IX bind to an identical site

on the enzyme (196). Data on HMR-1766 (Ataciguat) Figure 1.23, bottom left) was initially published in 2004 and was planned as a treatment for cardiovascular disease associated with either oxidative stress (197) or pulmonary hypertension (198). It specifically binds to the oxidised form (Fe^{3+}) of sGC (199). However, there has still not been any extensive investigation into the role of this compound clinically. The development of compound, CFM-1571 (Figure 1.23, bottom right) was based on the structure of YC-1 (178). It displays a weak activation of sGC but effectively synergises with NO to fully activate the enzyme (200).

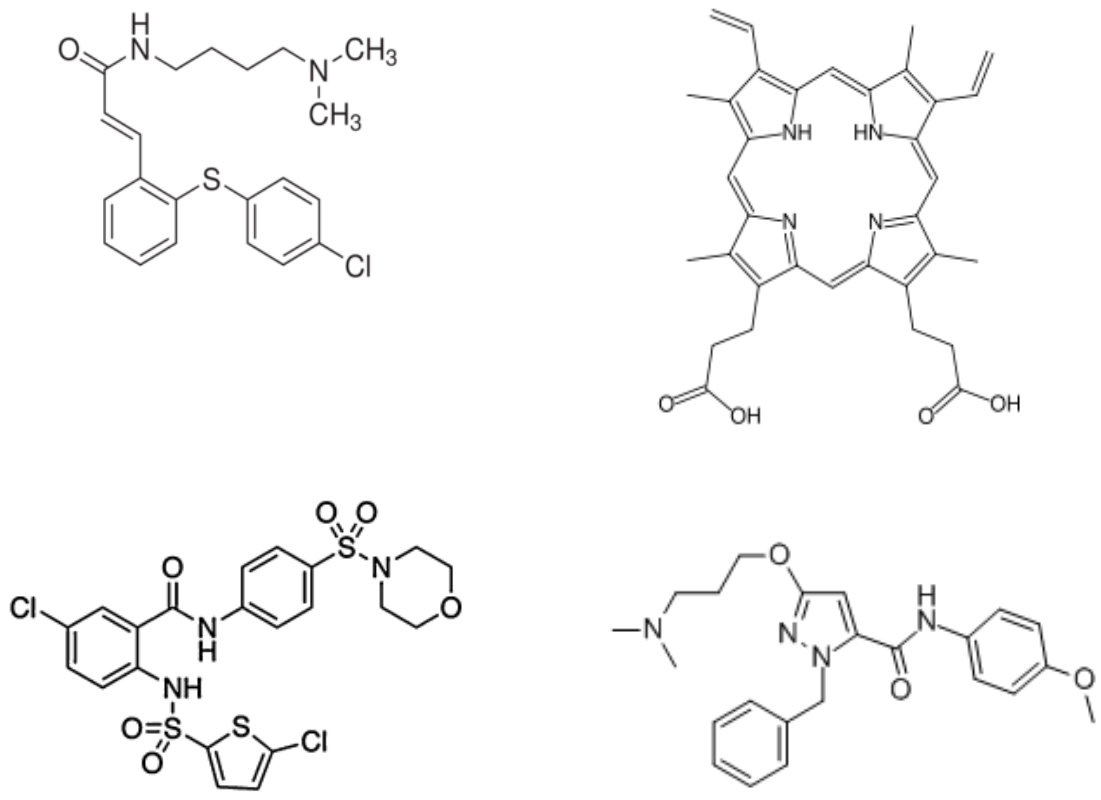

Figure 1.23: Structures of sGC activators. A-250619 (top left), protoporphyrin IX (top right), Ataciguat (bottom left) and CFM-1571 (bottom right). *Adapted (178, 199, 201).*

The activators and inhibitors described above have the ability to stimulate the enzyme in either a haem dependent/independent manner and in the absence/presence of NO. This thesis aimed to reveal whether sGC could be directly affected by O_2 to initiate relaxation of vascular smooth muscle. The binding of O_2 in sGC has been a topic of debate in this field and will be now introduced in more detail in section 1.8.2.3.

1.8.2.3 O_2 binding?

Using various spectral techniques Marletta's group have presented data to suggest that O_2 does not bind to human sGC (174, 192, 202, 203). Indeed the ligand discrimination between NO and O_2 by sGC has been thought to evolve due to the high O_2 concentrations (µM) in the body in contrast to lower NO concentrations (nM) (204). However, a particular subunit of sGC in the nematode, *Caenorhabditis elegans*, has been shown to have a haem binding domain that has the capacity to form a complex with O_2 (173). In addition to this, sGC of the bacterium, *Thermoanaerobacter tengcongensis*, exhibits high affinities for both diatoms, perhaps playing a role in O_2 sensing. Subsequently, the presence of a Tyrosine-140 residue in the haem pocket of sGC has been identified as an essential component for successful O_2 binding (205, 206). Domains such as these which can function as an isolated protein have now been termed the 'haem-nitric oxide and O_2 binding' cohort (H-NOX). It is thought that mammalian sGC as opposed to bacterial sGC does not contain this residue in the haem pocket therefore limiting O_2 binding.

In 2007, Marletta's group published evidence that the insect, *Drosophila melanogaster*, possessed an O_2-binding haemoprotein called Gyc-88E that could also bind NO and CO (207). These properties were found to be unique to GCs and may underlie a possible O_2-sensing role in *Drosophila.* More recently, a study on sGC purified from bovine lung, conducted by researchers in Japan demonstrated that when frozen at 77 Kelvin (-196.15 °C), the high spin haem of the ferrous enzyme (Fe^{2+}) converted to a low spin oxyhaem (Fe^{2+}-O_2). This ligation was confirmed using EPR spectroscopy with a cobalt-substituted enzyme (208). The O_2-binding form of the enzyme could also be produced under solutions maintained at -7 °C (266.15 Kelvin) however; O_2 was shown to have a low enzyme

affinity in conformational studies by x-ray absorption due to the weak formation of the His-Fe bond. This therefore illustrates that the formation of an O_2-sGC species can be formed even though the affinity for this gas is relatively weak.

1.8.3 S-nitrosation/nitrosylation

Recently, there has been much interest in s-nitrosation of sGC. The use of organic nitrates such as GTN and donor compounds such as SNOs to stimulate relaxation via the sGC/cGMP pathway is widespread. However, as explained in section 1.7.1, the use of GTN in patients has led to NO_3^- tolerance. Interestingly, Beuve and colleagues demonstrate that *in vivo*, NO_3^- tolerance is partly mediated by the desensitisation of sGC through GTN-dependent S-nitrosylation (209).

NO has the capacity to bind to sGC in the Fe^{2+} ferrous state to produce cGMP. However, sGC is desensitised to NO when the haem iron is oxidised to the Fe^{3+} state and this facet has since emerged as a potential therapeutic target for cardiovascular related disease. Within this setting, Fernhoff and colleagues provide evidence that the reductive S-nitrosylation of sGC is linked to the S-nitrosation of cysteines within the protein (210). Furthermore, the SNO formation occurs at cysteines 78 and 122 on the sGC β_1 subunit, rendering the enzyme desensitised to NO.

1.8.4 Inhibitors of sGC

Inhibitors of sGC have been used extensively as tools for examining the role of the enzyme in specific events. One of the main inhibitors used is ODQ (Figure 1.24, top left). When isolated, sGC possesses a Fe^{3+} haem moiety which is a 5-coordinate species, as previously reported in section 1.8.1.1. In the presence of ODQ, the Soret peak

(spectroscopy) shifts from 431 nm to 392 nm which subsequently leads to a reduction in NO-induced enzyme activity (211-213). The shift in Soret band is in agreement with oxidation of the ferrous haem to Fe^{3+}. Zhao and colleagues also confirmed that ODQ in fact inhibited other haem-containing proteins through oxidation, using Hb as an example (211).

6-anilino-5,8-quinolinedione (LY-83583) (Figure 1.24, top right) has also been used to inhibit sGC (214). Mülsch and colleagues discovered that LY-83583 could inhibit sGC activity in a purified enzyme assay, as well as inhibit endothelium-dependent relaxation in rabbit aortic strips in response to ACh or calcium ionophore A23187 (214).

Methylene blue (Figure 1.24, bottom) has been used over a number of years to inhibit sGC (215, 216). However, the use of methylene blue has also presented an issue due to the production of O_2^- radicals which of course can have a damaging affect to cells and tissues (217). More recently, the use of methylene blue as an inhibitor of sGC has diminished due to its indirect effects, including the inhibition of NOS (218). Methylene blue is therefore thought of as an unspecific inhibitor of sGC which is potentially less potent than first assumed.

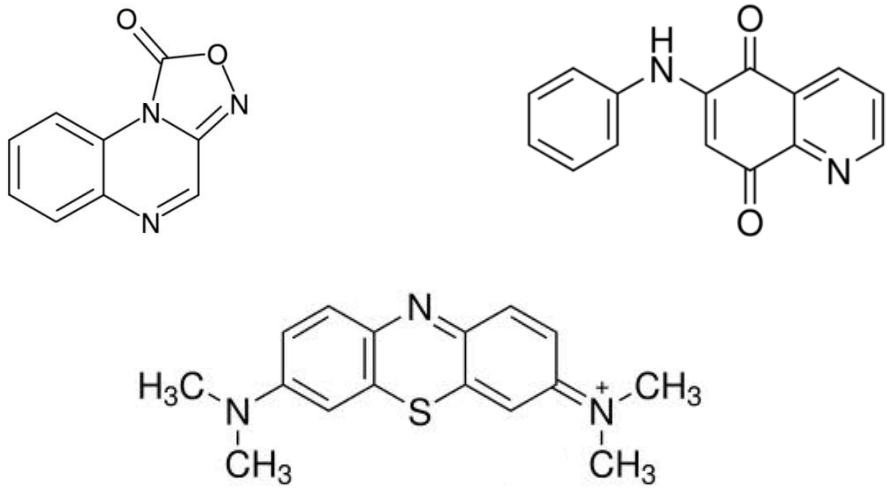

Figure 1.24: Structures of sGC inhibitors. ODQ (top left), LY-83583 (top right) and methylene blue (bottom). *Adapted (201).*

1.8.5 cGMP

The identification of cGMP was made after the discovery of cAMP in the late 1950's (219). Since then, an abundance of studies have aimed to characterise the role of cGMP within the cardiovascular system.

The main outcome of endothelial dysfunction is the decreased bioavailability of NO. It has been suggested that when the NO-sGC-cGMP pathway has been compromised, cGMP production via natriuretic peptides could supplement this reduced activity (220). Figure 1.25 highlights the broad spectrum of physiological effects arising from increased cGMP production.

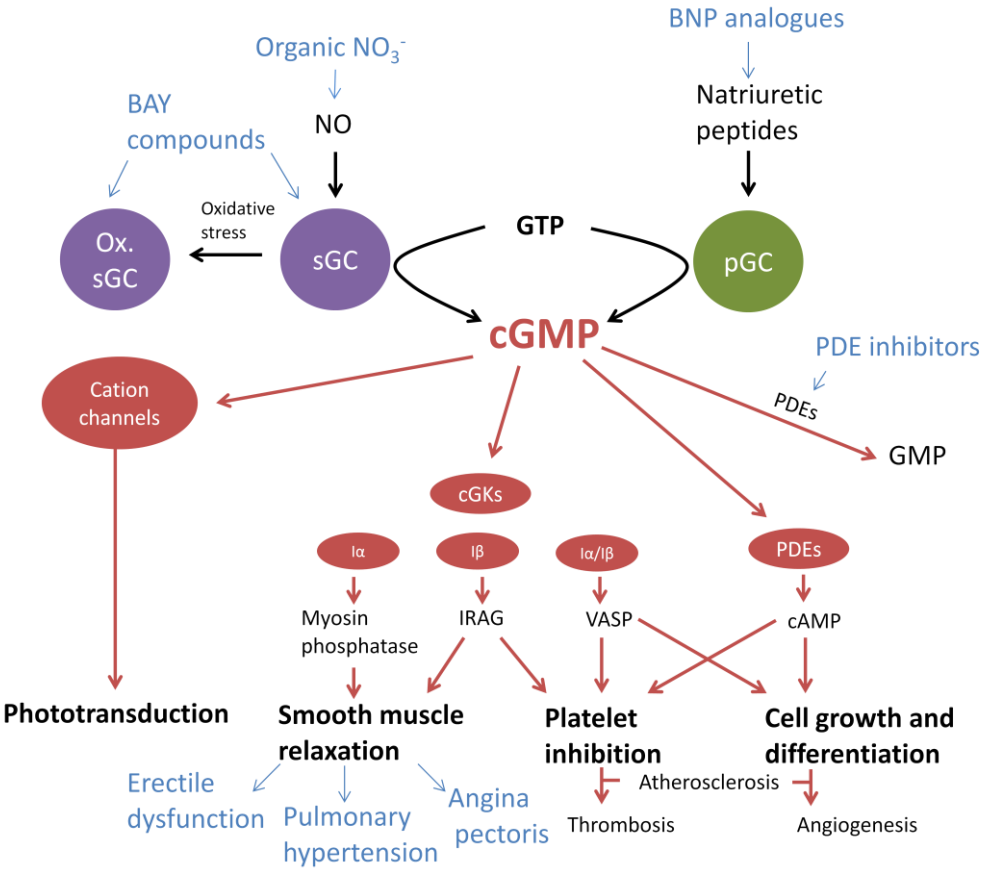

Figure 1.25: Summary of the cGMP signalling pathway. BNP: B-type Natriuretic peptide; IRAG: IP3 receptor associated cGKIβ substrate; VASP: vasodilator-stimulated phosphoprotein. The BAY compounds in blue target the NO binding site of sGC, leading to an elevation in cGMP production. *Adapted (221).*

1.8.5.1 cGMP-dependent protein kinases

Three types of cGMP-dependent protein kinases have been acknowledged in mammals: cGK type Iα (cGKIα) and cGK type Iβ (both found within the cytosol) and cGK type II (cGKII) which is membrane bound. In terms of cardiovascular function, the cGKI subtype is of great importance as this mediates the responses subsequent to elevations in cGMP (222).

Investigations into the role of cGKI in vascular regulation led to the development of cGKIα mutant mice. Due to the mutant genotype, these mice were unable to utilise the enzyme myosin phosphatase efficiently, leading to impaired vascular smooth muscle cell

growth. With this evidence, it was therefore acceptable to conclude that cGKIα has the ability to dilate blood vessels through vascular smooth muscle cell myosin phosphatase activity (221).

Research into cGKIβ proposed a specific communication with inositol 1, 4, 5-triphosphate receptor I associated protein (IRAG), consequentially inhibiting intracellular Ca^{2+} release. Data from a mouse model expressing mutant IRAG that therefore could not interact with the IP_3 receptor illustrated little relaxation of the aorta. Interestingly, mice with the dysfunctional IRAG did not develop hypertension, highlighting the significance of the cGKIβ-IRAG-Ca^{2+} pathway in smooth muscle function and not blood pressure regulation (223).

Furthermore, IRAG has been shown to be implicated in the anti-platelet function of exogenous NO. Studies established that the adhesion of vasodilator-stimulated phosphoprotein (VASP)-deficient platelets to the endothelium *in vivo* was increased after vessel damage; moreover, they were impassive to an NO stimulus. This indicates the association of the VASP pathway in the mechanism of platelet inhibition. (224).

1.8.5.2 Cyclic nucleotide phosphodiesterases (PDEs)

PDE activity was discovered in 1962 by Butcher and Sutherland (225). Since then, in excess of 100 variants of the enzyme have been identified and all are capable of hydrolysing the 3' cyclic phosphate bond of both cAMP and cGMP. Increased levels of cGMP can modify cAMP through altered PDE activity (226), presenting scenarios whereby cGMP pathways may act independently of signal transduction kinases.

Studies regarding the localisation and function of PDEs within specific cell types have revealed that several different enzyme family members can be expressed in any given cell. For instance, PDE 3A is expressed in vascular smooth muscle cells and has the capacity to modulate contraction. In addition, PDE 3A has also been implicated to play a vital role in oocyte maturation both *in vitro* and *in vivo* (227). PDEs are regulated in a variety of ways including phosphorylation, binding of cGMP/cAMP and binding of Ca^{2+}/CaM (227). Inhibiting PDE function has been of interest for a number of years for the treatment of various cardiovascular-related disorders such as pulmonary hypertension and erectile dysfunction (228). Newer drugs have been developed which are selective for certain PDEs, for example, PDE 5 has been a target for the development of several erectile dysfunction interventions including sildenafil, avanafil and zaprinast, among others (229, 230). The action of these compounds increases the half life of tissue cGMP, subsequent to inhibiting its degradation, thus prolonging cGMP-mediated effects/responses.

1.8.5.3 Measurement of cGMP

Since the 1970's, radioimmunoassay (RIA) and enzyme immunoassay (EIA) have been used to detect cGMP in tissue and fluid samples (231-233). RIA was first developed by Rosalyn Kalow in the early 1960's (234) in order to examine insulin concentrations within plasma samples in control versus early diabetic subjects.

EIA or enzyme-linked immunosorbent assay (ELISA) has a similar concept to that of RIA. However, there is no use of radioactive labels within this assay and so it has somewhat superseded the use of RIA due to safety. The label used within this system is an enzyme which is conjugated to primary or secondary antibodies or both (235).

As mentioned, ELISA usage has superseded RIA in many laboratories due to the potential hazards involved in using radioisotopes. In terms of sensitivity, ELISA and RIA are very similar. However theoretically, ELISA could possibly be more sensitive as each enzyme molecule has the potential to generate many colour products which can then be directly measured, whereas a radioisotope can only be decayed once. (236).

1.9 RBC-induced vasodilation in hypoxia

As detailed in section 1.4, NO has the ability to participate in a host of biochemical reactions in order to facilitate important biological actions. The preservation of NO in blood has been of particular interest since the early 1990's, when Stamler's group demonstrated that free thiols contained within certain proteins such as albumin (106) could react with NO to form SNO species that act as biological 'carriers' of NO in the circulation (237). More importantly, these SNO species were found to be biologically active in their own right and can inhibit platelet activation and induce vasodilation at sites distal to where they are produced/administered. Further investigation by Jia and colleagues, led to the discovery that the cysteine residue at position 93 of the β chain of Hb (Cysβ93) was a site at which SNO-Hb could be formed (110). Moreover, Jia confirmed that RSNOs behaved very differently from NO itself, demonstrated by the inability of RSNO compounds to react with either deoxy or oxy Hb. The RSNO compounds were said to possess NO^+ characteristics, thereby distinguishing it from the activity exerted by NO itself. Several other species have been implicated to serve in the preservation of NO bioactivity including lipids such as linoleic acid (238), found in RBC membranes and plasma. Nitrated lipid derivatives have been shown to mediate cGMP-dependent and independent signalling pathways (239).

The discovery that low O_2 tension facilitated the release of a bioactive species of NO from RBC/Hb led to further study into the local regulation of blood flow. This regulation was termed 'hypoxic vasodilation' by a number of groups. Most importantly, this refers to smooth muscle relaxation in hypoxic conditions as opposed to smooth muscle relaxation brought about by hypoxia. To date, several theories have been proposed. These theories centre on the ability of RBCs to release a mediator which transiently dilates hypoxic vessels in order to increase blood flow to match O_2 demand. Therefore, the mediator(s) involved must have the ability to cross the RBC membrane to act acutely upon the vascular endothelium or vascular smooth muscle. In addition to this, the relaxatory mediator must be impervious to the scavenging capacity of Hb to ensure its actions are executed outside of the RBC. The different theories and mediators published in the literature will now be introduced in more detail.

1.9.1 Proposed mechanisms

1.9.1.1 HbSNO

The formation of HbSNO has been extensively researched by Stamler and colleagues. This theory centres on Hb allostery and the conformational changes adopted during the respiratory cycle (240). Venous blood is only partially oxygenated (T state) and therefore has the ability to bind NO to form HbNO (see Figure 1.26).

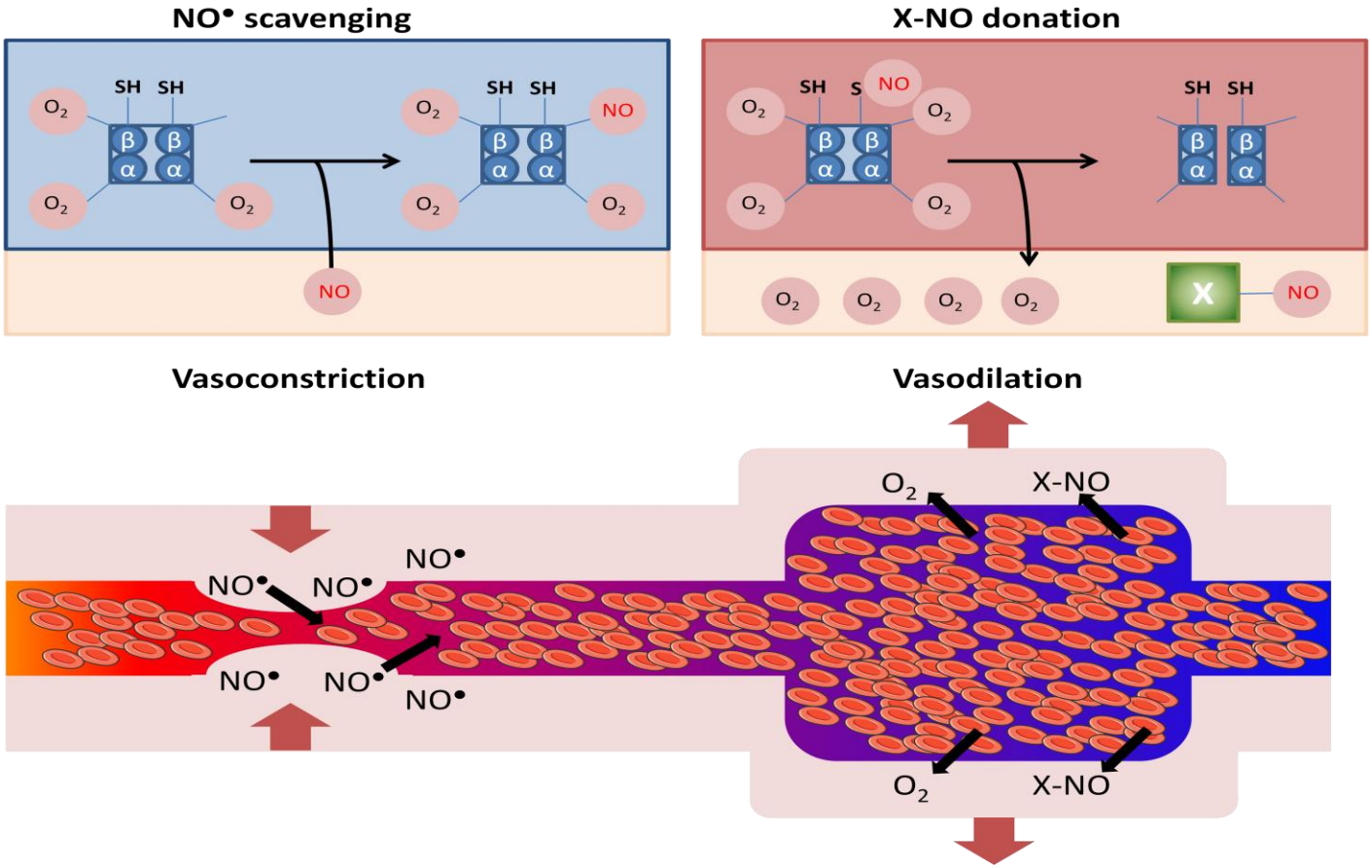

Figure 1.26: Interaction of NO and Hb during an arterial to venous transit. SNO and O_2 are released from Hb in the R state to vasodilate hypoxic vessels. *Adapted (241).*

The pulmonary circulation encompasses a change in saturation of blood in the lungs, leading to the displacement of NO by O_2 (T to R transition). Consequently, NO has the ability to bind to cysteine residues on the β chain of Hb to generate the R state conformation (HbSNO). After exit from the lungs, fully saturated RBCs carrying HbSNO deliver O_2 and SNO to respiring tissue, favouring the switch from R state Hb back to T state. Cysβ93 has been pinpointed to facilitate the release of SNO under low O_2 conditions (124, 242, 243) and is therefore essential to this theory.

The remaining questions regarding the SNO theory are centred on the ability of the NO species to exit the RBC on encountering areas of low tissue pO_2 without being recaptured by Hb. Pawloski and colleagues first reported that the anion transporter protein, AE-1, could be involved in transnitrosation reactions to transfer NO across the RBC membrane (244). They demonstrated that the interaction of HbSNO with this protein promoted the formation of the deoxygenated structure of Hb and subsequent dissociation of NO to the RBC membrane. Pawloski also demonstrated that the AE-1 inhibitor, DIDs, reduced the export of NO to the membrane. This was confirmed by a hypoxic rabbit aortic ring bioassay in which DIDs and NO were pre-incubated with RBCs before being introduced to pre-constricted rings. The DIDs treated RBCs produced a significantly reduced relaxation of hypoxic aortic rings compared with RBCs treated with NO alone.

Subsequent *in vivo* studies have also provided data to support this theory (124). In order to eliminate arterial to venous gradients of O_2, rats were exposed to 3 atmospheres of absolute pressure whilst inhaling 100 % O_2 in a hyperbaric chamber. Levels of both HbNO and HbSNO were then measured in cerebral blood from these animals. As reported by Jia a year earlier (110), there was an abundance of HbSNO present in arterial blood whereas a

higher proportion of HbNO was found in venous blood. This suggested that transnitrosation across the RBC membrane led to the differences between arterial and venous blood. In addition, Palmer *et al* used N-acetylcysteine (NAC) as an inducer of NO transfer reactions in blood in order to examine the effects of this transfer *in vivo* (245). A high dose of NAC administered to mice was converted to NAC-SNO and following a 3-week period, led to a subsequent decrease in RBC SNO concentration. Interestingly, high dose NAC treated mice developed pulmonary arterial hypertension, comparable to the effects witnessed in mice exposed to hypoxia alone for 3 weeks. In light of these observations, Palmer suggested that in NAC treated mice, oxyHb desaturation lead to NAC-SNO formation in systemic blood flowing back to the lungs. Taken together, these findings demonstrate the interaction of HbO_2 saturation with the formation of RSNO in blood and subsequent vascular effects upon the pulmonary circulation.

The SNO theory suggests that together with the release of O_2 to match demand of local tissue beds, the RBCs have the ability to release SNO from Hb which has a direct effect upon vascular tone and local blood flow.

1.9.1.2 NO_2^-

In the early 1950's, Furchgott discovered the importance of NO_2^- in altering vascular tone during experiments administering 100 µM $NaNO_2$ to strips of rabbit aortic tissue (94). Since then, a vast amount of research has been conducted on NO_2^- both *in vitro* and *in vivo*. *In vitro*, Zweier and colleagues demonstrated that NO can be generated in an ischaemic heart through the reduction of NO_2^- due to low pH (246). Furthermore, this production of NO from NO_2^- was not abrogated by NOS inhibitors and continued to occur during prolonged ischaemia. This non-enzymatic reduction of NO_2^- ultimately lead to a loss of contractile function of the heart. In addition, XO was shown to reduce NO_2^- to NO under anaerobic conditions in the presence of either NADH or xanthine (99). *In vivo*, Gladwin and colleagues devised an experiment examining the roles of both endothelial-derived NO and NO species on forearm blood flow, as well as levels of NO_2^-, low molecular weight SNOs, and high molecular weight SNOs in plasma and HbSNO (247). The results of this study demonstrated a gradient of plasma NO_2^- from artery to vein, indicative of a novel source of NO delivery to the vasculature. Moreover, Gladwin found that the consumption of NO_2^- increased significantly during forearm exercise and post NOS inhibition. Production of albumin-SNO was largely centred in the venous blood and was even formed during NOS inhibition, suggesting that albumin does not have the capacity to deliver NO from the lungs to the body. All of the aforementioned studies imply that NO_2^- is bioactive in its own right and *in vivo* could be reduced to NO to control vascular tone during metabolic stress (low pO_2).

In 2003, a clinical study tested the effects of a 5 minute $NaNO_2$ infusion on forearm blood flow measurements, with and without exercise and L-NMMA. The outcome of the

study demonstrated a rise in NO_2^- across the arm before and during exercise, which was also present in subjects that received L-NMMA (248). Cosby reported that the concentrations of $NaNO_2$ used in these studies were 'near physiological'. The *in vitro* portion of this study illustrated that a fall in pO_2 was potentiated by NO_2^- in the presence of Hb. However, in contradiction, a later study by the same group showed that addition of NO_2^- under hypoxic conditions in the presence of Hb did not affect the extent of relaxation compared to control rings (249). Moreover, Dalsgaard described that cell free deoxyHb enhanced the NO_2^--mediated response in hypoxic rat aortic rings however this was solely due to the presence of the allosteric effector, inositol hexaphosphate (IHP) (similar effect to 2,3-DPG, section 1.1.3.2.1) (250). It is noteworthy to mention that hypoxia alone potentiates NO_2^-- induced vasorelaxation in the absence of Hb, therefore questioning the role of deoxyHb as a NO_2^- reductase in this paradigm.

Huang and colleagues further investigated the role of Hb allostery in NO_2^- reduction as well as the ability of Hb to carry out this enzymatic function (251). Data collated from aortic ring bioassays illustrated that the reductase function of Hb and therefore NO-mediated vasodilation of tissue, is maximal at a HbO_2 saturation of 50 % (P_{50}) (tissue pO_2 20-40 mmHg). It was proposed that the reaction of NO_2^- with deoxyhaem involved the formation of two conformations of Hb, due to the ability of deoxyHb to display both T and R state characteristics. The reaction of NO_2^- with deoxyhaem in T state decreases as the deoxyhaem is consumed. However, this is balanced by the enhancement in the reaction between NO_2^- and R state deoxyhaem (forming methaem and iron nitrosyl haem). In addition, comparison between the addition of NO_2^- to deoxyHb and deoxymyoglobin (deoxyMb) highlighted that the rate constant for myoglobin (Mb) did not change, however the rate constant for

deoxyHb with NO_2^- increased exponentially. This finding supports the notion that reductase activity of deoxyHb increases as the reaction proceeds.

Collectively, the data presented implies that the level of HbO_2 saturation and subsequent cycling between T and R states as opposed to tissue pO_2 accounts for O_2 sensing under hypoxia. A recent study by Totzeck and colleagues in 2012 also implicated the role of Mb in the reduction of NO_2^- to NO (252). They provide evidence supporting the presence of Mb in vascular smooth muscle which contributes to hypoxic vasodilation *in vivo* and *ex vivo*. Furthermore, the use of Mb knockout mice models confirmed that Mb had a role in NO_2^--induced hypoxic vasodilation in these animals.

Similar to the HbSNO theory, the validity of the NO_2^- reduction hypothesis has also been questioned. For instance, it is well known that exercise increases O_2 debt to the muscles and therefore some tissues may have a low PO_2. However, the body has means to counteract the effects of local tissue hypoxia; increased respiration ensures O_2 requirement matches demand. Secondly, there has been some debate over the levels of NO that can exit the RBC and diffuse across the vascular wall to the smooth muscle cells. Hb has an extraordinary capacity to scavenge NO and therefore the levels that can escape the blood to act upon sGC when physiological levels of NO_2^- are present have been questioned. In addition, NO_2^- itself has the ability to induce relaxation under hypoxic conditions, regardless of the presence of Hb, suggesting that Hb and therefore RBCs per se, are not necessary for mediating vascular tone in this instance. Moreover, this relaxation is slow and gradual occurring over minutes, whereas the relaxation attributed to hypoxic vasodilation by RBCs is an immediate and transient response.

To date, the published data for both the SNO and NO_2^- theories have provided convincing evidence to support mechanisms contributing to hypoxic vasodilation. Yet neither completely fulfils the criteria that allow for rapid production and release of the relaxing species, that the mediator itself is easily replenished (as shown by RBC O_2 cycling experiments using bioassays), or whether these are relevant at physiological levels/conditions. Angelo *et al* goes some way to addressing this by providing evidence for the function of Hb as a SNO synthase, which appears to be dependent on the local concentration of NO_2^- (253). They demonstrate that physiological concentrations of NO_2^- with deoxyHb rapidly form a HbSNO precursor, producing HbSNO upon oxygenation. However, high NO_2^- concentrations inhibit the formation of HbSNO. This data connects the two theories together to some extent however the formation of this SNO precursor is not yet fully understood.

1.9.1.3 ATP

In 1992, Bergfeld and Forrester established that exercise-induced hypoxia led to a rise in RBC-derived ATP release (254). In most cells of the body, mitochondria consume ~85 % of O_2 present to allow for the process of oxidative phosphorylation which is the primary pathway for the production of ATP (255). It is thought that the ATP released from the RBC in hypoxia bind to P_2Y receptors on the endothelium (256), stimulating the release of NO and PGI_2. More recently, Sprague and colleagues conducted a study on rabbit skeletal muscle arterioles, examining the effect of ATP and O_2 release from RBCs following reduced tissue O_2 tension (257). The data illustrated that ATP release increased in proportion to the decrease in O_2 tension as hypothesised. In addition, a further experiment investigated the role of rabbit RBCs in the response of hamster cheek retractor arterioles to decreased extra-luminal

O_2 tension (~32 mmHg). The inclusion of rabbit RBCs in the buffer resulted in a dilation of the arterioles compared with buffer alone, supporting the hypothesis that RBCs contribute in delivery of ATP and O_2 to metabolically active skeletal muscle.

Experiments conducted by Stamler's group demonstrate that hypoxic vasorelaxation occurs in endothelium denuded vessels (258), suggesting that endothelium-dependent NO release by ATP may not be necessary here. Further investigation into this hypothesis illustrated that the levels of ATP in the blood rise relatively slowly in relation to a decreasing HbO_2 saturation. In relation to this paradigm, this change in mediator levels does not correspond to the transient resultant relaxation observed in the experimental models and *in vivo*, perhaps indicating that ATP may have more of a role in chronic hypoxia as opposed to hypoxia in the acute setting (254). Moreover, several groups agree that presence of L-NMMA in any experimental model does not affect the transient relaxation in response to hypoxia, confirming NOS is not a key player (101).

1.10 Thesis rationale

The mechanisms of local regulation of blood flow detailed in sections 1.9.1.1, 1.9.1.2 and 1.9.1.3, propose several ways in which RBCs are involved in the relaxation response to low O_2 tension. The main characteristics underlying the mechanisms described above can be summarised by the following:

- RBC-induced relaxation in hypoxia is largely sGC-mediated and endothelium-independent.
- Relaxation is dependent upon the HbO_2 saturation of RBCs.

The work contained within this thesis aims to address these findings and further investigate the mechanism behind the RBC-induced transient relaxation observed in hypoxia. These studies have centred on an *in vitro* myograph model utilising hypoxic rabbit aortic rings to demonstrate how RBCs affect vascular tone. Together with the notion that HbO_2 saturation is an important factor in this setting, as well as the lack of suitable oxygenated controls in previous experiments, Chapter 3 of this thesis aims to show the importance of O_2 itself on the control of vessel tone in hypoxia. In all experiments, buffer controls were equilibrated with 95 % O_2/5% CO_2 in order to mimic the O_2 carrying capacity of RBCs within blood.

Chapter 4 of this thesis further investigates the mechanism in terms of its sGC-dependence. As previously stated (section 1.8.1.1), NO is the primary ligand of sGC, catalysing the production of cGMP. However, sGC can also be activated via other haem-dependent and independent ligands which are also independent of NO. Much of the literature to date has argued against the interaction of sGC with O_2. The data within Chapter 4 further explores the interaction of O_2 with purified human sGC and whether O_2 influences other ligand binding.

Previous studies have used rabbit aortic rings to investigate mechanisms of RBC-induced relaxation in hypoxia. Physiologically, a conduit vessel such as the aorta is unlikely to experience hypoxia, since oxygenated blood deriving from the lungs flows into it. Chapter 5 addresses this by adopting a porcine coronary artery model, similar to the experimental model in Chapter 3. These vessels are more suitable for experimentation since blockages within coronary arteries, due to disease such as atherosclerosis, can cause local ischaemia distal to the site of occlusion.

1.11 Thesis Aims

The overall aim of this thesis is to study the acute effects of O_2 itself on vascular tone under hypoxic conditions. Specifically, this thesis aims to examine the following:

- The role of RBCs in mediating vasorelaxation in hypoxia, particularly focussing on the influence of O_2. This work will be conducted using the rabbit aortic ring model to study changes in isometric tension post introduction of O_2 to tissue under varied O_2 tensions.

- The role of O_2 in mediating sGC activation. The $\alpha_1\beta_1$ purified form of human sGC will be utilised in a model that will be utilised under normoxic and hypoxic conditions using the InVivo$_2$ hypoxia workstation (Ruskinn) to determine the effects of O_2 on enzyme activity. cGMP will be quantified by ELISA as a measure of sGC activity.

- Influence of vessel size and function on O_2-induced vasorelaxation by comparing studies conducted in both porcine coronary vessels and the rabbit aortic ring models.

1.11.1 Hypothesis

O_2 itself represents the mediator released by oxygenated RBCs that can induce relaxation of hypoxic vascular tissue.

2 General Methods

2.1 Reagent & Chemicals List

Table 2.1: Reagents and chemicals used.

Product	Company
Sodium chloride (NaCl)	Fisher Scientific UK
Potassium chloride (KCl)	
Potassium dihydrogen orthophosphate (KH_2PO_4)	
Magnesium sulphate ($MgSO_4$)	
Sodium hydrogen carbonate ($NaHCO_3$)	
Glucose ($C_6H_{12}O_6$)	
Calcium chloride ($CaCl_2$)	
Glacial acetic acid	
Hydrochloric acid	
DMSO	
Acetylcholine (ACh)	Sigma Aldrich UK
Phenylephrine (PE)	
Indomethacin	
Glibenclamide	
1H [1,2,4]oxadiazolo[4,3-a]quinoxalin-1-one (ODQ)	
Potassium iodide (KI)	
Iodine (I_2)	
Potassium hexacyanoferrate ($K_3Fe^{III}(CN_6)$)	
Sulphanilamide	
Mercury Chloride ($HgCl_2$)	
Antifoam	
PBS (tablet form)	
S-nitrosoglutathione (GSNO)	Alexis Biochemicals
MAHMA NONOate (NOC9)	
N^G-monomethyl-L-arginine (LNMMA)	
U46619	Tocris UK
Soluble guanylate cyclase (sGC) - human $\alpha_1\beta_1$	Axxorra

2.2 Myography

Male New Zealand white rabbits (2-2.5 kg) were euthanised by lethal injection (sodium pentobarbitone, 120 mg/kg, i.v). The thoracic aorta was removed carefully and placed in fresh Krebs-Henseleit (KH) buffer on ice (Composition mM: NaCl 109.2, KCl 2.7, KH_2PO_4 1.2, $MgSO_4$ 1.2, $NaHCO_3$ 25, Glucose 11, $CaCl_2$ 1.5). Excess adipose tissue was removed from the aorta and typically 8 rings of 2mm in width were prepared; care was taken not to damage the endothelium or smooth muscle.

The rings were mounted in baths containing 5 ml KH buffer at 37°C gassed with 95% O_2/5% CO_2. Resting tension was set to 2 g (94). Signals from the transducer were amplified and visualised on the Powerlab/Chart 4 for Windows software. Tissues were allowed to equilibrate for 60 minutes prior to experimentation.

Constriction-relaxation responses to 1μM PE and 10μM ACh, respectively, were performed to establish both smooth muscle and endothelial integrity. In most cases, three repeats established stable constriction-relaxation profiles. Figure 2.1 is a schematic of the myograph set up and typical curve generated by constriction-relaxation exercises.

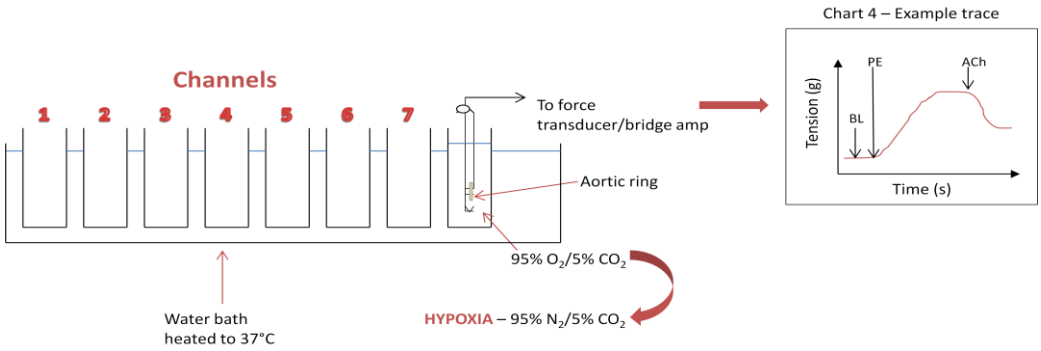

Figure 2.1: A schematic representation of an 8-channel myograph set-up. (BL – baseline).

2.2.1 Equilibration to varying O_2 concentrations

To equilibrate the rings to hypoxia (~0% O_2), the gas was switched to 95% N_2/5% CO_2 for 10 minutes. Other concentrations of O_2 used were 1, 5, 10 and 21%. The gas mixes (with 5% CO_2) were purchased from BOC UK and were similarly bubbled into the baths for 10 minutes to establish equilibrium.

Previous analysis of the O_2 content within the baths were made using O_2 electrodes and when equilibrated with 95% N_2/5% CO_2 under similar experimental conditions, confirmed this to be 0.9% O_2 (259). This represented the lowest possible O_2 concentration attainable in the open bath configuration. For the purpose of clarity only, this will be referred to as "zero" or "0%" for the remained of this thesis. Rings equilibrated to 0, 1 and 5% O_2 were constricted with 3 μM PE to achieve an equivalent sub-maximal constriction as normoxic rings (~95% O_2).

2.2.2 KH buffer samples

For certain myography experiments, bolus additions of 0, 21 or 95 % O_2 were added to the hypoxic vascular rings. These samples were prepared by bubbling N_2 (0 %) or 95 % O_2

into small septum-sealed bottles for 5 minutes. Air (21 % O_2) samples were allowed to reach ambient O_2 conditions by leaving open to the room conditions for at least 30 minutes.

2.2.3 KH buffer myography sample volumes

Samples were equilibrated for 5 minutes with 0, 21 or 95 % O_2 as outlined in section 2.2.2. Table 2.2 illustrates the relative final O_2 concentrations of each bath with respect to an addition of 200 µl of each sample (see 'Units Conversion' – XVII).

Table 2.2: Final bath O_2 concentration for 0, 21 and 95 % O_2 KH buffer samples.

Volume added to bath (µl)	**Final bath O_2 concentrations of KH buffer samples (µM)**		
	0 %	21 %	95 %
200	0	8.4	38

2.3 Blood Collection

Healthy participants gave their consent to have blood samples taken. These samples were taken by trained members of staff and in agreement with the Cardiff and Vale University Health Board and only where permitted by the Local Ethics Committee.

Blood was drawn from the median cubital vein or cephalic vein into vacutainers (K_3EDTA, Vacuette Greiner Bio-One^{TM}). After sample collection, the vacutainers were inverted to ensure adequate mixing with ethylenediaminetetraacetic acid (EDTA) to prevent clotting.

2.3.1 Blood Processing

Figure 2.2 below outlines the steps taken to isolate both the RBC and haem fractions. A former PhD student in our group, Dr Andrew Pinder, altered the O_2 saturation of RBC (as measured by the blood gas analysis (OSM3 Hemoximeter, Radiometer)) using a thin film rotating tonometer. This equipment required a relatively high dilution and volumes of RBC to be purged with gases of varying O_2 content. Therefore, in the studies conducted in this thesis, the O_2 saturation of RBCs held at physiological haematocrit was modulated by simply mixing with oxygenated PBS to achieve the target HbO_2 saturation.

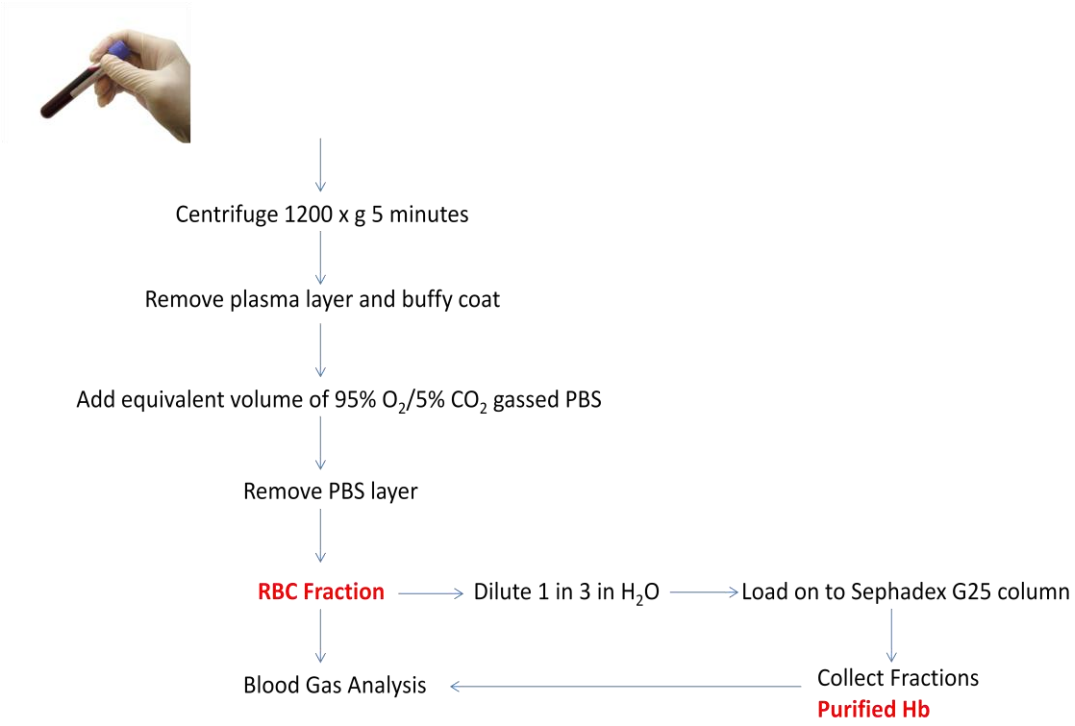

Figure 2.2: Human blood processing – separating whole blood into RBC and Hb fractions.

2.3.2 Blood and Hb myography sample volumes

In order to achieve a final bath O_2 concentration equal to that of KH buffer (section 2.2.3), the Hb concentration in each sample was factored in. The total Hb content (tHb in g %) was used from the OSM3 Hemoximeter data for each sample. It is noteworthy to mention that

this figure was higher than normal since the RBCs were taken from centrifuged blood and not whole blood. Purified Hb sample volumes were also calculated using the tHb. Each sample volume was calculated by working back from the Hb concentration to achieve a final bath concentration of 38 µM:Example:

tHb (g %) = 36.9

36.9 g % = 369 g/l

MW of Hb = 64,500 Da

369/64500 = 0.0057 M = 5.72 mM Hb

Volume in bath = 5000 µl (5 ml)

1 µl added to bath = 5.72/5000 = 1.144 µM Hb

4 O_2 molecules per Hb = 4 x 1.144 = 4.58 µM O_2 in 1 µl of RBCs

38 µM O_2 = 8.30 µl RBCs added

2.4 Purified enzyme experiments

Purified human sGC (10 μg) was reconstituted in 1 ml of enzyme buffer (personal communication, Professor John Garthwaite), divided into aliquots and stored at -80°C until use. Table 2.3 lists the buffer recipes used for all enzyme experiments.

All experiments were performed in an InVivo$_2$ Hypoxia Workstation 400 (Ruskinn). Normoxic experiments were carried out at 37°C and 20% O_2/5% CO_2 (maximum oxygenation for the hypoxia workstation) via a 25% O_2/5% CO_2 gas cylinder. Hypoxic experiments were maintained at 37°C and ~0% O_2/5% CO_2. Reagents were allowed to equilibrate for 1 hour before all tests were completed.

The reconstituted sGC enzyme was diluted 1 in 200 in assay buffer. GTP, dissolved in equimolar $MgCl_2$, was then added to a final concentration of 1 mM to start the reaction. All reactions were incubated for 10 minutes at 37°C immediately following GTP/$MgCl_2$ addition, after which boiling inactivation buffer was added in 4 times excess. Samples were then heated to boiling point before storage at -20°C for further analysis.

Table 2.3: Buffers used in sGC experiments.

Buffer	Constituents	Content	pH
Enzyme	Tris	50 mM	7.4
	DTT	1 mM	
	BSA	0.5 %	
Assay	Tris	50 mM	7.4
	EGTA	100 µM	
	$MgCl_2$	0.3 mM	
	BSA	0.045 %	
Inactivation	Tris	50 mM	7.5
	EDTA	4 mM	

DTT: dithiothreitol; BSA: Bovine serum albumin; EGTA: ethylene glycol tetraacetic acid; $MgCl_2$: magnesium chloride.

2.5 EPR Spectroscopy

EPR is a technique which detects species with unpaired electrons. The EPR phenomenon observed is the transition (resonance absorption of energy) between 2 energy states that can occur in an unpaired electron system in a magnetic field. An electron is a negatively charged spinning particle which possesses angular momentum (rotation due to inertia and velocity) (260). Subsequently, this angular momentum accounts for an electron possessing a magnetic moment. The momentum of the rotating electron produces a magnetic field and the axis of each spinning electron has an associated dipole moment. When an external magnetic field is applied to the sample, unpaired electrons are forced to take up specific orientations, governed by spin quantum number (S), either aligning with, or against, the direction of the external field. An electron has a S value of ½, allowing two

possible spin rotations; which are parallel (m_s = +1/2) and anti-parallel (m_s = −1/2) to the magnetic field (Zeeman's effect - see Figure 2.3) (261). In the absence of an external magnetic field, electrons are in random orientation and have an average energy state. In the presence of a magnetic field, parallel orientation (m_s = +1/2) occurs when the electron magnetic properties spin parallel to the external magnetic field (low energy) in comparison to anti-parallel (m_s = −1/2) where electron spin direction is opposed to the magnetic field (high energy). (261).

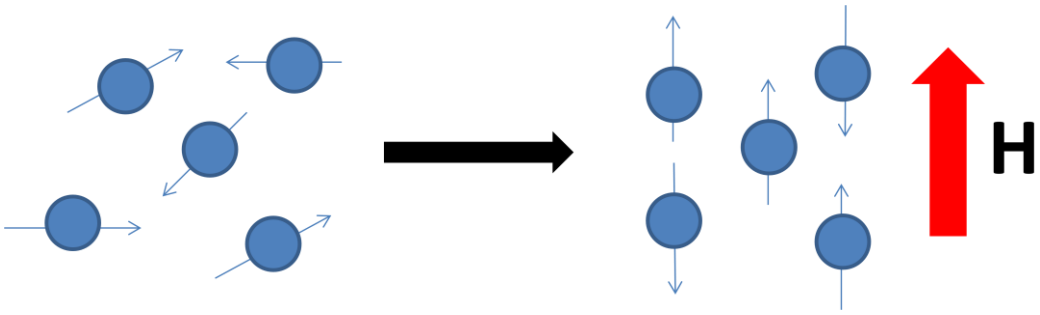

Figure 2.3: Zeeman's effect. *Adapted (262).*

When we supply an external magnetic field, the paramagnetic electrons can either orient in a direction parallel or anti-parallel to the direction of the magnetic field which creates two distinct energy levels for the unpaired electrons, in turn allowing the detection and measurement as electrons are driven between the two energy levels (Figure 2.4).

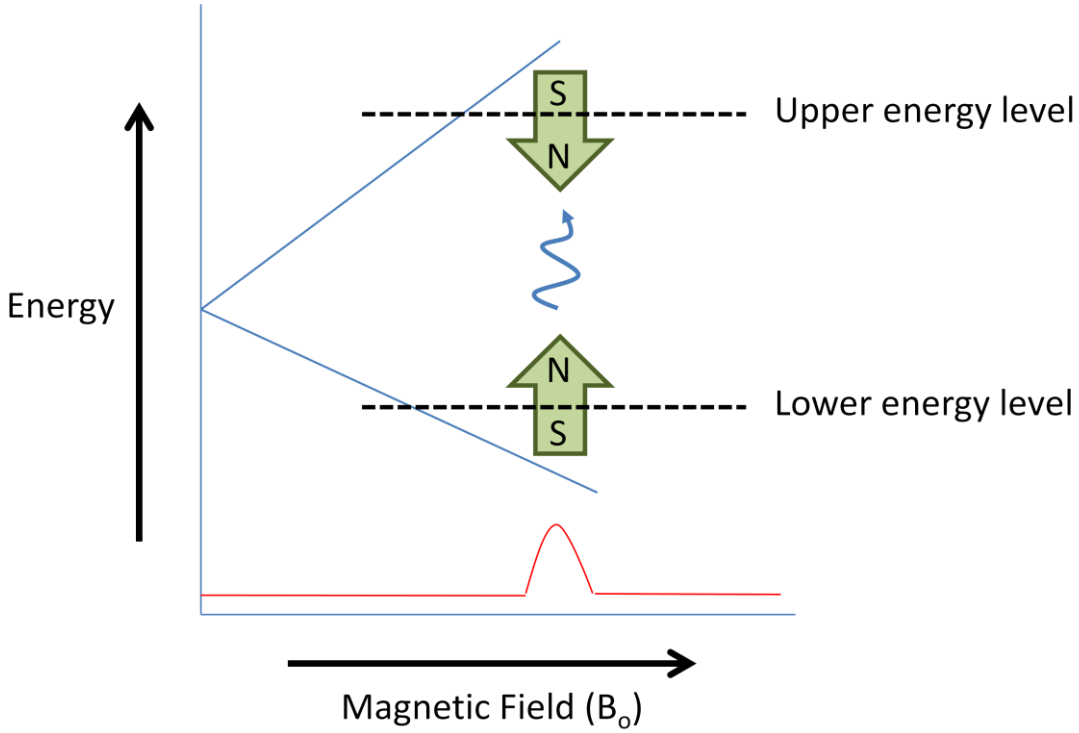

Figure 2.4: The excitation of electrons between energy levels during an applied magnetic field (262).

Therefore in the presence of a magnetic field (H) are two potential energy levels for an unpaired electron. 'h' represents the difference between the energy at the two levels (ΔE).

2.5.1 Oximetry

EPR oximetry relies on the fact that the ground state of molecular O_2 has 2 unpaired electrons. These two electrons will interact with other unpaired electron species and the extent of this interaction will be a function of the amount of O_2 present. This is reflected by the direct broadening of the ESR peak observed (263). This effect occurs with all paramagnetic materials although it is much larger in some materials than others and these are selected for oximetry. The spectral line width (measured in Gauss, G) (peak to peak splitting along the magnetic field axis) is measured and converted to pO_2 or concentration of O_2 using an appropriate calibration curve. It is crucial that the probe chosen for any oximetry studies does not affect the local O_2 present within the sample being tested, and

this is true for EPR oximetry because there is no physical or chemical interaction between O_2 and the probe – it simply recognises the presence of a secondary spin species.

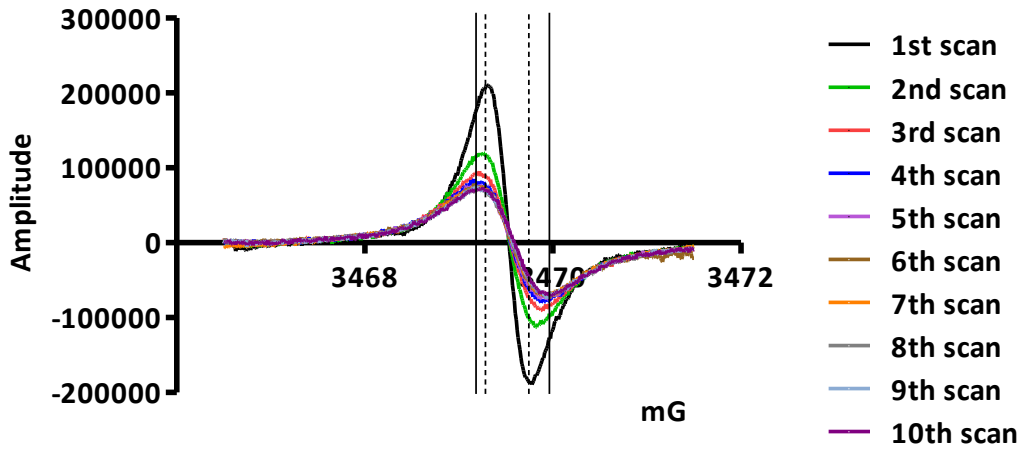

Figure 2.5: Incremental Y sweep (magnetic field) for a sample recorded in N_2 and then the perfusion gas switched to 95 % O_2 immediately after the first scan. Each scan had a 41 second duration and 10 scans were completed. The dashed lines represent the line width at low O_2 and the solid lines represent the line width at 95 % O_2.

The EPR machine used to conduct each experiment was the *Bruker escan*. Table 2.4 outlines the conditions set for oximetry. The modulation amplitude should be no more than one third of the expected line width (as a general rule) to ensure no artificial broadening of the peak to machine conditions (such as power).

Table 2.4: Experimental conditions for EPR oximetry.

	0 %	**21 %**	**95 %**
MW (dB)	18.00	18.00	18.00
Receiver Gain	2.24×10^3	4.48×10^3	4.48×10^3
Modulation Frequency (kHz)	86.00	86.00	86.00
Modulation Amplitude (G)	0.06	0.10	0.20
Modulation Phase (degrees)	17.37	17.37	17.37
Offset (%)	51.00	51.00	51.00
Conversion (msec)	81.92	81.92	81.92

2.5.2 Standard curve

The soluble oximetry probe, N^{15} per-deuterated tempone (PDT) (5 mM) was diluted 1 in 10 in double distilled water (d.H_2O) (500 µM). Three standards were prepared: 0, 21 and 95 % O_2. The air (21 %) standard was equilibrated to atmospheric O_2 by leaving open to the room conditions for at least 30 minutes prior to analysis. The diluted probe was even further diluted in order to detect O_2 accurately for each standard; 4 µl of diluted probe (500 µM) was added per 100 µl of distilled water used for each standard (1 in 25 dilution). The 0 and 95 % standards were achieved by drawing up the diluted probe (20 µM) into gas permeable tygon tubing and placing into a narrow hollow quartz tube used for EPR spectroscopy. The tube was perfused with either N_2 or 95 % O_2 to equilibrate to 0 or 95% O_2, respectively (Figure 2.6). The point at which the spectral line width no longer changed was taken as the standard. Figure 2.7 shows the typical data achieved for a standard curve over a 4 day period.

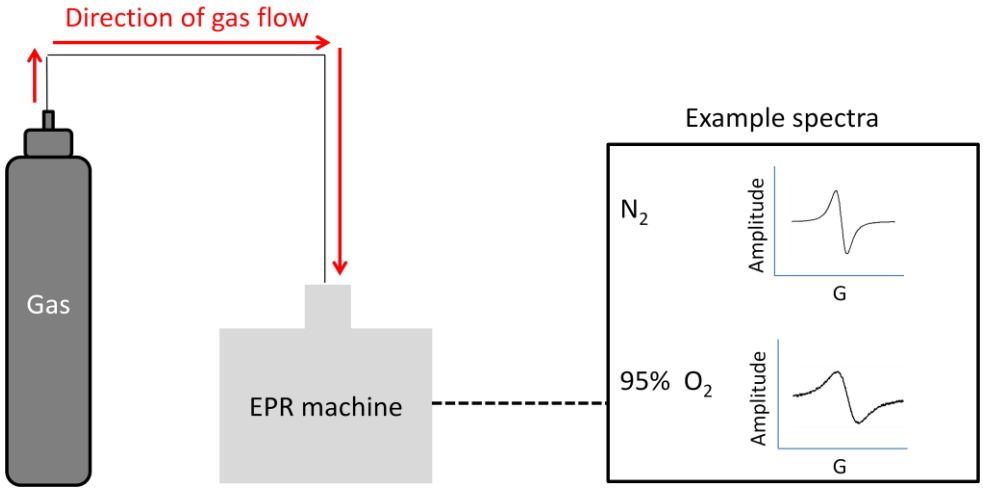

Figure 2.6: Standard curve preparation for EPR oximetry.

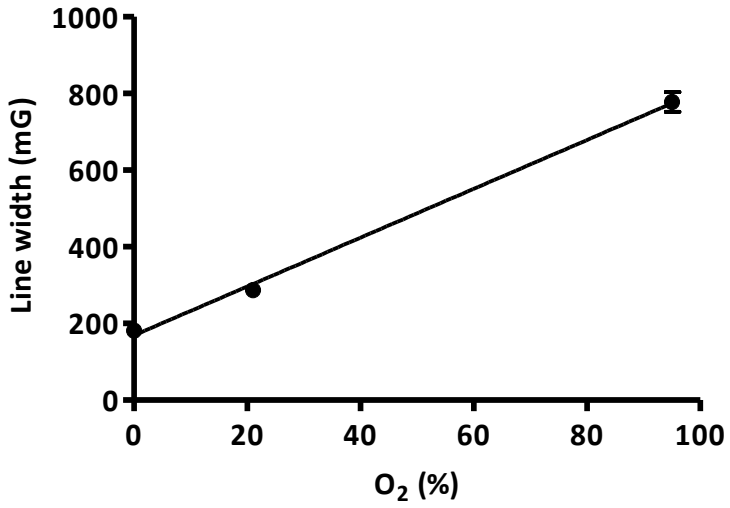

Figure 2.7: Standard curve for EPR oximetry (n=4) *Linear regression.*

2.5.2.1 EPR validation: Myography samples

In order to ascertain the O_2 content of the KH buffer samples that were added to each experiment (see section 2.2.2), EPR was used to determine the exact O_2 content present using the N^{15} PDT probe (20 μM). This was also to verify that the perfusion time of 5 minutes was enough to sufficiently deoxygenate (0 %) or oxygenate (95 %) the samples. After each time point, a glass capillary was used to draw up each sample and the fluid was contained by sealing each end with an air-tight sealant. The 0 % O_2 sample was drawn up in the hypoxic chamber to limit any contamination with air. The 95 % O_2 sample was taken as quickly as possible to limit gas escape. Figure 2.8 illustrates the line widths of each time point chosen.

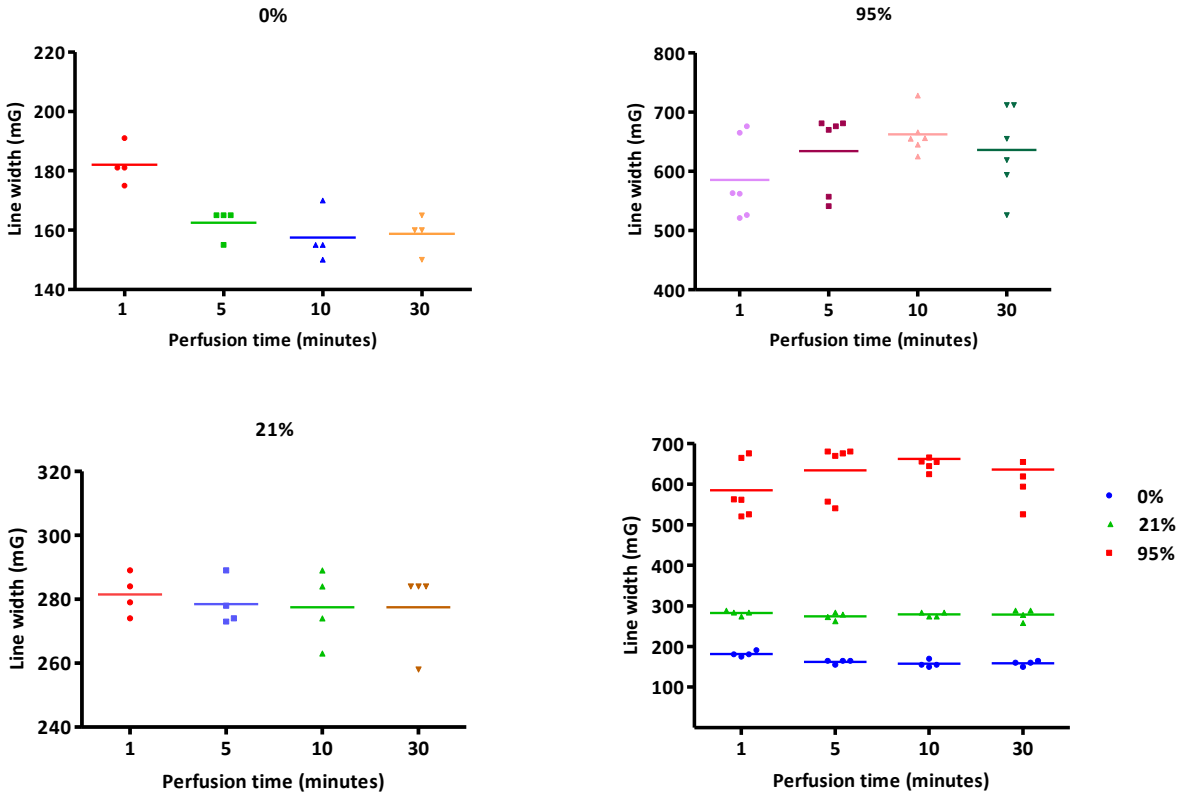

Figure 2.8: Validation of O_2 content in samples added to hypoxic vascular ring experiments. The bottom right graph is a summary of all O_2 samples analysed. Statistically, there was no difference in line width between those samples perfused for 10 minutes or 30 minutes with those perfused for 5 minutes. (n=4-6). *One-way ANOVA + Dunnett's post hoc test.*

2.5.2.2 EPR validation: Hypoxic chamber samples

Similarly to the myograph samples, the assay buffer utilised in the sGC experimental samples also needed to be tested to ensure that the buffer was of low O_2 and essentially hypoxic. Thus, identical volumes of assay buffer as those used in the experiments were added to vials and allowed to equilibrate for between 1 and 4 hours in the hypoxic chamber at 37°C (Figure 2.9).

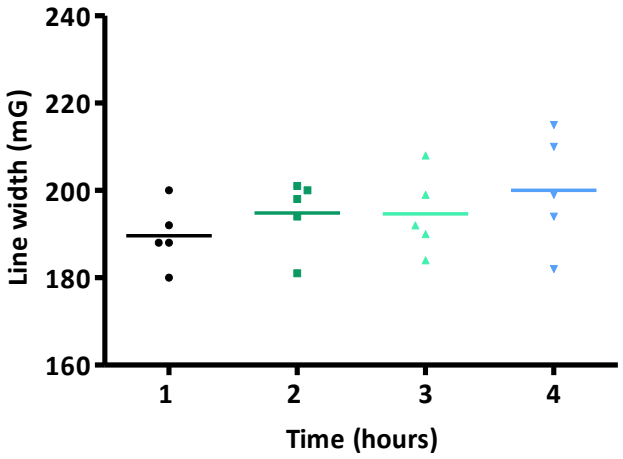

Figure 2.9: Validation of O_2 content in hypoxic chamber samples. Assay buffer samples were incubated for between 1 and 4 hours and analysed via EPR spectroscopy. There was no significant difference in the line width of each time point compared to a 1 hour incubation period. (n=5). *One-way ANOVA + Dunnett's post hoc test.*

2.6 cGMP ELISA

The kit used for all cGMP detection within this thesis was the *'R & D Systems Parameter™ cGMP Assay Kit'.* This particular kit was chosen as it had a wide range of detection (0-500 pmol/ml). This ELISA kit is based on competitive binding of the substrate (see Figure 2.10).

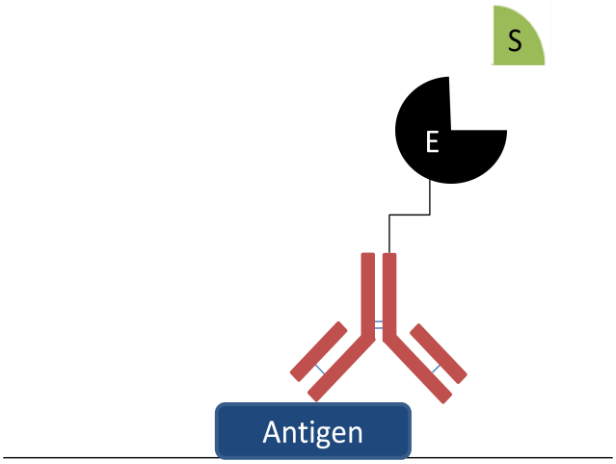

Figure 2.10: Direct competitive ELISA. A 96 well plate coated with an antigen secures the cGMP polyclonal antibody on to the plate. The cGMP-HRP conjugate directly competes with the cGMP in the sample for binding to the cGMP antibody already bound to the plate. *S: substrate; E: enzyme. Adapted from piercenet.com*

2.6.1 Kit constituents:

- ✓ Goat anti-rabbit microplate
- ✓ cGMP conjugate
- ✓ cGMP Standard
- ✓ Primary Antibody Solution
- ✓ Calibrator Diluent RDS-5
- ✓ Cell Lysis Buffer 5 Concentrate
- ✓ Wash Buffer Concentrate
- ✓ Colour Reagent A
- ✓ Colour Reagent B
- ✓ Stop Solution
- ✓ Adhesive Plate Sealers

2.6.2 Kit preparation

The wash buffer concentrate was diluted 1 in 25 in dH_2O. The cGMP standard was reconstituted in 1 ml of $d.H_2O$. This was then mixed and allowed to stand for a minimum of 15 minutes before the diluted standards were prepared.

2.6.3 Kit considerations

- ✓ All reagents must be allowed to equilibrate to room temperature before use.
- ✓ Opened kits are stable for up to 1 month at 4°C.
- ✓ Reagents must be kept away from light.
- ✓ Correct diluent was used – for enzyme experiments the Calibrator diluent was used.

2.6.4 Enzyme Sample Preparation

Samples collected from previous experiments in the hypoxic chamber (sGC diluted in enzyme assay buffer) were defrosted on the day of the cGMP assay and kept on ice. Each sample was allowed to equilibrate to room temperature and mixed thoroughly before being added to the plate.

2.6.5 Assay Procedure

2.6.5.1 Standard Preparation

- ✓ The reconstituted cGMP standard produced a stock solution of 5000 pmol/ml.
- ✓ 900 µl of Calibrator Diluent was added to a tube labelled 500 pmol/ml. 600 µl was added to each tube labelled 167, 56, 18.5, 6.2 and 2.1.
- ✓ 100 µl of the standard stock solution (5000 pmol/ml) was added to the 900 µl in the tube labelled 500 pmol/ml. A serial dilution was then carried out as shown in Figure 2.11 below. Standards were used within one hour of preparation.

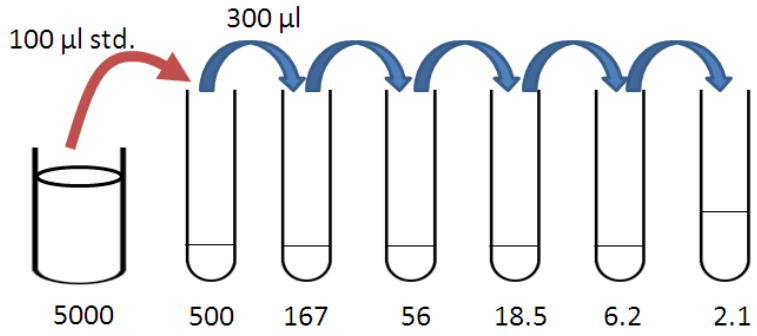

Figure 2.11: Process of cGMP standard serial dilutions.

Quantification

- ✓ 150 µl of Calibrator Diluent was added to the non-specific binding wells (NSB) and 100 µl was added to the zero standard wells.
- ✓ 100 µl of standard or sample was added to the wells.
- ✓ 50 µl of cGMP conjugate was added to each well which gave the wells a slight red colour.
- ✓ 50 µl of Primary Antibody Solution was added to each well, excluding the NSB wells. The addition of Primary Antibody caused the wells to turn a slight purple colour. The plate was covered with an adhesive strip.
- ✓ The plate was placed on a microplate shaker at 500 ± 50 rpm for 3 hours at room temperature.
- ✓ After the 3 hour incubation, the contents of the wells were aspirated and replaced with 400 µl of diluted wash buffer. This process was repeated for a total of 4 wash steps. After the final wash, the plate was blotted on clean paper towels to remove any excess fluid from the wells.

- ✓ Sufficient volumes of Colour reagents A and B (tetramethylbenzidine (TMB)/H_2O_2) were mixed together in equal quantities and protected from light. This solution was used within 15 minutes.
- ✓ 200 µl of prepared substrate solution was added to each well.
- ✓ The plate was then incubated for 30 minutes at room temperature. The plate was covered in foil to protect it against light.
- ✓ 50 µl of Stop solution (acidic solution – H_2SO_4) was added to each well after which the solution inside each well turned from a blue colour to yellow. Gentle tapping on the side of the plate ensured adequate mixing of the Stop solution with the contents of the wells.
- ✓ The absorbance of the plate was read at 450 nm within 30 minutes of adding the Stop solution. The wavelength was also corrected at 550 nm to account for any imperfections in the plate material. These readings, as well as the absorbance for the NSB wells were then subtracted from all standards and sample absorbances.

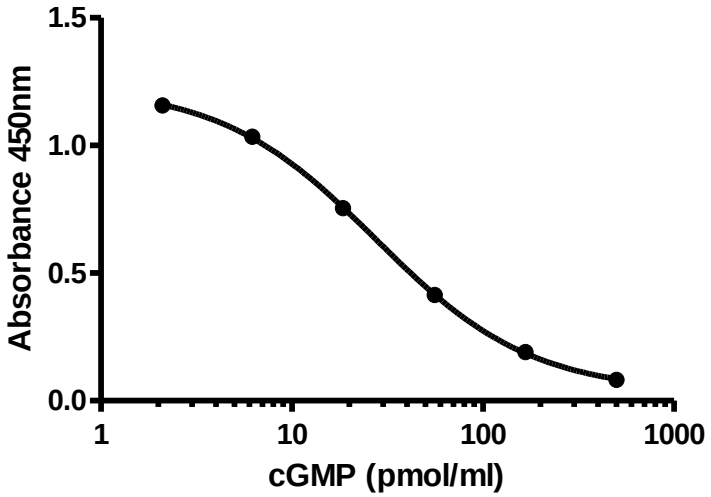

Figure 2.12: A typical standard curve achieved for the R & D parameter assay.

2.7 Ozone Based Chemiluminescence (OBC)

2.7.1 Background

OBC has been adopted by several laboratories worldwide, including our laboratory, to accurately measure a variety of NO species (116, 264, 265). The technique can detect NO species with a sensitivity of less than 1 pmol NO. Despite the potential for studying a wide range of NO concentrations, there has been many discrepancies over the levels of NO in whole blood. This may perhaps be due to the laboratory to laboratory variation in nitric oxide analysis (NOA) set-up or indeed the levels of NO_2^- contamination due to insufficient washing of equipment, in particular the Hamilton syringes used for injection. In plasma, the levels of NO_2^- and RSNO/RNNO are present in the nM range compared with a μM range for NO_3^-. This 1000-fold difference is due to the vast amount of NO_3^- obtained from the diet we eat and subsequent absorption into the bloodstream.

As explained, there have been several inconsistencies in the quantification of NO, a large proportion of which has been due to contamination and general laboratory practise. Our lab has minimised this by adopting specific protocols to ensure the consistency of measurements. For instance, we limit NO_2^- contamination by using HPLC grade water for washing equipment and diluting reagents/chemicals. This has been found to reduce standard error by around 5% (116). The timings of samples are also important, especially when dealing with patient blood; therefore it is crucial to keep this consistent. Blood samples are centrifuged immediately after being drawn from the patient/volunteer and the plasma snap frozen in liquid N_2. Samples are subsequently stored at -80°C until future analysis. In terms of freezing, our laboratory has shown that there were no differences in signal between samples run on the NOA fresh or stored at -80°C over six months. This was

on the proviso that the samples were thawed at 37°C (water bath) in the dark for 3 minutes (116).

2.7.2 Protocol: Tri-iodide

Figure 2.13 summaries the general NOA set up. The cleavage reagent, tri-iodide, was made up by dissolving 650 mg of iodine crystals with 70 ml glacial acetic acid under a fume hood. Another solution was made consisting of 1 mg potassium iodide dissolved in 20ml HPLC grade water. This was then added to the acid mix under the fume hood. The tri-iodide solution was then place on a stirrer for at least 30 minutes prior to use. Tri-iodide is used to reduce NO_2^- to NO and the presence of the acidic environment in the process is crucial for optimum cleavage of the thiol group.

A beaker of water was allowed to equilibrate to 50°C on the magnetic stirrer. The N_2 carrier gas was set at a flow rate of 200 ml/min. 5 ml of tri-iodide reagent was placed in the purge vessel and the glassware connected to the gas inlet and NaOH trap via Nalgene® tubing. 20 µl of anti-foam was used when injecting samples of plasma or RBCs to prevent the foaming of proteins within the samples. Hamilton syringes were used to inject samples into the purge vessel via the injection site. Sections 2.7.2.3 and 2.7.2.4 outline the specific protocols used to analyse various NO species.

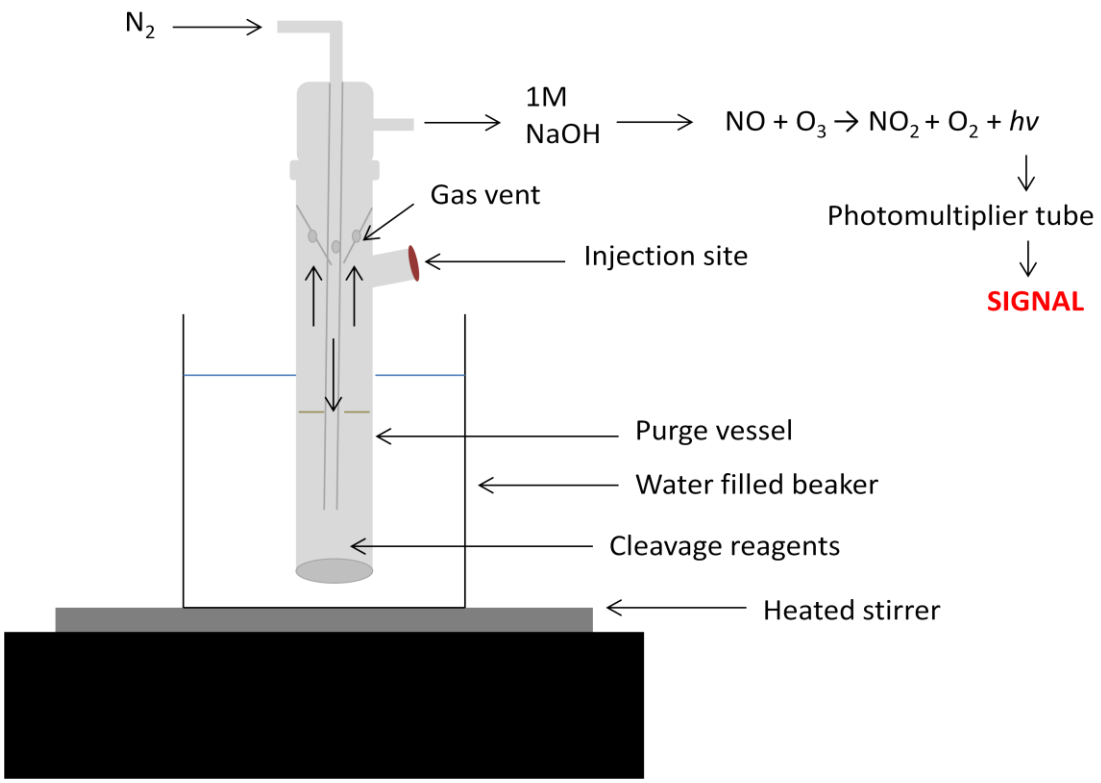

Figure 2.13: Schematic of the NOA set up.

2.7.2.1 NO_2^- standard curve

A 10 mM standard of $NaNO_2$ was made adding 69 mg $NaNO_2$ to 100 ml HPLC grade water. The 10 mM $NaNO_2$ stock was then further diluted to make the following standards (in nM): 62.5, 125, 250, 500 and 1000. 200 µl of each standard were injected. The linear standard curve was generated by plotting the $NaNO_2$ concentration versus area under the curve (Figure 2.14).

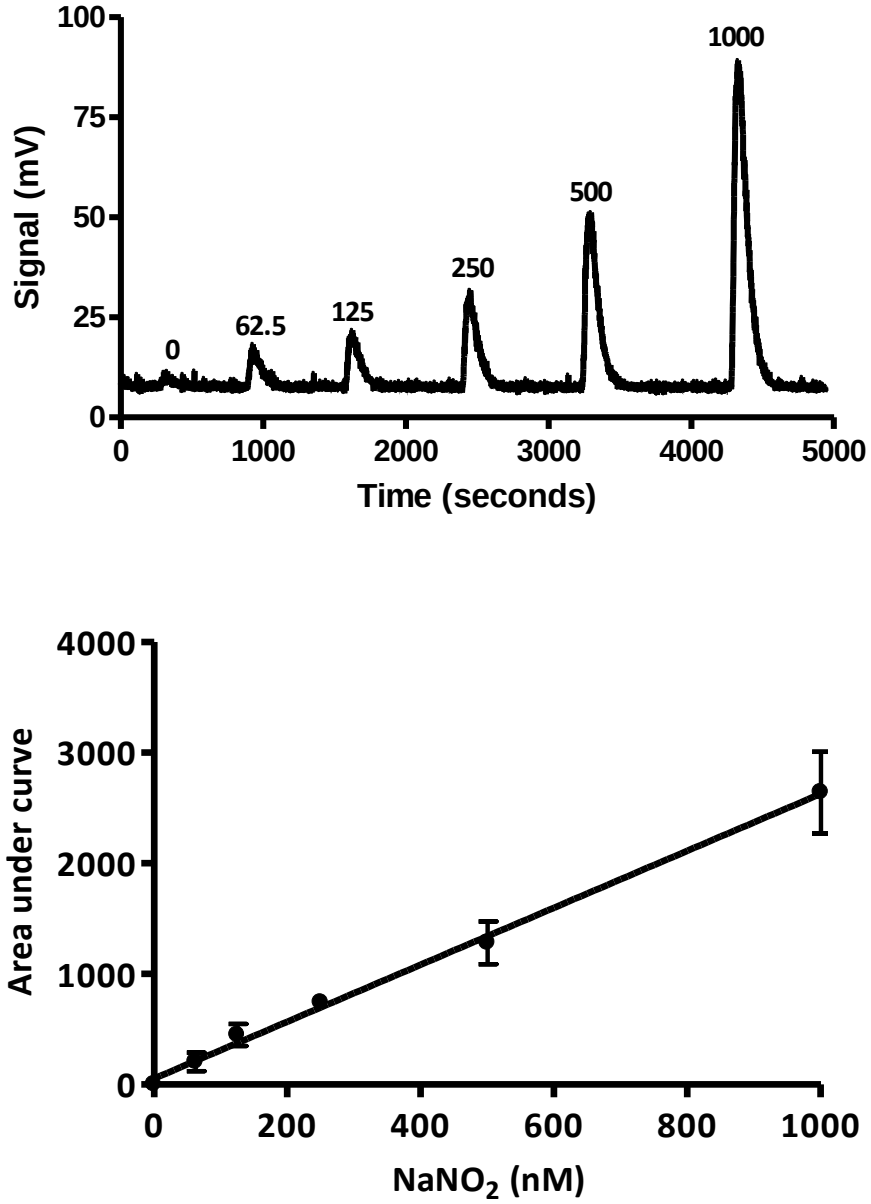

Figure 2.14: Standard curve achieved for NO_2^- in tri-iodide reagent. The top graph is the raw data plotted on the analysis program, Origin. The figures above each peak represent the concentrations of NO_2^- in nM. A typical standard curve of this data is shown underneath (n=3, r^2= 0.9703). *Linear regression*.

2.7.2.2 Reagents

Table 2.5: Reconstitution of reagents used in tri-iodide experiments.

Reagent	Method
5% Acidified Sulphanilamide	500 mg sulphanilamide + 10 ml 1N HCl, kept in the dark at room temperature.
Sulphanilamide water	1 ml 5% acidified sulphanilamide + 10ml HPLC grade water, kept in the dark at room temperature.
$HgCl_2$	67.9 mg $HgCl_2$ + 5 ml HPLC grade water, kept in the dark on ice.

The reagents listed above have been widely used in OBC in order to quantify the individual concentrations of NO-derived species within a biological sample. For the detection of species concerned herein, pre-incubation with acidified sulphanilamide removes NO_2^- over a relatively short period of time and the use of mercuric chloride selectively removes SNO (116).

2.7.2.3 Plasma

Table 2.6: Specific methods used for plasma samples.

Species	Method
RSNO/RNNO	9 parts plasma diluted in 1 part acidified sulphanilamide and incubated for 15 minutes in the dark. 200 µl injection into purge vessel.
NO_2^-/RSNO/RNNO	200 µl injection of plasma into purge vessel.

2.7.2.4 RBCs

Table 2.7: Specific methods used for RBC samples.

Species	Method
$HbNO_x$	RBC diluted in acidified sulphanilamide. 200 µl injection into purge vessel.
HbNO	9 parts of the acidified sample further diluted with 1 part $HgCl_2$. 200 µl injection into purge vessel.
Total RBC NO_x	RBCs diluted 1 in 5 with medical grade water. 200 µl injection into purge vessel.

The total RBC NO was diluted in medical grade water as opposed to injecting neat RBCs into the purge vessel. The cells were diluted for experimental accuracy of the quantification of NO. Using neat RBCs, a proportion of the sample was confined to the sides

of the purge vessel and as the RBC fraction was very viscous, the cells did not easily travel to the tri-iodide at the base of the tube. Simply attempting to inject neat RBCs directly into the tri-iodide proved fairly problematic. Therefore, diluting the RBCs by a fifth and correcting this dilution when calculating the concentration resulted in an overall more accurate result.

2.8 Statistics

The methods section of each results chapter summarises the statistical tests used. Individual experimental analyses are included in each figure legend.

3 Influence of O_2 on vascular smooth muscle under hypoxic conditions

3.1 Introduction

It is well understood that O_2 is generally a constrictor of systemic vascular tissue. In disease where O_2 may be limited, systemic vessels dilate in an attempt to increase the flow of blood to surrounding metabolically stressed tissue (266). In contrast, pulmonary vessels constrict under such conditions to prevent a decline in alveolar pO_2. This maintains the fine balance between the perfusion of O_2 across tissue beds and respiratory responses to hypoxia (267).

In terms of the local vasculature, the phenomenon of hypoxic vasorelaxation has been of interest for the past 20 years (258, 268-273). RBCs are thought to release a mediator which causes relaxation to dilate local hypoxic vessels (270). This would generally occur in the absence of disease, during an arterial to venous transit, where saturation of Hb with O_2 is high but the tissue pO_2 is low. As mentioned in Chapter 1, SNO release from the Hb moiety of RBCs has attracted much attention as well as NO_2^- reduction to NO by Hb (101, 110, 124, 274). However, investigation in our laboratory disputes these claims (275, 276). Certainly, NO_2^- in its own right has the capacity to dilate hypoxic tissue regardless of the presence of Hb, however, the kinetics of this relaxation is not coherent with the transient relaxation associated with hypoxic vasorelaxation.

The mediators proposed above as well as others (254, 277) have been extensively investigated in terms of mechanism and how they might be released from the RBCs to induce such a response. Nevertheless, none of these mediators fully satisfy the definition of acute hypoxic vasorelaxation and therefore the body of work displayed in this chapter aims to demonstrate how O_2 may not only be an important stimulus, but could be the mediator itself.

3.1.1 Aims

Based on pilot studies conducted by a previous PhD student, Dr Andrew Pinder (see Andrew George Pinder, PhD thesis, 2009), my aim was to investigate the role of O_2 in hypoxic vasorelaxation utilising the established rabbit aortic tissue model system.

The specific aims of this chapter were to:

- ✓ Compare vessel relaxation between RBCs, Hb and oxygenated KH buffer.
- ✓ Introduce varying quantities of O_2 to hypoxic aortic rings.
- ✓ Deduce the mechanism by which O_2 may be influencing vasorelaxation under hypoxic conditions.

3.1.2 Hypothesis

O_2 released from RBCs can cause relaxation of hypoxic vascular rings via the sGC-cGMP pathway.

3.2 General Methods

3.2.1 Myography

Rabbit thoracic aortae were excised and mounted as described in Chapter 2. All rings were equilibrated for 1 hour at a tension of 2 g before initial PE (1 μM) and ACh (10 μM) exercises. In order to equilibrate rabbit aortic rings to various O_2 tensions, the gas was switched to the appropriate mix and bubbled for 10 minutes in the baths. Normoxic studies referred to rings held at 95% O_2/5% CO_2 and hypoxic studies referred to rings held at 0% O_2/5% CO_2.

3.2.2 Human blood preparation

Blood was drawn from the antecubital vein as described in Chapter 2 and separated into RBC and Hb fractions (see section 2.3).

3.2.3 KH buffer sample preparation

Samples of KH buffer were prepared as described in Chapter 2 (see section 2.2.2) just before addition to the myograph.

3.3 Specific Methods

3.3.1 RBC-induced vasorelaxation

Dr Andrew Pinder performed an experiment during his PhD study within our group which highlighted the importance of RBC saturation and thus Hb allostery on this phenomenon (See Andrew George Pinder, PhD thesis, 2009). Briefly, blood was drawn from healthy volunteers into EDTA vacutainers and centrifuged at 1200 x g for 5 minutes at 4°C. The RBC fraction was diluted by approximately 1 in 10 to 3 g/dL in saline solution (0.9% w/v) and gassed with 95% O_2. The fully saturated RBCs were loaded into a thin film rotating

tonometer to achieve a range of HbO_2 saturations. 20 µl of each desired RBC sample was then carefully injected into the baths containing pre-constricted hypoxic aortic rings. Table 3.1 illustrates the extent of HbO_2 saturation as measured by the OSM3 Hemoximeter (Radiometer, Copenhagen).

Table 3.1: Summary of HbO_2 saturations of RBCs used in experiments by Dr Andrew Pinder.

Saturation	HbO_2 (%)	N
High	98.22 ± 0.45	13
Partial	51.43 ± 6.16	4
Low	20.40 ± 5.28	13

Samples were gassed with 95 % O_2 and/or 95 % N_2 to achieve the desired HbO_2 reported above.

3.3.2 A comparison of RBC, Hb and O_2

Rabbit aortic tissue was mounted in the myograph as described in Chapter 2. Following 10 minutes of equilibration to hypoxia, RBC, Hb or KH buffer samples were added to pre-constricted (3 µM PE) hypoxic vascular rings to induce relaxation (2 rings per treatment). The samples were added in a volume which would expose the hypoxic tissue to 38 µM O_2. sGC has been reported to function at concentrations between 20 and 40 µM O_2 (173), indicative of the ability of sGC to distinguish between ligands.

3.3.3 Addition of increasing O_2 to hypoxic tissue

In order to further investigate the effect of O_2 on vascular tone in hypoxia, it was key to confirm whether the effects observed were dependent upon the amount of O_2 exposed. Therefore, an experiment was conducted whereby KH buffer samples equilibrated at either 0 % O_2, 21 % O_2 or 95 % O_2 after which 200 µl was added to pre-constricted hypoxic aortic rings.

3.3.4 Inhibition of eNOS

Unless stated, all experiments involving rabbit aortic rings possess fully functioning endothelium. In order to ascertain if RBC-induced hypoxic vasorelaxation was NOS dependent, the inhibitor, L-NMMA (which competitively inhibits the generation of NO from its derivative, L-arginine) was used. L-NMMA was added to give a final concentration of 300 µM in the bath (278) and incubated with the rings for 20 minutes prior to switching the gas to favour hypoxic conditions. This particular concentration has been shown to effectively inhibit NOS function (278). The volume added did not have an effect on the baseline tension recorded. The N_2/CO_2 gas was then bubbled for 10 minutes which meant the total L-NMMA incubation time was 30 minutes. In order to verify that the inhibitor was functioning correctly, parallel experiments tested ACh-induced relaxation on rings incubated with L-NMMA. As expected, no relaxation was observed by these rings due to the inhibition of eNOS function (data not shown). After 10 minutes of equilibrating the rings to hypoxia, 3 µM PE was added to each bath and the developed tension was allowed to reach a plateau (approximately 6 minutes post addition). A bolus of KH buffer (200 µl) equilibrated with 95% O_2/5% CO_2 gas was then carefully added to the pre-constricted rings. The extent of vasorelaxation was calculated as in section 3.3.11.

3.3.5 Inhibition of sGC

To further investigate the intracellular mechanisms underlying hypoxic vasorelaxation, an experiment was conducted utilising the selective and irreversible haem moiety inhibitor of sGC, ODQ (213). ODQ has the ability to inhibit cGMP production initiated by endogenous and exogenous NO, however it does not inhibit the activity of pGC or AC (212, 213). ODQ (10 µM) was incubated with the vascular rings for 20 minutes plus a further 10 minutes whilst

the tissue equilibrated to hypoxic conditions. Following exposure to PE (3 μM), a bolus of 95% O_2 KH sample was added to the hypoxic rings.

3.3.6 Variation in tissue O_2 tension

A previous member of our group, Dr Stephen Rogers, carried out an experiment whereby fully saturated RBCs (~98% O_2) were added to isolated rabbit aortic rings pre-incubated at varied levels of ambient O_2 (unpublished work). This experiment aimed to address whether or not the extent to which vascular tissue dilates to introduction of O_2 bolus is directly related to the extent of tissue hypoxia. The results of this study are also included below and are considered critical for comparison.

3.3.7 Concentration response to NO donors

NO donors are used widely in vascular experiments to investigate the role of NO in cardiovascular physiology and pathophysiology. In this study, both NOC9 and GSNO were used as NO donors that are independent of endothelium. As detailed earlier, NOC9 has a very short half life compared to that of GSNO. The final concentrations of NOC9 used were (in M): 1 x 10^{-8}, 1 x 10^{-7}, 1 x 10^{-6} and 1 x10^{-5}. The final concentrations of GSNO used were (in M): 1 x 10^{-9}, 1 x 10^{-8}, 1 x 10^{-7}, 1 x 10^{-6} and 1 x10^{-5}. Both donor compounds were introduced in increasing concentrations into the myograph once the rings had reached a constricted plateau. The response to each concentration was allowed to reach a plateau before the next one was added.

3.3.8 ROS

The main experiment reported in this chapter is one which introduces O_2 into an essentially hypoxic environment. Although the period of hypoxia is short, the reperfusion of

O_2 into this environment may be sufficient to result in oxidative stress of the tissue, a phenomenon that has been studied at length in the context of ischaemia-reperfusion injury. To test this, a series of scavengers were used that act upon both extracellular and intracellular forms of ROS (Table 3.2).

Table 3.2: Summary of scavengers used.

Scavenger	Concentration	Site of action	Mechanism of action
SOD	100 U/ml	Extracellular	Catalyses the dismutation of O_2^- to $H_2O_2 + O_2$
PEG-SOD	100 U/ml	Intracellular/Extracellular	SOD conjugation to polyethylene glycol allows for passage through the cell membrane
MnTMPyP	10 µM	Intracellular/Extracellular	Permeates cellular membranes to catalyse dismutation of O_2^- and scavenge $ONOO^-$
PEG-CAT	250 U/ml	Intracellular/Extracellular	CAT conjugation to polyethylene glycol allows for passage through the cell membrane

All scavengers were incubated with the tissue for a total of 60 minutes, a pre-incubation time used by others (279, 280).

3.3.9 COX

With a view to understanding the mechanism of the hypoxic vasorelaxation observed, a thorough investigation of other potential pathways that could contribute to vasodilation was required. The main pathway considered here was COX. COX product, PGI_2 enhances

vasodilation by binding AC which leads to an increase in cAMP (148). Consequently, rabbit aortic rings were incubated for 30 minutes with the non-selective COX 1 and 2 inhibitor, indomethacin (10 µM), prior to constriction with PE.

3.3.10 Post-relaxation vasoconstriction

A characteristic feature of the raw data our group and others (258) obtained from hypoxic vasorelaxation experiments is that immediately following the induced period of relaxation, a vasoconstriction above that of the original constriction to PE is observed. To investigate this overshoot further, the ATP-sensitive K^+ (K_{ATP}) channel inhibitor glibenclamide (10 µM was incubated for 30 minutes with the aortic rings prior to experimentation.

3.3.11 Statistical Analysis

Hypoxic vasorelaxation was calculated by taking the maximum relaxation (see Figure 3.1) and expressing it as a percentage of the peak constriction induced by PE exposure to individual rings. Vasoconstriction was calculated in a similar manner; however the maximum constriction was expressed as a percentage of the peak constriction induced by PE. Raw data were presented as developed tensions from baseline values. Aortic rings which displayed impaired vascular function in terms of the curves achieved for PE/ACh exercises were not included in data analysis for that day.

Statistical analyses between different groups of data were compared either by using a Student's *t* test (paired or unpaired where applicable) or one-way ANOVA followed by a suitable *post-hoc* test (GraphPad Prism™ version 5.0). An n number of 1, for the majority of

experiments, is the average data of 2 paired rings. These analyses are described in complete detail within each figure legend.

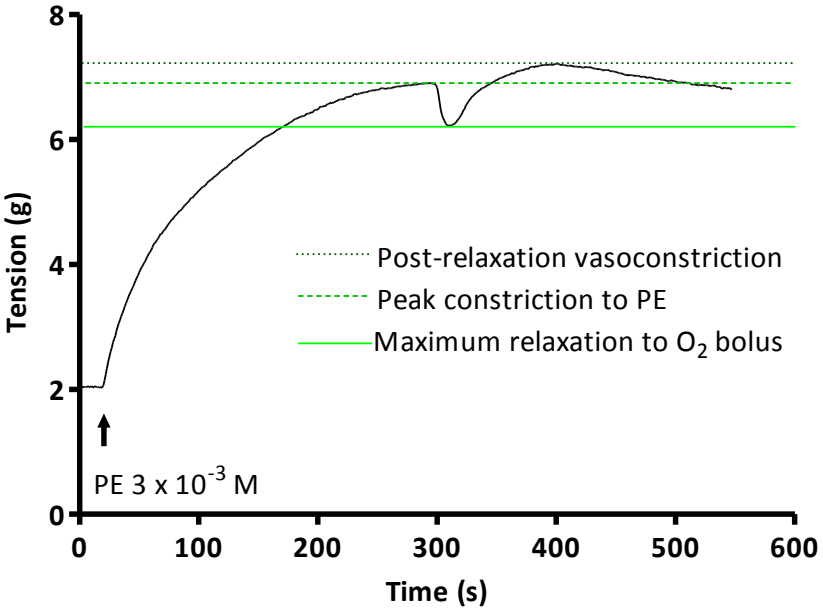

Figure 3.1: A typical raw data curve for hypoxic vasorelaxation.

3.4 Results

3.4.1 Hb Allostery

The data obtained by Dr Andrew Pinder is displayed in Figure 3.2. RBCs that were comprised of mainly R-state Hb relaxed hypoxic aortic rings significantly more than RBCs at low saturation (T-state Hb) and those that were partially saturated (a combination of R and T-state Hb). The results indicate the Hb allostery is a significant factor in the extent of relaxation displayed by hypoxic rabbit aortic rings.

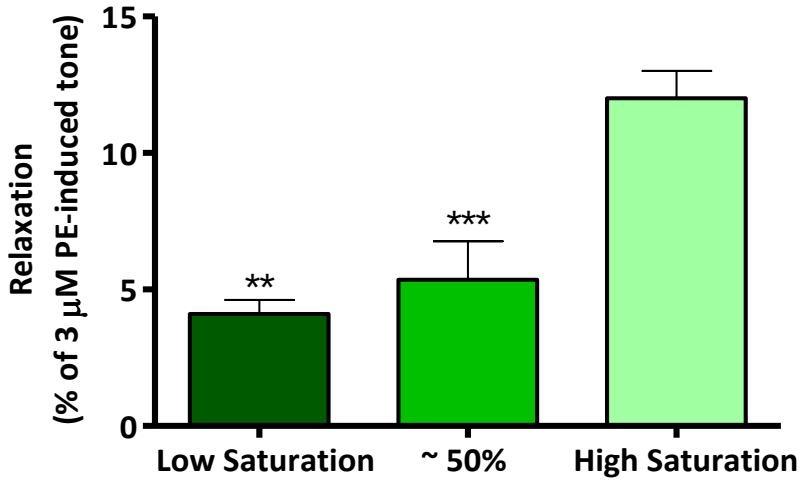

Figure 3.2: A comparison of highly saturated RBCs, partially saturated RBCs and RBCs at low saturation. Highly saturated RBCs relaxed hypoxic tissue to a greater extent than partially saturated RBCs and RBCs at low saturation (12.00 ± 1.00 % vs. 5.38 ± 1.42 % and 4.11 ± 0.51 %, respectively) (**p<0.01, ***p<0.001). *One-way ANOVA + Bonferroni's multiple comparison test. Reproduced with the permission of Dr A Pinder.*

3.4.2 Comparison of RBC, Hb and O_2

Data obtained by our group as well as others have shown that RBC can relax hypoxic vascular rings (101, 106, 248, 251, 254, 259, 271, 281). Since the RBCs that were being introduced to the hypoxic tissue were fully oxygenated, i.e. ~ 98 % HbO_2 saturation, a positive control would be needed to match the amount of O_2 within the RBCs, without the

RBCs physically present. Therefore, the rationale for the experiments in this section aimed to include an appropriately oxygenated control in the form of KH buffer equilibrated at ~ 95% O_2. As illustrated in Figure 3.3a, RBCs, Hb and KH buffer injected into the myograph with equivalent O_2 contents produced comparable relaxations. Figure 3.3b shows the same data in graphical form and is an average of 4 experiments.

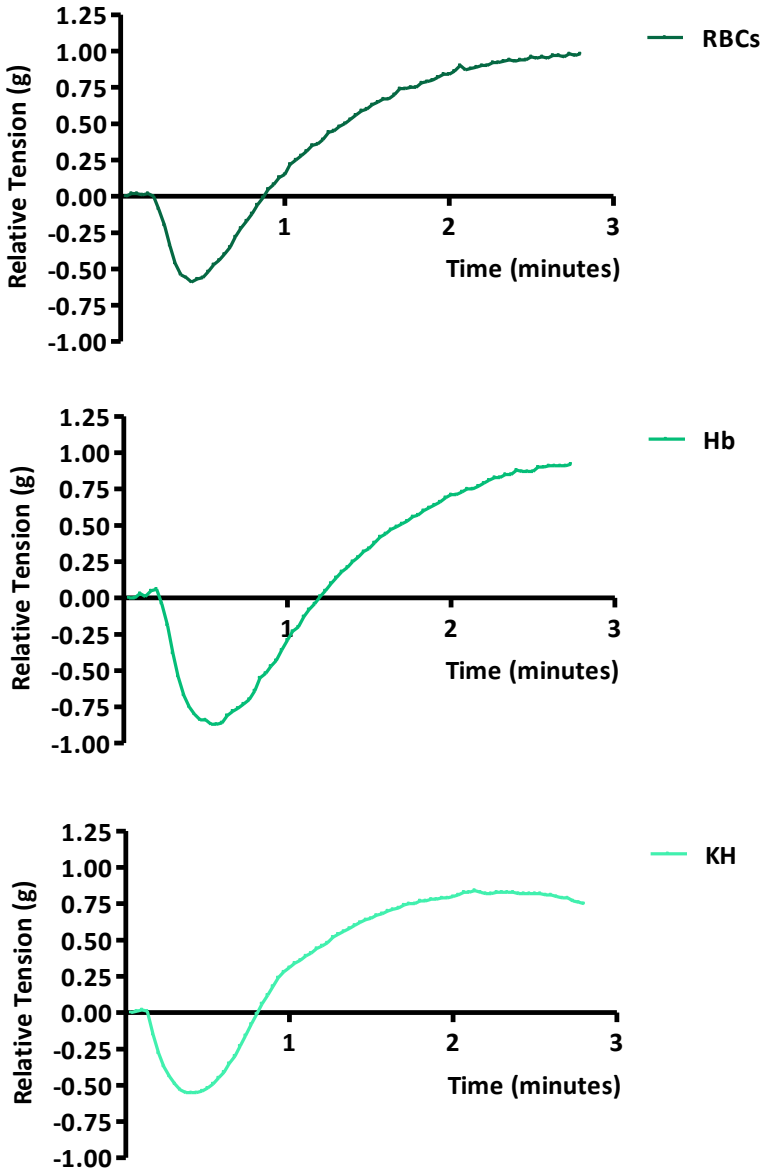

Figure 3.3a: Raw data curves depicting the relaxation and post-relaxation vasoconstriction to RBCs (top), Hb (middle) or KH buffer (bottom). All samples exposed the aortic rings to 38 µM O_2.

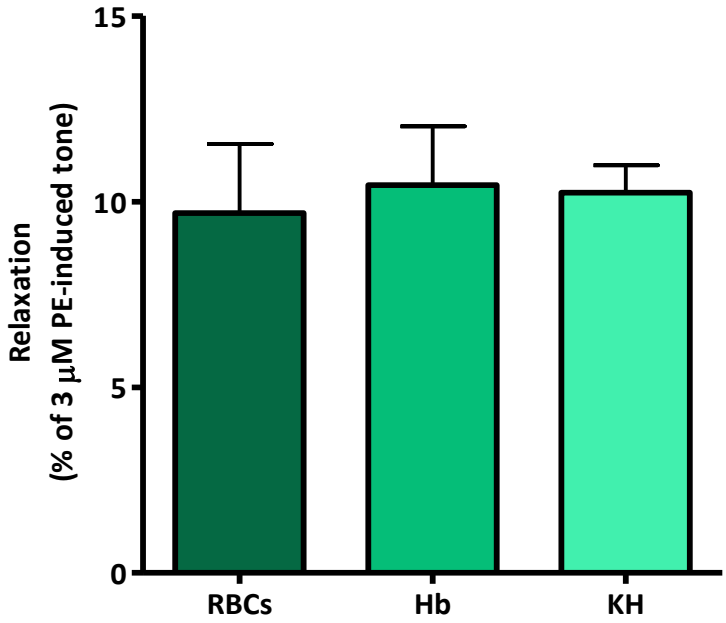

Figure 3.3b: Graphical summary of the raw data curves shown in Figure 3.3a. There was no difference in the magnitude of relaxations produced (n=4, p>0.05*) One-way ANOVA + Tukey's multiple comparison test.*

3.4.3 Effect of increasing O_2 on relaxation

The data shown in Figure 3.2 suggested the importance of Hb allostery in the degree of relaxation induced by RBCs. To examine whether this effect was a RBC effect or rather was proportional to the extent of O_2 delivery per se, KH buffer samples containing increasing O_2 contents were added to hypoxic aortic rings. Figure 3.4 illustrates that a similar effect is seen with KH buffer alone when appropriately oxygenated and ensuring delivery of the same package of O_2 to hypoxic tissue.

This experiment was completed in parallel with an equivalent number of rings in normoxia (95% O_2). The addition of these KH buffer samples to an already normoxic bath did not relax the tissue.

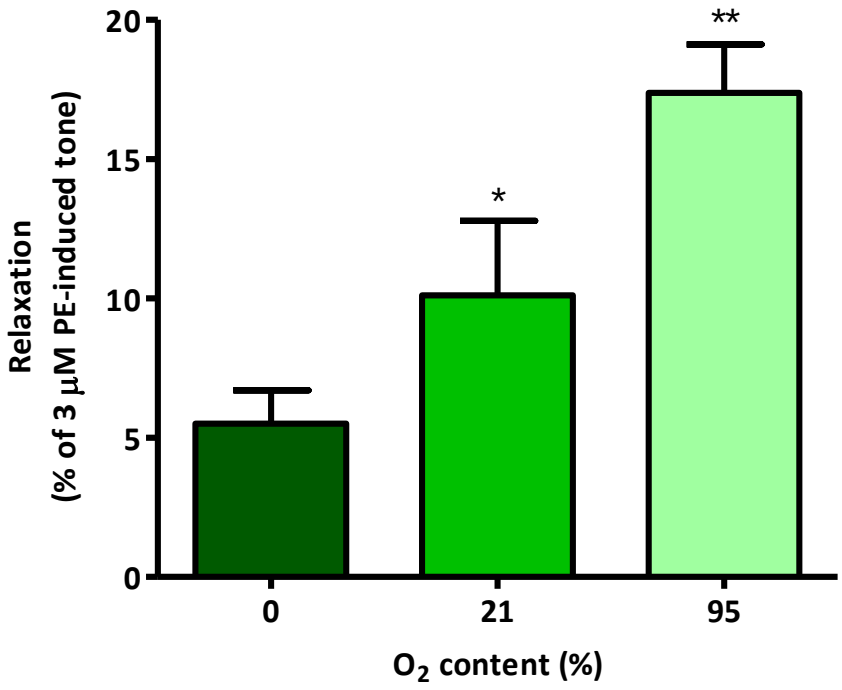

Figure 3.4: Relaxations produced by increasing O_2 content in KH buffer samples. As the KH buffer sample O_2 content increased, the relaxations produced also increased. Significant differences were observed between 0% and 95% samples (**p<0.01) and 21% and 95% samples (*p<0.05) (n=6) *One-way ANOVA + Tukey's multiple comparison test*.

3.4.4 Variation in tissue O_2 tension

As described above, Dr Stephen Rogers conducted an experiment whereby tissue O_2 tension of the rings was varied within the myograph, followed by the addition of fully oxygenated RBCs to the system.

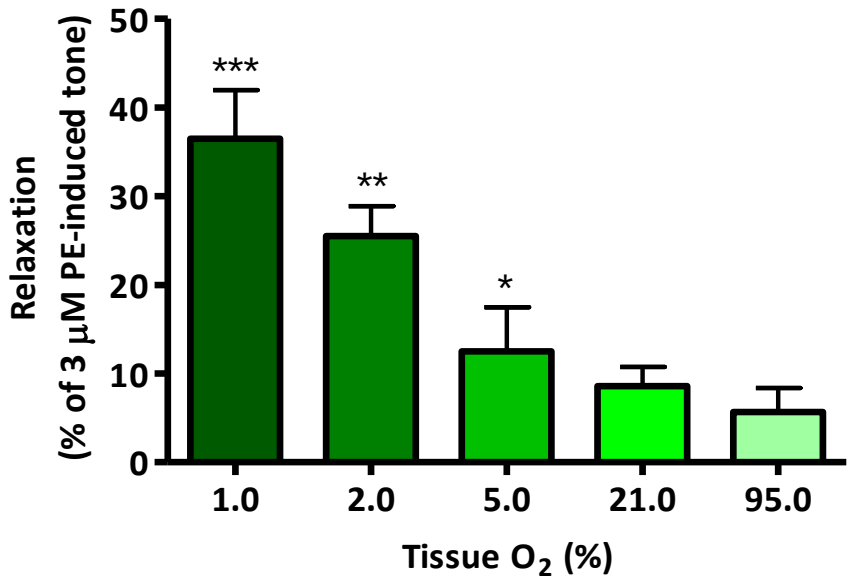

Figure 3.5: Effect of increasing tissue O_2 content on the magnitude of relaxation to RBCs. As the O_2 tension of the tissue increases, the relaxation induced by RBCs decreases. Significant differences in relaxation are observed for 1, 2 and 5% O_2 compared to 95% O_2 (***p<0.001, **p<0.01 and *p<0.05, respectively) (n=6) *One-way ANOVA + Newman Keuls post hoc test. Reproduced with the permission of Dr S Rogers.*

The data displayed in Figure 3.5 shows that the ability of fully oxygenated RBCs to induce relaxation of hypoxic rabbit aortic rings depends on the amount of O_2 already present within the tissue/surrounding milieu. Therefore, the less 'hypoxic' the tissue to begin with, the more diminished the effect induced by RBCs.

3.4.5 Pharmacological inhibition of eNOS

To ascertain whether endothelial-derived NO had an influence on the relaxation driven by O_2-containing samples, L-NMMA was pre-incubated with the aortic rings prior to experimentation as described in section 3.3.4. Figure 3.6 portrays the effects of this inhibitor on vasorelaxation of hypoxic aortic rings.

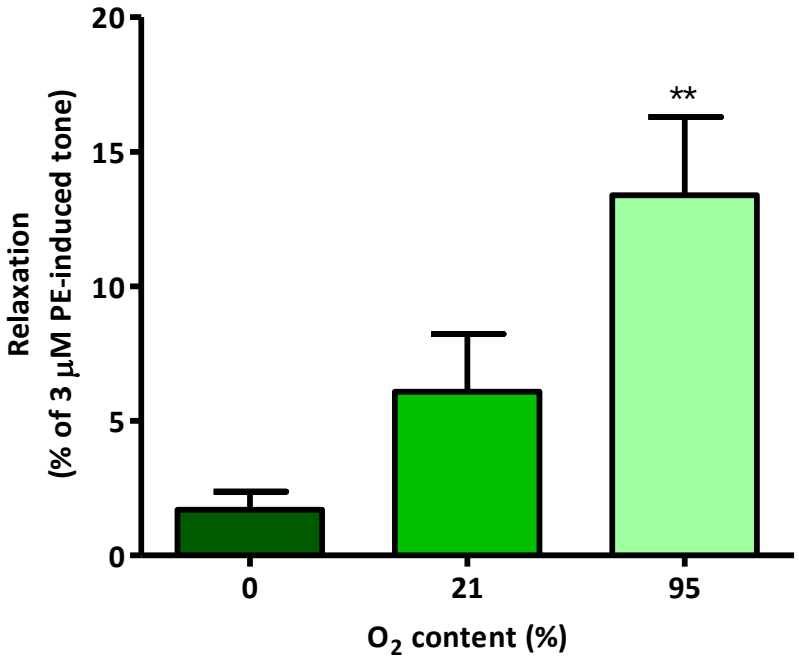

Figure 3.6: Relaxations produced by increasing O_2 content in KH buffer samples in the presence of 300 µM L-NMMA. A significant difference was observed between 0% and 95% samples (**p<0.01) (n=3-4) *One-way ANOVA+ Tukey's multiple comparison test.*

L-NMMA appears to have no effect on the relaxations induced by the KH buffer samples suggesting that endothelial-derived NO (from NOS) is unlikely to be involved in the mechanism of hypoxic vasorelaxation.

3.4.6 sGC

Previous literature has suggested that the enzyme, sGC, plays a major role in mediating hypoxic vasorelaxation. Therefore, in order to confirm the role of sGC in these experiments, an inhibitor of the catalytic haem moiety, ODQ (10 µM), was pre-incubated with the aortic rings as described in section 3.3.5.

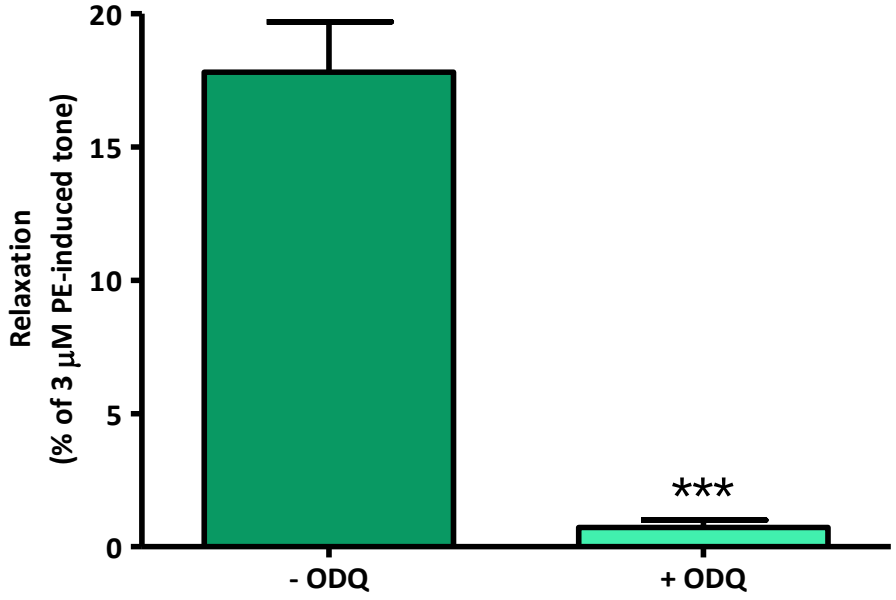

Figure 3.7: The effect of sGC haem inhibitor, ODQ, on O_2-mediated relaxation. The inhibition by ODQ (10 μM) almost abolished the effect of O_2 on the hypoxic aortic rings (17.51 ± 1.90 % vs. 0.72 ± 0.28 %) (***p<0.001) (n=7) *Paired t test.*

The results illustrated in Figure 3.7 confirm the importance of sGC in the relaxation induced by O_2 alone. The pre-incubation of ODQ (10 μM) with the aortic rings inhibited the relaxation by around 95% of the paired control. This data also suggests that the mechanism largely involves the smooth muscle as opposed to the vascular endothelium.

3.4.7 Effect of NO donors on normoxic and hypoxic tissue

This study also aimed to characterise the effect of hypoxia on the release of NO from two NO donors, NOC9 and GSNO.

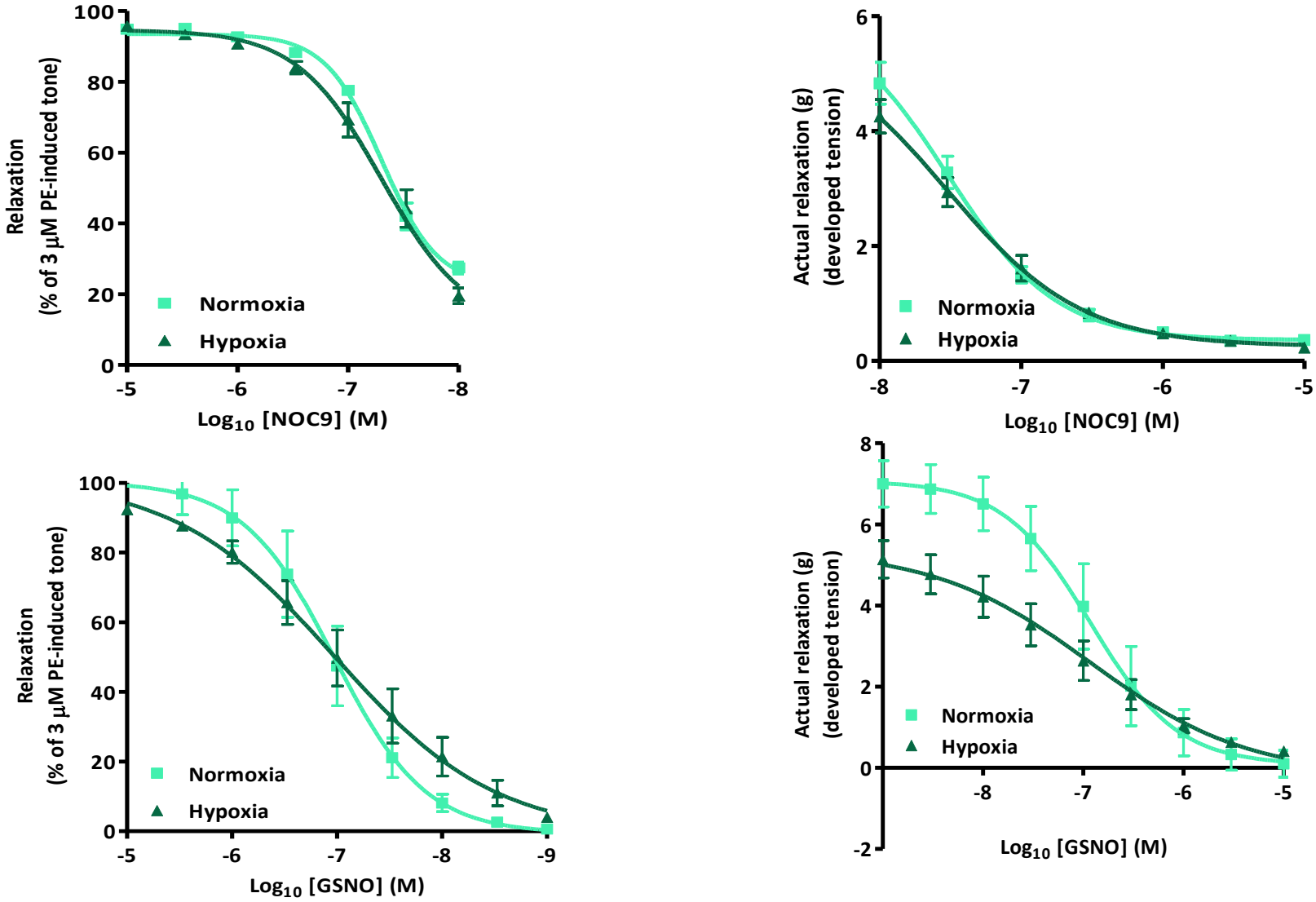

Figure 3.8: Concentration response curves to NOC9 (top) and GSNO (bottom). Evaluation of the pEC_{50} values (negative log of EC_{50}) for normoxia and hypoxia show that both NOC9 and GSNO show no significant differences (see Table 3.3) ($p>0.05$) (NOC9 n=3-8, GSNO n=4) *Non-Linear regression.*

Figure 3.8 presents the concentration response curves to NOC 9 (top) and GSNO (bottom). The calculated % relaxation data is shown on the left and the raw data is shown on the right.

Table 3.3: pEC_{50} values for each NO donor under normoxic and hypoxic conditions.

Conditions	pEC_{50} (M) from % relaxations		pEC_{50} (M) from raw tension in g	
	NOC9	GSNO	NOC9	GSNO
Normoxia	7.28	6.95	7.51	6.91
Hypoxia	7.59	7.07	7.60	7.10

The pEC_{50} values presented in Table 3.3 confirm that the comparison of NOC9 or GSNO in normoxia and hypoxia are not significantly different.

3.4.8 Inhibition of ROS

Inhibitors of O_2^- and H_2O_2 were pre-incubated with rabbit aortic rings in order to determine if the level of sGC activity (as measured by changes in cGMP level) was altered by these compounds.

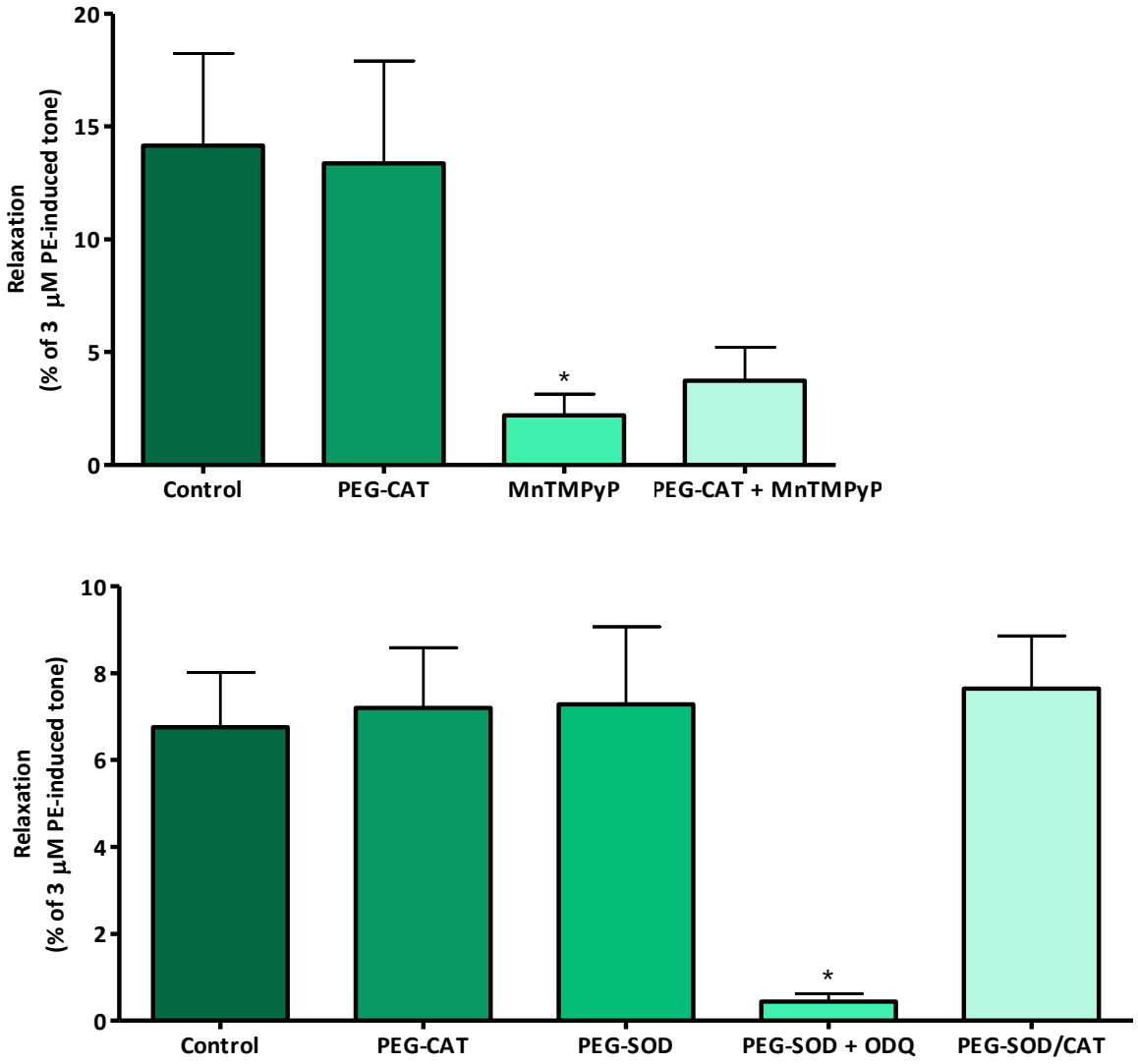

Figure 3.9: Vasorelaxation to 95% O_2 KH samples in the presence of various ROS inhibitors. Top: PEG-CAT (250 U/ml) had no effect on relaxation however the SOD mimetic, MnTMPyP (10 µM) significantly reduced the relaxation (n=5, *p<0.05). Bottom: PEG-SOD (100 U/ml) had no effect however in the combination with ODQ almost abolished any relaxation observed (n=3, *p<0.05) *One-way ANOVA + Dunnett's multiple comparison test.*

Pre-incubation with PEG-CAT, PEG-SOD or the combination of the two scavengers had no effect on the magnitude of the relaxation compared to control rings. Prior incubation with MnTMPyP dampened the relaxatory effect of KH samples. Furthermore, rings incubated with ODQ in addition to PEG-SOD displayed little relaxation to KH buffer samples (Figure 3.9).

3.4.9 Inhibition of COX

Aortic rings were exposed to indomethacin (10 μM) for a total of 30 minutes, in which during final 10 minutes, rings were exposed to hypoxic conditions as described previously (section 3.2.1).

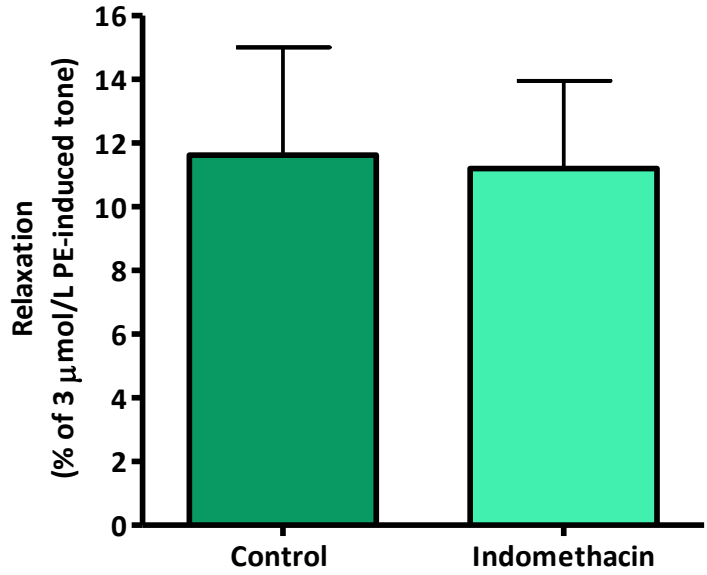

Figure 3.10: Vasorelaxation of hypoxic aortic rings in the absence and presence of COX inhibitor, indomethacin (10 μM). The drug had no effect on the magnitude of relaxation compared to the control (11.20 ± 2.75 % vs. 11.62 ± 3.39 %) ($p>0.05$) (n=4) *Paired t test*.

The results of this study show that inhibiting COX and therefore vascular effects of PGI_2 had no effect upon the relaxation induced by KH buffer samples (Figure 3.10).

3.4.10 Post-relaxation vasoconstriction – Inhibition of K_{ATP} channels

In hypoxic vascular experiments (section 3.4.2) a post-relaxation vasoconstriction above that of the maximum PE-induced constriction was consistently achieved in each experiment. Glibenclamide was pre-incubated with the vascular rings in an attempt to inhibit the potential role of K_{ATP} channels in this phenomenon.

Figure 3.11 illustrates the results of this experiment. Glibenclamide almost completely eliminates any post-relaxation constriction elicited by the hypoxic vascular rings.

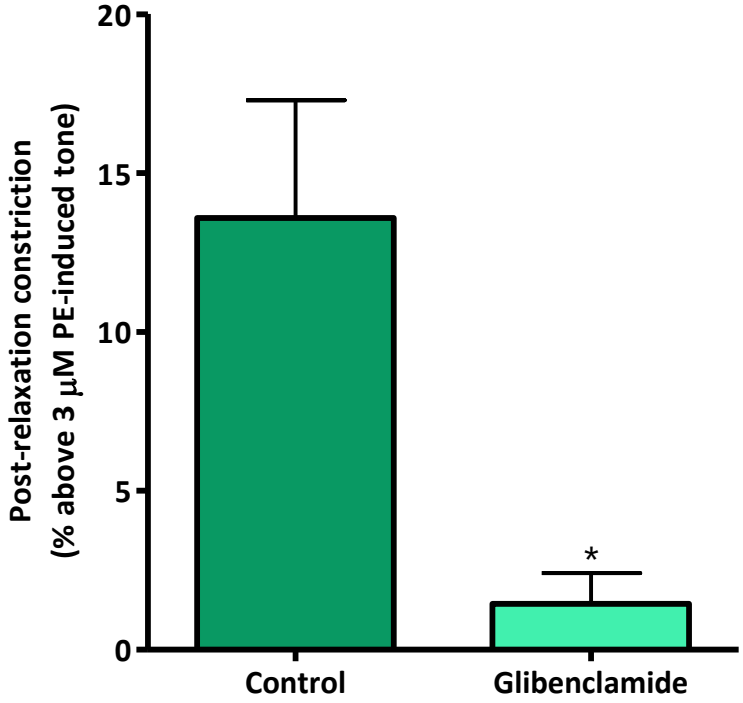

Figure 3.11: Post-relaxation vasoconstriction in the absence and presence of K_{ATP} channel inhibitor, Glibenclamide (10 µM). Glibenclamide reduced the degree of constriction ~9-fold compared to the control (13.59 ± 3.71 % vs. 1.45 ± 0.97 %) (p=0.0144) (n=3-4) *Unpaired t test*.

3.5 Discussion

3.5.1 Summary

The main findings of this chapter are:

I. RBCs with a high O_2 saturation induced a greater relaxation of hypoxic aortic rings than RBCs with a low O_2 saturation.

II. Purified oxygenated Hb induced relaxation of hypoxic aortic rings to a similar extent as RBC.

III. Oxygenated KH buffer induced relaxation of hypoxic aortic rings. When normalised for O_2 content, KH buffer exhibited equal relaxation capacity.

IV. The relaxations observed were sGC-dependent and endothelial NO-independent.

V. The magnitude of the relaxation was also inversely proportional to the tissue PO_2.

3.5.2 Chapter Review

Hypoxic vasorelaxation has attracted considerable interest in the NO field over the past two decades. A number of groups globally have suggested several mediators, none of which fully address the fundamental physiology of this response. The results obtained by Dr Andrew Pinder, (included in this chapter for illustration purposes), demonstrate Hb allostery to be of significance in terms of the magnitude of relaxation displayed by hypoxic aortic rings. Previously, similar experiments by Stamler's group have interpreted the increase in R state Hb to translate to an enhanced formation of HbSNO, leading to an increased level of free NO^+ in the bloodstream upon deoxygenation (124). Whilst this is physiologically feasible, there are two main caveats as to why this may not be the primary method of vasodilation. Firstly, Stamler and colleagues investigated the levels of T state bound HbNO versus R state bound HbSNO in this experiment (258). There was no observed decrease in

the level of HbNO upon oxygenation. This is somewhat surprising considering the shift in Hb allostery following RBC oxygenation. Secondly, Patel and colleagues conducted a knockout mouse study whereby the cysteine residue at position 93 on the β chain of Hb was replaced by an alanine residue (101). As highlighted earlier, this is the primary residue thought to release SNO from Hb to promote relaxation. *In vitro* myography experiments conducted with aortae from these knockout mice revealed that hypoxic vasorelaxation was still elicited in these vascular rings, demonstrating that SNO release from the RBC at this residue may not contribute to hypoxic vasorelaxation. This does not escape the fact that RSNO, including HbSNO, exhibit direct vasorelaxant properties. Rather, they are unlikely to mediate the acute hypoxic vasorelaxation studied herein.

The NO_2^- reduction theory proposed by Gladwin and colleagues (101, 248) has also been debated (258). Although the possibility exists for transnitrosation reactions to allow the free NO produced to leave the RBC, the levels of NO that could potentially escape are questionable. In addition, the theory was based on experimental conditions that were non-physiological. Supraphysiological concentrations of NO_2^- were used *in vitro* as well as a low haematocrit of Hb, promoting high rates of NO_2^- reduction and relatively low Hb scavenging of NO (248). Consequently, the conditions of the experiments used would need to be reconsidered in order to justify the theoretical claims. A recent study conducted by our laboratory further disputes Gladwin's hypothesis. As mentioned, their main study involved relatively large doses of $NaNO_2^-$ administered to human subjects, resulting in enhanced vasodilation and increased levels of HbNO (248). In our hands (116), administration of physiological concentrations of exogenous NO_2^- (100-300 nM) does not affect the levels of HbNO within RBCs under both hypoxic and normoxic conditions, indicating that perhaps

little NO reaches the inside the cell. These inconsistencies in data clearly present an issue for studies conducted using non-physiological concentrations of NO_2^-.

In order to investigate the nature of the mediator(s) involved, RBCs were first diluted and haemolysed before being loaded on a Sephadex column to purify the Hb. Importantly, our group (259), as well as others in early studies (124, 272), did not account for the O_2 content of the RBCs and so in the present studies the O_2 content was equalised in the form of a quantity of oxygenated buffer to act as a positive control. The degree of vasorelaxation was remarkably similar for RBCs, Hb and buffer of equalised O_2 content. These findings questioned the existing theories behind hypoxic vasorelaxation that perhaps were overshadowing a more simple answer. In order to address this, all further studies largely focussed on utilising oxygenated buffer as the primary method of inducing vasorelaxation.

As detailed earlier in this discussion, RBC samples containing an increased HbO_2 saturation promoted a greater degree of relaxation of hypoxic aortic rings. To test whether controlling the O_2 content of oxygenated buffer had the same effect, KH buffer was gassed to 0, 21 and 95% O_2 and added to hypoxic aortic rings. The samples produced very comparable relaxations to that of RBCs and corresponding purified Hb samples, indicative of an O_2-mediated influence over smooth muscle tone under hypoxic conditions.

Dr Stephen Rogers conducted an experiment to illustrate that varying tissue O_2 tension alters the effect of RBC samples on hypoxic vascular smooth muscle. Increases in tissue oxygenation lead to a reduction in relaxation responses. Physiologically, this certainly seems reasonable since tissues that already have a supply of O_2 do not need to dilate to the same extent in order to acquire an increased O_2 supply from the bloodstream.

A role for ATP-dependent release of endothelium-derived NO in mediating hypoxic vasorelaxation (254) would also seem to be refuted by the data presented in this thesis and in past literature (258). While a slight decrease in the maximum relaxation to 95 % O_2 compared to controls (~14% vs. 17%) in the presence of L-NMMA may suggest a small influence of endothelial-derived NO, however this seems unlikely since L-NMMA was pre-incubated with the rings in excess. L-NMMA incubation eliminates the possibility of all types of NOS, in mediating this relaxation and therefore is not just limited to endothelial dependent mechanisms. Indeed experiments performed with endothelium-denuded vascular rings further demonstrate that the mechanism underlying hypoxic vasorelaxation is solely limited to the vascular smooth muscle (258). That blood ATP concentration rises relatively slowly in relation to a decline in HbO_2 saturation and as such does not mirror the observed transient relaxation response described above, suggests that ATP may play a more significant role in chronic hypoxia as opposed to the acute RBC-induced relaxation.

The NO-sGC-cGMP pathway is the primary mechanism of vasodilation in vascular smooth muscle (170). To confirm that sGC was the principal enzyme acting in these hypoxic studies, experiments using the haem inhibitor, ODQ, were performed. The data confirmed that the sGC pathway did indeed mediate the vasodilation described herein. Interestingly, numerous studies in past literature suggest that O_2 does not bind to sGC (181, 202, 203). NO is widely regarded as the primary activator (168, 202, 282), though CO (283) can also bind but does not fully activate the enzyme. However, the data presented here clearly indicates that there may be an influence of O_2 upon sGC activity and that this interaction must be directly or indirectly related to the haem site of sGC since ODQ almost completely abolished vasorelaxation.

It is possible that the ability of O_2 to stimulate sGC depends on the concentration of O_2 already present at the tissue level. Indeed, lack of O_2 may alter (increase) the sensitivity of sGC to its primary activator, NO. Comparison of the concentration response curves for NOC9 and GSNO in normoxic and hypoxic conditions illustrated that there was not a significant difference between the release of NO at various O_2 tensions. However, analysis of the pEC_{50} in hypoxia shifted to the left compared to normoxia. Such an action may be due to a higher affinity/sensitivity of sGC to NO under hypoxic conditions compared to normoxic conditions where O_2 may be occupying 'free' sGC (143) and so partially prevents NO from binding. This represents a totally novel action for O_2 in the regulation of sGC activity with far reaching consequences in both health and disease. The experiments performed in this chapter could be seen as replicating a non-pathological form of reperfusion injury, in which essentially normal hypoxic vessels are reperfused with highly oxygenated blood (284). Importantly, free radicals are often formed under these conditions. Therefore, SOD, CAT and MnTMPyP were used as pharmacological tools to investigate the role of such species in the observed hypoxic relaxation responses. The data collected following pre-incubations with SOD and CAT suggested that there was no influence of O_2^- or H_2O_2 respectively, on vasorelaxation. However, in contrast pre-incubation with the cell permeable SOD mimetic, MnTMPyP, substantially diminished the relaxation responses and as such would indicate a significant influence of intracellular O_2^- or H_2O_2 in hypoxia. Evidence from the literature would suggest otherwise, given that MnTMPyP can in fact directly inhibit the function of sGC in the smooth muscle (285). In retrospect, it is therefore considered highly unlikely that free radicals underlie the O_2-mediated relaxation responses described herein. Potentially several other free radical scavengers could have been investigated including 5,10,15,20-tetrakis-[4-sulfonatophenyl]-porphyrinato-fer[III] (FeTPPS), a $ONOO^-$ scavenger and

decomposition catalyst (286) or histidine, which acts as a singlet O_2 scavenger (287). However, the concentrations of SOD and CAT investigated here have been widely used in similar experiments (279, 280) and therefore it is unlikely that other oxy radicals could have altered the cGMP levels achieved.

The results outlined in this chapter undoubtedly support sGC activation as the main pathway of vasorelaxation under hypoxic conditions. However, to rule out the possibility of further pathways being involved, namely COX-mediated PGI_2 signalling, experiments were performed in the presence of indomethacin. There was no significant difference between indomethacin treated and control tissues, confirming that the relaxations observed were not PGI_2-mediated.

The raw tension traces presented herein consistently exhibited (Fig 3.3a) two different components; acute vasorelaxation and post-relaxation vasoconstriction. As discussed, the central premise is that O_2 alone can relax the hypoxic vessels, a fact that is supported by the use of KH buffer controls. With regard to the mechanism underlying the post-relaxation vasoconstriction, Stamler and colleagues (1992) have previously suggested that this is due to the scavenging of NO by Hb which ultimately leads to constriction through decreased NO bioavailability. However, the results within this chapter suggest an alternative explanation involving ATP-sensitive potassium (K_{ATP}) channels. In the presence of intracellular ATP these channels are closed (288, 289). However, in hypoxia, mitochondria in the vascular smooth muscle have a suppressed ability to turnover ATP and in the presence of lower intracellular levels of O_2, some of the K_{ATP} channels may remain open, leading to hyperpolarisation and vasodilation. Exposure to O_2 would initiate the formation of ATP and subsequent closure of K_{ATP} channels, leading to vasoconstriction. Interestingly, in the presence of glibenclamide,

which inhibits K_{ATP} channels leading to their closure, the post-relaxation vasoconstriction is reduced. Therefore it is likely that O_2 directly affects the closure of K_{ATP} channels on the smooth muscle cell membrane during this phase.

3.5.3 Conclusions

The results presented in this chapter provide substantial evidence for an O_2-mediated mechanism underlying hypoxic vasorelaxation. Convincing arguments, supported experimentally, propose an alternate view to the theories previously put forward. Importantly, much of this data has recently been published (290) and supports the findings of all the chapters in this thesis. Taken together, the myography experiments have shown that oxygenated KH buffer alone can relax hypoxic rabbit aortic rings in an endothelial NO-independent, sGC-dependent mechanism. The magnitude of the relaxation to O_2 produced is dependent upon the tissue pO_2 and the amount of O_2 provided to the tissue.

4 Modification of sGC activity in normoxia

4.1 Introduction

4.1.1 sGC

sGC is central to the main pathway for regulating smooth muscle tone as described in Chapter 1. NO is the primary ligand for the enzyme (168) however other diatomic molecules such as CO can also enhance the activity of sGC (291).

The conclusions drawn from the experiments detailed in Chapter 3 provide substantial evidence for an O_2-mediated sGC-dependent mechanism underlying RBC-induced vasorelaxation. In order to further investigate this potential interaction between O_2 with sGC, experiments were designed to investigate how O_2 affects cGMP production following stimulation of sGC with various activators and stimulators.

4.1.2 Stimulators & Activators of sGC

A comprehensive review by Evgenov and colleagues (2006) explained that novel drugs developed to enhance the activity of sGC fall broadly into two categories, stimulators and activators (178). Stimulators were defined in the following terms, *'stimulate sGC directly and enhance sensitivity of the reduced enzyme to low levels of bioavailable NO'*. Activators, *'activate the NO-unresponsive, haem oxidised or haem free enzyme'*. Three types of NO-independent drugs will now be considered in more detail as they were utilised in this study to provide very different modes of sGC activation/modulation.

4.1.2.1 YC-1

YC-1, a benzyl indazole derivative, was first discovered by Yoshina and colleagues in 1978 (292) and initially utilised as a potent inhibitor of platelet aggregation (293). Since then, YC-1 has been shown to stimulate sGC independently of NO as well as having the

capacity to potentiate the effect of CO on the enzyme (294). Interestingly, spectra resulting from soret band analysis of unstimulated and stimulated sGC were not altered by the presence with YC-1 (294). This suggests that YC-1 activates via an allosteric site distal to the classic ligand binding site. YC-1 has also been shown to bind to haem-free sGC which further supports this hypothesis.

YC-1 was used in the studies presented herein in order to gain more clarity into the site at which O_2 affects the activity of sGC. YC-1 has been shown to potentiate the effect of CO on sGC and therefore, experiments reported here aimed to investigate O_2 in a similar manner.

4.1.2.2 BAY 41-2272

In the late 1990's to early 2000's, pyrazolopyridine, BAY 41-2272 was developed and shown to stimulate Cys238 and Cys243 regulatory sites on the α-subunit of sGC (295). Importantly, BAY 41-2272 stimulates the enzyme via an NO-independent mechanism while retaining the ability to potentiate NO and CO activity at the haem site (295). Furthermore, Stasch and colleagues also discovered that BAY 41-2272 was not able to stimulate haem free enzyme, illustrating that the compound acts in a haem-dependent manner. Soret band analysis of sGC in the presence or absence of NO demonstrated that there was no change in the spectral peak for NO in the presence of BAY 41-2272, suggesting that although haem-dependent, the compound does not directly bind the haem moiety. In terms of its clinical use, BAY 41-2272 reduces mortality in the low NO hypertensive rat model as well as lowering blood pressure and also has profound anti-platelet effects (178). BAY 41-2272 was used in the studies reported in this chapter in order to determine the haem-dependence of the effect of O_2 on sGC.

4.1.3 Aims

Having established that O_2 in the form of an oxygenated KH buffer bolus could relax vascular hypoxic rings via the sGC pathway, subsequent experiments aimed to further characterise the mechanisms by which O_2 influences sGC.

The specific aims of this chapter were to:

- ✓ Characterise the influence of O_2 upon sGC activity in the presence of various direct activators and modulators.
- ✓ Investigate the interaction of NO with sGC under normoxic and hypoxic conditions.

4.1.4 Hypothesis

Purified sGC can be stimulated directly by O_2 to stimulate cGMP production.

4.2 General Methods

4.2.1 Purified enzyme experiments

As outlined in Chapter 2 (section 0), the human $\alpha_1\beta_1$ form of the enzyme was reconstituted in 'enzyme buffer' before being diluted as appropriate for each sample. All experiments were performed at 37°C inside the hypoxic chamber (Ruskinn). Reagents and experimental vials were equilibrated in hypoxic conditions for at least 60 minutes prior to initiating the reaction with GTP/$MgCl_2$. All reactions were terminated by the addition of boiling inactivation buffer.

4.2.1.1 Enzyme Assay validation

Various sGC/buffer ratios were initially tested however the sGC/buffer ratio used in all experiments reported here was 1 in 200 (personal communication, Prof. Garthwaite, UCL,

London). Analysis of cGMP using the R&D ELISA system at this sGC/buffer meant that all tests (controls and stimulated samples) were within the range of the supplied standards.

4.2.2 cGMP ELISA

The R&D Parameter kit was used to measure the activity of sGC throughout all the experiments in this chapter. The main method is summarised in Chapter 2 (section 2.6).

4.2.3 Nitric Oxide Analyser (NOA)

The NOA was set up as described in section 2.7. In this case, PBS was used in place of a cleavage reagent (typically tri-iodide), given that NOC9 spontaneously liberates NO under neutral pH (1 mol NOC9 liberates 2 mols NO) with a $t_{1/2}$ of ~ 3 mins.

4.3 Specific Methods

4.3.1 Activity of sGC under normoxic and hypoxic conditions

In order to observe the direct effects of O_2 upon sGC, the enzyme was diluted 200 times in assay buffer in 1 ml glass vials. It was then incubated in the Invivo$_2$ hypoxic chamber for 60 minutes at either 20 % O_2/5 % CO_2 ('normoxia') or 0 % O_2/5 % CO_2 ('hypoxia') at 37°C. The initiation mix of GTP and $MgCl_2$ at equimolar concentration (1 mM) was then added to each vial and after gentle mixing, the samples were incubated for a further 10 minutes. Boiling inactivation buffer was added in 4 times excess to each vial and heated until the samples reached boiling point. The samples were then placed on ice and divided into aliquots and snap frozen in liquid N_2. Samples were stored at -20°C if not assayed on the day of experimentation. All frozen samples were assayed within 1 week of collection.

4.3.1.1 Activity of sGC under hyperoxic conditions

As an extension to the experiments described above (section 4.3.1) and to relate the findings to myography studies already completed, sGC was also incubated at 95 % O_2/5 % CO_2 (hyperoxia) for 10 minutes, in the presence of GTP/$MgCl_2$. A 0 % sample was also prepared as the hypoxic control. This experiment was performed in a water bath (outside the hypoxic chamber) sustained at 37°C.

4.3.2 O_2 consumption by sGC in vitro

To investigate whether the purified sGC utilised O_2, EPR spectroscopy was used to assess any changes in O_2 over time. As highlighted in detail in section 2.5.1, the spectral line width is used to report on the presence of O_2 within a sample. sGC was diluted in assay buffer to concentrations of either 50 µM (identical concentration used in all other experiments within this chapter) or 100 µM, as well as N^{15}-PDT (20 µM) and GTP/$MgCL_2$ (1 mM). A control of assay buffer of N^{15}-PDT (20 µM) and GTP/$MgCl_2$ (1mM) was used as a control. All samples were initially at atmospheric O_2 levels (~21 %) until the sample tube was sealed and quickly transferred to the cavity of the EPR spectrometer. A scan was then performed (Bruker escan) every 10 minutes over a period of 60 minutes for each sample. The settings for EPR were as described in Table 2.3 for 21 % O_2 equilibrated samples.

4.3.3 Inhibition of free radicals

In a similar approach to the *in vitro* myography experiments detailed in Chapter 3, it was also important to verify that free radical interactions with sGC did not account for the changes in cGMP production. As such sGC was incubated with SOD (100 U/ml), CAT (250 U/ml) or the two inhibitors combined for 60 minutes prior to the addition of GTP/$MgCl_2$.

Samples were then inactivated and tested for the presence of cGMP by ELISA in the same way as previous experiments.

4.3.4 Effect of NOC9 upon sGC activity in normoxia and hypoxia

As described above, NO is the primary ligand for sGC and potently activates the enzyme to increase the production cGMP. To examine how O_2 affected the production of cGMP following exposure to a NO donor, sGC was incubated for 10 minutes in normoxia or hypoxia with the following concentrations of NOC9 (in µM): 0; 0.118; 1.118; 11.8 and 118. After incubation, samples were immediately inactivated with inactivation buffer and analysed for cGMP by ELISA.

4.3.5 Release of NO from NOC9 under normoxic and hypoxic conditions

The experiment summarised in section 4.3.4 examined how O_2 affected the sGC-mediated cGMP production following exposure to a NO donor. In order to appropriately account for how O_2 might affect NO release from NOC9 per se, PBS at pH 7.4 was kept at 37°C in a reaction vessel purged with a flow of N_2 gas feeding into a NOA for on-line OBC detection of NO. NOC-9 was reconstituted in sodium hydroxide (NaOH) (0.1 M) to give a final stock concentration of 24 mM and kept on ice in the dark. For the experimental samples, the NOC-9 was further diluted in 1 ml of PBS (protected from light in a sealed vessel) to give the following final concentrations (in µM): 2.4; 1.2; 0.24; 0.12 and 0.024. In order to compare NO release under different conditions, the PBS was either pre-equilibrated to 0% or 95% O_2 by vigorous bubbling. Samples were incubated for 10 minutes at 37°C, after which 200 µl of the gas layer was drawn up using a Hamilton syringe and injected immediately into the purge vessel for OBC analysis. After the signal trace returned

to baseline values, 200 µl of the corresponding PBS sample was drawn up and injected into the purge vessel.

4.3.6 sGC activation

4.3.6.1 YC-1

YC-1 was used to investigate where on sGC that O_2 exerts its effects. The experiment was set up as described in section 4.2.1. YC-1 was added to each vial to achieve a final concentration of 100 µM. GTP/$MgCl_2$ was then added to initiate the reaction. After a 10 minute incubation, boiling inactivation buffer was added to terminate the reactions and these samples were then tested for the presence of cGMP by ELISA.

4.3.6.2 BAY 41-2272

Bayer healthcare have developed several activators/stimulators of sGC, some of which are used within the clinic. Riociguat® (BAY 41-2272) administered in tablet form is used to treat pulmonary hypertension (296-298). Following personal correspondence with Dr Andreas Knorr in Wuppertal, Germany, samples of BAY 41-2272 (available commercially) were obtained. Concentration response curves to these agents were produced in the isolated enzyme system in order to acquire a better understanding of how O_2 may be affecting sGC activity in their presence. Subsequently, the basic experiment was set up as outlined in section 0. BAY 41-2272 was utilised at the following concentrations based on previous methods (299, 300): 100 µM; 10 µM; 1 µM; 100 nM; 10 nM and 1 nM. This compound was added prior to the 10 minute incubation with GTP/$MgCl_2$. Following incubation, samples were inactivated as described in previous sections and analysed for cGMP content.

4.3.7 Statistical Analysis

cGMP was quantified as a measure of sGC activity. Chapter 2, section 2.6.5.1, shows a typical standard curve obtained from an assay. The concentrations of cGMP in the unknown samples were interpolated from the non-linear standard curve (GraphPad Prism™ version 5.0). A new standard curve was generated for each experimental day. The cGMP content within samples was compared by an unpaired Student's *t* test. All data is expressed as the mean ± standard error. Differences were considered significant where $p < 0.05$.

The data generated by EPR oximetry was analysed by recording the spectral line width (the difference between peak maximum and minimum in magnetic field units (mG) – see Figure 2.5) and comparing to the standard line widths obtained from this probe in N_2 and O_2.

The OBC signal was analysed by quantifying the area under the curve for each peak using the 'Liquid' software program (Analytix Ltd).

4.4 Results

4.4.1 Effect of O_2 on sGC

The data analysed from the cGMP assay confirmed that O_2 alone enhanced the activity of sGC and subsequent production of cGMP (Figure 4.1). These experiments were undertaken without addition of classic sGC stimulators. Perfusing the enzyme with 95 % O_2/5 % CO_2 (hyperoxia) further enhanced this production hyperoxia (411.50 ± 56.30 pmol/ml) in comparison to normoxic levels.

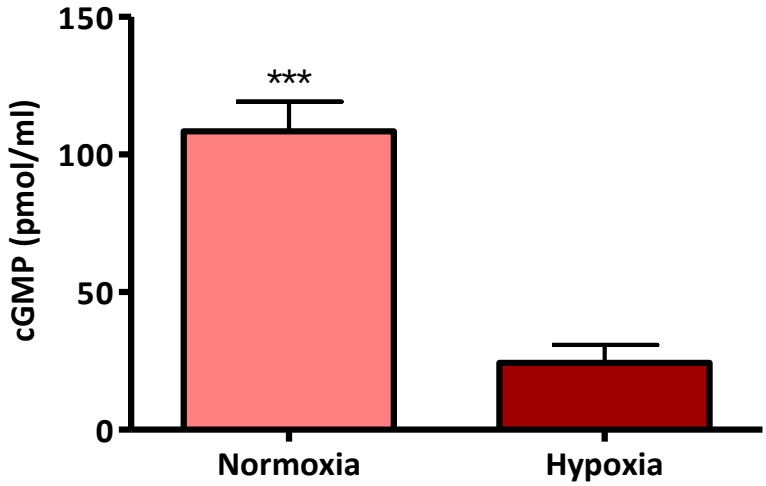

Figure 4.1: Effect of O_2 upon sGC activity. cGMP production was significantly greater for normoxia (108.40 ± 10.78 pmol/ml) and compared with hypoxia (24.34 ± 6.52 pmol/ml) following a 10 minute incubation post GTP/$MgCl_2$ addition (***p<0.001) (n=4-6) *Unpaired t test*.

4.4.2 Change in O_2 consumption over time by sGC – An EPR study

EPR was used to measure the O_2 change in a buffer solution containing sGC (plus GTP/$MgCl_2$) over time. Figure 4.2 presents the control samples for this study which contained either assay buffer alone (GTP) or assay buffer containing GTP/$MgCl_2$ (+GTP) (1 mM). As shown, the line widths of three separate samples for each test were comparable.

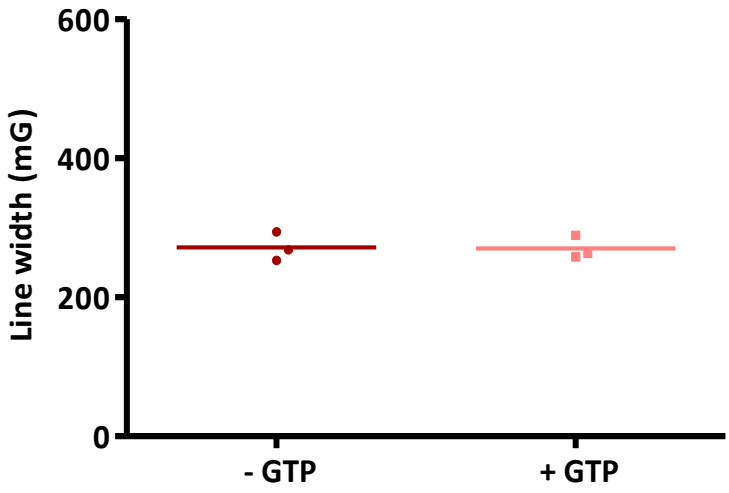

Figure 4.2: Measurement of line width following a 10 minute incubation in the presence or absence of GTP/$MgCl_2$ without sGC. The presence of GTP/$MgCl_2$ did not affect line width in the absence of the enzyme. ($p>0.05$) ($n=3$) *Paired t test.*

Following on from the control experiment with GTP, sGC was then introduced at 50 µM and 100 µM to investigate whether sGC can in fact 'consume' O_2 within the assay buffer (~21 % O_2), over a 60 minute time period. The results are displayed in Figure 4.3.

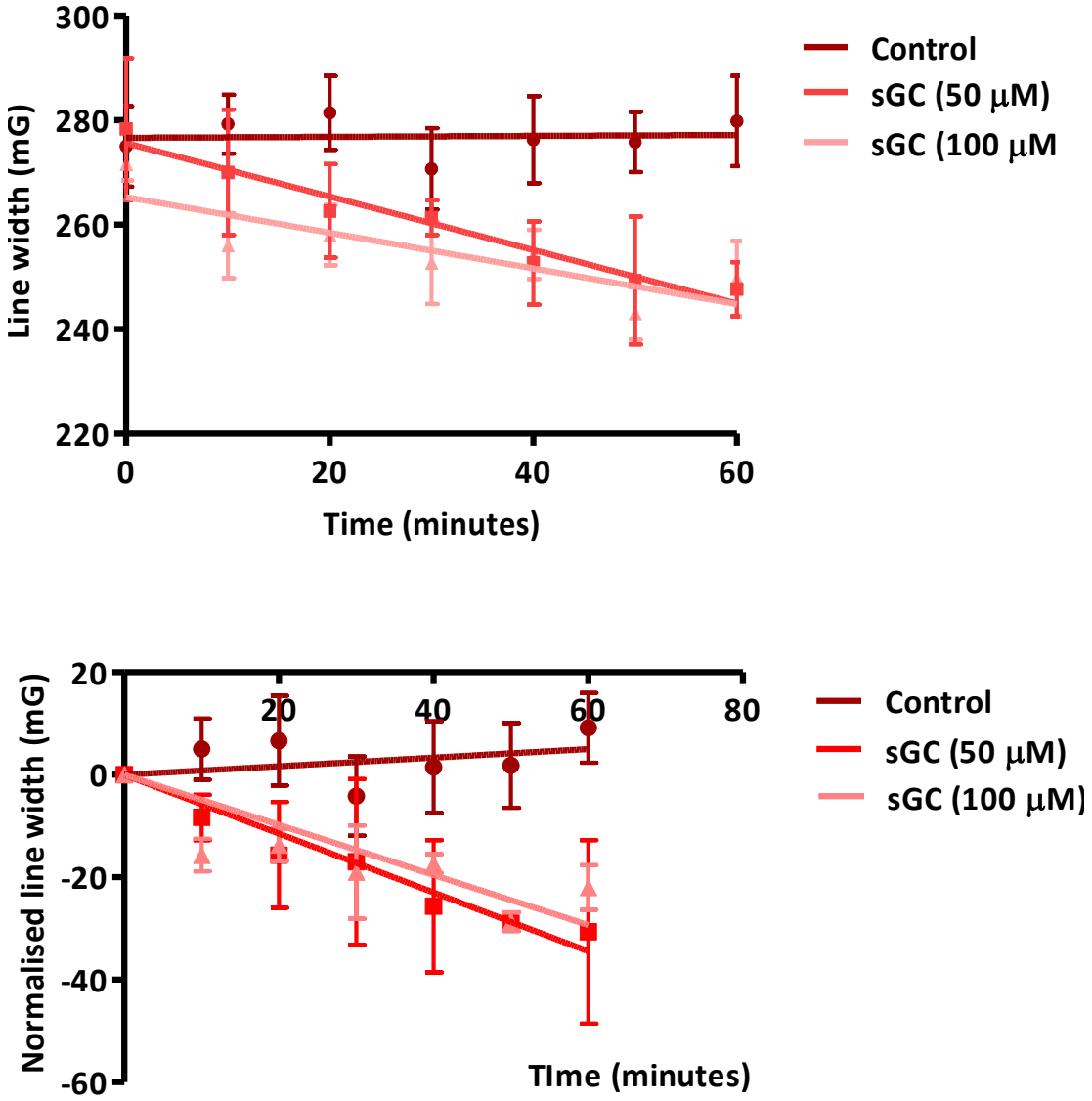

Figure 4.3: Effect of sGC on EPR spectral line width. The top graph represents the absolute raw values attained, the bottom graph is normalised for the line width at 0 minutes. The line width of the controls (210 µM O_2) were consistently stable over a 60 minute period (n=7). For both sGC concentrations, the line width decreased over time (n=3). There was a difference between the tests and controls when comparing the averaged data sets. *Linear regression*.

Figure 4.3 shows that the presence of sGC within an oxygenated sample decreases the line width of the spectrum obtained for O_2 sensitive spin-label, N^{15}-PDT. Samples containing both 50 and 100 µM sGC decreased the line width over time however, when comparing EC_{50} data, only samples containing 100 µM sGC were deemed statistically significant compared to control samples ($p = 0.0136$) (Figure 4.4).

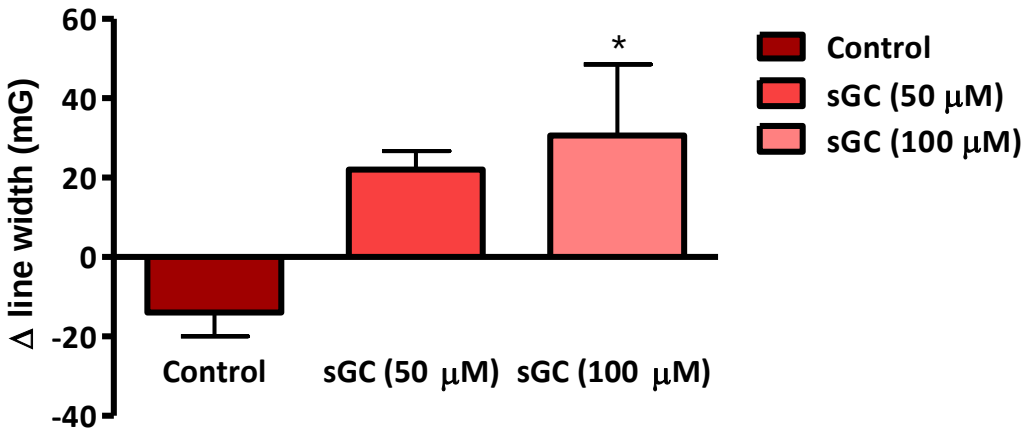

Figure 4.4: Change of line width over the 60 minute incubation during EPR spectroscopy. Samples containing 100 μM sGC displayed the largest decline in line width and therefore represented the greatest consumption of O_2 compared to the buffer controls (210 μM O_2) (n=3-6) (*$p < 0.05$) *One way ANOVA + Tukey's multiple comparison test.*

In terms of the amount of O_2 consumed, both samples containing sGC with oxygenated buffer displayed a reduction of between 20-25 mG. Based on the standard curves achieved for EPR oximetry (section 2.5.2), this would equate to around a 20 μM O_2 consumption.

4.4.3 Inhibition of Free Radicals

Experiments conducted for this section of work utilised SOD (100 U/ml) and CAT (250 U/ml) to inhibit potential generation of O_2^- and H_2O_2, respectively. cGMP was measured as described previously.

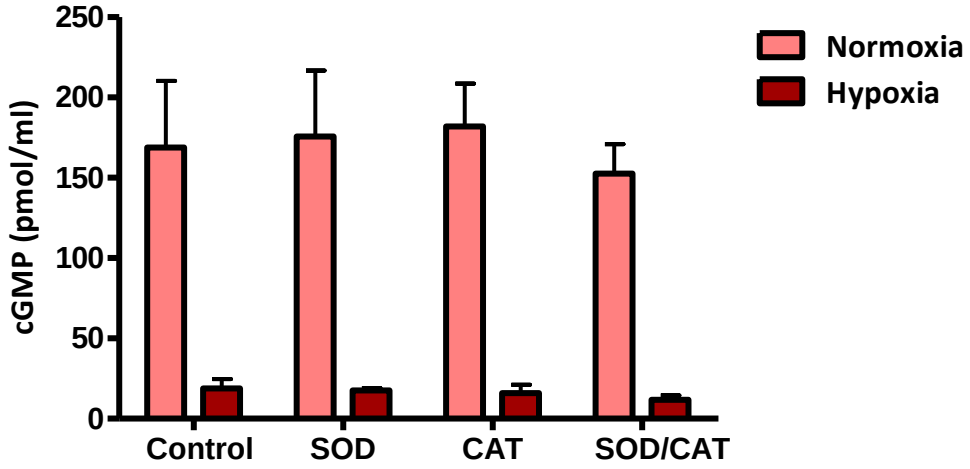

Figure 4.5: Inhibition of O_2^- and H_2O_2. There were marked differences across all groups between normoxia and hypoxia (***p < 0.05) however there was no difference in cGMP production within groups (n=3-4) *Two-way ANOVA + Bonferroni post test*.

As the data in Figure 4.5 suggests, there was no difference in cGMP production between control and test samples.

4.4.4 Influence of NOC9 on sGC activity

sGC was incubated with various concentrations of NOC9 under either normoxic or hypoxic conditions. The results are displayed in Figure 4.6.

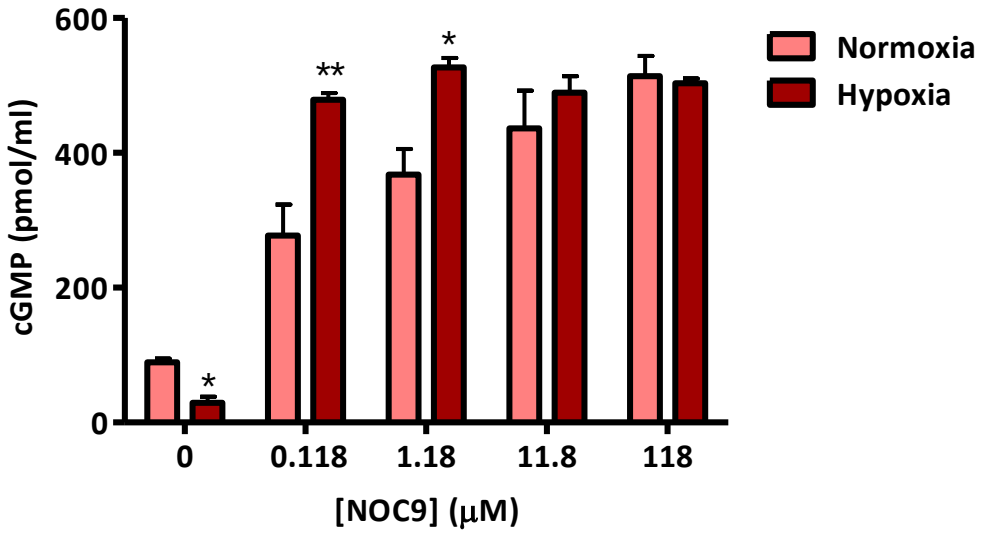

Figure 4.6: Effect of NOC9 on sGC activity in normoxia and hypoxia. Lower concentrations of NOC9 in hypoxia (0.118 and 1.18 μM NOC9) induced a greater production of cGMP than in normoxia, except in the absence of NOC9 (*p<0.05, **p<0.01) (n=3-6) *Two-way ANOVA + Bonferroni post test*.

NOC9 stimulated sGC to maximal activity in hypoxia even at the lowest concentration tested. In contrast, similar concentrations of NOC9 added in normoxia demonstrated increased cGMP with increased NOC9 added. However, it is important that whereas maximal activity was recorded at 0.118 μM in hypoxia, only 50 % activity was observed at this concentration in normoxia. At the highest concentration of NOC9 tested, maximal cGMP production was also observed in normoxia.

4.4.5 NOA: Release of NO by NOC9 in normoxia and hypoxia

Figure 4.7 illustrates that NO release from NOC9 increases in a linear fashion as the concentration of NOC9 in the sample increases. There were no differences between the slopes when normoxic and hypoxic data was compared.

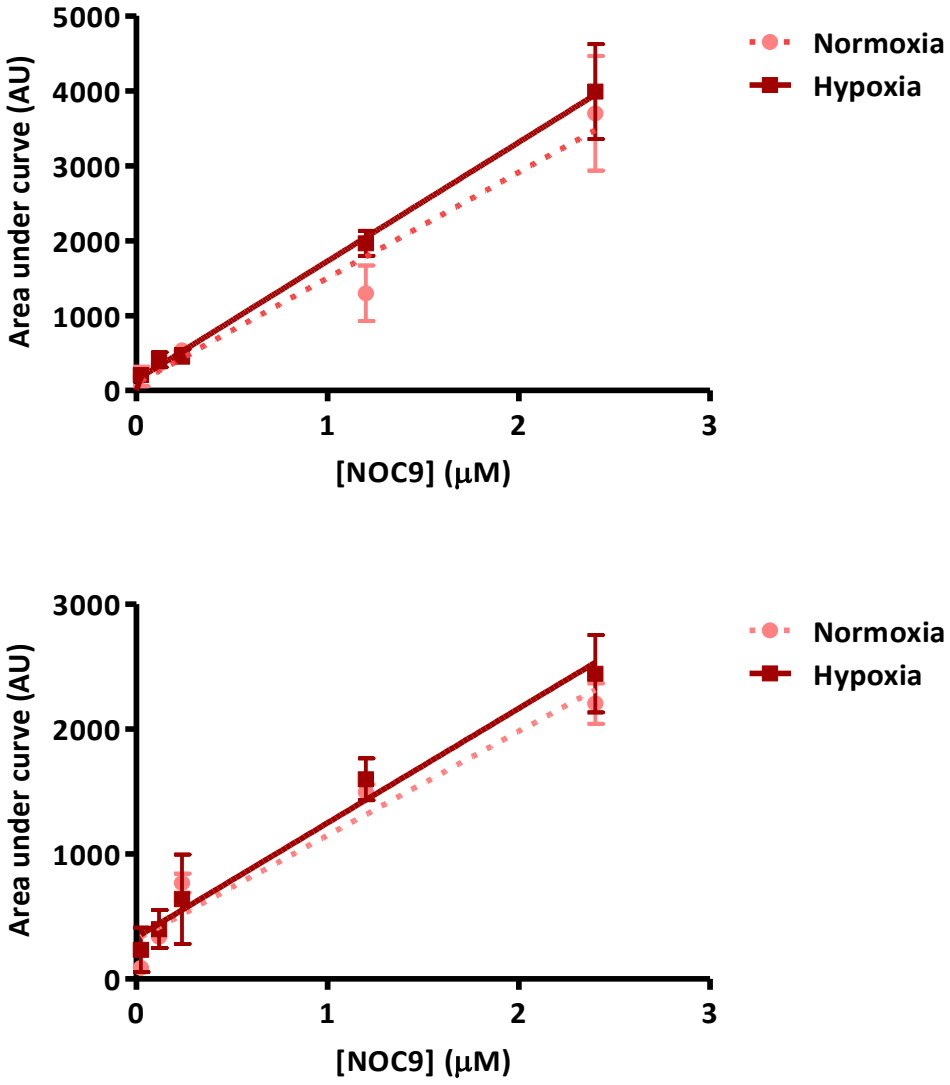

Figure 4.7: Release of NO from NOC9 under normoxia and hypoxia. Samples taken from both the gaseous phase (top) and liquid phase (bottom) following 10 minute incubation at 37 °C with NOC9 demonstrated a clear increase in the area under the curve with increasing NOC9 concentrations. The amount of NO released did not change between normoxic and hypoxic conditions for both gas and liquid samples ($p>0.05$) (n=3) *Linear regression*.

4.4.6 Effect of YC-1 on cGMP production

As explained in section 4.1.2.1, YC-1 binds to sGC via an allosteric site, promoting the stimulation of cGMP. Figure 4.8 depicts the levels of cGMP obtained for sGC incubated in the presence of YC-1 versus controls.

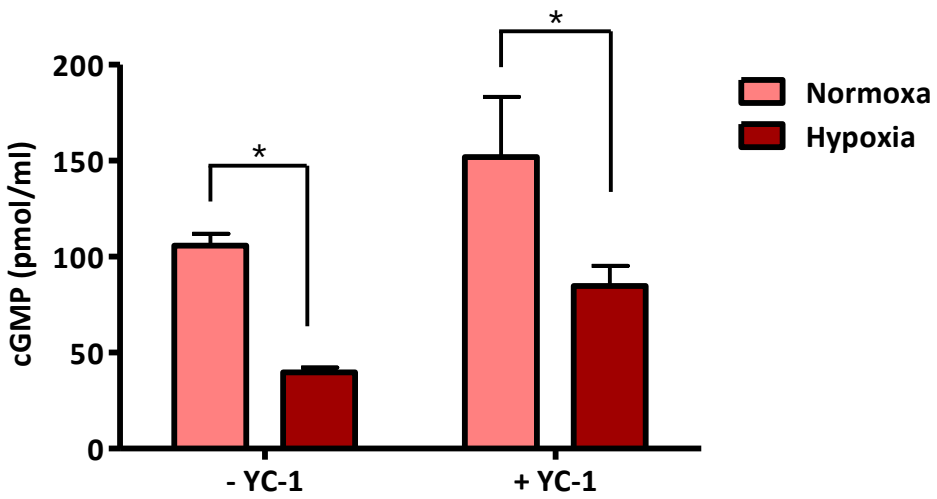

Figure 4.8: The effect of YC-1 on cGMP production under normoxic and hypoxic conditions. YC-1 enhanced the production of cGMP under both experimental conditions. Control samples (- YC-1) contained a significant amount more cGMP under normoxia compared with hypoxia (105.70 ± 6.23 pmol/ml vs. 39.82 ± 2.50 pmol/ml) (*p<0.05). The presence of YC-1 increased the cGMP production in normoxia versus hypoxia (*p<0.05) (n=4) *Two-way ANOVA + Bonferroni post test*.

Under both normoxic and hypoxic conditions, the presence of YC-1 enhanced the production of cGMP by approximately 50 pmol/ml. This suggests that the mechanism of action of YC-1 was independent of the presence of O_2. Moreover, in terms of the percent gain in cGMP levels, YC-1 in hypoxia increased 100% compared to the control. However, in normoxia, the presence of YC-1 increased the level of cGMP by 50% compared to the relative control value.

4.4.7 BAY 41-2272

BAY 41-2272 developed by Bayer® was used in this study in order to investigate how and where O_2 may be exerting its influence on sGC. Figure 4.9 displays the cGMP produced from samples stimulated with BAY 41-2272 under normoxic and hypoxic conditions. BAY 41-2272 stimulated a concentration-dependent increase in cGMP under hypoxic conditions. However in normoxia, even the weakest concentration of the drug maximally stimulated the enzyme. This suggests BAY 41-2272 activity is enhanced by O_2.

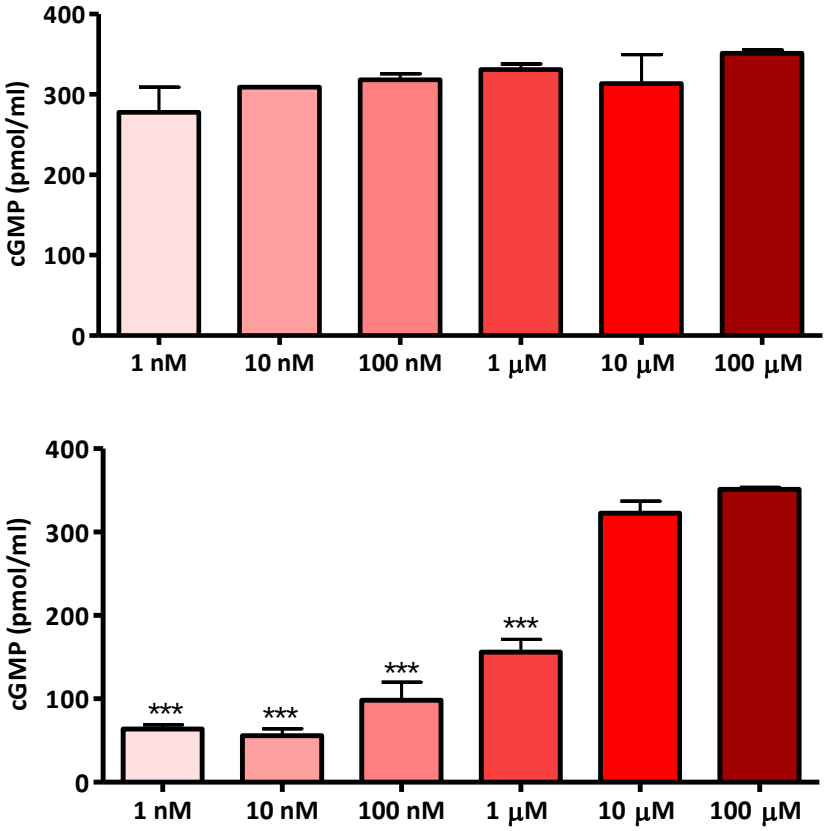

Figure 4.9: Concentration response curves to BAY 41-2272 in normoxia (top) and hypoxia (bottom). In hypoxia, BAY 41-2272 stimulates a concentration-dependent increase in cGMP; the lower concentrations between 1 nM and 1 µM stimulating significantly less cGMP production than 100 µM of the drug (***p<0.001) (n=3 for all) *One-way ANOVA + Tukey's multiple comparison test.*

4.5 Discussion

4.5.1 Summary

The main findings of this chapter are summarised below:

I. O_2 alone can increase the activity of sGC leading to a subsequent increase in cGMP production.

II. The level of cGMP produced is proportional to the amount of O_2 supplied to the enzyme.

III. sGC appeared to consume/utilise O_2 from the oxygenated assay buffer (as measured by EPR oximetry).

IV. Under hypoxic conditions, sGC was more sensitive to activation by NOC9 compared to normoxia.

V. YC-1 enhanced the production of cGMP to a similar extent in normoxia and hypoxia relative to control levels.

VI. BAY 41-2272 displayed a concentration-dependent increase in cGMP production under hypoxic conditions yet under normoxic conditions, the lowest concentration of BAY 41-2272 maximally activated the enzyme.

4.5.2 Chapter Review

As a progression of the work described in Chapter 3, the experiments detailed within this chapter aimed to determine whether O_2 alone had the capacity to stimulate/activate sGC directly. In previous literature, the interaction of sGC and O_2 has largely been dismissed (202, 301-304). These studies suggested that in order for human sGC to interact with O_2, a tyrosine residue needs to be present within the haem binding pocket of the enzyme. In contrast, the obligate anaerobe (killed by normoxic (21 %) levels of O_2),

Thermoanaerobacter tengcongensis, possesses a haem domain which can bind O_2 (304), much like a variety of other H-NOX family members (172, 305). Based on these findings, it would seem as though direct binding to the haem moiety of human sGC by O_2 as a direct ligand was unlikely. Nonetheless, O_2 could still potentially interact with the enzyme via an allosteric binding site or perhaps indirectly influence the activity of the haem site. Bearing this in mind, the experiments conducted aimed to address the haem-dependence of the O_2 effect, as well as show how O_2 affected the interaction of a variety of sGC stimulators and activators.

The novel experiments reported here were conducted with purified sGC enzyme equilibrated to hypoxic or normoxic conditions within a hypoxia workstation. The O_2 content within these samples was validated by EPR oximetry (see Chapter 2) in order to verify that hypoxic samples contained little or no O_2. sGC incubated under normoxic conditions (~21 % O_2) produced a significantly higher yield of cGMP compared to samples equilibrated to hypoxic conditions. Furthermore, an additional experiment was performed which gently introduced 95 % O_2/5 % CO_2 to the sample to test whether this effect of O_2 on sGC activity may be further enhanced by additional increases in O_2 content. The results achieved confirmed that there was a concentration-dependent increase in cGMP production with O_2, disputing the current understanding within this field of research and confidently demonstrating that the O_2 can affect the activity of the enzyme.

Having confirmed that O_2 brings about a direct and proportional increase in production of cGMP, the next step was to investigate whether sGC consumes the O_2 within the sample. sGC incubated at either 50 or 100 µM caused a decrease in the line width of the O_2-sensitive probe, N^{15}-PDT, over time, confirming that sGC in fact consumed or used the O_2 within the

sample. A study by Friebe provided evidence for the activation of sGC by SOD (306). In order to eliminate the possibility of any free radical species contributing to the mechanism of sGC activation/modulation, the scavengers SOD and CAT were pre-incubated with sGC in normoxia and hypoxia. No differences were observed in the analysis of cGMP levels of SOD or CAT incubated samples compared to controls. Overall, this data implied that O_2 does not enhance the formation of radical species in the presence of sGC in either of these experimental conditions.

NOC9 was chosen as the NO donor in these studies due to its short half life (~2 minutes at pH 7.4) (307). Under hypoxic conditions, the lowest concentration of NOC9 (0.118 µM) stimulated a significant rise in cGMP production from ~30 pmol/ml to ~500 pmol/ml, equivalent to that stimulated by the highest concentration of NOC9 in the normoxic studies. This would therefore suggest that catalytic saturation of the enzyme occurred with the lowest concentration of NOC9 as the primary ligand under hypoxic conditions. Normoxic data displayed a NOC9 concentration-dependent rise in cGMP. Given that 1 mol NOC9 is equivalent to 2 mols NO, 23.6 µM NO under normoxic conditions stimulated a rise in cGMP equivalent to that produced by 100-fold less NO in hypoxia. Thus the exclusion of O_2 decreases basal cGMP produced as well as rendering the enzyme more sensitive to lower concentrations of NO.

Aware that NO can be oxidised by O_2, a study was performed which aimed to determine the characteristics of NO release from NOC9 in hypoxia and normoxia. For both gaseous and liquid samples, there were no differences reported in the area under curve and thus the total amount of NO. In terms of the data acquired during this experiment, a much higher yield of NO was detected in the gaseous phase of each sample compared to the liquid

phase. This may well have been due to saturation of the buffer with NO and its subsequent release as a gas.

The next step taken was to investigate whether O_2 had an effect on NO-independent activators of sGC. Pre-incubation with YC-1 increased the total cGMP detected over control values. Moreover, the pmol/ml increase was parallel in normoxic and hypoxic samples indicating that the mechanism of YC-1 activation is not likely to be governed by O_2. This infers that the mechanism by which O_2 brings about sGC-dependent increases in cGMP production is by influencing a separate allosteric site, which is neither that of YC-1 binding or the haem moiety.

Bayer® compound, BAY 41-2272 was utilised to yield concentration response curve in the enzyme model to uncover potential differences in hypoxic and normoxic sGC activity. As described, this activator works independently of NO and is haem-dependent. A concentration-dependent response to BAY 41-2272 was observed in hypoxic conditions however this same effect was not achieved in normoxia, where cGMP was produced maximally. Collectively, the data presented within this chapter demonstrated that O_2 can directly stimulate sGC at a similar site as BAY 41-2272 and that this stimulation is independent of NO.

4.5.3 Conclusions

The novel results within this chapter confirm that O_2 can stimulate cGMP production by sGC in the absence of NO. Furthermore, the data suggests that O_2 can modulate the effects of NO on enzyme activation, a finding that is not due to the oxidation of NO by O_2. Experimental evidence using NO-independent activators of sGC have confirmed that the mechanism of YC-1 is not dependent on O_2 however cGMP production stimulated by BAY

41-2272 was potentiated under normoxic conditions. Taken together, the most coherent mechanism by which O_2 influences sGC would seem to be either directly via the haem moiety or an indirect involvement with the haem site via a separate secondary allosteric site.

5 Effect of vessel size & function on O_2-induced vasorelaxation

5.1 Introduction

In the heart, epicardial coronary arteries (left and right coronary arteries) serve as conduit vessels to transport blood to the entire myocardium. In addition, smaller intramyocardial coronary arterioles regulate the flow of blood according to the needs of the myocardium (308). Under normal conditions, blood flow through the epicardial coronary arteries is slightly higher than subendocardial arteries (309). However, when coronary flow becomes obstructed, frequently due to disease such as atherosclerosis, the variation in flow between epicardial and subendocardial arteries is significantly increased (310). Local arterial hypoxia dilates the epicardial coronary arteries in an attempt to increase flow and perfuse the surrounding tissue and subendocardial arteries and arterioles (311).

5.1.1 Coronary autoregulation

Normal resting coronary blood flow is ~250 ml/min and this increases 4 to 5 fold during vasodilation (312). Autoregulation maintains coronary blood flow over a wide range of coronary artery pressures when the determinants of myocardial O_2 consumption are kept constant, thereby matching supply with demand. This occurs via alterations in coronary vascular resistance which are mediated by a number of factors including the accumulation of local metabolites, endothelial-derived substances, autonomic innveration and paracrine factors (313). However, the dilatory capacity of coronary resistance arteries is exhausted when coronary pressure decreases below the lower autoregulatory limit. At this point, coronary blood flow becomes pressure dependent and further reductions in pressure will likely lead to the onset of ischaemia. The lower autoregulatory limit has been estimated from pre-clinical and clinical studies showing that coronary blood flow cannot be maintained at coronary pressure < 40 mmHg (314). This lower autoregulatory pressure limit increases

during tachycardia because of the increase in flow required as well as a reduction in the duration of diastole/perfusion time.

The resistance offered by large epicardial coronary conduit arteries is one of the major components in coronary blood flow. Under normal physiological circumstances, these vessels offer negligible resistance to flow as evidenced by the lack of a measurable drop in blood pressure in this section of the circulation (312). However, the contribution of this component to total coronary resistance increases in the presence of haemodynamically significant epicardial artery stenoses (> 50 % reduction in diameter) and may even reduce resting flow when the artery becomes severely narrowed (> 90%). A second component of coronary blood flow can be attributed to the resistance arteries and arterioles between 20-200 µm in diameter. The changes in coronary smooth muscle tone results from vasoactive signals arising in response to physical forces (shear stress – flow mediated dilatation (315)), endothelium-derived factors and changes in metabolic demand imposed by the tissue. A third component affecting coronary blood flow arises from extravascular compressive resistance brought about by a rise in contraction-mediated left ventricular pressure. This elevation during systole also increases coronary backpressure, which ultimately limits the driving pressure for coronary flow. (316).

5.1.2 Mechanisms of coronary vasodilation

Although the precise mechanisms underlying the regulation of coronary blood flow have not been clearly defined, several mediators that accumulate when myocardial metabolic activity is increased have been implicated. For instance, adenosine has attracted a lot of attention in terms of mediating vasodilation of resistance coronary arteries/arterioles via binding to A_{2A} receptors residing on the vascular smooth muscle. This leads to an increased

production of cAMP and the opening of calcium-dependent potassium channels (K_{ca}) channels (317). Even though adenosine does not directly dilate the larger conduit arteries, these vessels display flow mediated dilatation in response to local shear stress as arteriolar resistance decreases. It is important to note that the production of adenosine is directly related to the metabolic state of the cell (317) and therefore it would be very likely that it could function as a mediator of local vasodilation in response to change in metabolic demand.

NO derived from the vascular endothelium also plays an important role in coronary vascular tone. NO-mediated vasodilation in the coronaries is enhanced by shear stress and eNOS can also be activated during intermittent elevations in coronary blood flow, such as during exercise (318). However, although NO-mediated coronary vasodilation of both epicardial and resistance vessels occurs in response to increased blood flow *in vitro* and *in vivo* (319-321), data from studies using L-arginine analogues suggests that this response is not mandatory for exercise-induced increases in coronary blood flow to occur (322). Importantly, endothelial cells produce PGI_2 and other prostanoids via the metabolism of AA (323). These substances stimulate coronary vasodilation via an increase in smooth muscle cAMP and subsequent opening of K_{ATP} channels.

In addition to the endothelium-derived species described above, other substances have also been identified as mediators of coronary vasodilation. Similar to prostanoids, these substances have been found to hyperpolarise vascular smooth muscle cells and have therefore been termed as endothelium-derived hyperpolarising factors (EDHFs). To date, the exact identity of these EDHFs remains unknown, however, compounds such as

cytochrome P450-dependent metabolites of AA metabolism as well as H_2O_2 have been suggested (81, 324).

As documented above, there are several factors that regulate and modulate coronary vascular tone. The most important outcome of coronary vasodilation is adequate perfusion of the myocardium in order to supply respiring cells and tissues with O_2 and other nutrients. Importantly, it has been suggested that coronary vessels have the ability to sense changes in O_2. The fact that the O_2 gradient across coronary blood vessels within the myocardium is larger than any other vascular bed within the body (~98 % O_2 coronary arteries versus ~30-35 % coronary sinus), could suggest that the coronary vasculature require enhanced O_2 sensitivity compared to other tissues. Therefore, experiments within this chapter were designed to examine the effects of O_2 on coronary vascular tone *in vitro*.

5.1.3 Aims

The studies documented in this thesis so far have utilised rabbit aortic rings to determine the effects of O_2 on vascular tone. Having established that O_2 can (a) directly vasodilate in proportion to the extent of hypoxia, (b) directly stimulate sGC and (c) modulate sGC response to other stimuli, further studies focussed on assessing these actions in vessels that are more likely to encounter hypoxia *in vivo*. As such, porcine coronary vessels were chosen to study O_2-induced relaxation and vessel function across the vascular network. Sections of artery ≤ 2.0 mm in diameter were used and responses to O_2 administration, as well as endothelium-dependent and independent stimulation were investigated under different tissue pO_2.

The specific aims of this chapter were to:

- ✓ Characterise the effects of O_2 on isolated hypoxic porcine left anterior descending (LAD) coronary artery and compare this to the results obtained with rabbit aortic tissue.
- ✓ Investigate the effect of O_2 on hypoxic porcine coronary vessels of varying size.

5.1.4 Hypotheses

Given that the heart requires a large O_2 supply in order to meet the metabolic demand of the myocardium in supplying the body, in this *in vitro* model, coronary arterial rings would display a greater relaxatory effect to O_2 than conduit arteries (such as the aorta). Moreover, smaller coronary vessels would exhibit the greatest relaxation responses.

5.1.5 Acknowledgments

Prior to undertaking the studies outlined in this chapter, an undergraduate student project (conducted by Miss Natalie Price, BSc Medical Pharmacology) collated useful preliminary data for this body of work.

5.2 General Methods

5.2.1 Myography: Rabbit aortic tissue

The methods and experiments reported in this chapter have been previously described in detail in Chapter 3. Selected results are also included here for illustration purposes and to compare the responses of the two vessel types to O_2 under hypoxic conditions.

5.2.2 Myography: Porcine coronary tissue

5.2.2.1 Vessels > 2 mm diameter

Porcine hearts were collected from a local abattoir and immediately submerged in ice cold saline solution (0.9 % *w/v*). The LAD arteries were carefully dissected in 95% O_2/5 % CO_2-bubbled KH buffer (see section 2.2 for composition) and excess fat and minor vessels were removed. Any surplus dissected LAD vessels were stored in HEPES buffer (pH 7.4) (composition in mM: HEPES 25.0; NaCl 120.5; KCl 4.8; KH_2PO_4 1.5; $MgSO_4.7H_2O$ 1.2; $C_6H_{12}O_6$ 11.1 and $CaCl_2.2H_2O$ 1.4) at 4°C. These vessels were kept for a maximum of 3 days, during which time the HEPES buffer was changed daily.

On the day of experimentation, the vessels were cut into 2 mm wide rings. These were then mounted in baths containing 5 ml Krebs maintained at 37°C and gassed with 95% O_2/5% CO_2 (as previously described for rabbit aorta (section 2.2). The appropriate hypoxia level being tested was established as described in section 2.2.1. Preliminary studies were first carried out to establish a suitable resting tension for the porcine coronary rings. Tissues were set at either 2, 3 or 4g tension (95 % O_2/5 % CO_2) and exposed to 90 nM U46619 (thromboxane A_2 agonist). U46619 was used instead of PE since the porcine coronary LAD rings did not contract to this α_1 adrenergic receptor agonist. This observation was also made by Horst and colleagues in 1985 (325). The resting tension at which the maximum agonist-induced contraction response was achieved (in this case 3 g, see Figure 5.1) was then used for all further experiments.

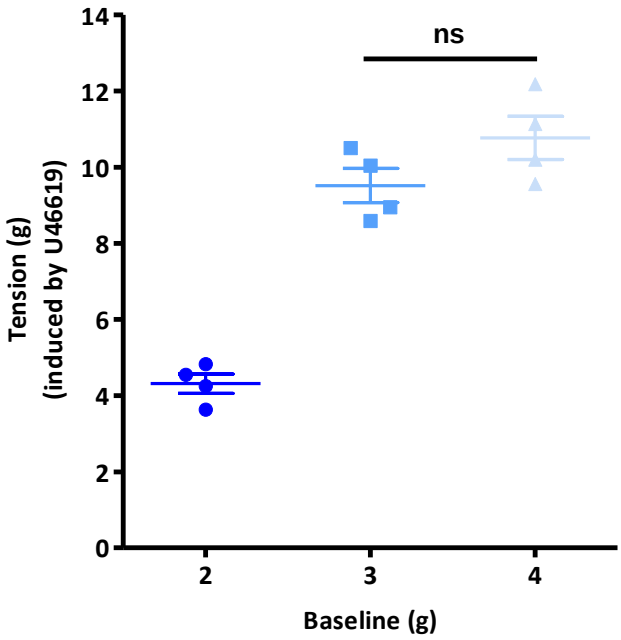

Figure 5.1: Determination of LAD resting tension. 3 g was used as the resting tension for all future coronary experiments as there was no statistical difference between the constriction generated at 3 and 4 g ($p>0.05$) (n=4).

For all further experiments, the established EC_{80} was used to constrict the LAD rings. Concentration response curves to U46619, in normoxia and hypoxia are displayed in Figure 5.2. An increased concentration of U46619 was required to constrict hypoxic rings to 80% of maximum (150 nM vs. 90 nM), to achieve an equivalent constriction to normoxic rings.

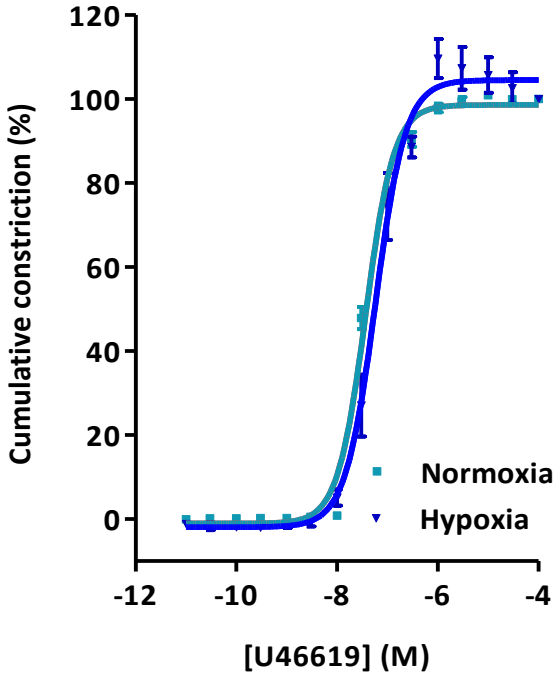

Figure 5.2: Concentration response curve to U46619. (n= 3-7) *Non-linear regression.*

Prior to daily experimentation, porcine coronary rings were 'exercised' with U46619 (90 nM) and BK (10 µM) to establish both smooth muscle and endothelial integrity. BK was used in place of ACh (rabbit aortic experiments) due to the reported lack of muscarinic receptors on porcine coronary endothelium (326, 327). The majority of rings required 3 exercises to establish a stable and repeatable response in constriction (this is similar to the experimental set up for aortae).

5.2.2.2 Vessels < 2 mm diameter

Hearts were collected as described in section 5.2.2.1. Septal and diagonal coronary vessels deriving from the LAD were carefully exposed under a dissection microscope and removed from the surrounding muscle and adipose tissue. These smaller vessels were harvested only on the day of heart collection and were not preserved overnight. Rings < 2mm in width were cut and the diameter recorded using callipers. The rings were then

mounted onto a DMT® myograph 610 M (pin mounts - see Figure 5.3) containing gassed KH buffer (95 % O_2/5 % CO_2). Resting tension was maintained at 5 mN as established by previous members of our group.

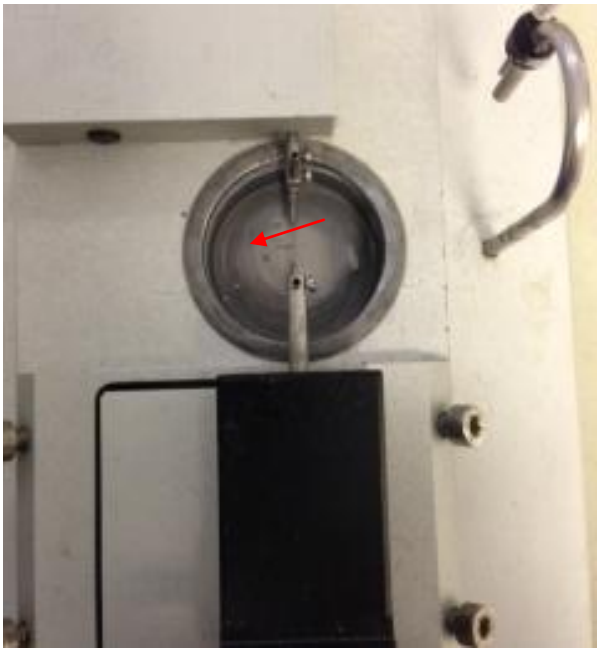

Figure 5.3: DMT® Wire Myograph 610M mounting pin set up. The red arrow indicates the location where the tissue is positioned within the bath.

5.2.2.2.1 Hypoxic chamber

Validation studies were performed whereby the chambers (see Figure 5.3) were gassed with 95 % N_2/5 % CO_2 for 10 minutes. Analysis of bath O_2 content by EPR demonstrated that the KH buffer did not decrease in O_2 content and therefore was not effectively 'hypoxic'. With the technical aid of Ruskinn Ltd, a protocol was developed that enabled the myograph to be placed inside the hypoxic chamber (Invivo$_2$), to prevent atmospheric air interfering with equilibration of KH buffer to hypoxia.

Once tissue rings were mounted on to the pins, the baths were placed in the hypoxic chamber and equilibrated to normoxic conditions (~21 % O_2) by purging O_2 and CO_2 into the

chamber. Individual baths were bubbled with 95 % O_2/5 % CO_2 from a gas source outside of the chamber. To achieve hypoxic conditions the chamber was set to 0 % O_2/5 % CO_2 and each bath was also gassed via the standard bubbling with 95% N_2/5% CO_2.

5.2.3 Western Blotting – sGC α_1 and β_1 subunits

5.2.3.1 Sample Preparation

Previous literature has stated that sGC subunits α_1 and β_1 are the most prevalent in vascular tissue for a range of animal species (328), therefore expression levels of these two subunits were investigated in further detail.

Tissue samples previously frozen at -80°C (rabbit aorta and porcine coronary artery denuded of endothelium) were removed from the freezer and placed into 1.5 ml Eppendorf tubes. Denuded rings were used here since the majority of sGC protein resides within the vascular smooth muscle. Immediately, 200µl of ice cold lysis buffer (20 mM Tris-HCl, pH 7.5) containing protease/phosphatase inhibitors (Roche) were added, plus 1.4 mm diameter stainless steel homogenising beads (at an equal bead to tissue weight ratio). The tissue samples were homogenised for 8 minutes at speed 8 on the 'Bullet Blender' (Next Advance). Subsequently, samples were centrifuged at 21,913 x g at 4°C for 30 minutes. The resulting supernatant was removed and placed into labelled 0.5 ml Eppendorf tubes. Samples were then stored on ice for use the same day or frozen and stored at -20°C.

5.2.3.2 Bradford Assay

The assay used to analyse total protein content within tissue samples was the Bradford assay which utilises a Coomassie reagent for colorimetric quantification. The assay is based on the binding of Coomassie dye to protein; in the presence of an acid there is a shift in

absorbance maximum from 465 nm to 595 nm and an associated colour change from brown to blue (329). BSA was used as the standard (Table 5.1). All standards and samples were diluted in 0.9 % *w/v* NaCl (Fresenius Kabi).

Table 5.1: Preparation of Bradford Assay BSA standards.

Tube	Volume of NaCl (µl)	Volume of BSA (µl)	[BSA] (µg/ml)
A	0	10	2000
B	20	60	1500
C	20	20	1000
D	20	20 of B	750
E	20	20 of C	500
F	20	20 of E	250
G	20	20 of F	125
H	80	20 of G	25
I	10	0	0

5.2.3.2.1 Protocol

The tissue homogenates were prepared as outlined in section 5.2.3.1. 5 µl of the BSA standard or unknown sample were added to a 96-well plate. 250 µl of Coomassie reagent was added to each well and then mixed on an orbital shaker for 30 seconds. The plate was then removed from the shaker, sealed and incubated on the bench for 10 minutes at room temperature. Following removal of the adhesive cover, the plate was then read at a wavelength of 595 nm.

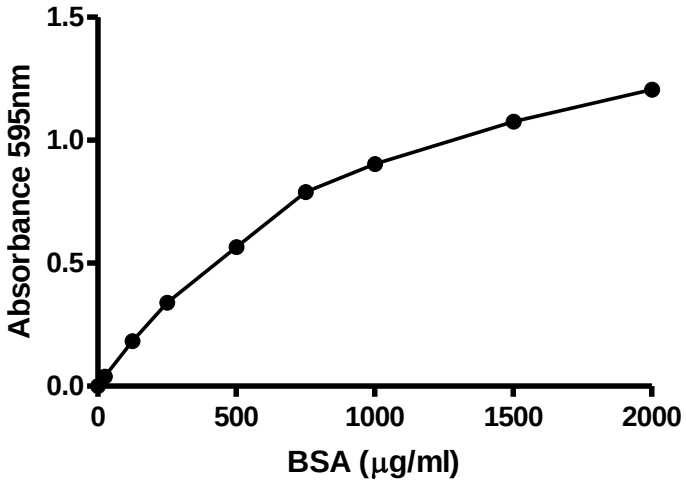

Figure 5.4: Typical standard curve achieved by the Bradford assay.

5.2.3.3 SDS-PAGE

Before loading on to the gel (see Table 5.2), the protein in the samples had to be denatured. This was accomplished by diluting the sample 1:1 with Laemmli buffer (see Table 5.2) followed by heating for 10 minutes at 95°C. The gel and running buffer constituents are detailed in Tables 5.2 and 5.3, respectively.

Table 5.2: SDS PAGE constituents.

Constituent	*Resolving Gel (ml)	*Stacking Gel (ml)
dH_2O	2.375	3.4
30% acrylamide mix	1.225	0.83
1.5M Tris (pH 8.8)	1.30	**0.63
10% SDS	0.05	0.05
10% APS	0.05	0.05
TEMED	0.004	0.005

**based on 5ml volume (resolving gel 7.5%), **1.0M Tris (pH 6.8), Acrylamide/Bis-acrylamide 30 % solution (37.5:1 ratio).*

Table 5.3: Running buffer (x10) constituents.

Constituent	Amount
Tris	30.3 g
SDS	10 g
Glycine	143 g
dH_2O	1 L

Diluted 1 in 10 before use

Standards and samples were loaded on to wells within the stacking gel to ensure each sample contained an equivalent protein concentration (determined by Bradford method). The gel was run at 200 V for 30 minutes or until the bands migrated to the base of the gel.

5.2.3.4 Transfer

After SDS-PAGE, the gel was placed in a transfer 'sandwich' as illustrated in Figure 5.5. The transfer cassette was filled up with cold transfer buffer (Table 5.4) and run at 100 V for 2 hours. This process encourages the movement of protein on to the PVDF membrane.

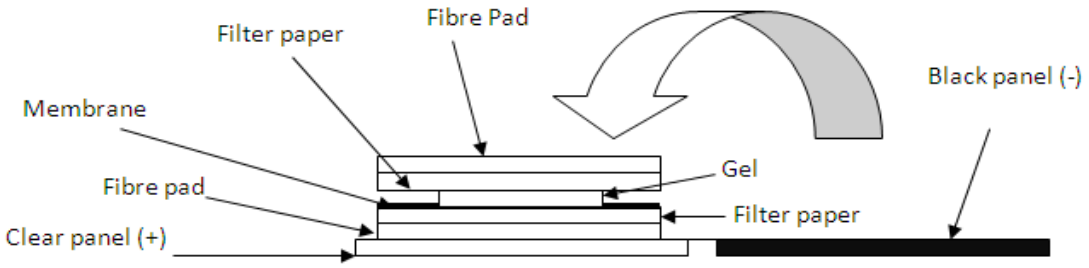

Figure 5.5: Schematic of the order of transfer in Western blotting.

After transfer, the gel was discarded and the membrane placed in blocking solution (5 % non-fat milk in wash buffer – see Table 5.5) on a rotator in a cold room overnight (~4 °C).

Table 5.4: Transfer buffer constituents.

Constituent	Amount
Tris	1.5 g
Glycine	7.2 g
Methanol	100 ml
dH_2O	400 ml

25 mM Tris, 192 mM Glycine, 20 % Methanol

Table 5.5: Wash buffer (Tris buffered saline + Tween 20 (TBST)) constituents.

Constituent	Amount
Tris	6.1 g
NaCl	8.8 g
Tween-20	1 ml

pH to 7.6 prior to Tween-20 addition. Blocking solution was made by adding 5 g non-fat milk powder to 100 ml of wash buffer.

5.2.3.5 Incubation with antibodies

After cold incubation overnight, the membrane was removed from the blocking solution and incubated with the primary antibody (sGC mouse monoclonal or β-actin, 1 in 200 in 5 % milk-TBST) for one hour at room temperature. After incubation, the membrane was washed 3 x 10 minutes in 5% milk-TBST at room temperature. The secondary antibody (goat anti-mouse) was added at a concentration of 1 in 1000 made up in 5% milk-TBST and incubated on the rocker for 1 hour at room temperature. Again, the membrane was washed however, the 3 x 10 minute washes were in TBST only. Following the washes, the membrane was incubated in luminol reagent (Santa Cruz) for 5 minutes with agitation.

5.2.3.6 Dark room procedure

X-ray film was exposed to the membrane for 5 minutes in the dark, after which the film was developed and bands quantified by densitometry.

5.2.4 Western Blotting

Tissue homogenates were prepared as described in section 5.2.3.1. Table 5.6 states the specific antibodies used for these experiments.

Table 5.6: Antibodies used for Western Blotting.

Antibody	Details	Source	Dilution
Primary	sGC α_1 mouse monoclonal sGC β_1 mouse monoclonal β-actin mouse monoclonal	Abcam Santa Cruz Santa Cruz	1:200
Secondary	Goat anti-mouse	Abcam	1:1000

5.3 Specific Methods

Most experiments within this chapter replicated as close as possible the studies completed using rabbit aortic rings. Porcine coronary rings were used to highlight any differences in responses which may be due to the vessel type and its specific function.

5.3.1 O_2-induced relaxation in LAD rings

In order to establish whether O_2-mediated relaxation occurs in large epicardial porcine coronary vessels in the same way as rabbit aortic rings, LAD rings were mounted in the myograph as described in section 5.2.2.1. Following 10 minute incubation under hypoxic conditions, rings were pre-constricted with 150 nM U46619. Once a plateau was established (~15 g tension), a bolus of KH buffer was administered to give final bath O_2 concentrations of 0 ('0 %'), 8.4 ('21 %') or 38 µM ('95 %'). RBCs were also prepared as outlined in section 2.3 and administered in the same way as the KH buffer bolus.

5.3.2 Inhibition of eNOS and sGC

L-NMMA (300 µM) and ODQ (10 µM) were pre-incubated with LAD rings for 30 minutes prior to experimentation to inhibit both eNOS and sGC, respectively. Bolus injections of either KH buffer or RBCs were administered to give a final bath O_2 concentration of 38 µM.

5.3.3 Effect of O_2 on the response to GSNO

Concentration responses (1 nM to 10 µM) to GSNO were performed on porcine LAD rings under various O_2 conditions. Baths were equilibrated either at 0, 10, 21 or 95 % O_2 by bubbling appropriate gases mixed with 5 % CO_2. The response to each concentration was allowed to reach a plateau before the next one was added.

5.3.4 Vessel size

5.3.4.1 Concentration response to U46619

The EC_{80} concentration of U46619 was established for large epicardial coronary vessels in the same way as rabbit aorta (section 5.2.2.1). The next stage was to investigate whether vessel size had an influence on the extent of O_2-mediated vasorelaxation. Second and third order branches originating from the LAD were dissected and prepared for isometric tension studies as outlined in section 5.2.2.2. Concentration responses (0.1 nM to 10 µM) to U46619 were then carried out for vessel rings between 0.5 mm and 1.0 mm diameter in order to establish an EC_{80} under hypoxic conditions for each size ring. This concentration would then be used in future experiments for rings of equivalent size.

5.3.4.2 O_2-induced relaxation in < 2mm porcine coronary rings

Porcine coronary rings between 0.5 mm and 1.0 mm inner diameter were equilibrated under hypoxic conditions as described in section 5.2.2.2.1. The appropriate EC_{80} of U46619

(1 nM to 10 μM) was applied to each ring. Once a contraction plateau was established a bolus injection of KH buffer containing 38 μM O_2 was administered. RBCs were also prepared as outlined in section 2.3 and administered in the same way as the KH buffer bolus.

5.3.5 Statistical Analysis

O_2-induced vasorelaxation was calculated by taking the maximum relaxation and expressing it as a percentage of the peak constriction induced by U46619. In general, an n value of 1 was an average of 2 paired rings. The majority of concentration response curves presented in this chapter are analysed by comparison of pEC_{50} values. Group data was compared using a Student's *t* test (paired or unpaired as appropriate) or one-way ANOVA followed by a suitable *post hoc* test (GraphPad Prism™ version 5.0). The exact statistical test used is stated in each figure legend. A p value < 0.05 was deemed statistically significant.

Western blotting analysis was expressed as a ratio of the density units of the test band and respective actin control. Since separate blots were used to probe control and test proteins, an unpaired *t* test was performed to calculate any statistical differences in band density. P values of < 0.05 were taken as statistically significant.

5.4 Results

5.4.1 O_2-induced vasorelaxation

Having confirmed that introducing a bolus of O_2, regardless of source, can influence vascular tone in rabbit aortic rings, KH buffer (oxygenated to various levels) was also introduced to hypoxic porcine coronary rings. Figure 5.6 illustrates that exposure of hypoxic

coronary rings to 95 % O_2 induced greater relaxation compared to little or no O_2 (0 %) (37.28 ± 2.37 % vs. 1.43 ± 0.69 %).

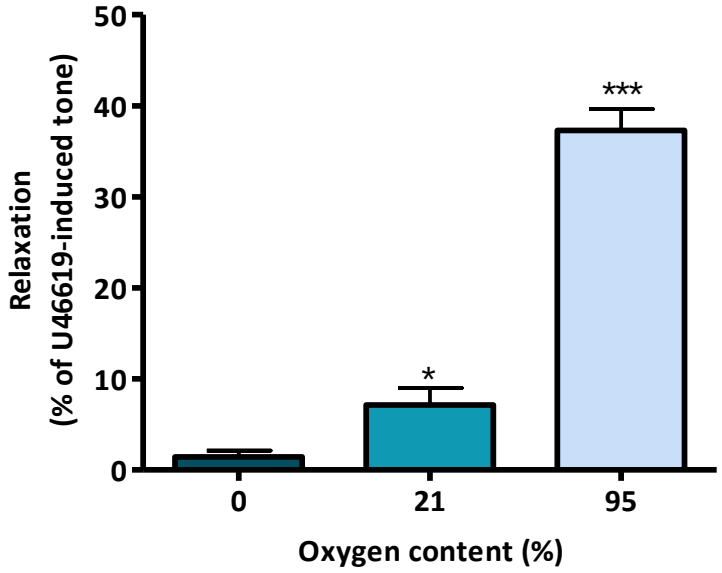

Figure 5.6: Porcine coronary vasorelaxation in hypoxia produced by increasing O_2 content in KH buffer samples. Significant differences were observed between 0 % and 21 % samples (*p<0.05), 0 % and 95 % samples (***p<0.001) and 21 % and 95 % samples (***p<0.001) (n=5-7) *One-way ANOVA + Tukey's multiple comparison test*.

As explained previously in Chapter 3, section 3.4.2, a bolus injection of either RBCs, Hb or KH buffer to hypoxic rabbit aortic rings induced a transient vasorelaxation followed by a rebound constriction, the latter having been shown to be of equal magnitude to the relaxation (see Andrew George Pinder, PhD Thesis, 2009). As shown in Figure 5.6, porcine LAD coronary rings were also shown to relax to a bolus of oxygenated buffer. An example trace of the raw data is depicted in Figure 5.7, along with the data for rabbit aortic rings from Chapter 3. Porcine LAD rings appear to display a much greater relaxation to O_2 than rabbit aortic rings. In addition, porcine LAD rings do not appear to constrict post-relaxation, in contrast to rabbit aortic rings.

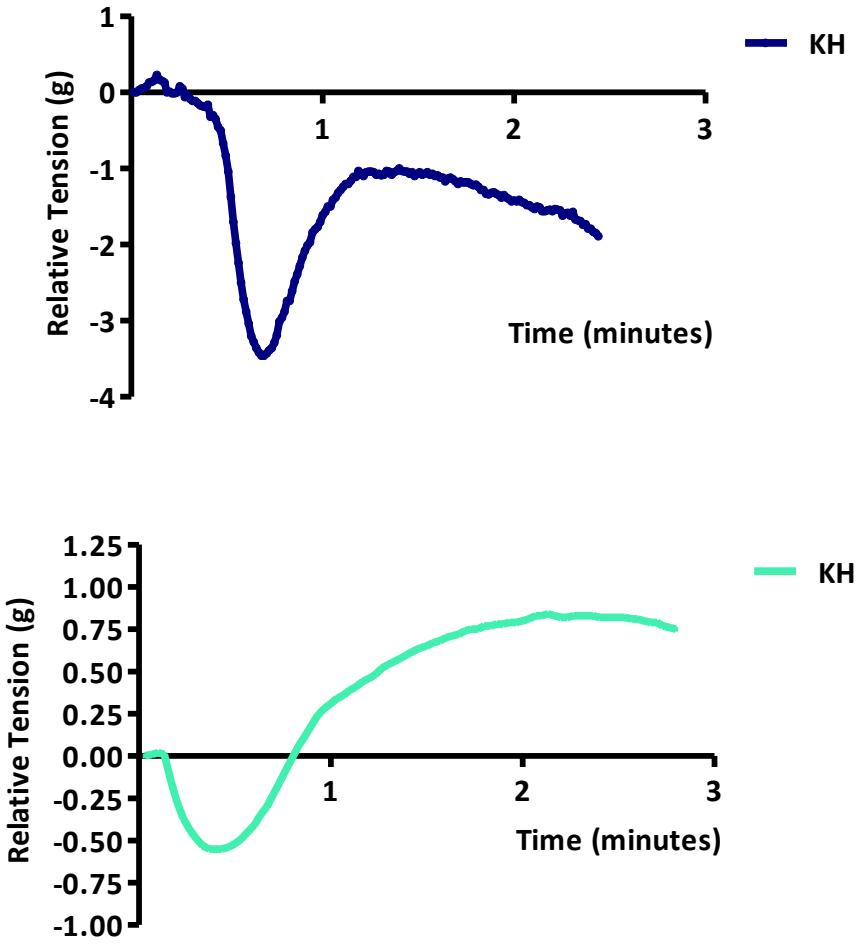

Figure 5.7: Raw data curves illustrating the relaxation induced by KH buffer equilibrated at 95 % O_2 (38 µM O_2 final bath concentration). The top trace represents the relaxation induced in porcine coronary tissues. The bottom trace represents data from rabbit aortic ring studies (from Chapter 3, section 3.4.2) and is shown here for comparison.

To compare the effects of the oxygenated KH buffer (control) to RBC-induced hypoxic vasorelaxation, paired rings received 38 µM O_2 in the form of either KH buffer or fully oxygenated isolated human RBCs. Figure 5.8 demonstrates that there was no difference in the magnitude of relaxation induced.

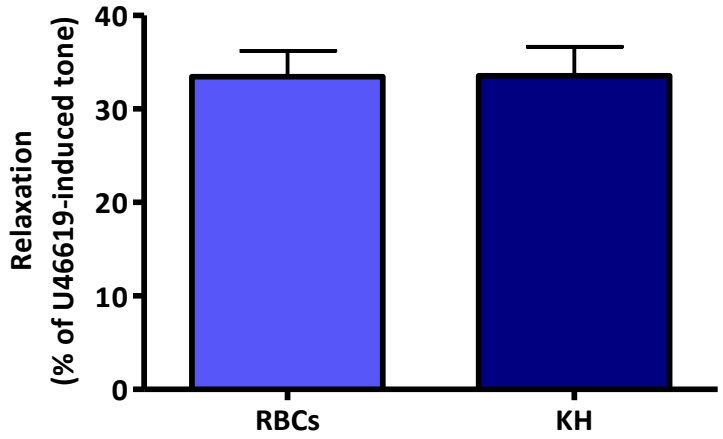

Figure 5.8: Comparison of relaxation induced by either KH buffer or RBCs (95 % O_2 delivery). There was no difference in the extent of relaxation by the two modes of delivery (n=3-4, p>0.05) *Unpaired t test.*

5.4.2 Post-relaxation vasoconstriction

The tension recordings post O_2 addition show coronary arteries did not exhibit a post-relaxation vasoconstriction (section 5.4.1, Figure 5.7). In Chapter 3, an experiment aimed to investigate the involvement of K_{ATP} channels in the post-constriction observed in the myograph model with rabbit aortae. Data presented in Figure 3.11 demonstrated that there was a ~15 % increase in constriction above that of the maximum PE-induced tone. The raw traces displayed in section 5.4.1 of this chapter suggest that porcine coronary vessels subjected to O_2 do not display a post-relaxation vasoconstriction, a fact further confirmed on repetition (Figure 5.9).

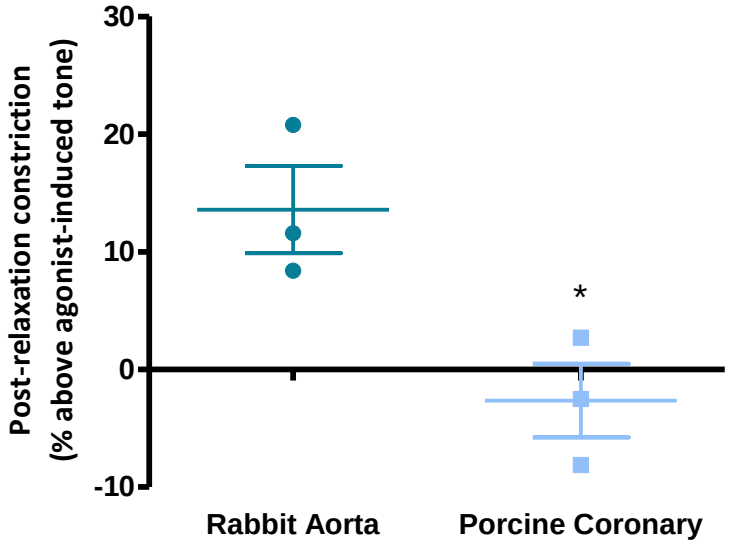

Figure 5.9: Post-relaxation vasoconstriction following addition of oxygenated (95 % O_2) KH buffer to either rabbit aortic rings or porcine coronary rings. Porcine coronary rings displayed a significantly reduced constriction compared to rabbit aortic rings (n=3, *p<0.05) *Unpaired t test*.

5.4.3 Inhibition of eNOS and sGC

Having shown that both KH buffer and RBCs of identical O_2 concentrations relax large epicardial porcine coronary tissue to the same extent, subsequent experiments aimed to establish the mechanism by which the relaxations occured. As with rabbit aorta ring experiments, L-NMMA and ODQ were used to investigate the involvement of eNOS and sGC in this relaxation process, respectively. Pre-incubation with L-NMMA (300 µM) did not affect the relaxation to KH buffer or RBCs (Figures 5.10 and 5.11, respectively). Moreover ODQ (10 µM) abrogated the relaxation to both KH buffer and RBCs (Figures 5.10 and 5.11, respectively) as in the rabbit aorta. These data would suggest that like rabbit aortic rings, the O_2-induced relaxation of large epicardial porcine coronary arteries under hypoxic conditions does not involve eNOS and is largely mediated via activation of vascular smooth muscle sGC.

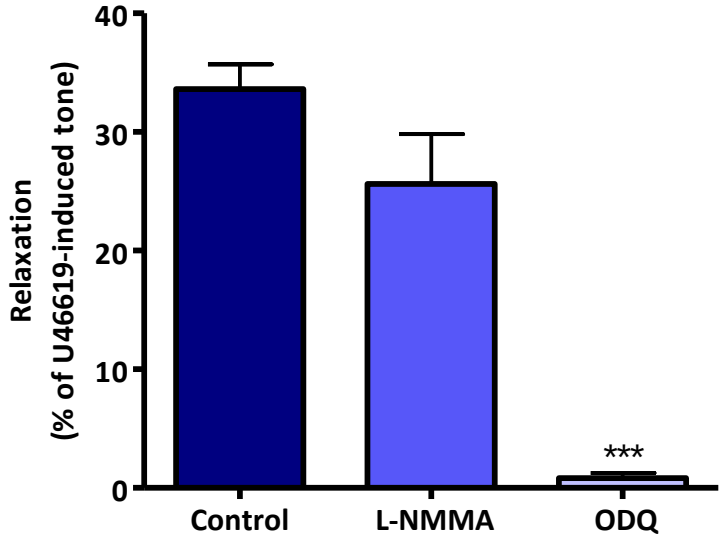

Figure 5.10: The effect of eNOS and sGC inhibitors on relaxation induced by an oxygenated KH buffer bolus (95 % O_2). No difference in the extent of relaxation (compared to control) was observed in rings incubated with L-NMMA ($p>0.05$). Conversely ODQ almost completely abolished RBC-induced vasorelaxation (n=4-5, ***$p<0.001$) *One-way ANOVA + Dunnett's multiple comparison test.*

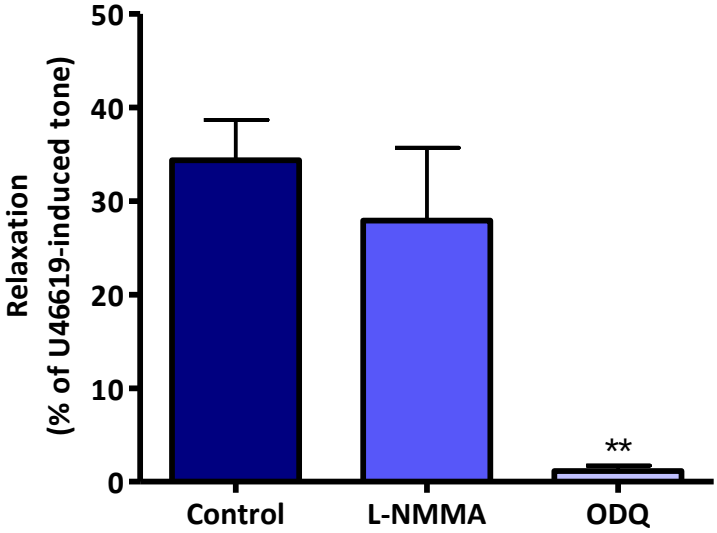

Figure 5.11: The effect of eNOS and sGC inhibitors on relaxation induced by RBCs (95 % O_2). No difference in the extent of relaxation (compared to control) was observed in rings incubated with L-NMMA ($p>0.05$). Conversely ODQ almost completely abolished RBC-induced vasorelaxation (n=4-5, **$p<0.01$) *One-way ANOVA + Dunnett's multiple comparison test.*

5.4.4 Effect of O_2 on NO donor response

GSNO was administered to endothelium-intact LAD coronary rings equilibrated at various O_2 concentrations. This was an important experiment to investigate whether the smooth muscle sGC response to exogenous NO was affected by the amount of O_2 present in the tissue. In the presence of endothelium (Figure 5.12), no differences between the GSNO pEC_{50} or indeed maximum relaxation were observed.

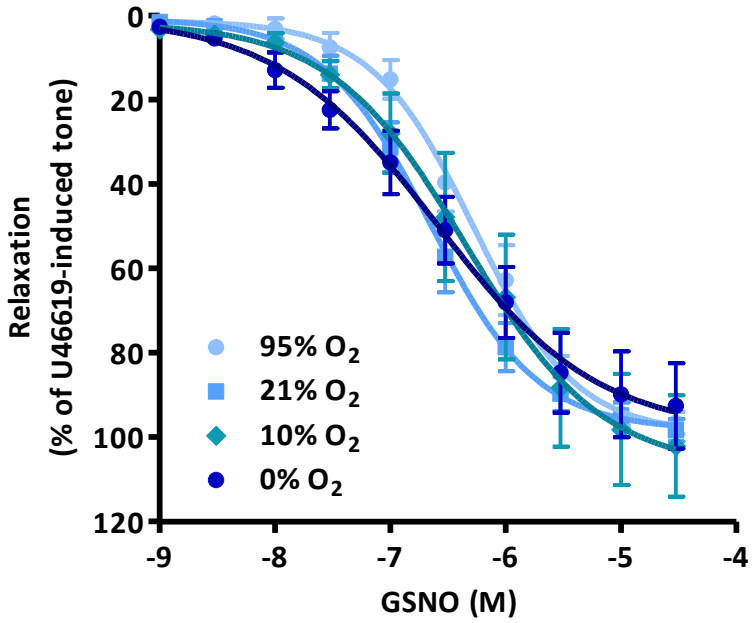

Figure 5.12: Concentration response curves to GSNO. No significant difference in potency of GSNO (pEC_{50}) to endothelium intact rings was witnessed under 0, 10, 21 or 95 % O_2 bathing solutions (n=4-6) (p = >0.05).

5.4.5 Rabbit Aorta vs. Porcine coronary artery

Table 5.7 summarises the key experiments performed with both rabbit aortic rings and large epicardial porcine LAD coronary rings. The results report a degree of disparity between the responses in hypoxia to both RBCs and oxygenated KH buffer. In particular porcine tissues relaxed ~20 % more than tissues to KH buffer or RBCs of equal O_2 content.

Since porcine coronary rings displayed a greater relaxation, one possible explanation could be related to the level of expression of sGC in porcine coronary tissue. The results displayed in Figure 5.13 clearly confirm that there was no marked difference in expression of either sGC subunit between porcine and rabbit vascular tissue after normalising for β-actin content.

Table 5.7: Comparison of main experimental results for rabbit aorta and porcine coronary tissue experiments.

Conditions	Rabbit Aorta		Porcine Coronary		Difference in response?
	Mean ± SEM	n	Mean ± SEM	n	
KH buffer (95 % O_2)	10.25 ± 0.73 %	4	33.57 ± 2.79 %	4	~ 23 % > relaxation by porcine rings
RBCs (95 % O_2)	9.69 ± 1.86 %	4	33.43 ± 2.79 %	3	~23 % > relaxation by porcine rings
+ ODQ (10 µM)	0.72 ± 0.28 %	7	0.83 ± 0.42 %	4	No difference
+ L-NMMA (300 µM)	13.38 ± 2.91 %	4	25.64 ± 4.19 %	5	No difference between each group and respective controls
sGC α_1	0.31 ± 0.08 ODu	3	0.36 ± 0.11 ODu	3	No difference
sGC β_1	0.31 ± 0.01 ODu	3	0.25 ± 0.07 ODu	3	No difference

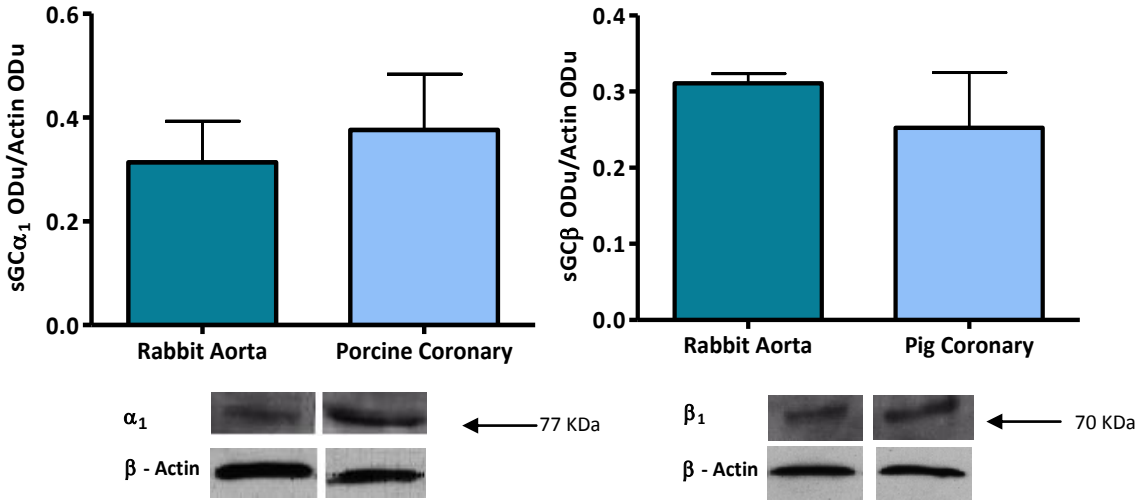

Figure 5.13: Comparison of the relative levels of sGC α_1 and β_1 subunits in rabbit aortic and large epicardial porcine coronary tissues. No differences in the amount of either subunit were observed between vessel types (n=3, p>0.05) *Unpaired t test*.

5.4.6 Effects of vessel size

Initial concentration response curves to U46619 were performed in order to ascertain whether the difference in coronary diameter affected the contractility to this agonist. Only a small number of vessels were tested and for this reason no statistical analysis could be performed. However, the data in Figure 5.14 suggest that pEC_{50} to U46619 was not different between vessel sizes.

BK and GSNO were administered to rings of various inner diameters under hypoxic conditions to compare the effects on endothelium-dependent and independent relaxation responses. Figure 5.15 as well as the pEC_{50} data displayed in Table 5.8, clearly indicate that BK had a greater relaxatory effect compared to GSNO.

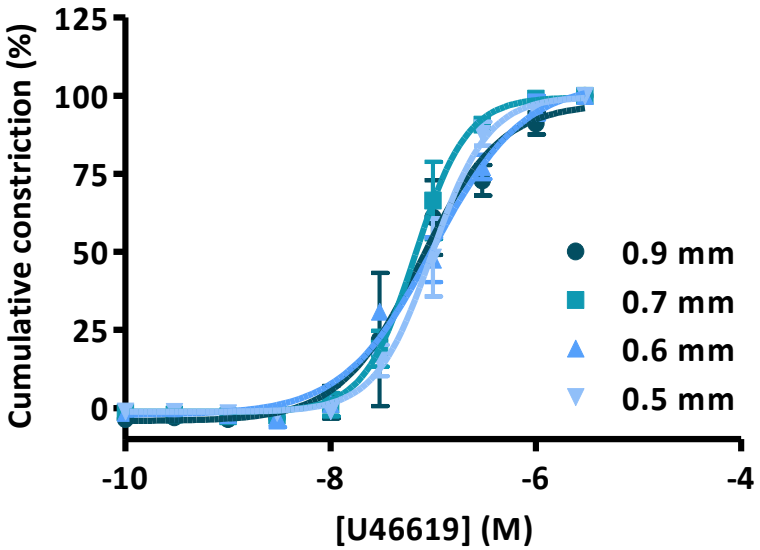

Figure 5.14: Concentration response curves to U46619 under hypoxic conditions (~0 % O_2) in porcine LAD coronary branch rings of varying internal diameter. The pEC_{80} values are shown in Table 5.8 (n=2-5 per vessel diameter) *Non linear regression.*

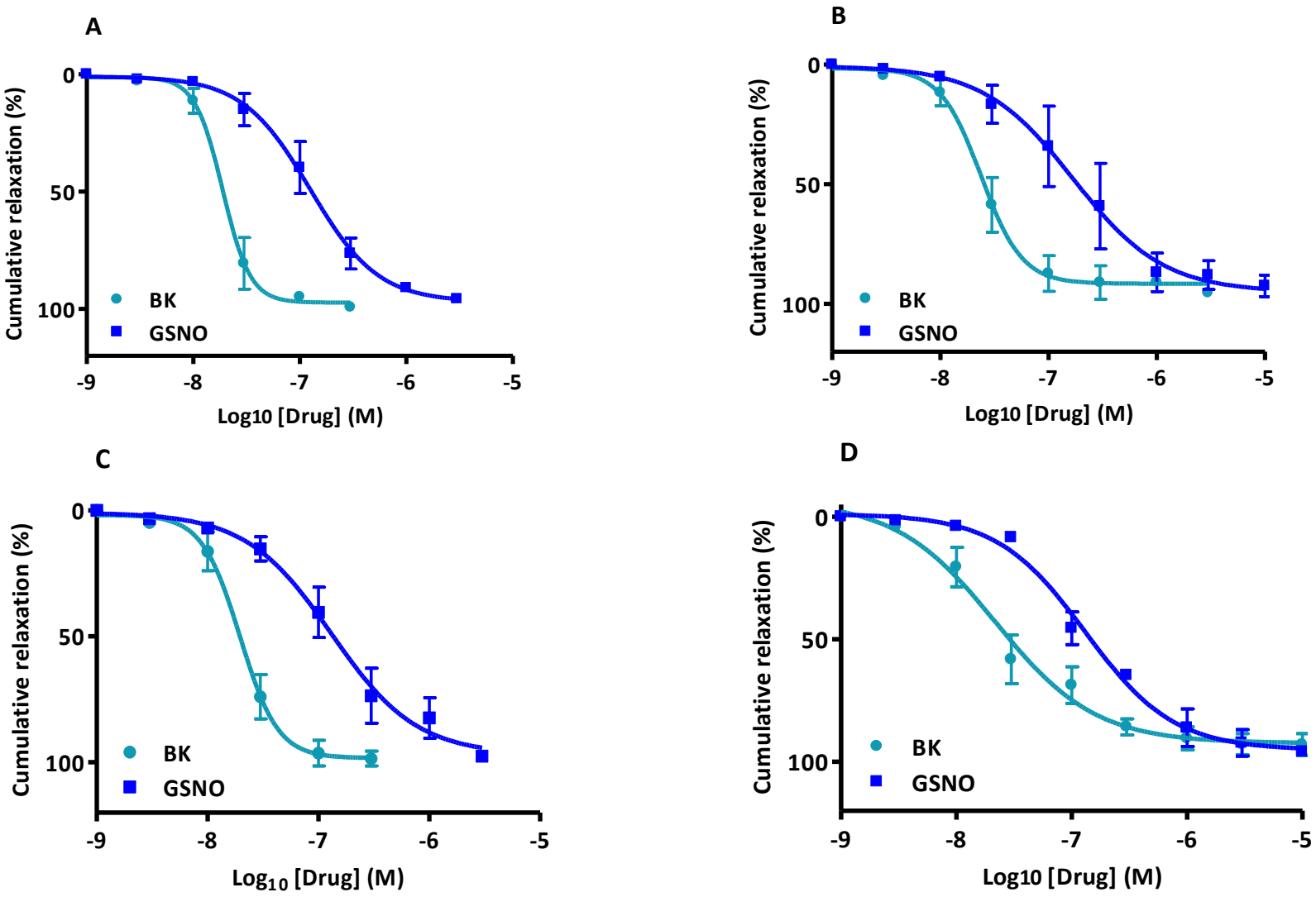

Figure 5.15: Concentration response curves to BK and GSNO for hypoxic porcine coronary rings with inner diameters of (A) 0.9 mm (B) 0.70 mm (C) 0.6 mm and (D) 0.5 mm. BK induced a greater relaxatory response than GSNO. (n=2 -3) *Non-linear regression*.

In terms of pEC_{50} (Table 5.8 and Figure 5.16), there were no large differences across a range of inner vessel diameters for both BK and GSNO.

Table 5.8: Average pEC_{50} values calculated from concentration response curves shown in Figure 5.15.

Inner diameter (mm)	Average pEC_{50} (nM)	
	BK	**GSNO**
0.9	7.72	6.90
0.7	7.62	6.77
0.6	7.71	6.88
0.5	7.66	6.88

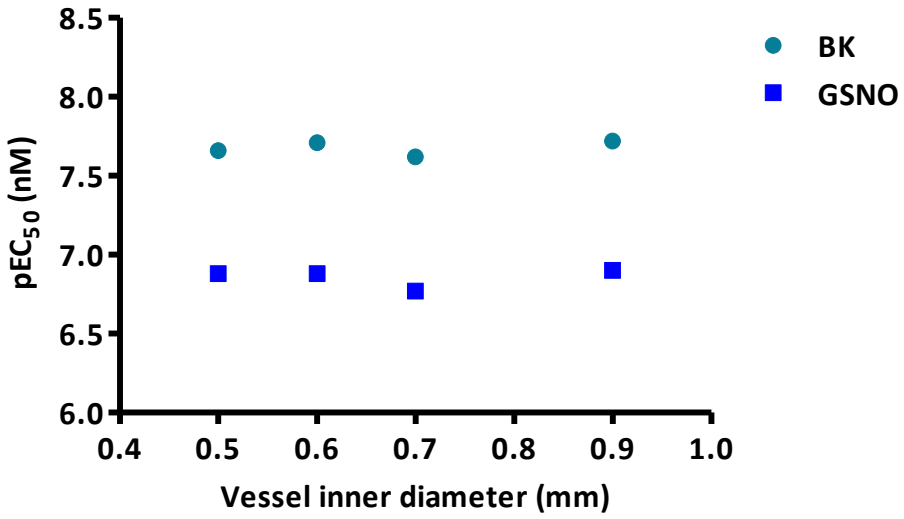

Figure 5.16: Correlation analysis between inner vessel diameter and average pEC_{50} for BK and GSNO. *Pearson r = -0.37 (BK) and -0.06 (GSNO), p = 0.63 (BK) and 0.94 (GSNO).*

Figure 5.17 presents a correlation analysis of percent relaxation versus vessel sizes. A negative correlation between the extent of relaxation and vessel size is demonstrated across the dataset indicating that smaller vessels are more sensitive to the administration of O_2.

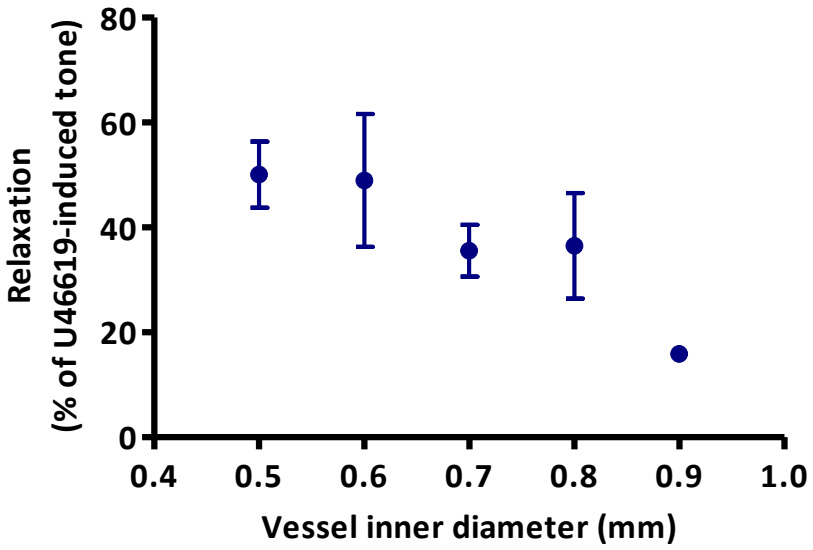

Figure 5.17: Correlation analysis between inner vessel diameter and average % relaxation to a 38 µM O_2 KH buffer bolus. *Pearson r = -0.73, n=4-6, *p = 0.024*.

5.5 Discussion

5.5.1 Summary

The main findings of this chapter are listed below:

I. Porcine coronary arterial rings display vasorelaxation in response to O_2 and this relaxation is largely sGC-mediated.

II. Hypoxic porcine LAD rings relaxed ~20 % more than rabbit aortic rings to a matched O_2 bolus.

III. There is no difference in sGC α1 and β1 subunit expression between rabbit aortic and porcine coronary tissue when normalised for actin.

IV. The magnitude of O_2-mediated vasorelaxation in hypoxia was inversely related to the vessel diameter for porcine coronary rings originating from the LAD.

5.5.2 Chapter Review

In vitro isometric tension studies in Chapter 3 characterised O_2-induced relaxation under hypoxic conditions in rabbit aortic tissue. Given that *in vivo* the aorta would be highly unlikely to encounter hypoxic conditions, this chapter focussed on characterising the phenomenon in porcine coronary arteries.

Previous literature regarding the study of RBC-induced vasorelaxation in hypoxia have typically utilised rabbit aortic tissue (249, 258). The data reported within this thesis show that rabbit aortic rings display around a ~15 % relaxation to oxygenated RBCs and an equivalent buffer control which contained an equal content of O_2. In comparison, tension recordings with porcine LAD rings displayed an enhancement of 20 % relaxation in response to an identical O_2 bolus. This would seem to support the hypothesis outlined at the start of

this chapter which proposed that porcine coronary arterial rings would display a greater relaxation to O_2 compared to rabbit aortic rings. Indeed the vessels within the heart, even under normal physiological conditions, are exposed to RBCs at various saturations of O_2, with a gradient that ranges from 95% in coronary artery to ~25% in the coronary sinus, representing the greatest physiological tissue O_2 gradient (330, 331). Therefore the relevance of this finding could be key to understanding how coronary vascular tone is maintained under areas of low pO_2. In terms of the kinetics of the response, this occurs over seconds and is therefore relevant to the acute and rapid response of the vessel. In relation to physiology, the myocardium needs to maintain an adequate supply of oxygenated blood in order for the heart to sustain efficient delivery of blood to the circulation and peripheral tissues (332). Failure of the vasculature to supply highly O_2-saturated blood could lead to local myocardial ischaemia. Therefore, the enhanced ability for the coronaries to respond to O_2 at low pO_2 would lead to a transient vasodilation allowing an increased perfusion of blood.

Initial experiments with ODQ and L-NMMA demonstrated that like rabbit aortic rings, porcine coronary arteries relaxed in hypoxia to a bolus of O_2 and this process was shown to be largely sGC-dependent and endothelium-independent. Porcine coronary arterial rings relaxed significantly more than rabbit aortic rings to an identical O_2 bolus. To investigate the underlying reasons for this disparity between blood vessels, the expression of sGC protein in both tissue types was undertaken. Western blot analysis confirmed that there were indeed no differences in the relative expression of either α_1 or β_1 subunits, perhaps ruling out the possibility that an increase in the amount of enzyme potentiated the relaxation response to O_2. However, upon examination, porcine coronary tissue is much more muscular than rabbit

aorta. This could suggest that even though the western blot data is expressed per mg of protein, the porcine coronary tissue could have an overall increased amount of protein relative to the vessel size, potentially accounting for the enhanced vasorelaxatory response to O_2.

Assessment of the raw traces for porcine coronary artery and rabbit aorta revealed clear differences, with porcine coronary arteries not exhibiting a post-relaxation vasoconstriction. In Chapter 3, further investigation with rabbit aortic rings lead to the proposal that this constriction may be accounted for by the closure of K_{ATP} channels post-O_2 addition. Coronary vascular smooth muscle cells express K_{ATP} channels which have been identified in the regulation of coronary metabolic and autoregulatory state (316). This concept has been supported by the evidence that inhibition of K_{ATP} channels by glibenclamide, causes constriction of coronary vessels which reduces coronary flow (333). Therefore, this suggests that in this setting, the introduction of O_2 to hypoxic coronary vessels leads to a further enhancement in vasodilation which dampens any constrictive effects caused by the immediate availability of ATP.

Experiments detailed in Chapter 4 of this thesis concluded that sGC was more sensitised to NO under hypoxic conditions compared to normoxia. In this chapter, further experiments aimed to examine the effects of vessel size on vasorelaxation to endothelium-dependent and independent substances. Vessel size did not alter the vasodilatory profiles of BK or GSNO, however, the coronary rings were an order of magnitude more sensitive to BK. There is evidence to suggest that NO has a greater effect on larger epicardial vessels whereas EDHF and adenosine affects smaller resistance coronary arteries (321, 334, 335). The smallest coronaries used in these studies had diameters of ~0.5 mm. Even though small

coronaries of < 0.2 mm (312) are most responsive to EDHF, clearly the results presented here indicate that BK might stimulate an enhanced vascular smooth muscle cell hyperpolarisation when compared to GSNO stimulation exclusively via sGC. However, the data displayed within this chapter suggest a sGC-dependent response due to the inhibitory effects of ODQ.

Further experiments examined the effect of vessel size on the magnitude of O_2-induced vasorelaxation under hypoxic conditions. Coronary rings with a smaller inner diameter relaxed ~30 % more than those with the largest inner diameter. This suggests that smaller coronaries are more responsive to O_2 under hypoxic conditions through increased sensitivity to sGC. One possibility for the enhanced relaxation to O_2 by porcine coronary rings compared to rabbit aortic rings could be accounted for by the response of O_2-sensitive K_{ATP} channels and subsequent hyperpolarisation of smooth muscle cells, but this remains to be elucidated in further studies.

5.5.3 Conclusions

The results within this chapter suggest that the porcine coronary artery displays an enhanced hypoxic vasodilatory response to the administration of O_2, either as RBCs or an equivalent oxygenated KH buffer, when compared to rabbit aortic tissue. Relaxations observed in hypoxia by coronary and aortic tissue are largely sGC mediated, as confirmed by the attenuation of the response by ODQ. Smaller coronary vessels were found to relax considerably more to a defined O_2 bolus, indicating that smaller coronary vessels may display a greater sensitivity to O_2 under hypoxic conditions.

6 Pilot Study: O_2 offloading by abnormal Hb under hypoxic conditions

6.1 Introduction

Patients with sickle cell disease possess the variant HbS, characterised by the substitution of glutamic acid (negatively charged) by valine (neutral charge) at position 6 of the β-globin chain (336). Importantly, the severity of the disease is very much dependent upon genotype. For instance, homozygous sickle cell haemoglobin (HbSS) leads to the severe disease phenotype of sickle cell anaemia, whereas heterozygous genotypes (HbS/C, HbS/β^o, HbS/β^+, HbS/HPHP, HbS/E) present varying clinical symptoms. The more rarely occurring HbS/β^o-thalassemia is phenotypically indistinguishable from homozygous HbSS (337).

The substitution of residues on the β-globin chain renders RBCs susceptible to 'sickling' in areas of low O_2 tension, hindering their capacity to carry O_2 efficiently. This sickling process, known as HbS polymerisation, is caused by hydrophobic interactions by adjacent amino acids with the substituted valine residue. Consequently, HbS forms rigid, rod like structures which results in the production of deformed RBCs. Even under normal pO_2 these cells often maintain low saturation, leading to symptoms of anaemia. Moreover, homozygous patients are frequently affected by painful 'vaso-occlusive crises' which occur due to the conformational changes of RBCs into sickle shaped cells, leading to vessel obstruction and ischaemic injury (338).

Decreased NO bioavailability has been implicated in the vasculopathy associated with sickle cell disease (339). Despite an observed upregulation of NOS (340), this reduced bioavailabilty is thought to arise as a consequence of the rapid scavenging of NO by cell-free Hb (341) and oxy radicals (342), as well as low levels of L-arginine (343). In addition to this,

the fact that sickle RBCs have an impaired ability to deliver O_2 could also contribute to this vasculopathy.

The O_2 dissociation curve for sickle cell disease is shifted to the right compared with normal Hb (P_{50} relates to a pO_2 of ~21 mmHg for normal Hb compared to ~45 mmHg for HbSS (344)). As a result, affected individuals are characterised by a reduced ability to deliver O_2 efficiently under low pO_2. Importantly, the extent of this dysfunction correlates to the severity of the disease, and that for heterozygous patients is not as profound as the shift observed in homozygotes (344). Based on this knowledge, the main rationale for conducting the pilot study reported here was to investigate whether the extent of RBC-induced relaxation under hypoxic conditions was altered by the presence of HbS.

6.1.1 Aims

Patients with disorders such as sickle cell disease possess Hb which displays a reduced ability to deliver O_2 efficiently under low partial pO_2. The specific aim of this study was to examine the effect of abnormal Hb on O_2-induced hypoxic vasorelaxation of porcine coronary rings held at various O_2 tensions.

6.1.2 Hypothesis

RBCs containing abnormal HbS would display an impaired ability to relax pre-constricted hypoxic porcine coronary rings compared to normal Hb.

6.1.3 Acknowledgements

I would like to thank Dr Alison May for all her advice in setting up this pilot study. I am indebted to Mr Lawrence King and staff within the haemoglobinopathy diagnostic laboratory at UHW for assisting with sample collection and performing HPLC analyses.

6.2 Methods

6.2.1 Sample collection & preparation

Venous blood was collected from appropriate patients and immediately stored at 4°C. Samples were transferred to the laboratory, on ice and then centrifuged at 1200 x g for 5 minutes at 4°C. Control venous blood was collected from healthy volunteers within the Wales Heart Research Institute and centrifuged in the same way. After centrifugation, surplus RBCs and plasma samples from both cohorts were snap frozen in liquid N_2 and stored at -80°C until required for NO analyses. RBCs to be used in myograph studies were washed in an equivalent volume of oxygenated PBS and centrifuged for a second time and the PBS fraction discarded prior to use.

6.2.1.1 Sample criteria

Included:

- ✓ Untransfused patients with sickle cell disorder caused by either homozygous HbS or heterozygous HbSβ^o.

Excluded:

- × Transfused patients.
- × Blood from patients receiving hydroxyurea/carbamide due to the increased synthesis of HbF (345).

6.2.2 Myography

Porcine coronary rings (~2 mm diameter) were dissected and mounted as described in section 5.2.2. Rings were incubated with L-NMMA (300 µM) for 20 minutes, followed by a

further 10 minute incubation at 0, 1 or 5 % O_2/5 % CO_2. Initial experiments also included 10, 21 and 95 % O_2 however, O_2-induced relaxation in hypoxia could only be observed at 5 % O_2 or lower and therefore a relaxation curve to O_2 under a full range of tissue pO_2's could not be presented. RBCs were added into each bath to expose tissue to 38 µM O_2 in concurrence with previous experiments in Chapters 3 and 5. Relaxation data reported are averaged from two rings receiving identical treatment.

6.2.3 Ion Exchange HPLC

Ion Exchange HPLC was carried about by staff in the haemoglobinopathy diagnostic laboratory at UHW immediately after sample collection. The method followed was the 'Variant^{TM} II β-thalassemia Short Program' (Bio-Rad) in order to determine the content of adult Hb variant A_2 (HbA_2) and foetal Hb (HbF). A brief description of the method is outlined below.

Healthy adult Hb consists mostly of HbA, < 3.5 % HbA_2 and < 2 % HbF. Carriers of β-thalassemia have increased levels of both HbA_2 (> 3 %) and sometimes, HbF (> 2 %) (346). Ion exchange HPLC separates molecules based on their charge. The sample to be analysed is injected into the mobile phase (solvents) which runs through the column (stationary phase comprising of solid particles such as silica). Local ionic interactions occur between the stationary phase and the sample, which ultimately determine the retention time of each analyte. Ions of the same charge do not interact with the stationary phase and therefore pass through the system quickly. (347). Using the Variant β-thalassemia short program, HbE which is present in a high proportion in blood is eluted within the HbA_2 retention time window and subsequent presumptive identification of the variants is made from the area

percent from the sample report (348). Full identification is made following cellulose acetate electrophoresis at alkali pH 8.6 and citrate gel electrophoresis at acid pH 6.4.

6.2.4 OBC

Total plasma and RBC NO metabolites were measured as outlined in section 2.7.2. Most of the samples collected were of small sample volume and therefore only total RBC measures were made instead of individual measures of RBC-associated NO_2^- and Hb bound NO.

6.3 Results

6.3.1 Hb composition

Control blood samples were drawn from volunteers as described in section 6.2.1. The average total Hb for the 5 samples analysed was 14.66 ± 0.41 g/dL^{-1}. Table 6.1 displays the composition of HbA_2 and HbF in samples from diseased patients. Each patient was either homozygous or heterozygous for sickle cell disease. It is noteworthy to mention that the HbA_2 present on HPLC on these patients, includes glycated components of HbS, so is always overestimated. This is one of the reasons HbA_2 levels on sickle cell carriers/disorders are not usually reported.

Table 6.1: Hb variant composition in patient samples.

Patient	Gender	HbF (%)	HbA_2 (%)**	Hb (g/dL^{-1})
1	M	15.1	4.2	10.2
2*	F	0.2	4.1	6.7
3*	F	0.3	3.9	11.8
4	M	7.6	4.0	10.8
5	F	5.5	5.0	10.4

** HbSS. All other patients heterozygous HbS/ β-thalassemia, ** % includes glycated HbS.*

RBCs were added to the myograph in appropriate volumes to give a final bath concentration of 38 µM (see section 2.3.2).

6.3.2 OBC

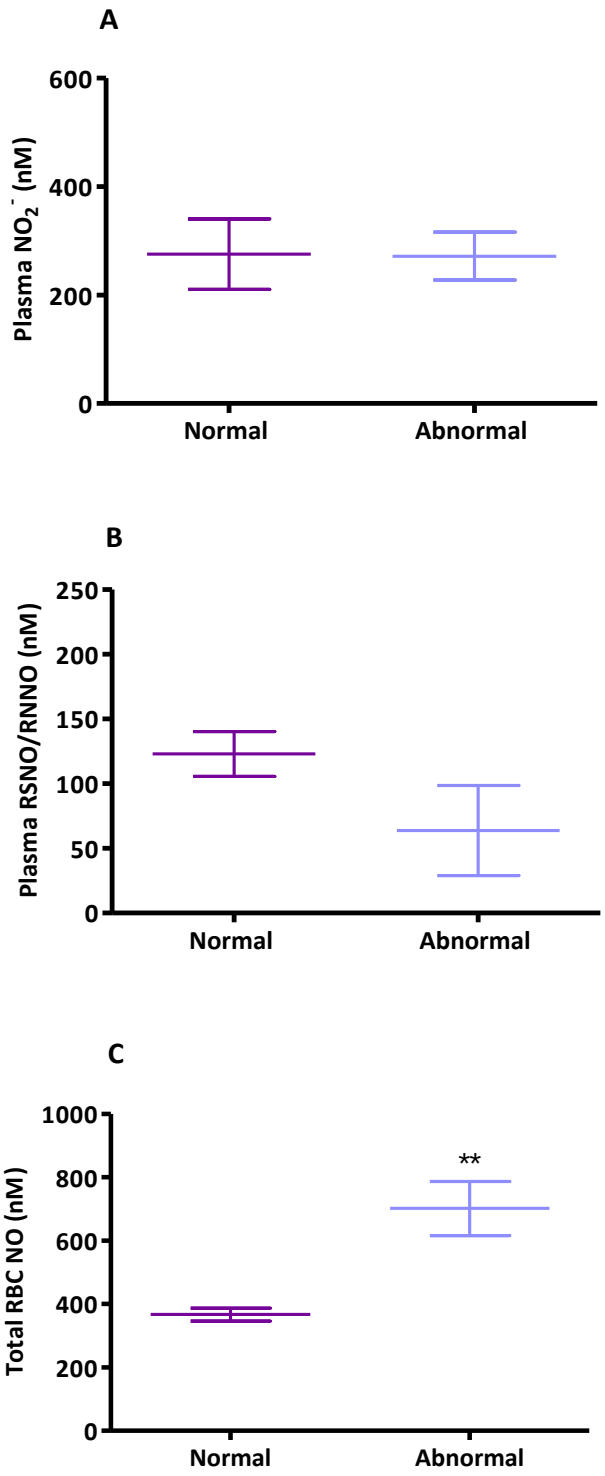

Figure 6.1: NO metabolite levels as measured by OBC. A – Plasma NO_2^- levels, B – Plasma RSNO/RNNO, C – Total RBC NO (all nM). No statistical differences were observed between normal and abnormal Hb for both plasma NO_2^- and RSNO/N-nitrosamine (RNNO) ($p>0.05$). Total RBC NO was significantly raised in RBCs containing abnormal Hb compared with control RBCs (366.90 ± 20.52 nM vs. 701.80 ± 85.63 nM) (**$p=0.0052$) (n=5) *Unpaired t test*.

Plasma NO_2^- and RSNO/RNNO levels were not statistically different in patients with sickle cell disease/sickle cell trait compared to normal plasma. However, measurement of the total RBC-associated NO revealed elevated levels of metabolite species in abnormal blood samples compared to control blood. However, it is important to mention that in both cohorts, plasma RSNO/RNNO and total RBC NO were present at levels far greater than reported in the literature (349, 350).

6.3.3 O_2-induced vasorelaxation

Administration of both normal and abnormal RBC samples into porcine coronary rings held at various O_2 tensions transiently relaxed rings held at 0, 1 and 5 % O_2 (Figure 6.2). Preliminary testing of normal RBCs revealed that rings held higher than 5 % O_2 did not relax to oxygenated RBCs and therefore are not presented here.

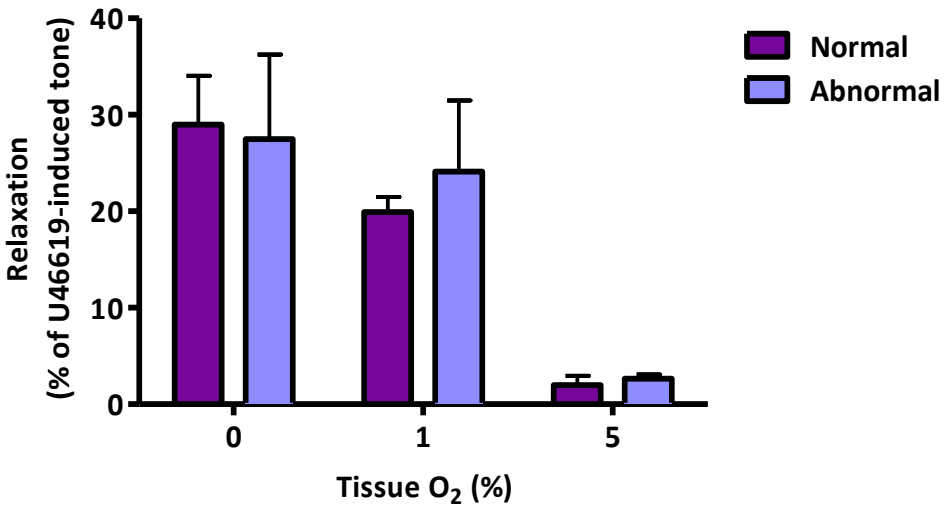

Figure 6.2: Effect of increasing tissue O_2 content on O_2-induced vasorelaxation. An increase in tissue O_2 content decreased the magnitude of porcine coronary relaxation to RBC-derived O_2. There were no statistical differences between the extent of relaxation induced by administration of abnormal RBCs compared with healthy RBCs ($p>0.05$) (n=5) *Two-way ANOVA + Bonferroni post test.*

In order to establish whether sample Hb content influenced the observed relaxations, data from Figure 6.2 was normalised for the Hb content of each sample (Figure 6.3). Statistically, no such association was observed.

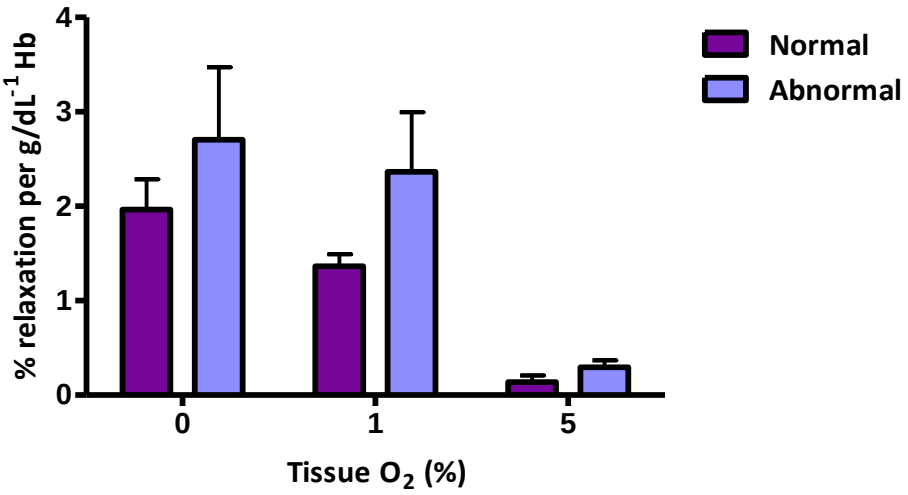

Figure 6.3: Effect of increasing tissue O_2 content on O_2-induced vasorelaxation. Data from normal and abnormal samples (Figure 6.2) were normalised for Hb content. There were no differences in relaxation at each tissue O_2 between groups ($p>0.05$) *Two-way ANOVA + Bonferroni post test.*

6.4 Discussion

Chapters 3 and 5 of this thesis provide convincing evidence for the role of O_2 in mediating relaxation in acute hypoxia. The data within this pilot study suggests that venous RBCs originating from sickle cell disease patients do not display an impaired ability to relax vascular smooth muscle under hypoxic conditions compared with healthy RBCs. As such, the hypothesis proposed in this chapter is rejected.

In this study, there were five different patient blood samples, each with an individual genetic variation of sickle cell disease. The rationale behind sample preparation allowed for the oxygenation of RBCs prior to sample administration in order to encourage a fully saturated state of Hb (R state (40)). Thus, any differences in the relaxations produced by porcine coronary rings would be due to the sickling effect of patient Hb upon administration into the hypoxic tissue baths. Clearly, the occurrence of a transient relaxation of coronary tissue under hypoxic conditions suggests that the transient contact of sickle cells with hypoxia (seconds) does not allow sufficient time for HbS polymerisation and inhibition of the relaxatory response. In addition, considering sickle cells have a lower affinity for O_2 (351), one would have anticipated that perhaps during the oxygenation of samples, sickle cell RBCs would not be able to become as saturated as normal Hb, therefore minimising the amount of O_2 available for offloading and subsequent mediation of relaxation of vascular tissue. However, the volume of RBCs administered to each bath was calculated on the basis that mutated HbS would bind O_2 to a similar extent as HbA and therefore have the potential to offload an equivalent amount of O_2. Given that the experiments conducted here only studied one patient sample per sickle cell genotype, the correlation between the extent of relaxation and haemoglobinopathy could not be elucidated.

NO analyses of patient and control samples revealed high levels of both plasma RSNO/RNNO and total RBC NO. Such measurements, made by several different techniques, have received close scrutiny, not least because of the inconsistency in values published by different research groups (106, 350, 352). Compared to data published by Marley and Nagababu, the levels of RSNO achieved here were approximately 2 to 4 fold greater (118, 350). Conversely the levels of plasma NO_2^- for both normal and abnormal samples were approximately 275 nM which compares favourably with previously published values (248, 275). A likely explanation for the elevated levels of plasma RSNO/RNNO could be the lack of patient/control fasting prior to blood collection. Since dietary intake is well known to increase plasma metabolite levels, the latter is a significant cofounder of the present study (353).

Interestingly, total RBC associated NO was significantly elevated in abnormal RBC samples. Moreover, both normal and abnormal sample levels deviated substantially from previously from published data (248). A study by Pawloski and colleagues reported a decreased level of Hb bound SNO in sickle cell RBCs compared to controls (354). Further NO analysis of the samples collected would have verified the distribution of NO inside the RBC and confirmed whether Hb associated NO_2^- as well as other unbound metabolites contributed to the overall rise in the total RBC NO measured.

In summary, this pilot study has shown that sickle cells have the capacity to relax hypoxic vascular tissue. This is likely to be due to the fact that transient exposure of low levels of O_2 does not affect hydrophobic interaction between HbS chains and therefore the O_2 offloading capacity of mutated Hb.

7 Conclusions

The main aims of this thesis were to further investigate the role of O_2 in the relaxation of hypoxic vascular smooth muscle. Building on the work of previous and more recent findings within our research group, the experiments described herein were designed to establish the mechanism underlying O_2-induced relaxation and to explore how this is related to the phenomenon of hypoxic vasorelaxation by RBCs.

The biochemical role of NO within RBCs as a mediator of this effect has been intensely debated over the past two decades (244, 248, 355). In particular, research interests have focused on two interactions of NO with Hb. Firstly, thiol bound NO forming HbSNO and secondly, the capacity of Hb (in deoxy state) to function as a NO_2^- reductase. With regard to HbSNO, it is well recognised that released SNO has the capacity to promote vasorelaxation (270). However the research presented within this thesis, and previously within our laboratory, suggests that SNO may not be the direct cause of vascular relaxation in hypoxia.

The interest in NO_2^- and its subsequent reduction by Hb (247, 274, 356), originated from the evidence that there is an arterial to venous gradient of plasma NO_2^- present in blood (248), suggestive of the utilisation of NO_2^- across a vascular bed. In the context of RBC-induced vasorelaxation, our group has demonstrated that NO_2^- can directly relax hypoxic vascular tissue in the absence of Hb (357) *in vitro*, suggesting that Hb may not be necessary to facilitate changes in vessel tone. In addition, an *in vivo* NO_2^- infusion study confirmed that Hb has little effect on NO_2^- reduction, providing further evidence to reject this theory (275). The latter *in vivo* experiment was performed with physiological concentrations of NO_2^- in contrast to several studies that draw rigid conclusions on the basis of supraphysiological concentrations of NO_2^-. Our group has also provided evidence that

differences in NO metabolite levels in various compartments in the body are due to reapportionment of metabolites as opposed to a net loss/gain from that compartment. Most importantly, the overall level of NO (in terms of total NO metabolites measureable) in blood remains consistent. This is likely due to the difference in utilisation of tissue NO_2^- compared to NO_2^- contained within the plasma compartment which can also be augmented in the face of hypoxia (275).

Both of the theories outlined above are dependent upon the allosteric state of Hb and the level of tissue oxygenation, which allows for the release of vasoactive forms of NO, leading to vasorelaxation. Important data emerged from the previous project which shaped the work within this thesis. Most importantly, this data illustrated that the vasorelaxant species released from RBCs was replenishable upon re-oxygenation. Therefore, such a mediator would be completely restored during T to R cycling. It is important to mention that the mechanism of hypoxic vasorelaxation cannot be mistaken for the series of events which occurs during the adaptive response to chronic/prolonged hypoxia but instead serves to quickly deliver O_2 to local tissue which may have a reduced blood supply.

The novel work reported within this thesis provides convincing evidence for the direct role of O_2 in the relaxation of hypoxic vascular tissue. The initial rationale for investigation with O_2 in this setting came about by the inclusion of an appropriate control for classical RBC hypoxic vessel studies. O_2, in the form of an oxygenated buffer bolus (comparable to RBC HbO_2 saturation), was able to induce a transient relaxation of hypoxic rabbit aortic rings which was of identical magnitude to that induced by RBCs, illustrated in Chapter 3 of this thesis. Our lab has previously reported a rise in O_2 concentration in hypoxic myograph experiments post-administration of oxygenated RBCs, as measured by an O_2

electrode (259). Interestingly, the post-relaxation vasoconstriction attributable to RBC-induced relaxation was also present for O_2 alone. Moreover, the content of O_2 within the buffer sample was directly correlated to the extent of vessel relaxation. This finding is closely related to the relationship between HbO_2 saturation and the extent of vessel relaxation illustrated in Chapter 3. In addition, further analysis of this correlation suggests that the line of regression runs through the origin therefore if no relaxation occurs, no post-constriction results. This questions the proposed theory of Hb scavenging of NO, since a prior vasorelaxation is not essential. A study presented in Chapter 3 demonstrates that the K_{ATP} channel inhibitor, glibenclamide, almost completely abolishes the post relaxation vasoconstriction induced in rabbit aortic rings. This suggests the role of O_2 in this setting could be partly attributed to the turnover of energy source, ATP. All tissue experiments in Chapter 3 utilised an increased concentration of PE due to the relaxant effect of hypoxia on basal vascular tone. Thus, a second mechanism of vasoconstriction could be limited to the effect of O_2 upon cellular respiration and subsequent turnover of mitochondrial ATP, giving rise to an increased energy store for further constriction by excess PE present within the tissue bath.

The simple idea that molecular O_2 could cause relaxation in hypoxia was one which posed many research questions, the most significant being, what is the mechanism by which O_2 acts? Our laboratory and others (250, 258) have shown that RBC-induced vasorelaxation in hypoxia can be largely inhibited by ODQ. This is also true for O_2-induced vasorelaxation presented in Chapter 3 and signifies a sGC-dependent mechanism.

The data presented in Chapter 4 are the first to provide evidence for the stimulation of purified human sGC by O_2. Numerous publications have stated that human sGC cannot

bind O_2 (283, 301, 303), mainly due to its primary function in NO signalling. However, levels of cGMP detected by ELISA were significantly increased by atmospheric levels of O_2 compared to hypoxia and more importantly, this occurred in the absence of preferential ligand, NO. In addition, the activity of hypoxic sGC was 'sensitised' to lower concentrations of NO compared to the normoxic enzyme. The question remains as to the physiological or indeed pathological role of this action.

In terms of conditions such as coronary heart disease, where myocardial tissue oxygenation is limited distal to the site of occlusion (358), NO donors are extremely beneficial to enhance vasodilation. Chronic treatment with drugs such as GTN are associated with developed tolerance in patients (359) and the search for alternative treatments is ongoing. Looking from a different perspective, an unexpected mechanism by which NO donor treatment could improve vascular function is through this increased sensitivity of sGC. Although the work within this chapter did not confirm the location of O_2 stimulation of sGC, it is likely that O_2 has a direct influence upon the haem moiety of the enzyme in a site similar to that where BAY 41-2272 acts. This is a completely novel finding which is important to the field of sGC biochemistry and could benefit the development of sGC-targeted therapeutics. In the clinic today, O_2 therapy has vastly improved the well-being of patients with acute coronary syndromes by improving the saturation of Hb and subsequent tissue oxygenation (360). The theory we propose is that O_2 delivery in this setting could lead to enhanced vasodilatory functions which are not attributable to NO. Excessive O_2 exposure however does lead to negative effects due to the increased formation of radical species (360) which would need to be taken into consideration prior to therapy.

The research conducted for this thesis, as well as other publications (258, 271), used the isolated rabbit aortic ring model to explore the mechanisms underlying hypoxic vasorelaxation. However, *in vivo* the aorta is unlikely to experience such hypoxic conditions and the aim of Chapter 5 was to characterise these findings in porcine coronary artery. This particular subset of vessels was chosen due to the relative diameter of the vessels in relation to human coronary vessels as well as rabbit aortic vessels used in previous experiments within this thesis. Coronary vessels and the myocardial tissue which surround them can become ischaemic when myocardial O_2 supply does not meet demand (358). Since coronary blood flow is ~250 ml/min^{-1} at rest (312), it is imperative that the blood can flow freely to the heart to meet this demand (332). Coronary thrombosis and conditions where blood flow to the heart muscle is compromised leads to a decreased perfusion of the myocardium and subsequent myocardial ischaemia (361). These studies therefore had direct pathological significance. O_2-induced vasorelaxation in porcine coronary LAD rings produced significantly enhanced relaxations compared with rabbit aortic rings of the same inner diameter. Since O_2 could enhance the activity of sGC, the sGC α_1 and β_1 content in both tissue types was examined and shown to be similar in porcine coronary and rabbit aortic tissue per mg of protein. Although of similar size in terms of inner diameter, porcine coronary vessels possess a thicker vessel wall than rabbit aorta. Thus the amount of total sGC protein in porcine coronary vessels was higher, allowing more O_2 to bind sGC. *In vivo* this increased O_2 binding to sGC and subsequent vasorelaxation could benefit patients with endothelial dysfunction, where NO bioavailabilty is lacking (362). Further investigation into the effect of O_2-induced vasorelaxation of porcine coronary vessels of different size illustrated that smaller porcine coronary rings (~0.5 mm inner diameter) deriving from the LAD, demonstrated an enhanced relaxatory response compared to vessels of a larger inner

diameter. This finding is important in understanding how various coronary vessels supplying the myocardial tissue bed respond to O_2. For instance, in a clinical setting, vessels and myocardial tissue downstream from the site of occlusion would benefit from increased O_2 sensitivity post-bypass surgery.

In summary, through the use of *in vitro* techniques, the data within this thesis provides convincing evidence to support the role of O_2 in mediating relaxation under acute hypoxic conditions. In comparison with the classical RBC-induced vasorelaxation bioassay performed by ourselves and others, this data supports the hypothesis that O_2 is the mediator released from RBCs to transiently dilate hypoxic tissue. Our myograph studies utilise RBCs at a < 0.5 % haematocrit and still we see ~15 % relaxation induced in rabbit aortic rings and ~30 % relaxation in porcine coronary tissue. *In vivo*, where the haematocrit is ~40 %, this could have a significant effect upon matching O_2 supply with demand, especially in the heart where myocardial O_2 supply is vital. Further evidence is needed to support the studies presented here with regards to the direct interaction of sGC with O_2. Structural studies conducted to date have focussed on the binding of NO to sGC under de-gassed conditions, mainly due to the rapid oxidation of NO by O_2. However, in order to confirm whether O_2 binds sGC, structural studies would need to be attempted under conditions where O_2 concentration is strictly controlled and in the absence of NO.

Publications & Presentations

Publications

- **Dada, J**., Pinder, A.G., Lang, D. and James, PE. (2013). Oxygen mediates vascular smooth muscle relaxation in hypoxia. *PLOS ONE,* Vol 8, 2, pp. e57162.
- **Dada, J**., Pinder, A.G., Lang, D, and James, PE. Oxygen can mediate relaxation of hypoxic vascular smooth muscle. *Nitric Oxide*, Vol 27. Suppl. S27.
- James P.E., Bundhoo, S., Sagan, E., **Dada, J**., Halcox, J.P., Morris, K. and Anderson R.A. Thienopyridine-derived nitrosothiol. (2012). *Platelets*, Vol 23, 4, pp. 322-330.
- Bundhoo SS, Anderson RA, Sagan E, **Dada J**, Harris R, Halcox JP, Lang D and James PE. (2011) Direct vasoactive properties of thienopyridine-derived nitrosothiols. *J. Cardiovasc Pharmacol,* Vol 58(5), pp. 550-558.
- Anderson, RA, Bundhoo, S., Sagan, E, **Dada, J**, Lang, D, James, PE. (2011).The formation of S-nitrosothiols from thienopyridines inhibit platelet transformation without biotransformation: Novel mechanism of action? *JACC* 57(14) Suppl. 1; E1917.
- Anderson, RA, Bundhoo, S., Sagan, E, **Dada, J**, Harris, R , James, PE. (2011). From thienopyridines to nitrosothiols: A novel potential mechanism of thienopyridines bioactivity. *JACC* 57(14) Suppl. 1; E1918.
- Anderson, RA, Bundhoo, S, Sagan, E, **Dada, J**, Harris, R, Halcox, J, Lang, D, and James PE. (2010). Direct Vasoactive properties of Thienopyridine derived Nitrosothiols. *JACC,* Vol 56, 13, Suppl B.

Presentations

- 22nd – 26th July 2012: The 7th International Conference on the Biology, Chemistry & Therapeutic Application of Nitric Oxide (NO2012), Edinburgh, UK – Poster presentation.
- 13th – 18th February 2011 – Gordon Research Conference on Nitric Oxide, California – Chairman's Choice oral presentation.
- 11th November 2011 – Cardiff University Postgraduate Research Day – Poster finalist.
- 12th – 15th July 2010 – Bristol Heart Institute Summer School – Poster presentation.

References

1. Gonzalez C, Almaraz L, Obeso A, Rigual R. Carotid body chemoreceptors: from natural stimuli to sensory discharges. Physiological reviews. 1994;74(4):829.
2. Germann WJ, Stanfield CL. Principles of Human Physiology. Education P, editor. San Francisco: Benjamin Cummings; 2005.
3. Prabhakar NR. Oxygen sensing by the carotid body chemoreceptors. Journal of Applied Physiology. 2000;88(6):2287-95.
4. Prabhakar NR. Invited Review: Oxygen sensing during intermittent hypoxia: cellular and molecular mechanisms. Journal of Applied Physiology. 2001;90(5):1986-94.
5. Rausch SM, Whipp BJ, Wasserman K, Huszczuk A. Role of the carotid bodies in the respiratory compensation for the metabolic acidosis of exercise in humans. The Journal of Physiology. 1991;444(1):567-78.
6. Lahiri S, Semenza GL, Prabhakar NR. Oxygen sensing: Responses and adaptation to hypoxia: CRC Press; 2003.
7. Lahiri S, Roy A, Baby SM, Hoshi T, Semenza GL, Prabhakar NR. Oxygen sensing in the body. Progress in biophysics and molecular biology. 2006;91(3):249-86.
8. Morio Y, McMurtry IF. Ca2+ release from ryanodine-sensitive store contributes to mechanism of hypoxic vasoconstriction in rat lungs. Journal of Applied Physiology. 2002;92(2):527-34.
9. Williams SE, Wootton P, Mason HS, Bould J, Iles DE, Riccardi D, et al. Hemoxygenase-2 is an oxygen sensor for a calcium-sensitive potassium channel. Science. 2004;306(5704):2093-7.
10. Adachi T, Ishikawa K, Hida W, Matsumoto H, Masuda T, Date F, et al. Hypoxemia and blunted hypoxic ventilatory responses in mice lacking heme oxygenase-2. Biochemical and biophysical research communications. 2004;320(2):514-22.
11. Ortega-Sáenz P, Pascual A, Gómez-Díaz R, López-Barneo J. Acute oxygen sensing in heme oxygenase-2 null mice. The Journal of general physiology. 2006;128(4):405-11.
12. Ortega-Sáenz P, Pascual A, Piruat JI, López-Barneo J. Mechanisms of acute oxygen sensing by the carotid body: lessons from genetically modified animals. Respiratory physiology & neurobiology. 2007;157(1):140-7.
13. Carrera S, de Verdier PJ, Khan Z, Zhao B, Mahale A, Bowman KJ, et al. Protection of cells in physiological oxygen tensions against DNA damage-induced apoptosis. Journal of Biological Chemistry. 2010;285(18):13658-65.
14. Chandel NS, Budinger GS, Schumacker PT. Molecular oxygen modulates cytochrome c oxidase function. Journal of Biological Chemistry. 1996;271(31):18672-7.
15. Chance B, Williams G. Respiratory enzymes in oxidative phosphorylation I. Kinetics of oxygen utilization. Journal of Biological Chemistry. 1955;217(1):383-94.
16. Korshunov SS, Skulachev VP, Starkov AA. High protonic potential actuates a mechanism of production of reactive oxygen species in mitochondria. FEBS letters. 1997;416(1):15-8.
17. Dawson TL, Gores GJ, Nieminen A-L, Herman B, Lemasters JJ. Mitochondria as a source of reactive oxygen species during reductive stress in rat hepatocytes. American Journal of Physiology-Cell Physiology. 1993;264(4):C961-C7.
18. Lopez-Barneo J, Lopez-Lopez JR, Urena J, Gonzalez C. Chemotransduction in the carotid body: K+ current modulated by PO2 in type I chemoreceptor cells. Science. 1988;241(4865):580-2.
19. Buckler K. A novel oxygen-sensitive potassium current in rat carotid body type I cells. The Journal of Physiology. 1997;498(Pt 3):649-62.
20. López-Barneo J. Oxygen-sensing by ion channels and the regulation of cellular functions. Trends in neurosciences. 1996;19(10):435-40.
21. Fearon I, Palmer A, Balmforth A, Ball S, Varadi G, Peers C. Modulation of recombinant human cardiac L-type Ca2+ channel α1C subunits by redox agents and hypoxia. The Journal of physiology. 1999;514(3):629-37.

22. Babior BM. NADPH oxidase. Current opinion in immunology. 2004;16(1):42-7.
23. Wang D, Youngson C, Wong V, Yeger H, Dinauer MC, De Miera EV-S, et al. NADPH-oxidase and a hydrogen peroxide-sensitive K+ channel may function as an oxygen sensor complex in airway chemoreceptors and small cell lung carcinoma cell lines. Proceedings of the National Academy of Sciences. 1996;93(23):13182-7.
24. Marshall C, Mamary A, Verhoeven A, Marshall B. Pulmonary artery NADPH-oxidase is activated in hypoxic pulmonary vasoconstriction. American journal of respiratory cell and molecular biology. 1996;15(5):633-44.
25. Jones RD, Hancock JT, Morice AH. NADPH oxidase: a universal oxygen sensor? Free Radical Biology and Medicine. 2000;29(5):416-24.
26. Archer SL, Reeve HL, Michelakis E, Puttagunta L, Waite R, Nelson DP, et al. O2 sensing is preserved in mice lacking the gp91 phox subunit of NADPH oxidase. Proceedings of the National Academy of Sciences. 1999;96(14):7944-9.
27. James PE, Parton J, Jackson SK, Frenneaux MP. Oxygen indirectly regulates nitric oxide availability. Adv Exp Med Biol. 2003;510:139-43.
28. Semenza G. HIF-1: using two hands to flip the angiogenic switch. Cancer and Metastasis Reviews. 2000;19(1):59-65.
29. Semenza G. Surviving ischemia: adaptive responses mediated by hypoxia-inducible factor. Journal of Clinical Investigation. 2000;106(7):809-12.
30. Semenza GL. Regulation of mammalian O2 homeostasis by hypoxia-inducible factor 1. Annual review of cell and developmental biology. 1999;15(1):551-78.
31. Russell N, Powell G, Jones J, Winterburn P, Basford J. Blood Biochemistry. Kent: Croom Helm Ltd; 1982.
32. Elliott SG, Foote MA, Molineux G. Erythropoietins, erythropoietic factors, and erythropoiesis: molecular, cellular, preclinical, and clinical biology: Springer; 2009.
33. CROSBY WH. Normal functions of the spleen relative to red blood cells: a review. Blood. 1959;14(4):399-408.
34. Kiefer CR, Snyder LM. Oxidation and erythrocyte senescence. Current opinion in hematology. 2000;7(2):113-6.
35. Sherwood L. Human physiology: from cells to systems: Thomson Brooks/Cole; 2012.
36. Kavanaugh J, Moo-Penn W, Arnone A. Accommodation of insertions in helices: The mutation in hemoglobin Catanosville (Pro 37α-Glu-Thr 38α) generates a 3 10 α bulge. Biochemistry. 1993;32:2509-13.
37. Adair G. The hemoglobin system. Journal of Biological Chemistry. 1925;63(2):529.
38. Haurowitz F, Hardin RL, Dicks M. Denaturation of hemoglobins by alkali. The Journal of Physical Chemistry. 1954;58(2):103-5.
39. Andrzej Brzozowski Z, Eleanor Dodson G, Mieczyslaw Grabowski R. Bonding of molecular oxygen to T state human haemoglobin. 1984.
40. Perutz MF, Ladner JE, Simon SR, Ho C. Influence of globin structure on the state of the heme. I. Human deoxyhemoglobin. Biochemistry. 1974;13(10):2163-73.
41. Lukin JA, CHIEN H. The structure-function relationship of hemoglobin in solution at atomic resolution. Chemical reviews. 2004;104(3):1219-30.
42. Paulev P-E. Textbook in Medical Physiology and Pathophysiology: Essentials and clinical problems: Copenhagen Medical Publishers; 1999.
43. Brunori M, Engel J, Schuster TM. The effect of ligand binding on the optical rotatory dispersion of myoglobin, hemoglobin, and isolated hemoglobin subunits. Journal of Biological Chemistry. 1967;242(4):773-4.
44. Popel AS. Theory of oxygen transport to tissue. Critical reviews in biomedical engineering. 1988;17(3):257-321.

45. Krogh A. The number and distribution of capillaries in muscles with calculations of the oxygen pressure head necessary for supplying the tissue. The Journal of physiology. 1919;52(6):409-15.
46. Rhoades RA, Bell DR. Medical physiology: principles for clinical medicine: Wolters Kluwer Health; 2009.
47. Bronzino JD. The biomedical engineering handbook. 2: CRC press; 2000.
48. Fantini S. Dynamic model for the tissue concentration and oxygen saturation of hemoglobin in relation to blood volume, flow velocity, and oxygen consumption: Implications for functional neuroimaging and coherent hemodynamics spectroscopy (CHS). NeuroImage. 2013.
49. Bohr C, Hasselbalch K, Krogh A. Concerning a biologically important relationship–the influence of the carbon dioxide content of blood on its oxygen binding. Skand Arch Physiol. 1904;16:402.
50. Murray R, Granner D, Mayes P, Rodwell V. 26th ed: McGraw-Hill Medical; 2003.
51. Maynard R, Waller R. Carbon monoxide. In: Air pollution and Health. New York: Academic Press; 1999.
52. Christiansen J, Douglas C, Haldane J. The absorption and dissociation of carbon dioxide by human blood. The Journal of Physiology. 1914;48(4):244-71.
53. Siems W, Sommerburg O, Grune T. Erythrocyte free radical and energy metabolism. Clinical nephrology. 2000;53(1 Suppl):S9.
54. Nepal O, Rao JP. Haemolytic effects of hypo-osmotic salt solutions on human erythrocytes. Kathmandu University Medical Journal. 2012;9(2):35-9.
55. Dzik WH. The air we breathe: three vital respiratory gases and the red blood cell: oxygen, nitric oxide, and carbon dioxide. Transfusion. 2011;51(4):676-85.
56. Schaller J, Gerber S, Kaempfer U, Lejon S, Trachsel C. Human blood plasma proteins: structure and function: Wiley; 2008.
57. Thomas C, Lumb AB. Physiology of haemoglobin. Continuing Education in Anaesthesia, Critical Care & Pain. 2012;12(5):251-6.
58. McArdle WD, Katch FI, Katch VL. Exercise physiology: nutrition, energy, and human performance: Lippincott Williams & Wilkins; 2010.
59. Bradford JR, Dean HP. The pulmonary circulation. The Journal of physiology. 1894;16(1-2):34.
60. Euler Uv, Liljestrand G. Observations on the pulmonary arterial blood pressure in the cat. Acta Physiologica Scandinavica. 1946;12(4):301-20.
61. Ingram TE, Pinder AG, Bailey DM, Fraser AG, James PE. Low-dose sodium nitrite vasodilates hypoxic human pulmonary vasculature by a means that is not dependent on a simultaneous elevation in plasma nitrite. Am J Physiol Heart Circ Physiol. 2010;298(2):H331-9.
62. Dipp M, Evans AM. Cyclic ADP-ribose is the primary trigger for hypoxic pulmonary vasoconstriction in the rat lung in situ. Circulation research. 2001;89(1):77-83.
63. Dipp M, Nye PC, Evans AM. Hypoxic release of calcium from the sarcoplasmic reticulum of pulmonary artery smooth muscle. American Journal of Physiology-Lung Cellular and Molecular Physiology. 2001;281(2):L318-L25.
64. Evans AM, Hardie DG, Peers C, Mahmoud A. Hypoxic pulmonary vasoconstriction: mechanisms of oxygen-sensing. Current opinion in anaesthesiology. 2011;24(1):13.
65. Galley HF, Webster NR. Physiology of the endothelium. British journal of anaesthesia. 2004;93(1):105-13.
66. Gallagher G, Sumpio BE. Vascular endothelial cells. Basic Science of Vascular Disease Mt Kisco: Futura Publishing Co. 1997:151-86.
67. Otsuka F, Finn AV, Yazdani SK, Nakano M, Kolodgie FD, Virmani R. The importance of the endothelium in atherothrombosis and coronary stenting. Nature Reviews Cardiology. 2012.
68. Moncada S, Higgs A. The Vascular Endothelium I: Springer; 2010.

69. Csortos C, Kolosova I, Verin AD. Regulation of vascular endothelial cell barrier function and cytoskeleton structure by protein phosphatases of the PPP family. American Journal of Physiology-Lung Cellular and Molecular Physiology. 2007;293(4):L843-L54.
70. Rubanyi GM. The role of endothelium in cardiovascular homeostasis and diseases. Journal of cardiovascular pharmacology. 1993;22:S1&hyhen.
71. Levi M, ten Cate H, van der Poll T. Endothelium: interface between coagulation and inflammation. Critical care medicine. 2002;30(5):S220-S4.
72. Pober JS, Cotran RS. The role of endothelial cells in inflammation. Transplantation. 1990;50(4):537-44.
73. Varani J, Ward PA. Mechanisms of endothelial cell injury in acute inflammation. Shock. 1994;2(5):311-2.
74. Lawrence T, Willoughby DA, Gilroy DW. Anti-inflammatory lipid mediators and insights into the resolution of inflammation. Nature Reviews Immunology. 2002;2(10):787-95.
75. Harrison DG, Widder J, Grumbach I, Chen W, Weber M, Searles C. Endothelial mechanotransduction, nitric oxide and vascular inflammation. Journal of internal medicine. 2006;259(4):351-63.
76. Tedgui A, Mallat Z. Anti-inflammatory mechanisms in the vascular wall. Circulation Research. 2001;88(9):877-87.
77. Halliwell B, Gutteridge JMC. Lipid peroxidation: a radical chain reaction. Free radicals in biology and medicine. 1989;2:188-218.
78. Wang DH. Molecular sensors for cardiovascular homeostasis: Springer; 2007.
79. Wolin MS, Ahmad M, Gupte SA. The sources of oxidative stress in the vessel wall. Kidney international. 2005;67(5):1659-61.
80. Darley-Usmar V, Halliwell B. Blood radicals: reactive nitrogen species, reactive oxygen species, transition metal ions, and the vascular system. Pharmaceutical research. 1996;13(5):649-62.
81. Liu Y, Zhao H, Li H, Kalyanaraman B, Nicolosi AC, Gutterman DD. Mitochondrial sources of H2O2 generation play a key role in flow-mediated dilation in human coronary resistance arteries. Circulation research. 2003;93(6):573-80.
82. Wolin MS. Interactions of oxidants with vascular signaling systems. Arteriosclerosis, thrombosis, and vascular biology. 2000;20(6):1430-42.
83. Förstermann U. Oxidative stress in vascular disease: causes, defense mechanisms and potential therapies. Nature Clinical Practice Cardiovascular Medicine. 2008;5(6):338-49.
84. Wolin MS. Reactive oxygen species and the control of vascular function. American Journal of Physiology-Heart and Circulatory Physiology. 2009;296(3):H539-H49.
85. Bredt DS, Hwang PM, Glatt CE, Lowenstein C, Reed RR, Snyder SH. Cloned and expressed nitric oxide synthase structurally resembles cytochrome P-450 reductase. Nature. 1991;351(6329):714-8.
86. Bredt DS, Hwang PM, Snyder SH. Localization of nitric oxide synthase indicating a neural role for nitric oxide. Nature. 1990;347(6295):768-70.
87. Xie Q-W, Cho HJ, Calaycay J, Mumford RA, Swiderek KM, Lee TD, et al. Cloning and characterization of inducible nitric oxide synthase from mouse macrophages. Science. 1992;256(5054):225-8.
88. Stuehr DJ, Griffith OW. Mammalian nitric oxide synthases. Advances in Enzymology and Related Areas of Molecular Biology, Volume 65. 1992:287-346.
89. Alderton WK, Cooper CE, Knowles RG. Nitric oxide synthases: structure, function and inhibition. Biochemical Journal. 2001;357(Pt 3):593.
90. Marletta MA. Nitric oxide synthase structure and mechanism: ASBMB; 1993.
91. Stuehr DJ. Structure-function aspects in the nitric oxide synthases. Annual review of pharmacology and toxicology. 1997;37(1):339-59.
92. Rang HP, Dale MM, Ritter JM, Moore PK. Pharmacology. 5th. London: Churchill Livingston. 2003:490-502.

93. Hord NG, Tang Y, Bryan NS. Food sources of nitrates and nitrites: the physiologic context for potential health benefits. The American journal of clinical nutrition. 2009;90(1):1-10.
94. Furchgott RF, Bhadrakom S. Reactions of strips of rabbit aorta to epinephrine, isopropylarterenol, sodium nitrite and other drugs. Journal of Pharmacology and Experimental Therapeutics. 1953;108(2):129-43.
95. Classen HG, Stein-Hammer C, Thöni H. Hypothesis: the effect of oral nitrite on blood pressure in the spontaneously hypertensive rat. Does dietary nitrate mitigate hypertension after conversion to nitrite? Journal of the American College of Nutrition. 1990;9(5):500-2.
96. Haas M, Classen HG, Thöni H, Classen UG, Drescher B. Persistent antihypertensive effect of oral nitrite supplied up to one year via the drinking water in spontaneously hypertensive rats. Arzneimittelforschung. 2011;49(04):318-23.
97. Beier S, Classen HG, Loeffler K, Schumacher E, Thöni H. Antihypertensive effect of oral nitrite uptake in the spontaneously hypertensive rat. Arzneimittel-Forschung. 1995;45(3):258-61.
98. Tsuchiya K, Takiguchi Y, Okamoto M, Izawa Y, Kanematsu Y, Yoshizumi M, et al. Malfunction of vascular control in lifestyle-related diseases: formation of systemic hemoglobin-nitric oxide complex (HbNO) from dietary nitrite. Journal of pharmacological sciences. 2004;96(4):395-400.
99. Godber BL, Doel JJ, Sapkota GP, Blake DR, Stevens CR, Eisenthal R, et al. Reduction of nitrite to nitric oxide catalyzed by xanthine oxidoreductase. Journal of Biological Chemistry. 2000;275(11):7757-63.
100. Gautier C, van Faassen E, Mikula I, Martasek P, Slama-Schwok A. Endothelial nitric oxide synthase reduces nitrite anions to NO under anoxia. Biochemical and biophysical research communications. 2006;341(3):816-21.
101. Gladwin M, Crawford J, Patel R. The biochemistry of nitric oxide, nitrite, and hemoglobin: role in blood flow regulation* 1. Free Radical Biology and Medicine. 2004;36(6):707-17.
102. Larsen FJ, Ekblom B, Sahlin K, Lundberg JO, Weitzberg E. Effects of dietary nitrate on blood pressure in healthy volunteers. New England Journal of Medicine. 2006;355(26):2792-3.
103. Webb AJ, Patel N, Loukogeorgakis S, Okorie M, Aboud Z, Misra S, et al. Acute blood pressure lowering, vasoprotective, and antiplatelet properties of dietary nitrate via bioconversion to nitrite. Hypertension. 2008;51(3):784-90.
104. Kapil V, Webb A, Ahluwalia A. Inorganic nitrate and the cardiovascular system. Heart. 2010;96(21):1703-9.
105. Gow AJ, Chen Q, Hess DT, Day BJ, Ischiropoulos H, Stamler JS. Basal and stimulated protein S-nitrosylation in multiple cell types and tissues. Journal of Biological Chemistry. 2002;277(12):9637-40.
106. Stamler J, Jaraki O, Osborne J, Simon D, Keaney J, Vita J, et al. Nitric oxide circulates in mammalian plasma primarily as an S-nitroso adduct of serum albumin. Proceedings of the National Academy of Sciences. 1992;89(16):7674.
107. Broillet M-C. S-nitrosylation of proteins. Cellular and Molecular Life Sciences CMLS. 1999;55(8-9):1036-42.
108. Martínez-Ruiz A, Villanueva L, de Orduña CG, López-Ferrer D, Higueras MÁ, Tarín C, et al. S-nitrosylation of Hsp90 promotes the inhibition of its ATPase and endothelial nitric oxide synthase regulatory activities. Proceedings of the National Academy of Sciences of the United States of America. 2005;102(24):8525-30.
109. Gaston B, Reilly J, Drazen JM, Fackler J, Ramdev P, Arnelle D, et al. Endogenous nitrogen oxides and bronchodilator S-nitrosothiols in human airways. Proceedings of the National Academy of Sciences. 1993;90(23):10957-61.
110. Jia L, Bonaventura C, Bonaventura J, Stamler J. S-nitrosohaemoglobin: a dynamic activity of blood involved in vascular control. Nature. 1996;380:221-6.
111. Kluge I, Gutteck-Amsler U, Zollinger M, Do KQ. S-Nitrosoglutathione in Rat Cerebellum: Identification and Quantification by Liquid Chromatography-Mass Spectrometry. Journal of neurochemistry. 1997;69(6):2599-607.

112. Mathews WR, Kerr SW. Biological activity of S-nitrosothiols: the role of nitric oxide. Journal of Pharmacology and Experimental Therapeutics. 1993;267(3):1529-37.
113. Grube R, Kelm M, Motz W, Stauer B, Moncada S, Feelisch M, et al. Enzymology, Biochemistry and Immunology. London: Portland Press; 1994.
114. Kelm M. Nitric oxide metabolism and breakdown. Biochimica et Biophysica Acta (BBA)-Bioenergetics. 1999;1411(2):273-89.
115. Marley R, Patel RP, Orie N, Ceaser E, Darley-Usmar V, Moore K. Formation of nanomolar concentrations of S-nitroso-albumin in human plasma by nitric oxide. Free Radical Biology and Medicine. 2001;31(5):688-96.
116. Pinder AG, Rogers SC, Khalatbari A, Ingram TE, James PE. The measurement of nitric oxide and its metabolites in biological samples by ozone-based chemiluminescence. Methods Mol Biol. 2009;476:10-27.
117. Nagababu E, Rifkind JM. Measurement of plasma nitrite by chemiluminescence. Free Radicals and Antioxidant Protocols: Springer; 2010. p. 41-9.
118. Nagababu E, Rifkind JM. Determination of S-NitrosothiolsS-Nitrosothiols in Biological Fluids by ChemiluminescenceChemiluminescence. Nitric Oxide: Springer; 2011. p. 27-37.
119. Cassoly R, Gibson QH. Conformation, co-operativity and ligand binding in human hemoglobin. Journal of molecular biology. 1975;91(3):301-13.
120. Rohlfs RJ, Bruner E, Chiu A, Gonzales A, Gonzales ML, Magde D, et al. Arterial blood pressure responses to cell-free hemoglobin solutions and the reaction with nitric oxide. Journal of Biological Chemistry. 1998;273(20):12128-34.
121. Wolf EW, Banerjee A, Soble-Smith J, Dohan Jr FC, White RP, Robertson JT. Reversal of cerebral vasospasm using an intrathecally administered nitric oxide donor. Journal of neurosurgery. 1998;89(2):279-88.
122. Huang Z, Ucer K, Murphy T, Williams RT, King SB, Kim-Shapiro DB. Kinetics of nitric oxide binding to R-state hemoglobin. Biochemical and biophysical research communications. 2002;292(4):812-8.
123. Sharma VS, Ranney HM. The dissociation of NO from nitrosylhemoglobin. Journal of Biological Chemistry. 1978;253(18):6467-72.
124. Stamler J, Jia L, Eu J, McMahon T, Demchenko I, Bonaventura J, et al. Blood flow regulation by S-nitrosohemoglobin in the physiological oxygen gradient. Science. 1997;276(5321):2034.
125. Gow AJ, Stamler JS. Reactions between nitric oxide and haemoglobin under physiological conditions. Nature. 1998;391(6663):169-73.
126. May JM, Qu Z-C, Xia L, Cobb CE. Nitrite uptake and metabolism and oxidant stress in human erythrocytes. American Journal of Physiology-Cell Physiology. 2000;279(6):C1946-C54.
127. Kosaka H, Imaizumi K, Imai K, Tyuma I. Stoichiometry of the reaction of oxyhemoglobin with nitrite. Biochimica et Biophysica Acta (BBA)-Protein Structure. 1979;581(1):184-8.
128. Zavodnik I, Lapshina E, Rekawiecka K, Zavodnik L, Bartosz G, Bryszewska M. Membrane effects of nitrite-induced oxidation of human red blood cells. Biochimica et Biophysica Acta (BBA)-Biomembranes. 1999;1421(2):306-16.
129. Shingles R, Roh MH, McCarty RE. Direct measurement of nitrite transport across erythrocyte membrane vesicles using the fluorescent probe, 6-methoxy-N-(3-sulfopropyl) quinolinium. Journal of bioenergetics and biomembranes. 1997;29(6):611-6.
130. Doyle MP, Pickering RA, DeWeert TM, Hoekstra JW, Pater D. Kinetics and mechanism of the oxidation of human deoxyhemoglobin by nitrites. Journal of Biological Chemistry. 1981;256(23):12393-8.
131. Bayliss WM. On the local reactions of the arterial wall to changes of internal pressure. The Journal of physiology. 1902;28(3):220-31.
132. Meininger GA, Davis MJ. Cellular mechanisms involved in the vascular myogenic response. American Journal of Physiology-Heart and Circulatory Physiology. 1992;263(3):H647-H59.

133. Horowitz A, Menice CB, Laporte R, Morgan KG. Mechanisms of smooth muscle contraction. Physiological reviews. 1996;76(4):967-1003.
134. Sakurada S, Takuwa N, Sugimoto N, Wang Y, Seto M, Sasaki Y, et al. Ca2+-dependent activation of Rho and Rho kinase in membrane depolarization-induced and receptor stimulation-induced vascular smooth muscle contraction. Circulation research. 2003;93(6):548.
135. Kamm KE, Stull JT. The function of myosin and myosin light chain kinase phosphorylation in smooth muscle. Annual review of pharmacology and toxicology. 1985;25(1):593-620.
136. Spudich JA. The myosin swinging cross-bridge model. Nature Reviews Molecular Cell Biology. 2001;2(5):387-92.
137. Hughes AD. Calcium channels in vascular smooth muscle cells. Journal of vascular research. 2008;32(6):353-70.
138. Walsh MP. Vascular smooth muscle myosin light chain diphosphorylation: mechanism, function, and pathological implications. IUBMB life. 2011;63(11):987-1000.
139. Karaki H, Ozaki H, Hori M, Mitsui-Saito M, Amano K-I, Harada K-I, et al. Calcium movements, distribution, and functions in smooth muscle. Pharmacological Reviews. 1997;49(2):157-230.
140. Fukata Y, Amano M, Kaibuchi K. Rho-Rho-kinase pathway in smooth muscle contraction and cytoskeletal reorganization of non-muscle cells. Trends in pharmacological sciences. 2001;22(1):32.
141. Dimopoulos GJ, Semba S, Kitazawa K, Eto M, Kitazawa T. Ca2+-dependent rapid Ca2+ sensitization of contraction in arterial smooth muscle. Circulation research. 2007;100(1):121-9.
142. Strijdom H, Chamane N, Lochner A. Nitric oxide in the cardiovascular system: a simple molecule with complex actions. Cardiovasc J Afr. 2009;20(5):303-10.
143. Mergia E, Friebe A, Dangel O, Russwurm M, Koesling D. Spare guanylyl cyclase NO receptors ensure high NO sensitivity in the vascular system. Journal of Clinical Investigation. 2006;116(6):1731.
144. Yang J, Clark JW, Bryan RM, Robertson CS. Mathematical modeling of the nitric oxide/cGMP pathway in the vascular smooth muscle cell. American Journal of Physiology-Heart and Circulatory Physiology. 2005;289(2):H886-H97.
145. Wautier JL, Pintigny D, Maclouf J, Wautier MP, Corvazier E, Caen J. Release of prostacyclin after erythrocyte adhesion to cultured vascular endothelium. The Journal of laboratory and clinical medicine. 1986;107(3):210.
146. Mueck AO, Seeger H, Korte K, Lippert TH. The effect of 17 beta-estradiol and endothelin 1 on prostacyclin and thromboxane production in human endothelial cell cultures. Clinical and experimental obstetrics & gynecology. 1993;20(4):203.
147. Zhang Q-H, Zu X-Y, Cao R-X, Liu J-H, Mo Z-C, Zeng Y, et al. An involvement of SR-B1 mediated PI3K–Akt–eNOS signaling in HDL-induced cyclooxygenase 2 expression and prostacyclin production in endothelial cells. Biochemical and biophysical research communications. 2012;420(1):17-23.
148. Salvemini D, Currie MG, Mollace V. Nitric oxide-mediated cyclooxygenase activation. A key event in the antiplatelet effects of nitrovasodilators. Journal of Clinical Investigation. 1996;97(11):2562.
149. Triggle CR, Samuel SM, Ravishankar S, Marei I, Arunachalam G, Ding H. The endothelium: influencing vascular smooth muscle in many ways. Canadian journal of physiology and pharmacology. 2012;90(6):713-38.
150. Chaytor AT, Martin PE, Edwards DH, Griffith TM. Gap junctional communication underpins EDHF-type relaxations evoked by ACh in the rat hepatic artery. American Journal of Physiology-Heart and Circulatory Physiology. 2001;280(6):H2441-H50.
151. Chaytor AT, Taylor HJ, Griffith TM. Gap junction-dependent and-independent EDHF-type relaxations may involve smooth muscle cAMP accumulation. American Journal of Physiology-Heart and Circulatory Physiology. 2002;282(4):H1548-H55.
152. Griffith TM. Endothelium-dependent smooth muscle hyperpolarization: do gap junctions provide a unifying hypothesis? British journal of pharmacology. 2004;141(6):881-903.

153. Chaytor AT, Bakker LM, Edwards DH, Griffith TM. Connexin-mimetic peptides dissociate electrotonic EDHF-type signalling via myoendothelial and smooth muscle gap junctions in the rabbit iliac artery. British journal of pharmacology. 2005;144(1):108-14.
154. Edwards DH, Li Y, Griffith TM. Hydrogen peroxide potentiates the EDHF phenomenon by promoting endothelial Ca2+ mobilization. Arteriosclerosis, thrombosis, and vascular biology. 2008;28(10):1774-81.
155. Sandow SL, Hill CE. Incidence of myoendothelial gap junctions in the proximal and distal mesenteric arteries of the rat is suggestive of a role in endothelium-derived hyperpolarizing factor–mediated responses. Circulation Research. 2000;86(3):341-6.
156. Nagao T, Vanhoutte PM. Hyperpolarization as a mechanism for endothelium-dependent relaxations in the porcine coronary artery. The Journal of physiology. 1992;445(1):355-67.
157. Shimokawa H, Yasutake H, Fujii K, Owada MK, Nakaike R, Fukumoto Y, et al. The importance of the hyperpolarizing mechanism increases as the vessel size decreases in endothelium-dependent relaxations in rat mesenteric circulation. Journal of cardiovascular pharmacology. 1996;28(5):703-11.
158. Félétou M, Vanhoutte PM. Endothelium-Derived Hyperpolarizing Factor Where Are We Now? Arteriosclerosis, thrombosis, and vascular biology. 2006;26(6):1215-25.
159. Busse R, Edwards G, Félétou M, Fleming I, Vanhoutte PM, Weston AH. EDHF: bringing the concepts together. Trends in pharmacological sciences. 2002;23(8):374-80.
160. Ignarro LJ, Napoli C, Loscalzo J. Nitric Oxide Donors and Cardiovascular Agents Modulating the Bioactivity of Nitric Oxide An Overview. Circulation research. 2002;90(1):21-8.
161. Feelisch M. The use of nitric oxide donors in pharmacological studies. Naunyn-Schmiedeberg's archives of pharmacology. 1998;358(1):113-22.
162. Ignarro LJ. Biosynthesis and metabolism of endothelium-derived nitric oxide. Annual review of pharmacology and toxicology. 1990;30(1):535-60.
163. Sanchez Luna M, Luisa Franco M, Bernardo B. Therapeutic Strategies in Pulmonary Hypertension of the Newborn: Where Are We Now? Current medicinal chemistry. 2012;19(27):4640-53.
164. Nelin LD, Hoffman GM. The use of inhaled nitric oxide in a wide variety of clinical problems. Pediatric Clinics of North America. 1998;45(3):531-48.
165. Keefer LK. Nitric oxide (NO)-and nitroxyl (HNO)-generating diazeniumdiolates (NONOates): emerging commercial opportunities. Current topics in medicinal chemistry. 2005;5(7):625-36.
166. Zai A, Rudd MA, Scribner AW, Loscalzo J. Cell-surface protein disulfide isomerase catalyzes transnitrosation and regulates intracellular transfer of nitric oxide. Journal of Clinical Investigation. 1999;103(3):393-9.
167. Gerzer R, Radany EW, Garbers DL. The separation of the heme and apoheme forms of soluble guanylate cyclase. Biochemical and biophysical research communications. 1982;108(2):678-86.
168. Gerzer R, Böhme E, Hofmann F, Schultz G. Soluble guanylate cyclase purified from bovine lung contains heme and copper. FEBS letters. 1981;132(1):71.
169. Lucas KA, Pitari GM, Kazerounian S, Ruiz-Stewart I, Park J, Schulz S, et al. Guanylyl cyclases and signaling by cyclic GMP. Pharmacological reviews. 2000;52(3):375-414.
170. Poulos T. Soluble guanylate cyclase. Current opinion in structural biology. 2006;16(6):736-43.
171. Koesling D. Studying the structure and regulation of soluble guanylyl cyclase. Methods. 1999;19(4):485-93.
172. Karow DS, Pan D, Tran R, Pellicena P, Presley A, Mathies RA, et al. Spectroscopic characterization of the soluble guanylate cyclase-like heme domains from Vibrio cholerae and Thermoanaerobacter tengcongensis. Biochemistry. 2004;43(31):10203-11.
173. Boon E, Marletta M. Ligand specificity of H-NOX domains: from sGC to bacterial NO sensors. Journal of inorganic biochemistry. 2005;99(4):892-902.
174. Winger JA, Marletta MA. Expression and characterization of the catalytic domains of soluble guanylate cyclase: interaction with the heme domain. Biochemistry. 2005;44(10):4083-90.

175. Kosarikov DN, Young P, Uversky VN, Gerber NC. Human soluble guanylate cyclase: functional expression, purification and structural characterization. Archives of biochemistry and biophysics. 2001;388(2):185-97.
176. Koesling D, Friebe A. Soluble guanylyl cyclase: structure and regulation. Reviews of Physiology, Biochemistry and Pharmacology, Volume 135: Springer; 1999. p. 41-65.
177. Karow D, Pan D, Davis J, Behrends S, Mathies R, Marletta M. Characterization of Functional Heme Domains from Soluble Guanylate Cyclase†. Biochemistry. 2005;44(49):16266-74.
178. Evgenov OV, Pacher P, Schmidt PM, Haskó G, Schmidt HHHW, Stasch J-P. NO-independent stimulators and activators of soluble guanylate cyclase: discovery and therapeutic potential. Nature Reviews Drug Discovery. 2006;5(9):755-68.
179. Arnold WP, Mittal CK, Katsuki S, Murad F. Nitric oxide activates guanylate cyclase and increases guanosine 3': 5'-cyclic monophosphate levels in various tissue preparations. Proceedings of the National Academy of Sciences. 1977;74(8):3203-7.
180. Buechler WA, Nakane M, Murad F. Expression of soluble guanylate cyclase activity requires both enzyme subunits. Biochemical and biophysical research communications. 1991;174(1):351-7.
181. Stone J, Marletta M. Soluble guanylate cyclase from bovine lung: activation with nitric oxide and carbon monoxide and spectral characterization of the ferrous and ferric states. Biochemistry. 1994;33(18):5636-40.
182. Zhao Y, Schelvis JPM, Babcock GT, Marletta MA. Identification of histidine 105 in the β1 subunit of soluble guanylate cyclase as the heme proximal ligand. Biochemistry. 1998;37(13):4502-9.
183. Stone J, Sands R, Dunham W, Marletta M. Electron paramagnetic resonance spectral evidence for the formation of a pentacoordinate nitrosyl-heme complex on soluble guanylate cyclase. Biochemical and Biophysical Research Communications. 1995;207(2):572-7.
184. Stone J, Marletta M. Spectral and Kinetic Studies on the Activation of Soluble Guanylate Cyclase by Nitric Oxide†. Biochemistry. 1996;35(4):1093-9.
185. Martin E, Berka V, Sharina I, Tsai A-L. Mechanism of binding of NO to soluble guanylyl cyclase: implication for the second NO binding to the heme proximal site. Biochemistry. 2012;51(13):2737-46.
186. Maines MD. Heme oxygenase: function, multiplicity, regulatory mechanisms, and clinical applications. The FASEB Journal. 1988;2(10):2557-68.
187. Willis D, Moore A, Frederick R, Willoughby D. Heme oxygenase: a novel target for the modulation of inflammatory response. Nature medicine. 1996;2(1):87-93.
188. Brüne B, Schmidt K, Ullrich V. Activation of soluble guanylate cyclase by carbon monoxide and inhibition by superoxide anion. Eur J Biochem. 1990;192(3):683-8.
189. Kharitonov VG, Sharma VS, Pilz RB, Magde D, Koesling D. Basis of guanylate cyclase activation by carbon monoxide. Proceedings of the National Academy of Sciences. 1995;92(7):2568-71.
190. Deinum G, Stone JR, Babcock GT, Marletta MA. Binding of nitric oxide and carbon monoxide to soluble guanylate cyclase as observed with resonance Raman spectroscopy. Biochemistry. 1996;35(5):1540-7.
191. Miller LN, Nakane M, Hsieh GC, Chang R, Kolasa T, Moreland RB, et al. A-350619: a novel activator of soluble guanylyl cyclase. Life sciences. 2003;72(9):1015-25.
192. Stone J, Marletta M. Spectral and Kinetic Studies on the Activation of Soluble Guanylate Cyclase by Nitric Oxide. Biochemistry. 1996;35(4):1093-9.
193. Mingone CJ, Gupte SA, Chow JL, Ahmad M, Abraham NG, Wolin MS. Protoporphyrin IX generation from δ-aminolevulinic acid elicits pulmonary artery relaxation and soluble guanylate cyclase activation. American Journal of Physiology-Lung Cellular and Molecular Physiology. 2006;291(3):L337-L44.
194. Ohlstein EH, Wood KS, Ignarro LJ. Purification and properties of heme-deficient hepatic soluble guanylate cyclase: effects of heme and other factors on enzyme activation by NO, NO-heme, and protoporphyrin IX. Archives of biochemistry and biophysics. 1982;218(1):187-98.

195. Ignarro LJ, Wood KS, Wolin MS. Activation of purified soluble guanylate cyclase by protoporphyrin IX. Proceedings of the National Academy of Sciences. 1982;79(9):2870-3.
196. Hobbs A. Soluble guanylate cyclase: the forgotten sibling. Trends in Pharmacological sciences. 1997;18(4):484-91.
197. Zhou Z, Pyriochou A, Kotanidou A, Dalkas G, van Eickels M, Spyroulias G, et al. Soluble guanylyl cyclase activation by HMR-1766 (ataciguat) in cells exposed to oxidative stress. American Journal of Physiology-Heart and Circulatory Physiology. 2008;295(4):H1763-H71.
198. Lasker GF, Maley JH, Pankey EA, Kadowitz PJ. Targeting soluble guanylate cyclase for the treatment of pulmonary hypertension. Expert review of respiratory medicine. 2011;5(2):153-61.
199. Priviero FBM, Webb RC. Heme-dependent and independent soluble guanylate cyclase activators and vasodilation. Journal of cardiovascular pharmacology. 2010;56(3):229.
200. Hahn M, Lampe T, Stasch J-p, Schlemmer K-h, Wunder F, Becker E-m, et al. Branched 3-phenylpropionic acid derivatives and their use. US Patent 20,130,079,412; 2013.
201. Derbyshire ER. Investigating the Heme Environment and Mechanism of Activation of Soluble Guanylate Cyclase: ProQuest; 2008.
202. Derbyshire ER, Marletta MA. Biochemistry of soluble guanylate cyclase. Handb Exp Pharmacol. 2009(191):17-31.
203. Karow D, Pan D, Davis J, Behrends S, Mathies R, Marletta M. Characterization of Functional Heme Domains from Soluble Guanylate Cyclase□. Biochemistry. 2005;44(49):16266-74.
204. Burstyn JN, Yu AE, Dierks EA, Hawkins BK, Dawson JH. Studies of the heme coordination and ligand binding properties of soluble guanylyl cyclase (sGC): characterization of Fe (II) sGC and Fe (II) sGC (CO) by electronic absorption and magnetic circular dichroism spectroscopies and failure of CO to activate the enzyme. Biochemistry. 1995;34(17):5896-903.
205. Cary S, Winger J, Derbyshire E, Marletta M. Nitric oxide signaling: no longer simply on or off. Trends in biochemical sciences. 2006;31(4):231-9.
206. Tsai A-l, Martin E, Berka V, Olson JS. How Do Heme-Protein Sensors Exclude Oxygen? Lessons Learned from Cytochrome c', Nostoc puntiforme Heme Nitric Oxide/Oxygen-Binding Domain, and Soluble Guanylyl Cyclase. Antioxidants & Redox Signaling. 2012;17(9):1246-63.
207. Huang SH, Rio DC, Marletta MA. Ligand binding and inhibition of an oxygen-sensitive soluble guanylate cyclase, Gyc-88E, from Drosophila. Biochemistry. 2007;46(51):15115-22.
208. Makino R, Park SY, Obayashi E, Iizuka T, Hori H, Shiro Y. Oxygen binding and redox properties of the heme in soluble guanylate cyclase: implications for the mechanism of ligand discrimination. J Biol Chem. 2011;286(18):15678-87.
209. Sayed N, Kim DD, Fioramonti X, Iwahashi T, Durán WN, Beuve A. Nitroglycerin-induced S-nitrosylation and desensitization of soluble guanylyl cyclase contribute to nitrate tolerance. Circulation research. 2008;103(6):606-14.
210. Fernhoff NB, Derbyshire ER, Underbakke ES, Marletta MA. Heme-assisted S-Nitrosation Desensitizes Ferric Soluble Guanylate Cyclase to Nitric Oxide. Journal of Biological Chemistry. 2012;287(51):43053-62.
211. Zhao Y, Brandish PE, DiValentin M, Schelvis JPM, Babcock GT, Marletta MA. Inhibition of soluble guanylate cyclase by ODQ. Biochemistry. 2000;39(35):10848-54.
212. Garthwaite J, Southam E, Boulton CL, Nielsen EB, Schmidt K, Mayer B. Potent and selective inhibition of nitric oxide-sensitive guanylyl cyclase by 1H-[1,2,4]oxadiazolo[4,3-a]quinoxalin-1-one. Mol Pharmacol. 1995;48(2):184-8.
213. Schrammel A, Behrends S, Schmidt K, Koesling D, Mayer B. Characterization of 1H-[1,2,4]oxadiazolo[4,3-a]quinoxalin-1-one as a heme-site inhibitor of nitric oxide-sensitive guanylyl cyclase. Mol Pharmacol. 1996;50(1):1-5.
214. Mülsch A, Busse R, Liebau S, Förstermann U. LY 83583 interferes with the release of endothelium-derived relaxing factor and inhibits soluble guanylate cyclase. Journal of Pharmacology and Experimental Therapeutics. 1988;247(1):283-8.

215. Hwang TL, Wu CC, Teng CM. Comparison of two soluble guanylyl cyclase inhibitors, methylene blue and ODQ, on sodium nitroprusside-induced relaxation in guinea-pig trachea. British journal of pharmacology. 1998;125(6):1158-63.
216. Dierks E, Burstyn J. The deactivation of soluble guanylyl cyclase by redox-active agents. Archives of Biochemistry and Biophysics. 1998;351(1):1-7.
217. Wolin MS, Cherry PD, Rodenburg JM, Messina EJ, Kaley G. Methylene blue inhibits vasodilation of skeletal muscle arterioles to acetylcholine and nitric oxide via the extracellular generation of superoxide anion. Journal of Pharmacology and Experimental Therapeutics. 1990;254(3):872-6.
218. Mayer B, Brunner F, Schmidt K. Inhibition of nitric oxide synthesis by methylene blue. Biochemical pharmacology. 1993;45(2):367-74.
219. Rall TW, Sutherland EW. Formation of a cyclic adenine ribonucleotide by tissue particles. Journal of Biological Chemistry. 1958;232(2):1065-76.
220. Cerra M, Pellegrino D. Cardiovascular cGMP-generating systems in physiological and pathological conditions. Current medicinal chemistry. 2007;14(5):585-99.
221. Feil R, Kemp-Harper B. cGMP signalling: from bench to bedside. EMBO reports. 2006;7(2):149.
222. Hofmann F, Ammendola A, Schlossmann J. Rising behind NO: cGMP-dependent protein kinases. Journal of cell science. 2000;113(10):1671-6.
223. Geiselhöringer A, Werner M, Sigl K, Smital P, Wörner R, Acheo L, et al. IRAG is essential for relaxation of receptor-triggered smooth muscle contraction by cGMP kinase. The EMBO journal. 2004;23(21):4222-31.
224. Massberg S, Grüner S, Konrad I, Arguinzonis MIG, Eigenthaler M, Hemler K, et al. Enhanced in vivo platelet adhesion in vasodilator-stimulated phosphoprotein (VASP)–deficient mice. Blood. 2004;103(1):136-42.
225. Butcher R, Sutherland EW. Adenosine 3', 5'-phosphate in biological materials. I. Purification and properties of cyclic 3', 5'-nucleotide phosphodiesterase and use of this enzyme to characterize adenosine 3', 5'-phosphate in human urine. The Journal of biological chemistry. 1962;237:1244.
226. Beavo J. Cyclic nucleotide phosphodiesterases: functional implications of multiple isoforms. Physiological reviews. 1995;75(4):725.
227. Bender AT, Beavo JA. Cyclic nucleotide phosphodiesterases: molecular regulation to clinical use. Pharmacological reviews. 2006;58(3):488-520.
228. Francis SH, Busch JL, Corbin JD. cGMP-dependent protein kinases and cGMP phosphodiesterases in nitric oxide and cGMP action. Pharmacological Reviews. 2010;62(3):525-63.
229. Corbin JD, Francis SH. Molecular Biology and Pharmacology of PDE-5—Inhibitor Therapy for Erectile Dysfunction. Journal of andrology. 2003;24(S6):S38-S41.
230. Corbin JD, Francis SH, Webb DJ. Phosphodiesterase type 5 as a pharmacologic target in erectile dysfunction. Urology. 2002;60(2):4-11.
231. Wood PJ, Marks V. Direct measurement of cGMP in blood plasma and urine by radioimmunoassay. Annals of clinical biochemistry. 1978;15(1):25.
232. Mizuno T, Watanabe M, Sakamoto T, Sunamori M. L-arginine, a nitric oxide precursor, attenuates ischemia-reperfusion injury by inhibiting inositol-1, 4, 5-triphosphate. The Journal of thoracic and cardiovascular surgery. 1998;115(4):931-6.
233. Zhang Y, Dufield D, Klover J, Li W, Szekely-Klepser G, Lepsy C, et al. Development and validation of an LC–MS/MS method for quantification of cyclic guanosine 3', 5'-monophosphate (cGMP) in clinical applications: A comparison with a EIA method. Journal of Chromatography B. 2009;877(5):513-20.
234. Yalow RS, Berson SA. Plasma insulin concentrations in nondiabetic and early diabetic subjects. Determinations by a new sensitive immuno-assay technic. Diabetes. 1960;9:254.
235. Overview of ELISA [cited 2013 09/05/13]. Available from: http://www.piercenet.com/browse.cfm?fldID=F88ADEC9-1B43-4585-922E-836FE09D8403.

236. Elgert KD. Immunology: understanding the immune system: Wiley. com; 2009.
237. Stamler J, Simon D, Osborne J, Mullins M, Jaraki O, Michel T, et al. S-nitrosylation of proteins with nitric oxide: synthesis and characterization of biologically active compounds. Proceedings of the National Academy of Sciences of the United States of America. 1992;89(1):444.
238. Baker PR, Schopfer FJ, Sweeney S, Freeman BA. Red cell membrane and plasma linoleic acid nitration products: synthesis, clinical identification, and quantitation. Proceedings of the National Academy of Sciences of the United States of America. 2004;101(32):11577-82.
239. Freeman BA, Baker PR, Schopfer FJ, Woodcock SR, Napolitano A, d'Ischia M. Nitro-fatty acid formation and signaling. Journal of Biological Chemistry. 2008;283(23):15515-9.
240. McMahon TJ, Moon RE, Luschinger BP, Carraway MS, Stone AE, Stolp BW, et al. Nitric oxide in the human respiratory cycle. Nat Med. 2002;8(7):711-7.
241. Lane P, Gross S. Hemoglobin as a chariot for NO bioactivity. Nature Medicine. 2002;8(7):657-8.
242. McMahon TJ, Stone AE, Bonaventura J, Singel DJ, Stamler JS. Functional Coupling of Oxygen Binding and Vasoactivity inS-Nitrosohemoglobin. Journal of Biological Chemistry. 2000;275(22):16738-45.
243. Pezacki JP, Ship NJ, Kluger R. Release of nitric oxide from S-nitrosohemoglobin. Electron transfer as a response to deoxygenation. Journal of the American Chemical Society. 2001;123(19):4615.
244. Pawloski J, Hess D, Stamler J. Export by red blood cells of nitric oxide bioactivity. Nature. 2001;409(6820):622-6.
245. Palmer LA, Doctor A, Chhabra P, Sheram ML, Laubach VE, Karlinsey MZ, et al. S-nitrosothiols signal hypoxia-mimetic vascular pathology. Journal of Clinical Investigation. 2007;117(9):2592-601.
246. Zweier JL, Wang P, Samouilov A, Kuppusamy P. Enzyme-independent formation of nitric oxide in biological tissues. Nature medicine. 1995;1(8):804-9.
247. Gladwin MT, Shelhamer JH, Schechter AN, Pease-Fye ME, Waclawiw MA, Panza JA, et al. Role of circulating nitrite and S-nitrosohemoglobin in the regulation of regional blood flow in humans. Proceedings of the National Academy of Sciences. 2000;97(21):11482-7.
248. Cosby K, Partovi K, Crawford J, Patel R, Reiter C, Martyr S, et al. Nitrite reduction to nitric oxide by deoxyhemoglobin vasodilates the human circulation. Nature medicine. 2003;9(12):1498-505.
249. Isbell TS, Gladwin MT, Patel RP. Hemoglobin oxygen fractional saturation regulates nitrite-dependent vasodilation of aortic ring bioassays. American Journal of Physiology-Heart and Circulatory Physiology. 2007;293(4):H2565-H72.
250. Dalsgaard T, Simonsen U, Fago A. Nitrite-dependent vasodilation is facilitated by hypoxia and is independent of known NO-generating nitrite reductase activities. American Journal of Physiology-Heart and Circulatory Physiology. 2007;292(6):H3072.
251. Huang Z, Shiva S, Kim-Shapiro D, Patel R, Ringwood L, Irby C, et al. Enzymatic function of hemoglobin as a nitrite reductase that produces NO under allosteric control. Journal of Clinical Investigation. 2005;115(8):2099-107.
252. Totzeck M, Hendgen-Cotta UB, Luedike P, Berenbrink M, Klare JP, Steinhoff H-J, et al. Nitrite Regulates Hypoxic Vasodilation via Myoglobin-Dependent Nitric Oxide GenerationClinical Perspective. Circulation. 2012;126(3):325-34.
253. Angelo M, Singel DJ, Stamler JS. An S-nitrosothiol (SNO) synthase function of hemoglobin that utilizes nitrite as a substrate. Proceedings of the National Academy of Sciences. 2006;103(22):8366-71.
254. Bergfeld G, Forrester T. Release of ATP from human erythrocytes in response to a brief period of hypoxia and hypercapnia. Cardiovascular research. 1992;26(1):40.
255. Solaini G, Baracca A, Lenaz G, Sgarbi G. Hypoxia and mitochondrial oxidative metabolism. Biochimica et Biophysica Acta (BBA)-Bioenergetics. 2010;1797(6):1171-7.

256. Corr L, Burnstock G. Analysis of P2-purinoceptor subtypes on the smooth muscle and endothelium of rabbit coronary artery. Journal of cardiovascular pharmacology. 1994;23(5):709.
257. Sprague RS, Hanson MS, Achilleus D, Bowles EA, Stephenson AH, Sridharan M, et al. Rabbit erythrocytes release ATP and dilate skeletal muscle arterioles in the presence of reduced oxygen tension. Pharmacological reports: PR. 2009;61(1):183.
258. Diesen D, Hess D, Stamler J. Hypoxic vasodilation by red blood cells: evidence for an S-nitrosothiol-based signal. Circulation research. 2008;103(5):545.
259. James P, Lang D, Tufnell-Barret T, Milsom A, Frenneaux M. Vasorelaxation by red blood cells and impairment in diabetes: reduced nitric oxide and oxygen delivery by glycated hemoglobin. Circulation research. 2004;94(7):976.
260. Weil JA, Bolton JR, Wertz JE, Nugent JA. Electron paramagnetic resonance: elementary theory and practical applications: Wiley New York; 1994.
261. Jen CK. The Zeeman effect in microwave molecular spectra. Physical Review. 1948;74(10):1396.
262. Eaton GR, Eaton SS, D.P B, Weber RT. Quantitative EPR. Germany2010.
263. Smirnova TI, Smirnov AI, Clarkson RB, Linn Belford R. Accuracy of oxygen measurements in T2 (line width) EPR oximetry. Magnetic resonance in medicine. 1995;33(6):801-10.
264. MacArthur PH, Shiva S, Gladwin MT. Measurement of circulating nitrite and< i> S</i>-nitrosothiols by reductive chemiluminescence. Journal of Chromatography B. 2007;851(1):93-105.
265. Yang F, Troncy E, Francœur M, Vinet B, Vinay P, Czaika G, et al. Effects of reducing reagents and temperature on conversion of nitrite and nitrate to nitric oxide and detection of NO by chemiluminescence. Clinical chemistry. 1997;43(4):657-62.
266. Gonzalez-Alonso J, Olsen D, Saltin B. Erythrocyte and the regulation of human skeletal muscle blood flow and oxygen delivery: role of circulating ATP. Circulation research. 2002;91(11):1046.
267. Gupte SA, Wolin MS. Oxidant and redox signaling in vascular oxygen sensing: implications for systemic and pulmonary hypertension. Antioxidants & redox signaling. 2008;10(6):1137-52.
268. Nagababu E, Ramasamy S, Abernethy D, Rifkind J. Active nitric oxide produced in the red cell under hypoxic conditions by deoxyhemoglobin-mediated nitrite reduction. Journal of Biological Chemistry. 2003;278(47):46349.
269. Allen B, Piantadosi C. How do red blood cells cause hypoxic vasodilation? The SNO-hemoglobin paradigm. American Journal of Physiology- Heart and Circulatory Physiology. 2006;291(4):H1507.
270. Allen BW, Stamler JS, Piantadosi CA. Hemoglobin, nitric oxide and molecular mechanisms of hypoxic vasodilation. Trends Mol Med. 2009;15(10):452-60.
271. Crawford J, Isbell T, Huang Z, Shiva S, Chacko B, Schechter A, et al. Hypoxia, red blood cells, and nitrite regulate NO-dependent hypoxic vasodilation. Blood. 2006;107(2):566.
272. Gladwin M, Raat N, Shiva S, Dezfulian C, Hogg N, Kim-Shapiro D, et al. Nitrite as a vascular endocrine nitric oxide reservoir that contributes to hypoxic signaling, cytoprotection, and vasodilation. American Journal of Physiology- Heart and Circulatory Physiology. 2006;291(5):H2026.
273. Isbell T, Sun C, Wu L, Teng X, Vitturi D, Branch B, et al. SNO-hemoglobin is not essential for red blood cell□dependent hypoxic vasodilation. Nature medicine. 2008;14(7):773-7.
274. Kim-Shapiro DB, Gladwin MT, Patel RP, Hogg N. The reaction between nitrite and hemoglobin: the role of nitrite in hemoglobin-mediated hypoxic vasodilation. J Inorg Biochem. 2005;99(1):237-46.
275. Ingram T, Pinder A, Bailey D, Fraser A, James P. Low-dose sodium nitrite vasodilates hypoxic human pulmonary vasculature by a means that is not dependent on a simultaneous elevation in plasma nitrite. American Journal of Physiology- Heart and Circulatory Physiology. 2010;298(2):H331.
276. Pinder A, Pittaway E, Morris K, James P. Nitrite directly vasodilates hypoxic vasculature via nitric oxide-dependent and-independent pathways. British journal of pharmacology. 2009;157(8):1523-30.

277. Cao Z, Bell JB, Mohanty JG, Nagababu E, Rifkind JM. Nitrite enhances RBC hypoxic ATP synthesis and the release of ATP into the vasculature: a new mechanism for nitrite-induced vasodilation. Am J Physiol Heart Circ Physiol. 2009;297(4):H1494-503.
278. Rees DD, Palmer RMJ, Schulz R, Hodson HF, Moncada S. Characterization of three inhibitors of endothelial nitric oxide synthase in vitro and in vivo. British journal of pharmacology. 1990;101(3):746-52.
279. Volk KA, Roghair RD, Jung F, Scholz TD, Lamb FS, Segar JL. Coronary endothelial function and vascular smooth muscle proliferation are programmed by early-gestation dexamethasone exposure in sheep. American Journal of Physiology-Regulatory, Integrative and Comparative Physiology. 2010;298(6):R1607-R14.
280. Cooke C-LM, Davidge ST. Endothelial-dependent vasodilation is reduced in mesenteric arteries from superoxide dismutase knockout mice. Cardiovascular research. 2003;60(3):635-42.
281. Ellsworth M, Forrester T, Ellis C, Dietrich H. The erythrocyte as a regulator of vascular tone. American Journal of Physiology- Heart and Circulatory Physiology. 1995;269(6):H2155.
282. Zhao Y, Brandish P, Ballou D, Marletta M. A molecular basis for nitric oxide sensing by soluble guanylate cyclase. Proceedings of the National Academy of Sciences of the United States of America. 1999;96(26):14753.
283. Ma X, Sayed N, Beuve A, van den Akker F. NO and CO differentially activate soluble guanylyl cyclase via a heme pivot-bend mechanism. EMBO J. 2007;26(2):578-88.
284. Angelos MG, Kutala VK, Torres CA, He G, Stoner JD, Mohammad M, et al. Hypoxic reperfusion of the ischemic heart and oxygen radical generation. Am J Physiol Heart Circ Physiol. 2006;290(1):H341-7.
285. Pfeiffer S, Schrammel A, Koesling D, Schmidt K, Mayer B. Molecular actions of a Mn (III) porphyrin superoxide dismutase mimetic and peroxynitrite scavenger: reaction with nitric oxide and direct inhibition of NO synthase and soluble guanylyl cyclase. Molecular pharmacology. 1998;53(4):795-800.
286. Fleischer EB, Palmer JM, Srivastava TS, Chatterjee A. Thermodyamic and kinetic properties of an iron-porphyrin system. Journal of the American Chemical Society. 1971;93(13):3162-7.
287. Fridovich I. Superoxide dismutases: defence against endogenous superoxide radical. Oxygen free radicals and tissue damage. 1979;65:77-93.
288. Quayle J, Nelson M, Standen N. ATP-sensitive and inwardly rectifying potassium channels in smooth muscle. Physiological reviews. 1997;77(4):1165.
289. Brayden J. Functional roles of KATP channels in vascular smooth muscle. Clinical and Experimental Pharmacology and Physiology. 2002;29(4):312-6.
290. Dada J, Pinder AG, Lang D, James PE. Oxygen Mediates Vascular Smooth Muscle Relaxation in Hypoxia. PloS one. 2013;8(2):e57162.
291. Friebe A, Schultz G, Koesling D. Sensitizing soluble guanylyl cyclase to become a highly CO-sensitive enzyme. The EMBO Journal. 1996;15(24):6863.
292. Yoshina S, Tanaka A, Kuo SC. Studies on heterocyclic compounds. XXXIV. Synthesis of furo [3, 2-c] pyrazole derivatives.(2). Electrophilic substitution of 1, 3-diphenylfuro [3, 2-c] pyrazole (author's transl)]. Yakugaku zasshi: Journal of the Pharmaceutical Society of Japan. 1978;98(2):204.
293. Ko F-N, Wu C-C, Kuo S-C, Lee F-Y, Teng C-M. YC-1, a novel activator of platelet guanylate cyclase. Blood. 1994;84(12):4226-33.
294. Friebe A, Koesling D. Mechanism of YC-1-induced activation of soluble guanylyl cyclase. Molecular pharmacology. 1998;53(1):123.
295. Stasch J-P, Becker EM, Alonso-Alija C, Apeler H, Dembowsky K, Feurer A, et al. NO-independent regulatory site on soluble guanylate cyclase. Nature. 2001;410(6825):212-5.
296. Grimminger F, Weimann G, Frey R, Voswinckel R, Thamm M, Bölkow D, et al. First acute haemodynamic study of soluble guanylate cyclase stimulator riociguat in pulmonary hypertension. European Respiratory Journal. 2009;33(4):785-92.

297. Ghofrani HA, Hoeper MM, Halank M, Meyer FJ, Staehler G, Behr J, et al. Riociguat for chronic thromboembolic pulmonary hypertension and pulmonary arterial hypertension: a phase II study. European Respiratory Journal. 2010;36(4):792-9.
298. Ghofrani H-A, Voswinckel R, Gall H, Schermuly R, Weissmann N, Seeger W, et al. Riociguat for pulmonary hypertension. Future Cardiology. 2010;6(2):155-66.
299. Bawankule DU, Sathishkumar K, Sardar KK, Chanda D, Krishna AV, Prakash VR, et al. BAY 41-2272-Induced Dilation in Ovine Pulmonary Artery: Role of Sodium Pump. Journal of Pharmacology and Experimental Therapeutics. 2005.
300. Toque HA, Mónica FZT, Morganti RP, De Nucci G, Antunes E. Mechanisms of relaxant activity of the nitric oxide-independent soluble guanylyl cyclase stimulator BAY 41-2272 in rat tracheal smooth muscle. European journal of pharmacology. 2010;645(1-3):158-64.
301. Martin E, Berka V, Bogatenkova E, Murad F, Tsai AL. Ligand selectivity of soluble guanylyl cyclase: effect of the hydrogen-bonding tyrosine in the distal heme pocket on binding of oxygen, nitric oxide, and carbon monoxide. J Biol Chem. 2006;281(38):27836-45.
302. Ma X, Sayed N, Beuve A, van den Akker F. NO and CO differentially activate soluble guanylyl cyclase via a heme pivot-bend mechanism. The EMBO Journal. 2007;26(2):578.
303. Derbyshire ER, Deng S, Marletta MA. Incorporation of tyrosine and glutamine residues into the soluble guanylate cyclase heme distal pocket alters NO and O2 binding. J Biol Chem. 2010;285(23):17471-8.
304. Boon E, Huang S, Marletta M. A molecular basis for NO selectivity in soluble guanylate cyclase. Nature chemical biology. 2005;1(1):53-9.
305. Pellicena P, Karow DS, Boon EM, Marletta MA, Kuriyan J. Crystal structure of an oxygen-binding heme domain related to soluble guanylate cyclases. Proceedings of the National Academy of Sciences of the United States of America. 2004;101(35):12854-9.
306. Friebe A, Schultz G, Koesling D. Stimulation of soluble guanylate cyclase by superoxide dismutase is mediated by NO. Biochemical Journal. 1998;335(Pt 3):527.
307. Homer K, Wanstall J. In vitro comparison of two NONOates (novel nitric oxide donors) on rat pulmonary arteries. European journal of pharmacology. 1998;356(1):49-57.
308. Herzog E, Chaudhry F. Echocardiography in acute coronary syndrome: Diagnosis, treatment and prevention. Saric M, editor2009.
309. Davies SW, Wedzicha JA. Hypoxia and the heart. British heart journal. 1993;69(1):3.
310. Verhoeff B-J. Simultaneous pressure and flow velocity measurements in diagnosis and treatment of coronary artery disease2010.
311. Taggart MJ, Wray S. Hypoxia and smooth muscle function: key regulatory events during metabolic stress. The Journal of physiology. 1998;509(2):315-25.
312. Ramanathan T, Skinner H. Coronary blood flow. Continuing Education in Anaesthesia, Critical Care & Pain. 2005;5(2):61-4.
313. van de Hoef TP, Nolte F, Rolandi MC, Piek JJ, van den Wijngaard JP, Spaan JA, et al. Coronary pressure-flow relations as basis for the understanding of coronary physiology. Journal of molecular and cellular cardiology. 2012;52(4):786-93.
314. Canty Jr JM. Coronary Blood Flow and Myocardial Ischemia. Essential Cardiology: Springer; 2013. p. 387-403.
315. Kelm M. Flow-mediated dilatation in human circulation: diagnostic and therapeutic aspects. American Journal of Physiology- Heart and Circulatory Physiology. 2002;282(1):H1.
316. Essential Cardiology: Principles and Practice. 3rd edition ed. Rosendorff C, editor. New York: Springer; 2013.
317. Heusch G. Adenosine and maximum coronary vasodilation in humans: myth and misconceptions in the assessment of coronary reserve. Basic research in cardiology. 2010;105(1):1-5.
318. Laughlin MH, Bowles DK, Duncker DJ. The coronary circulation in exercise training. American Journal of Physiology-Heart and Circulatory Physiology. 2012;302(1):H10-H23.

319. Canty J, Schwartz JS. Nitric oxide mediates flow-dependent epicardial coronary vasodilation to changes in pulse frequency but not mean flow in conscious dogs. Circulation. 1994;89(1):375-84.
320. Kuo L, Davis MJ, Chilian WM. Endothelium-dependent, flow-induced dilation of isolated coronary arterioles. American Journal of Physiology-Heart and Circulatory Physiology. 1990;259(4):H1063-H70.
321. Nishikawa Y, Stepp DW, Chilian WM. In vivo location and mechanism of EDHF-mediated vasodilation in canine coronary microcirculation. American Journal of Physiology-Heart and Circulatory Physiology. 1999;277(3):H1252-H9.
322. Altman JD, Kinn J, Duncker DJ, Bache RJ. Effect of inhibition of nitric oxide formation on coronary blood flow during exercise in the dog. Cardiovascular research. 1994;28(1):119-24.
323. Duffy SJ, Castle SF, Harper RW, Meredith IT. Contribution of vasodilator prostanoids and nitric oxide to resting flow, metabolic vasodilation, and flow-mediated dilation in human coronary circulation. Circulation. 1999;100(19):1951-7.
324. Campbell WB, Harder DR. Endothelium-derived hyperpolarizing factors and vascular cytochrome P450 metabolites of arachidonic acid in the regulation of tone. Circulation research. 1999;84(4):484-8.
325. Horst MA, Robinson CP. Action of agonists and antagonists on adrenergic receptors in isolated porcine coronary arteries. Canadian journal of physiology and pharmacology. 1985;63(7):867-71.
326. GRÄSER T, LEISNER H, TIEDT N. Absence of role of endothelium in the response of isolated porcine coronary arteries to acetylcholine. Cardiovascular research. 1986;20(4):299-302.
327. Gräser T, Leisner H, Vedernikov Y, Tiedt N. The action of acetylcholine on isolated coronary arteries of different species. Cor et vasa. 1987;29(1):70.
328. Papapetropoulos A, Cziraki A, Rubin JW, Stone CD, Catravas JD. cGMP accumulation and gene expression of soluble guanylate cyclase in human vascular tissue. Journal of cellular physiology. 1996;167(2):213-21.
329. Kruger NJ. The Bradford method for protein quantitation. Basic protein and peptide protocols: Springer; 1994. p. 9-15.
330. Beltrame JF, Limaye SB, Wuttke RD, Horowitz JD. Coronary hemodynamic and metabolic studies of the coronary slow flow phenomenon. American heart journal. 2003;146(1):84-90.
331. McNulty PH, King N, Scott S, Hartman G, McCann J, Kozak M, et al. Effects of supplemental oxygen administration on coronary blood flow in patients undergoing cardiac catheterization. American Journal of Physiology-Heart and Circulatory Physiology. 2005;288(3):H1057-H62.
332. Ardehali A, Ports TA. Myocardial oxygen supply and demand. CHEST Journal. 1990;98(3):699-705.
333. Gross GJ, Auchampach JA. Role of ATP dependent potassium channels in myocardial ischaemia. Cardiovascular research. 1992;26(11):1011-6.
334. Kuo L, Davis MJ, Chilian WM. Longitudinal gradients for endothelium-dependent and-independent vascular responses in the coronary microcirculation. Circulation. 1995;92(3):518-25.
335. Quyyumi AA, Dakak N, Andrews NP, Gilligan DM, Panza JA, Cannon RO. Contribution of nitric oxide to metabolic coronary vasodilation in the human heart. Circulation. 1995;92(3):320-6.
336. INGRAM D, NEW A. A SPECIFIC CHEMICAL DIFFERENCE BETWEEN THE GLOBINS OF NORMAL HUMAN AND SICKLE-CELL AN/EMIA H/EMOGLOBIN. Nature. 1956;178.
337. Stuart MJ, Nagel RL. Sickle-cell disease. The Lancet. 2004;364(9442):1343-60.
338. Epstein FH, Bunn HF. Pathogenesis and treatment of sickle cell disease. New England Journal of Medicine. 1997;337(11):762-9.
339. Reiter CD, Gladwin MT. An emerging role for nitric oxide in sickle cell disease vascular homeostasis and therapy. Current opinion in hematology. 2003;10(2):99-107.
340. Gladwin MT, Schechter AN, Ognibene FP, Coles WA, Reiter CD, Schenke WH, et al. Divergent nitric oxide bioavailability in men and women with sickle cell disease. Circulation. 2003;107(2):271-8.

341. Reiter CD, Wang X, Tanus-Santos JE, Hogg N, Cannon RO, Schechter AN, et al. Cell-free hemoglobin limits nitric oxide bioavailability in sickle-cell disease. Nature medicine. 2002;8(12):1383-9.
342. Aslan M, Ryan TM, Adler B, Townes TM, Parks DA, Thompson JA, et al. Oxygen radical inhibition of nitric oxide-dependent vascular function in sickle cell disease. Proceedings of the National Academy of Sciences. 2001;98(26):15215-20.
343. Morris CR, Kuypers FA, Larkin S, Sweeters N, Simon J, Vichinsky EP, et al. Arginine therapy: a novel strategy to induce nitric oxide production in sickle cell disease. British journal of haematology. 2000;111(2):498-500.
344. Rodman T, Close HP, Cathcart R, Purcell MK. The oxyhemoglobin dissociation curve in the common hemoglobinopathies. The American journal of medicine. 1959;27(4):558-66.
345. Cokic VP, Smith RD, Beleslin-Cokic BB, Njoroge JM, Miller JL, Gladwin MT, et al. Hydroxyurea induces fetal hemoglobin by the nitric oxide–dependent activation of soluble guanylyl cyclase. Journal of Clinical Investigation. 2003;111(2):231-9.
346. Haematology ICfSi. Recommendations for Selected Methods for Quantitative Estimation of Hb A2 and for Hb A2 Reference Preparation. Br J Haematol. 1978;38:573.
347. Ou C-N, Buffone GJ, Reimer GL, Alpert AJ. High-performance liquid chromatography of human hemoglobins on a new cation exchanger. Journal of Chromatography A. 1983;266:197-205.
348. Bunn HF, Forget BG. Hemoglobin: molecular, genetic and clinical aspects: WB Saunders Company Philadelphia; 1986.
349. Rogers SC, Khalatbari A, Gapper PW, Frenneaux MP, James PE. Detection of human red blood cell-bound nitric oxide. Journal of Biological Chemistry. 2005;280(29):26720-8.
350. Marley R, Feelisch M, Holt S, Moore K. A chemiluminescense-based assay for S-nitrosoalbumin and other plasma S-nitrosothiols. Free radical research. 2000;32(1):1-9.
351. Becklake MR, Griffiths S, McGregor M, Goldman H, Schreve J. Oxygen dissociation curves in sickle cell anemia and in subjects with the sickle cell trait. Journal of Clinical Investigation. 1955;34(5):751.
352. Goldman RK, Vlessis AA, Trunkey DD. Nitrosothiol quantification in human plasma. Analytical biochemistry. 1998;259(1):98-103.
353. Bryan NS. Food, Nutrition and the nitric oxide pathway: biochemistry and bioactivity: DEStech Publications, Inc; 2010.
354. Pawloski JR, Hess DT, Stamler JS. Impaired vasodilation by red blood cells in sickle cell disease. Proceedings of the National Academy of Sciences of the United States of America. 2005;102(7):2531-6.
355. Dietrich H, Ellsworth M, Sprague R, Dacey Jr R. Red blood cell regulation of microvascular tone through adenosine triphosphate. American Journal of Physiology- Heart and Circulatory Physiology. 2000;278(4):H1294.
356. Dejam A, Hunter C, Schechter A, Gladwin M. Emerging role of nitrite in human biology. Blood Cells, Molecules, and Diseases. 2004;32(3):423-9.
357. Ingram TE, Pinder AG, Milsom AB, Rogers SC, Thomas DE, James PE. Blood vessel specific vaso-activity to nitrite under normoxic and hypoxic conditions. Adv Exp Med Biol. 2009;645:21-5.
358. Vlodaver Z. Coronary heart disease: Springer Science+ Business Media; 2012.
359. Münzel T, Daiber A, Gori T. Nitrate Therapy New Aspects Concerning Molecular Action and Tolerance. Circulation. 2011;123(19):2132-44.
360. Shuvy M, Atar D, Steg PG, Halvorsen S, Jolly S, Yusuf S, et al. Oxygen therapy in acute coronary syndrome: are the benefits worth the risk? European heart journal. 2013.
361. Granger DN. Ischemia-reperfusion: mechanisms of microvascular dysfunction and the influence of risk factors for cardiovascular disease. Microcirculation. 1999;6(3):167-78.
362. Vanhoutte PM. Endothelial dysfunction: the first step toward coronary arteriosclerosis. Circulation journal: official journal of the Japanese Circulation Society. 2009;73(4):595-601.